

# Nonlinear Macromechanical Analysis of Polymeric Materials

by

Hossein Sepiani

A thesis

presented to the University of Waterloo

in fulfillment of the

thesis requirement for the degree of

Doctor of Philosophy

in

Civil Engineering

Waterloo, Ontario, Canada, 2017

© Hossein Sepiani 2017

## Examining Committee Membership

The following served on the Examining Committee for this thesis. The decision of the Examining Committee is by majority vote.

External Examiner

Kenneth W. Neale

Professor Emeritus at University of Sherbrook

Supervisor

Maria Anna Polak

Professor at Civil and Environmental Engineering  
Department, University of Waterloo

Internal Member

Wei-Chau Xie

Professor at Civil and Environmental Engineering  
Department, University of Waterloo

Internal Member

Wayne Brodland

Professor at Civil and Environmental Engineering  
Department, University of Waterloo

Internal-external Member

Alexander Penlidis

Professor at Chemical Engineering Department,  
University of Waterloo

## **AUTHOR'S DECLARATION**

I hereby declare that I am the sole author of this thesis. This is a true copy of the thesis, including any required final revisions, as accepted by my examiners.

I understand that my thesis may be made electronically available to the public.

## Abstract

A new methodology for predicting the short term and long term responses of viscoelastic and viscoplastic materials is developed in this research. The methodology aims to predict the behaviour of viscoelastic/viscoplastic isotropic material subjected to loading in isochronous condition (temperature effects are not included). The methodology is implemented in a finite element (FE) procedure through a user defined material subroutine (UMAT) which is linked to ABAQUS software and is called at each increment and material calculation point. The built-in viscoelastic ABAQUS procedure is not able to analyze the nonlinear behaviour of viscoelastic and viscoplastic materials, hence, a specific procedure needs to be defined, which justifies the application of user generated subroutines for material definition in this work.

The development of the methodology consists of four major parts: 1) development of material models for Nonlinear Viscoelastic (NVE) and Nonlinear Viscoplastic (NVP) materials; 2) development of macromechanical NVE and NVP models; 3) development of failure model; 4) implementation in finite element procedure.

For the first part, a new approach is developed for macromechanical constitutive formulations for time-dependent materials. In particular, two phenomenological constitutive models for polymer materials are illustrated, describing time-dependent and nonlinear mechanical behaviour, the Nonlinear Viscoelastic (NVE) and Nonlinear Viscoplastic (NVP) material models. In the proposed approach, short term creep test data are used for modelling both short term and long term responses. A major part of the experiments were done by Liu (Liu, 2007), while the rest have been provided by ExxonMobil, a division of Imperial Oil. The differential form of the model is used to simulate typical Nonlinear Viscoelastic polymeric behaviour using a combination of springs and dashpots. Unified plasticity theory is then used to develop the second model, the Nonlinear Viscoplastic one. Least squares fitting is applied for the determination of material parameters for both models based on experimental results. Due to practical constraints, experimental data are usually available for short term time-frames only. In the presented proposed formulation, the material parameters determined from short term testing are used to obtain material parameter relationships for predicting the long term material response. This is done by extending short term information for longer time frames.

The second part, which is the development of macromechanical NVE and NVP models, is done using two theories: multiple integral and single integral representations of constitutive equations. Multiple

integral representation for three-dimensional behaviour is an extension of linear superposition to the nonlinear range. The method is based on the small strain assumption, but is extended to large deformation for materials in which the stress-strain relation is nonlinear and the concept of incompressibility is governing. Similar to the material modelling (first part), the modelling process uses springs and dash-pots, and a power-law approximation function method for viscoelastic and viscoplastic nonlinear behaviour, respectively. Single integral representation, on the other hand, is a simplified form of multiple integral representation. Based on Schapery's single integral constitutive law, a solution procedure has been provided to solve nonlinear viscoelastic behaviour. This procedure is applicable to three dimensional problems and uses time- and stress-dependent material properties to characterize the nonlinear behaviour of the material. The approximation equations describing material behaviour are defined based on the material response in a short test time frame. For this estimation, Prony series method is used the basis of the constitutive relations is the non-separable form of the equations.

For the failure modelling (third part), an energy based method of delayed failure is presented. The delayed failure approach is applicable to both NVE and NVP modelling for both multiple integral and single integral theories. The approach works with limiting the strain energy of the material to a boundary which is the resilience limit. Here, based on Schapery's single integral constitutive law, the delayed failure criterion is employed for NVE modelling, which helps to solve for the polymer's time to failure involving material nonlinearity.

In the last part, the proposed viscoelastic and viscoplastic models, as well as the delayed failure criterion, are implemented in a user material algorithm of the FE general purpose program ABAQUS and the validity of the models is assessed by comparisons with experimental observations from tests on polyethylene material samples in one-dimensional tensile loading (these tests are done by others). The experiments are short term loading, long term loading, and step loading. Comparisons show that the proposed constitutive model can satisfactorily represent the time-dependent mechanical behaviour of polymers even for long term predictions and the developed formulation provides a flexible and reliable framework for predicting load responses of polymers. It is also concluded that with proper material properties to reflect the deformation involved in the mechanical tests, the deformation behaviour observed experimentally can be accurately predicted using the Finite Element Method (FEM) simulation.

## **Acknowledgements**

This research was undertaken under the supervision of Professor Maria Anna Polak. Without Professor Polak's direction, help, and encouragement, this thesis could hardly be accomplished as presented. Thus, I would like to express my greatest gratitude to her.

I am also grateful to professor Alexander Penlidis for his encouragement and guidance throughout the development of this research and the expertise shared with me on this subject.

My special thanks go to my wife, Atefeh. I owe my deepest gratitude to her, for her understanding, constant support and patience and for being my primary motivation.

## **Dedication**

To my Family.

# Table of Contents

Examining Committee Membership .....	ii
AUTHOR'S DECLARATION.....	iii
Abstract.....	iv
Acknowledgements.....	vi
Dedication .....	vii
List of Figures .....	xii
List of Tables .....	xviii
Nomenclature.....	xx
Chapter 1 Introduction .....	1
1.1 Research significance.....	1
1.2 Objectives .....	3
1.3 Outline of the Research.....	3
Chapter 2 Background and Literature Review.....	7
2.1 Introduction.....	7
2.1.1 Micromolecular background to viscous and solid behaviour.....	7
2.1.2 Types of polymers and their tensile and compressive behaviour.....	9
2.1.3 Experimental considerations .....	14
2.2 Constitutive modelling.....	20
2.2.1 Micro- and macro-scale modelling .....	21
2.2.2 Viscoelastic modelling.....	22
2.2.3 Viscoplastic modelling.....	24
2.3 Parameter estimation for linear modelling.....	25
2.4 Nonlinear modelling .....	28



2.4.1 Classic method of nonlinearization by Liu (Liu, 2007).....	29
2.4.2 Optimized method of nonlinearization (present research).....	30
2.5 Extending the material parameters to longer times frames .....	33
2.5.1 Using short term testing for predictions at longer time frames .....	34
2.5.2 Viscoelastic (NVE) and viscoplastic (NVP) long term responses.....	35
2.6 Modelling the response under varying stress .....	38
2.6.1 Modified superposition principle (MSP).....	38
2.7 Modelling Methodology .....	41
2.8 Practical applications of the present work.....	45
2.9 Conclusion.....	46
Chapter 3 Modelling Short and Long Term Time-dependent Nonlinear Behaviour of Polyethylene..	48
3.1 Introduction .....	48
3.2 Problem Definition .....	51
3.3 Material characteristics.....	52
3.4 Non-linear Viscoelastic (NVE) Model Development .....	53
3.5 Non-linear Viscoplastic ( NVP) Model Development .....	57
3.6 Modelling Long term Behaviour .....	61
3.7 Error Analysis.....	62
3.8 Results .....	64
3.9 Conclusions .....	65
Chapter 4 Finite Element Implementation of Viscoelastic and Viscoplastic Models based on Multi- Integral Formulation.....	77
4.1 Introduction .....	77
4.2 The Constitutive Model.....	82

4.3 Determination of material functions .....	87
4.4 Extending the material parameters to longer times frames .....	96
4.5 Implementation in the Finite Element Program ABAQUS.....	98
4.6 Results and Discussion .....	101
4.7 Conclusions.....	107
Chapter 5 Constitutive equations and finite element implementation of linear modelling for viscoelastic materials .....	110
5.1 Introduction.....	110
5.2 Constitutive Equations .....	114
5.3 Finite deformation formulation of Model B.....	118
5.3.1 Extending to Three-Dimensional Viscoelastic Constitutive Relations .....	121
5.4 FEM implementation .....	124
5.5 Results, materials and comparison.....	125
5.6 Conclusion .....	132
Chapter 6 Constitutive equations and finite element implementation of isochronous nonlinear viscoelastic behaviour .....	134
6.1 Introduction.....	134
6.2 Constitutive Equations .....	137
6.3 Extending to Multi-Dimensional Relations .....	141
6.4 Material Properties.....	143
6.5 FEM implementation .....	149
6.6 Results and comparisons.....	151
6.6.1 Case 1: Short term loading.....	151
6.6.2 Case 2: Long term loading.....	156

6.6.3 Case 3: Step loading .....	164
6.7 Conclusions .....	167
Chapter 7 A Review on Failure Analysis of Viscoelastic Materials .....	170
7.1 Introduction .....	170
7.2 Delayed Failure .....	171
7.2.1 Uniaxial Delayed Failure.....	173
7.2.2 Multi-axial Failure.....	175
7.2.3 FEM implementation.....	177
7.3 Conclusions .....	183
Chapter 8 Conclusions and Future Work .....	184
8.1 Conclusions .....	184
8.2 Future Work .....	187
Bibliography .....	190
Appendix A Viscous Material Analysis Instructions .....	204

## List of Figures

Figure 1: Amorphous and crystalline phases within the polymer materials .....	9
Figure 2: Creep curve for viscous materials subjected to constant load (Brinson, et al., 2008).....	11
Figure 3: Strain recovery in both thermoelastic and thermoset polymers (Brinson, et al., 2008).....	11
Figure 4: Relaxation behaviour for both thermoelastics and thermosets and the definition of the 10 second relaxation modulus (Brinson, et al., 2008).....	12
Figure 5: The stress relaxation modulus $E(t)$ vs $\log(t)$ (Brinson, et al., 2008).....	13
Figure 6: Strain-time curves for 24-hour creep tests on HDPE-pipe (left), and HDPE-resin (right) (Liu, 2007) .....	14
Figure 7: Strain versus time tests (Liu, et al., 2008) .....	16
Figure 8: Strain after 8 hours of creep test at 10 MPa versus hardening stiffness (Behjat, et al., 2014) .....	18
Figure 9: Sample stress-strain curves for ETFE film tested in tension in both directions (Charbonneau, 2011) .....	20
Figure 10: Experimental (continuous line) (Liu, 2007), and non-linear viscoelastic model (dashed line) results for 24-hour creep tests for an HDPE resin .....	32
Figure 11: Experimental (continuous line) (Liu, 2007), and non-linear viscoplastic model (dashed line) results for 24-hour creep tests for an HDPE resin .....	33
Figure 12: Experimental (continuous line) (Liu, 2007), and present NVE model prediction (dashed line) in 40 hours test time (pipe material) .....	36
Figure 13: Experimental (continuous line) (Liu, 2007), and present NVE model prediction (dashed line) in 7 days test time (pipe material).....	36
Figure 14: Experimental (continuous line) (Liu, 2007), and present NVP model prediction (dashed line) in 40 hours test time (pipe material) .....	37
Figure 15: Experimental (continuous line) (Liu, 2007), and present NVP model prediction (dashed line) in 7 days test time (pipe material).....	37
Figure 16: Strain vs time for HDPE resin. Stress level 1 = 2.90 MPa, stress level 2 = 5.80 MPa, stress level 3 = 8.70 MPa, (blue continuous line: experimental data (Liu, 2007), red dashed line: present model) .....	40

Figure 17: Strain vs time for HDPE pipe. Stress level 1 = 1.50 MPa, stress level 2 = 2.90 MPa, stress level 3 = 4.38 MPa, stress level 4 = 5.84 MPa, stress level 5 = 7.30 MPa, (blue continuous line: experimental data (Liu, 2007), red dashed line: present model) .....	41
Figure 18: Strain resultant due to the assumed constant stress increments; representation of superposition principle. ....	43
Figure 19: Experimental (continuous line) (Liu, 2007), and nonlinear viscoelastic model (dashed line) results for 24 hour creep tests (PIPE) using Eqs. (61), (64) and (66) . (Material properties and fitting parameters are cited in Table 3 and Table 4, respectively) .....	59
Figure 20 Experimental (continuous line) (Liu, 2007), and nonlinear viscoelastic model (dashed line) results for 24 hour creep tests (Resin1) using Eqs. (61), (64) and (66) . (Material properties and fitting parameters are cited in Table 3 and Table 5, respectively) .....	59
Figure 21 Experimental (continuous line) (Liu, 2007) and nonlinear viscoplastic model (dashed line) results for 24 hour creep tests (PIPE) using Eqs. (67) and (68). (Material properties and fitting parameters are cited in Table 6 and Table 7, respectively) .....	60
Figure 22 Experimental (continuous line) (Liu, 2007), and nonlinear viscoplastic model (dashed line) results for 24 hour creep tests (Resin1) using Eqs. (67) and (68). (Material properties and fitting parameters are cited in Table 6 and Table 8, respectively) .....	60
Figure 23: Experimental (continuous line) (Liu, 2007), and present nonlinear viscoelastic model (dashed line) results for 24 hour creep test showing erroneous behaviour at 5.97 MPa (PIPE) using Eqs. (61), (64) and (66). Other stress levels are shown in grey (dotted lines) .....	67
Figure 24: Experimental (continuous line) (Liu, 2007), and present nonlinear viscoplastic model (dashed line) results for 24 hour creep test showing erroneous behaviour at 5.97 MPa (PIPE) using Eqs. (67) and (68). Other stress levels are shown in grey (dotted lines) .....	68
Figure 25: Experimental (continuous line) (Liu, 2007), and present nonlinear viscoelastic model prediction (dashed line) in 40 hours test time (PIPE) using Eqs. (61), (64), (66) and (69). (Material properties and fitting parameters are cited in Table 4 and Table 9, respectively) .....	68
Figure 26: Experimental (continuous line) (Liu, 2007), and present nonlinear viscoelastic model prediction (dashed line) in 7 days (170 hours) test time (PIPE) using Eqs. (61), (64), (66) and (69). (Material properties and fitting parameters are cited in Table 4 and Table 9, respectively) .....	69

Figure 27: Experimental (continuous line) (Liu, 2007), and present nonlinear viscoplastic model prediction (dashed line) in 40 hours test time (PIPE) using Eqs. (67), (68) and (70). (Material properties and fitting parameters are cited in Table 8 and Table 10, respectively) .....	69
Figure 28: Experimental (continuous line) (Liu, 2007), and present nonlinear viscoplastic model prediction (dashed line) in 7 days (170 hours) test time (PIPE) using Eqs. (67), (68) and (70). (Material properties and fitting parameters are cited in Table 8 and Table 10, respectively).....	70
Figure 29: Strain resultant due to the assumed constant stress increments. Representation of superposition Principle.....	83
Figure 30: Experimental (continuous line) (Liu, 2007), and nonlinear viscoelastic model (dashed line) results for 24 hour creep tests (PIPE).....	91
Figure 31: Experimental (continuous line) (Liu, 2007), and nonlinear viscoelastic model (dashed line) results for 24 hour creep tests (RES1) .....	92
Figure 32: Experimental (continuous line) (Liu, 2007), and nonlinear viscoplastic model (dashed line) results for 24 hour creep tests (PIPE).....	93
Figure 33: Experimental (continuous line) (Liu, 2007), and nonlinear viscoplastic model (dashed line) results for 24 hour creep tests (RES1) .....	94
Figure 34: Viscoelastic (dashed-dotted line -.-) and viscoplastic (dashed line - - -) model responses compared to 24 HRS test data (solid line) (Liu, 2007), for PIPE material .....	104
Figure 35: One week (7 days) viscoelastic VE (dashed-dotted line -.-) and viscoplastic VP (dashed line - - -) models responses compared to test data (solid line) (Liu, 2007), for PIPE material.....	104
Figure 36: Experimental (continuous line) (Liu, 2007), and viscoelastic VE (dotted dashed line) and viscoplastic VP (dashed line) models prediction (dashed line) in 40 hours test time (PIPE). Analyses done using UMAT in Abaqus .....	105
Figure 37: Two weeks (14 days) unadjusted viscoelastic and viscoplastic (dashed-dotted lines -.- and dashed lines - - -, respectively) as well as adjusted viscoelastic and viscoplastic (rhombus marked lines -◇-◇- and star marked lines -*-*- , respectively) model responses compared to 24 HRS test data (solid line) (Liu, 2007), for PIPE material .....	106
Figure 38: A 3-parameter Model A.....	115
Figure 39: Multi Kelvin Solid configuration Model B. ....	117
Figure 40: Applied step-load stress history.....	119
Figure 41: Dog-bone shape material sample test used by Liu (Liu, 2007) .....	126

Figure 42: Test results (continuous line) (Liu, 2007) vs. present FEA (dashed line) for HDPE-PIPE material.....	128
Figure 43: Test results (continuous line) (Liu, 2007) vs. present FEA (dashed line) for HDPE-RES1 material.....	128
Figure 44: Test results (continuous line) (Liu, 2007) vs. present FEA (dashed line) for HDPE-RES2 material.....	129
Figure 45: Finite element results for PIPE material under 7.71MPa, Model A (N=1) compared to experiments, see Table 22 for material parameters for each case .....	131
Figure 46: Finite element results for PIPE material under 7.71MPa, using Model A (N=1), and Model B (N=2 & N=3) compared to experiments (Liu, 2007).....	132
Figure 47: Multi Kelvin Solid configuration.....	139
Figure 48: Single 3D element made in ABAQUS and meshed by one quadratic hexahedron solid element, C3D20R .....	152
Figure 49: Short term (24 hour) results comparison for PIPE material between test data (solid lines) (Liu, 2007) and present FEA (dashed lines).....	153
Figure 50: Short term (24 hour) results comparison for RES1 material between test data (solid lines) (Liu, 2007) and present FEA (dashed lines).....	154
Figure 51: Short term (24 hour) results comparison for RES2 material between test data (solid lines) (Liu, 2007) and present FEA (dashed lines).....	154
Figure 52: Short term (24 hour) results comparison for RES4 material between test data (solid lines) (Liu, 2007) and present FEA (dashed lines).....	155
Figure 53: Short term (24 hour) results comparison for PE80 material between test data (solid lines) (Liu, 2007) and present FEA (dashed lines).....	155
Figure 54: Long term (40 hour) response prediction for PIPE material, test data (solid lines) (Liu, 2007) and present FEA (dashed lines).....	157
Figure 55: Long term (170 hour) response prediction for PIPE material, test data (solid lines) (Liu, 2007) and present FEA (dashed lines).....	157
Figure 56: Finite element (solid lines) vs. experimental (dashed lines) (by Imperial Oil), creep results for LL-8461 at 23°C.....	159
Figure 57: Finite element (solid lines) vs. experimental (dashed lines) (by Imperial Oil), creep results for LL-8461 at 50°C.....	160

Figure 58: Finite element (solid lines) vs. experimental (dashed lines) (by Imperial Oil), creep results for LL-8461 at 60°C .....	160
Figure 59: Finite element (solid lines) vs. experimental (dashed lines) (by Imperial Oil), creep results for HD-8660 at 23°C .....	161
Figure 60: Finite element (solid lines) vs. experimental (dashed lines) (by Imperial Oil), creep results for HD-8660 at 50°C .....	161
Figure 61: Finite element (solid lines) vs. experimental (dashed lines) (by Imperial Oil), creep results for HD-8660 at 60°C .....	162
Figure 62: Finite element (solid lines) vs. experimental (dashed lines) (by Imperial Oil), creep results for Paxon-7004 at 23°C .....	162
Figure 63: Finite element (solid lines) vs. experimental (dashed lines) (by Imperial Oil), creep results for Paxon-7004 at 50°C .....	163
Figure 64: Finite element (solid lines) vs. experimental (dashed lines) (by Imperial Oil), creep results for Paxon-7004 at 60°C .....	163
Figure 65: Two step loading for PIPE material, test data (solid lines) (Liu, 2007) and present FEA (dashed lines) .....	165
Figure 66: Two step loading for PIPE material, test data (solid lines) (Liu, 2007) and present FEA (dashed lines) .....	166
Figure 67: Multi step loading for PIPE material, test data (solid lines) (Liu, 2007) and present FEA (dashed lines) .....	166
Figure 68: Multi step loading and unloading for PIPE material, test data (solid lines) (Liu, 2007) and present FEA (dashed lines) .....	167
Figure 69: Multi Kelvin Solid configuration subject to uniaxial stress. ....	174
Figure 70: A cubic single element solid model made in ABAQUS and meshed by one quadratic hexahedron solid element, C3D20R .....	178
Figure 71: Axial deviatoric free energy (W1) per time for PIPE material .....	179
Figure 72: Transverse deviatoric free energy (W2) per time for PIPE material .....	179



Figure 73: Time to fail vs. stress for A) polyethylene, T=296K and B) polymethyl methacrylate (PMMA), T=297K (McKenna, et al., 1980) .....	180
Figure 74: Time to failure (hrs) vs. applied stress for material Resin 2, using the delayed failure approach .....	182
Figure 75: Logarithmic time to failure (hrs) vs. applied stress for material Resin 2, using the delayed failure approach .....	182

## List of Tables

Table 1: List of tested polyethylene materials (Liu, 2007) .....	71
Table 2: Fitting parameters for $X_0$ .....	71
Table 3: Fitting parameters for NVE model .....	72
Table 4: Material parameters for “PIPE” (Viscoelastic).....	72
Table 5: Material parameters for “Resin1” (Viscoelastic).....	72
Table 6: Fitting parameters for NVP model.....	73
Table 7: Material parameters for “PIPE” (Viscoplastic).....	73
Table 8: Material parameters for “Resin1” (Viscoplastic).....	73
Table 9: Fitting parameters for NVE long term model .....	74
Table 10: Fitting parameters for NVP long term model .....	75
Table 11: Fitting error, PIPE material (test time of 40 hours, case I) per Eq. (71) .....	76
Table 12: Fitting error, PIPE material (test time of 7 days, case II) per Eq. (71) .....	76
Table 13: List of tested polyethylene (Liu, 2007).....	88
Table 14: Material fitting parameters for $X_0$ (Eq. (93)) .....	94
Table 15: Material fitting parameters for NVE model (Eq. (92) & Eq. (94)).....	95
Table 16: Material fitting parameters for NVP model (Eq. (97)) .....	96
Table 17: Material fitting parameters for long term Viscoelastic (Eq. (98)) and Viscoplastic (Eq. (99)) models for “PIPE” material sample .....	98
Table 18: Material constants (properties) for “PIPE” (Viscoelastic).....	102
Table 19: Material constants for “PIPE” (Viscoplastic) .....	102
Table 20: List of tested polyethylene (Liu, 2007).....	126
Table 21: Prony series parameters (material parameters) (Liu, 2007).....	127
Table 22: Prony series parameters for PIPE under 7.71MPa uniaxial force for Model A (N=1) .....	130
Table 23: Prony series parameters for PIPE under 7.71MPa uniaxial force.....	131
Table 24: List of tested polyethylene materials (dog-bone shape samples) by Liu (Liu, 2007) .....	146
Table 25: List of tested polyethylene* (from ExxonMobil Chemical Canada) .....	146
Table 26: Fitting parameters for materials listed in Table 24 .....	147
Table 27: Fitting parameters for materials listed in Table 25 .....	148
Table 28: Error (%) for the readings of strain (FE model vs. experiment) for short term prediction	153

Table 29: Error (%) for the readings of strain (FE model vs. experiment) for long term predictions (40 hour and 170 hour) based on 24 hour material parameters for PIPE material .....	158
Table 30: Error (%) for the readings of strain (FE model vs. experiment) at time = 1007 hr .....	164
Table 31: TTF (Time To Failure) for Resin 2, based on delayed failure approach.....	181

## Nomenclature

$a_0 \sim a_2$	Model fitting parameters
$a_{\sigma T}^t$	Shift factor
$b_0 \sim b_6$	Model fitting parameters
$b'_0 \sim b'_6$	Model fitting parameters
$c_0 \sim c_4$	Model fitting parameters
$c'_0$	Model fitting parameter
$d_0 \sim d_6$	Model fitting parameters
$e_{ij}$	Strain tensor components
$f$	A function of time
$f_t$	Value of function $f$ at time $t$
$f^e$	denotes the elastic strain
$f^v$	denotes the time dependent strain
$g_{ij}$	A function of stress and time
$g_0, g_1, g_2$	material functions of stress and temperature
$h_{ij}$	A function of stress
$m$	Model fitting parameter
$\tilde{m}$	Model fitting parameter
$m_1, m_2, m'_1, m'_2$	Model fitting parameters
$n_1, n_2$	Model fitting parameters
$p$	hydrostatic pressure
$q_n$	Modelling parameter
$s_{ij}$	Deviatoric stress
$s'$	Model fitting parameter
$s_a, s'_a$	Model fitting parameter
$t$	Time
$t_i$	Start time for $i$ -th time increment
$tr()$	Indicates the trace of tensor
$u, u_{ij}$	Displacement vector, components

$x_i$	Material point coordination
$A_n$	Material parameters
$A_0$	Material parameter at $t_0$
$A_\infty$	Material parameter at $t_\infty$
$B_n$	Material parameters
$B_n^t$	Modelling parameter
$C_n$	Material parameters
$\mathbb{C}$	Elastic moduli of the material
$\mathbf{C}$	coefficients matrix
$\bar{C}_1, \bar{C}_2$	Constants
$D(t)$	Creep compliance
$\mathbb{D}$	Material compliance matrix
$D_0$	instantaneous elastic compliance
$D_n$	n-th equivalent creep compliance
$D_t$	instantaneous compliance at time $t$
$E_0$	Elastic modulus of elasticity
$E_i$	Elastic modulus for i-th Kelvin unit
$\bar{E}^t$	hereditary strain at time $t$
$E^t$	Equivalent modulus of elasticity at time $t$
$E^e$	Elastic modulus
$E^i$	Equivalent inelastic/viscous modulus
$E_g$	“glassy” modulus
$F_j$	Material external force component
$G$	Shear modulus
$G_0$	instantaneous shear compliance
$G_i$	shear compliances for $i^{th}$ Kelvin unit
$H_{ij}$	Modelling parameter
$\mathbf{I}$	Unit tensor
$J$	shear compliance
$J_0$	instantaneous shear compliance
$K$	Bulk modulus

$K_i$	Functions of time called Kernells
$N$	Order of polynomial equation
$N_t$	Number of strain measurements recorded for each creep test
$Q_{ij}^t$	Modelling parameter
$R$	Resilient factor
$T$	Material parameter
$T$	Temperature
$T_1, T_2, T'_1$	Model fitting parameter
$T_0$	reference temperature
$T_g$	glass transition temperature
$T_n$	relaxation time for shear
$V$	Material viscoelastic domain
$W^s$	Total strain energy
$W_i^s$	Energy stored in direction $i$
$X_0$	Elastic creep compliance
$X_n$	Equivalent creep compliances
$\bar{X}_i$	Original material point coordination
$X_{i,j}$	creep compliances tensor components
$\alpha$	Model fitting parameter
$\tilde{\alpha}$	Model fitting parameter
$\beta_{ij}$	A function of stress and strain
$\gamma_{ij}$	Strain tensor components
$\delta(t)$	Dirac delta function
$\varepsilon, \varepsilon_{ij}$	Strain, strain tensor components
$\dot{\varepsilon}$	Strain rate
$\varepsilon^e$	Elastic strain
$\varepsilon^p$	Inelastic/plastic strain
$\varepsilon_i, \hat{\varepsilon}_i$	Predicted and measured strain vlues at time $t_i$
$\varepsilon^i$	inelastic strain
$\varepsilon_V$	Volumetric strain
$\varepsilon_n$	strain associated with n-th Kelvin unit

$\dot{\varepsilon}_k$	Strain rate for i-th Kelvin unit
$\varepsilon_c$	Constant strain
$\varepsilon'$	recovery strain
$\varepsilon''$	Second strain
$\zeta^t$	reduced time scale parameter
$\theta$	dilatational strains
$\lambda$	Time factor in long term modelling
$\lambda$	Lame parameter
$\lambda'$	Equivalent test time for dimensional consistency
$\mu$	Lame parameter
$\mu_i$	Coefficient of viscosity for i-th Kelvin unit
$\nu$	Poisson's ratio
$\bar{v}, \bar{v}_i$	Material point velocity vector, components
$\xi, \xi_i$	Integration variable
$\rho$	material density
$\sigma, \sigma_{ij}$	Stress, stress tensor components
$\bar{\sigma}$	Equivalent stress for dimensional consistency
$\dot{\sigma}$	Stress rate
$\sigma_{eff}$	Equivalent stress
$\sigma_v$	Volumetric stress
$\sigma_y$	tensile stress at yield
$\sigma_i$	Principle stress in $i$ direction / i-th increment stress
$\sigma_{jn}$	Equivalent stress in $i$ direction for Kelvin unit $n$
$\sigma^{(i)}$	Material constants
$\sigma_f$	Failure stress
$\sigma_c$	Constant stress
$\tau_n$	Material parameters, relaxation times
$\chi(t)$	Time dependent relaxation compliance
$\chi_i$	Time dependent material functions
$\psi(t, \sigma)$	Creep compliance function
$\psi^e$	Elastic strain energy

$\psi^i$	Inelastic strain energy
$\Pi$	coefficients matrix
$\Psi_i$	Functions of time



# Chapter 1

## Introduction

### 1.1 Research significance

Polymers and plastics are commonly used in structural and mechanical applications such as pipes, automotive parts and medical implants. During the last few decades, a significant amount of research has been done on polymers in order to predict their behaviour under different loading and environmental conditions. The application of polymers in industry has led to the development of different approaches of investigation in forms of theoretical, experimental, numerical and finite element approaches. In particular, two specific approaches are important to mention. These are molecular (micro-mechanical) and macroscopic (macro-mechanical) in nature. Micromechanical models emphasize the relation between the macroscopic properties of materials and their microstructure. For predicting mechanical response of polymers for structural analysis, the macromechanical approach is employed.

Research presented in this thesis is focused on macromechanical analysis. Although many scientific works have been carried out on this topic there are still gaps that need to be filled. A common problem in the area of macromechanical investigation of polymers is defining the behaviour of materials, which involves consideration of viscoelasticity and/or viscoplasticity, as well as nonlinearity in response. This has always been one of the main concerns of researchers in this area, which involves two procedures. First is the development of constitutive equations and second is defining material properties. The first procedure includes two major formulation approaches, which are differential and integral.

The first step is based on an approximation process. For the differential approach, a configuration of spring and dash-pot elements, which best describes the behaviour, needs to be chosen. Approximation functions describing material behaviour need to be selected. The right selections of these components of formulations have always been of interest to researchers. Herein, a multi Kelvin solid configuration of springs and dash-pot elements is chosen for the differential formulation. For the integral formulation, on the other hand, exponential and power law functions are approximated for viscoelastic and viscoplastic analysis, respectively. The suitability of all these selections is analyzed.

The second step involves employment of experimental results in defining material parameters using the developed constitutive formulation in step 1. The technique involves fitting the resultant constitutive relations to the test data and optimizing the solution for the unknown material parameters. In this work, a nonlinear optimization approach is developed in MATLAB workspace, which defines the material properties, using 24-hour unidirectional creep test results. It is then shown that the methodology used in step 1 and the resultant material properties from step 2 are useful and easy to be implemented in finite element procedures.

Another important consideration is predicting the response in a long term time-frame. Running long term experiments is expensive and time consuming. Although many researchers have used the Time-Temperature Superposition Principle (TTSP) for predicting long term behaviour of polymers, to the best knowledge of the author, no work is available on other methods and this research aims to fill this gap by providing an efficient empirical procedure. In the proposed approach one means of generating relevant design data is to investigate prototype structures within a shorter time-frame. Based on this investigation, the constitutive equations are modified accordingly.

For the main objective of this research, to accomplish, which is finite element (FE) implementation of constitutive models in a commercial software, a user defined material subroutine is generated. Abaqus is used for the Finite Element Analysis (FEA). The current version of the commercial software Abaqus allows only linear viscoelastic modeling, which can be used for both small and large strain problems. It has to be used in conjunction with linear elastic behaviour or hyperelastic behaviour. Material parameters are defined either by direct specification of Prony series parameters, or by direct inclusion of creep, relaxation or frequency test data. The built-in procedure in Abaqus software is not able to analyze the nonlinear behaviour of viscoelastic and viscoplastic materials. Noting that nonlinear time domain analysis requires application of time- and stress-dependent material properties, a specific procedure needs to be defined, which justifies the application of user generated subroutines for material definition. For this, two procedures are developed using integral formulation of material behaviour. The first procedure is based on the multi-integral formulation of viscoelastic and viscoplastic analyses, and the second one is based on Schapery's single integral formulation. The formulations are modified in such a way that the material parameters can be employed for the long term analysis. These properties are based on a multi-Kelvin configuration of spring and dash-pot elements for viscoelastic behaviour and power law functions for viscoplastic behaviour. Both analyses are nonlinear and based on the user defined material subroutine.

A failure analysis, based on maximum distortion energy, is also studied and used in further improvement of the FE procedure. Consequently, this makes the procedure able to predict the ultimate life time of the material for the long term.

## **1.2 Objectives**

The objectives of the thesis are outlined below.

1. Development of a mathematically rational modelling of polymeric material behaviour and optimization using results of the tested polymers (macromechanical constitutive modelling). The modelling should include time dependent and nonlinear characteristics of the behaviour and, at the same time, be simple enough for easy implementation into a commercial finite element package such as ABAQUS.

2. Development of the mathematical modelling for long term response prediction. The strategy is to use short term test data for optimizing the model parameters.

3. Development of a mathematical failure model based on ultimate failure energy criteria, which is easy to implement in FE analysis through a user defined material subroutine.

4. Implementation of the developed mathematical model along with failure criteria (steps 1~3) into the commercial software ABAQUS, by developing an appropriate procedure. For this a user defined material subroutine is generated, which is invoked by FE software ABAQUS, during the nonlinear analysis.

5. Validating both the mathematical model and the FE procedure by comparing the present results with experimental ones.

## **1.3 Outline of the Research**

The thesis is written in a form composed of several published and planned journal papers.

### **Chapter 1:**

Provides a description of the research significance and justification, as well as objectives of the research, and the steps taken to achieve these objectives.

### **Chapter 2: Background and Literature Review**

Parts of this chapter are based on the book chapter:

Polak, M.A., H. Sepiani and A. Penlidis. Modelling Material Behaviour of Polymers, Chapter in Computational Modelling, Optimization, and Manufacturing Simulation of Advanced Engineering Materials, (Pablo Munoz-Rojas, Ed.), by Springer, ISBN 978-3-319-04265-7

In this chapter a background is provided on viscoelastic and viscoplastic materials, their application, and micromolecular and macromolecular characteristics. Also, experimental investigations that have been done previously at the University of Waterloo are described. An introduction to the modelling methods is provided. The theoretical approaches adopted in the thesis are explained.

### **Chapter 3: Modelling Short and Long Term Time-dependent Nonlinear Behaviour of Polyethylene**

Contents of this chapter is published in the journal of “Mechanics of Advanced Materials and Structures”. In this chapter a new methodology for developing macromechanical constitutive formulations for time-dependent materials is developed which describes nonlinear behaviour. Differential formulation as well as unified plasticity theory is used for development of 1-D nonlinear viscoelastic and viscoplastic models, respectively. Models are extended to long term, based on short term experimental observations. Materials parameters are obtained using nonlinear optimization, which is a minimization technique of an error function. The resultant models describe nonlinear time dependent behaviour, and are easy to use in finite element procedures.

### **Chapter 4: Finite Element Implementation of Long Term Behaviour of Viscoelastic and Viscoplastic Materials**

In this chapter, a multiple integral approach, which is essentially an extension of the Boltzmann’s linear superposition principle to nonlinear range, is employed for three-dimensional behaviour of viscoelastic and viscoplastic materials. Some simplifications are considered in order to obtain a particularly useful theory, namely the fully incompressible behaviour assumption of the material, the superposition of small time dependent deformations, and finally the simplifications of the material functions. Differential formulation (exponential form), and unified plasticity (power-law function) approximations are used for viscoelastic and viscoplastic modelling, respectively.

The equations describing material behaviour are modified based on the measured material properties through an empirical approach, by fitting the results to experimental data. The models are optimized for long-term responses which are beyond the test time. Finite element procedures are implemented in

the user-defined material algorithm in Abaqus (UMAT). The validity of the models is assessed by comparison with experimental observations on high density polyethylene (HDPE) for a single element under uniaxial loading. The comparisons show that the proposed constitutive model can satisfactorily represent the time-dependent mechanical behaviour of polymers.

### **Chapter 5: Constitutive Equations and Finite Element Implementation of Linear Behaviour for Viscoelastic Materials**

This chapter is concerned with the formulation and constitutive equations of finite strain viscoelastic materials using the superposition principle in a thermodynamically consistent manner. Based on the proposed constitutive equations, a finite element (FE) procedure is developed, and is implemented in a User Material FE code. For validation, the material properties are used, which have been previously obtained experimentally by Liu (Liu, 2007). The model is used to predict the response of sample materials and the results are compared to experimental ones.

### **Chapter 6: Constitutive Equations and Finite Element Implementation of Isochronous Nonlinear Viscoelastic Behaviour**

In this chapter, based on Schapery's single integral constitutive law, a nonlinear solution procedure is used to solve problems involving material nonlinearity. To simulate the viscoelastic behaviour of materials, a multi Kelvin solid configuration of spring and dash-pot elements is used to construct the constitutive equations. Time- and stress-dependent material properties (based on a generalized multi Kelvin simulation) are used to characterize the nonlinear behaviour of material.

For finite element analysis purposes, the three dimensional formulation is developed and material functions are defined and modified to include the long term response of the material. For this, the parameters within the equations describing material behaviour are set to be functions of test time by observing the parameters trend versus different examined test times.

The presented model can be used for the development of a unified computer code that can handle both linear as well as nonlinear viscoelastic material behavior. The proposed viscoelastic model is implemented in a user-defined material algorithm in Abaqus (UMAT). The validity of the models is assessed by comparison with experimental observations on high density polyethylene (HDPE) specimens test results under uniaxial loading.

### **Chapter 7: A Review and Analysis on Failure of Polyethylene**

In this chapter a brief introduction is provided on failure criteria for polymers. Out of the many criteria, the maximum strain energy is chosen for finite element application. The results are compared with results published in the literature.

### **Chapter 8: Conclusions and Future Works**

In this chapter the outcome of the research is discussed and future possible research opportunities are suggested.

## **Chapter 2**

### **Background and Literature Review**

Polymers are the most widespread materials in nature. Silk, wool, DNA, cellulose, rubber and proteins are typical examples. In contrast, synthetic polymers, like polyethylene, nylon, polyesters, Teflon and epoxy, are industrially derived from petroleum oil. They are often formulated for specific applications. Polymers are widely used in the automotive, aerospace and computer industries, building trades and many other applications. Some important areas of applications of polymers are: fiber reinforced plastics, adhesives, insulation applications, optical applications, fibers and plastic pipes.

This chapter provides a background and literature review on the polymeric material and the constitutive equations. First a background on micromolecular behaviour of viscous and solid materials are presented. Types of polymers and their applications are discussed and the experimental methods of investigating polymers are provided.

Constitutive modelling of viscoelastic and viscoplastic materials are discussed later. This will follow with parameter estimation for linear modelling which has been performed previously at University of Waterloo. Methods of nonlinear modelling (vs. linear modelling) are provided and techniques of extending the material parameters to longer time frames are discussed. Also, the widely-used superposition principle is mentioned. Finally, modelling methodology which will be used in this research is explained briefly.

#### **2.1 Introduction**

##### **2.1.1 Micromolecular background to viscous and solid behaviour**

There are numerous ways to classify polymers from a micromolecular point of view. Most of the polymers can be classified as either thermoplastics or thermosets. These names are associated with general structural, thermal and processing characteristics. Basic structural differences greatly impact material properties. The fundamental physical difference between the two classes comes from the way the polymer molecules are connected with each other. Thermosets consist of cross-linked molecules; hence they have a network structure. This influences the specific behaviour of these materials. In

contrast to thermoset polymers, thermoplastic polymers can be made to flow over many processing cycles and they can be melted or molded.

Many polymers are two-phase materials consisting of an amorphous and a crystalline phase. What distinguishes the crystalline phase from the amorphous phase is that in crystals the macromolecules are packed together in an organized fashion as opposed to forming a random shape as in the case of the amorphous phase. When the polymer is subsequently subjected to a load, each phase behaves differently. The crystalline lamellae provide high yield stress, while the amorphous phase provides flexibility and hence a recoverable elastic response. Figure 1 shows a schematic representation of the two phases in polyethylene. The parallel lines at the centre of the figure represent the crystalline phase and the random configuration at the two sides represents the amorphous phase.

What gives most polymers, especially polyethylene, their uniform resistance to load is the existence of covalent bonds between carbon atoms. A covalent bond is a chemical bond in which the electrons are shared between the atoms. The angular relations between atoms in a polymer determine the strength of the covalent bond. To create a polymeric chain each central atom needs to have at least two bonds with other atoms. However, two carbon atoms can have double or triple bonds.

The cohesive properties of a polymer are due to van der Waals forces, which come from interactions between different molecules. There are two mechanisms that are at play when it comes to van Der Waals forces: one is the mass attraction and the other is related to momentary electron fluctuations. The strength of the van Der Waals force relative to a covalent bond is usually about 1%. However, there are several factors that can help increase this value to 10%. Some of these factors are: proximity of molecules, increase in molecule size, and multiple bonds between carbon atoms.

Two general modes of deformation in polymer crystals are described. (1) Within chains of the polymer: This mode of deformation can be caused by stretching of covalent chains (this stretching is strongly resisted and therefore does not account for much of the deformation), change of angle between adjacent covalent bonds (which is more easily accommodated than the previous mode), and rotation of one bond with respect to the next adjacent bond (which is easier than the previous modes). (2) Between chains, which refers to deformations that are perpendicular to the chains. This type of deformation happens with much less resistance than the ones within the chains.



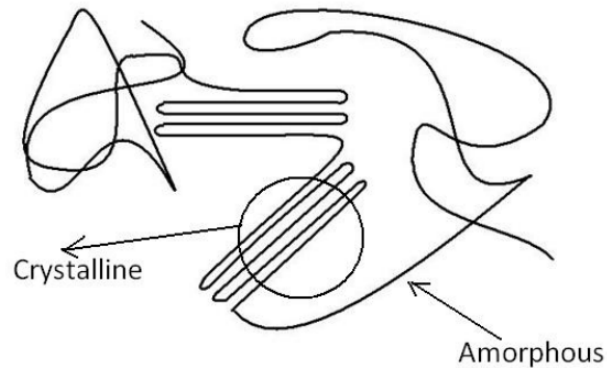


**Figure 1: Amorphous and crystalline phases within the polymer materials**

### 2.1.2 Types of polymers and their tensile and compressive behaviour

As mentioned previously, there are two main categories of polymeric material behaviour.

**Thermoplastic polymers:** They can be made to flow and one can melt or mold them during processing. The crystalline phase is denser than the amorphous part. This results in enhancement in some properties like hardness, corrosion resistance or resistance to environmental stress cracking (ESC), friction and wear, and less creep or time-dependent behaviour.

Examples include polyethylene, polypropylene, Polyamides (nylon), polytetrafluoroethylene, polyvinyl Chloride (PVC), polystyrene, polycarbonate, and polymethyl Methacrylate.

**Thermoset polymers:** These are used generally where high thermal and dimensional stability are required. They are suitable for electrical and thermal insulation, high performance composite applications and where high strength and modulus are required. Phenolics, polyurethanes, and epoxy-polymers are typical examples.

**Tensile and compressive behaviour:** Polymers show solid and viscous as well as time-dependent behaviour. The induced stress and strain are functions of time. They generally can be thought of as a three-dimensional surface. The stress-strain-time relationship, or time-dependent constitutive law, can be determined by loading a polymer specimen with constant stress (results in creep phase response) or constant strain (results in relaxation or isometric response). These two types of behaviour and corresponding experiments will be discussed further in the following sections.

**Creep phase:** Viscous materials deform continuously when subjected to constant load. The initial strain is produced due to the pure elastic property of a polymer and is predicted by its stress-strain modulus. The elastic region is followed by the viscoelastic or viscoplastic response. The deformation slowly continues until rupture or yielding occurs. As seen in Figure 2, the primary region is the early stage of loading when the creep rate decreases rapidly with time. Then, the creep rate reaches a steady-state, which is called the secondary creep stage. The next region is characterized by a rapid increase in strain (tertiary stage) and, finally, fracture.

The creep response depends on material properties and type, magnitude of applied stress, temperature and time. Thermoplastics and thermosets show different behaviour. As seen in Figure 3, the strain will tend to a constant value after a long time for a thermoset, while the strain will increase without limit for a thermoplastic. Upon removal of the applied load, an immediate elastic recovery equal to the elastic deformation occurs for both types of polymers. It is then followed by a period of slow recovery. For an ideal thermoset material, a decay to zero can be seen, which happens after a long time interval (compared to the loading time).

**Relaxation phase:** This behaviour is defined as a gradual decrease in stress with time under a constant deformation or strain. The resultant response is shown in Figure 4. After a long period of time, both curves decay to a constant value. This asymptotic value is equal to zero for thermoplastic materials.

The relaxation and creep tests observations reveal both solid and fluid characteristics related to polymeric materials. The relation  $E_{(t=0)} = \sigma_0/\varepsilon_c$  shows the instantaneous modulus of elasticity corresponding to the elastic solid behaviour in a relaxation test, where index  $c$  shows the constant value and index 0 shows the initial one. In similar fashion, the relation  $D_{(t=0)} = \varepsilon_0/\sigma_c$  indicates the initial relaxation compliance which is related to the elastic solid portion of the material behaviour.

Fluid behaviour of polymers is defined by considering a time-dependent relaxation modulus as  $E(t) = \sigma(t)/\varepsilon_c$ . Plotting this modulus versus log time (Figure 5) reveals that at short times, the stress is at a high plateau corresponding to a “glassy” modulus  $E_g$ , and then falls exponentially to a lower equilibrium “rubbery” modulus  $E_r$ .

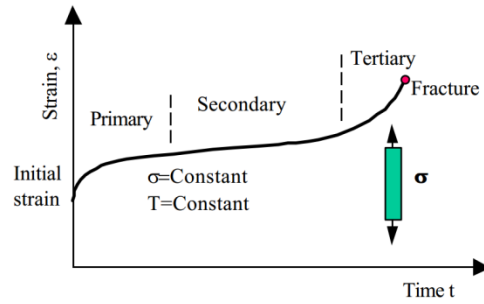


**Figure 2: Creep curve for viscous materials subjected to constant load (Brinson, et al., 2008)**

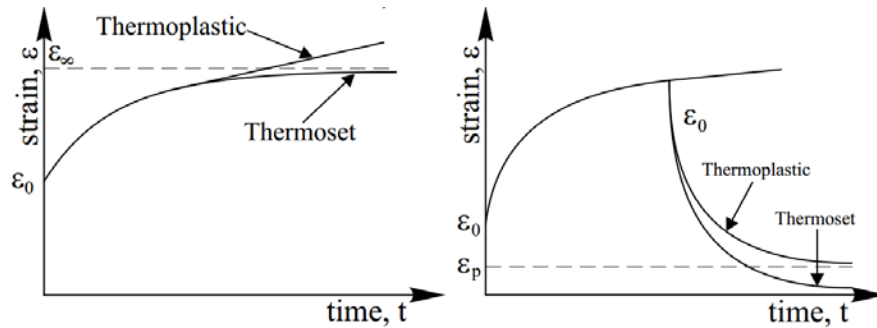


**Figure 3: Strain recovery in both thermoelastic and thermoset polymers (Brinson, et al., 2008)**

**Modulus vs. compliance:** Creep and relaxation are both illustrations of the same molecular mechanism, and are related to each other. However, even though  $E = 1/D$  in both glassy and rubbery regions, in general  $E \neq 1/D$ . In particular, the relaxation response moves toward its equilibrium value more quickly than does the creep response. These factors are related by a convolution integral (Ferry, 1980)

$$\int_0^t E(t - \tau)D(\tau)d\tau = t \quad (1)$$

where  $t$  is time and  $\tau$  is an integration parameter with time unit. Several approximation methods of interconversion between transient relaxation modulus,  $E(t)$ , and creep compliance,  $D(t)$ , are used in the literature. They are mostly based on adjustment of the elastic-like reciprocal relationship between these two parameters. The simplest interrelationship which is recommended for weakly viscoelastic materials is based on the quasi-elastic interrelationship defined as  $E(t) D(t) \approx 1$  (Park, et al., 1999).

For linear viscoelastic materials in which the relaxation modulus and creep compliance can be represented by simple power laws over their transition zones, Leaderman (Leaderman, 1943), Christensen (Christensen, 1971), Denby (Denby, 1975) and Park (Park, et al., 1999) presented the following interconversion formulas, respectively.

$$E(t)D(t) = \frac{\sin n\pi}{n\pi} \quad (2)$$

$$E(t)D(t) \cong \frac{1}{1 + \frac{n^2\pi^2}{4}} \quad (3)$$

$$E(t)D(t) \cong \frac{1}{1 + \frac{n^2\pi^2}{6}} \quad (4)$$

$$E(\alpha t)D(t) = E(t)D(t/\alpha) = 1 \quad (5)$$

in which  $\alpha = \left(\frac{\sin n\pi}{n\pi}\right)^{1/n}$  and  $n$  is the local slope of the source function  $F(t)$  ( $= E(t)$  or  $= D(t)$ ), defined as

$$n = \left| \frac{d \log F(\tau)}{d \log \tau} \right|_{at \tau=t} \quad (6)$$

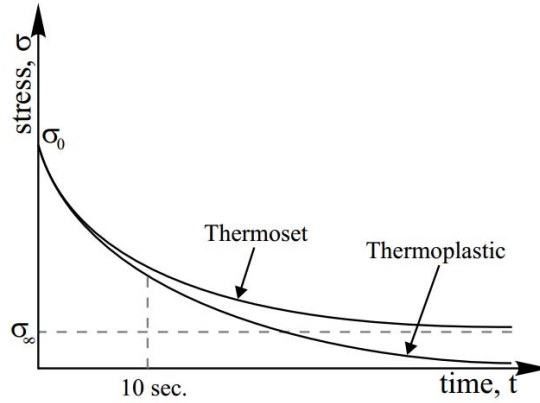


**Figure 4: Relaxation behaviour for both thermoelastics and thermosets and the definition of the 10 second relaxation modulus (Brinson, et al., 2008)**

**Linearity, nonlinearity and the concept of isochronous modulus:** Two important definitions of linearity (or nonlinearity) are usually employed: the first is material linearity which deals with Hookean stress-strain behaviour or linear relation between stress and strain; and the second is geometric linearity (or nonlinearity).

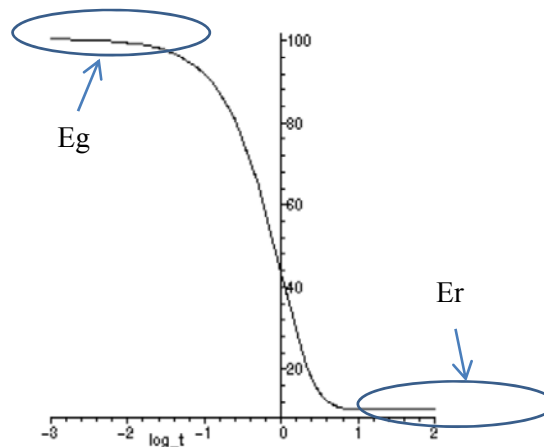


**Figure 5: The stress relaxation modulus  $E(t)$  vs  $\log(t)$  (Brinson, et al., 2008)**

One of the main points in analysis is to determine if the material behaviour under specific conditions is linear or nonlinear. This can be accomplished by determining if the creep compliance (or relaxation modulus) is independent of stress (or strain). This can be performed by plotting the stress-strain curves for different times. It can be seen in Figure 6 and is called isochronous stress-strain diagram. If this isochronous variation of stress versus strain at any given time,  $t_i$ , is linear, the material is linear. In this case the creep compliance (or relaxation modulus) can be determined by  $D(t_i) = \varepsilon_i/\sigma_i$  (or  $E(t_i) = \sigma_i/\varepsilon_i$ ). This property is characterized as linear viscoelasticity. In the linear range the compliance (or modulus) is independent of stress (strain). By increasing the applied stress or strain, a transition from linear to nonlinear viscoelasticity can be observed (Figure 6). In the nonlinear region, the slope of isochronous stress-strain curve is no longer constant, meaning that the compliance (or modulus) is a function of stress (or strain).

It is worth pointing out that polymers generally exhibit linear behaviour at low stresses, while at moderate or higher stress levels, the material is assumed to be nonlinear and will not obey the linear Hookean relationship.

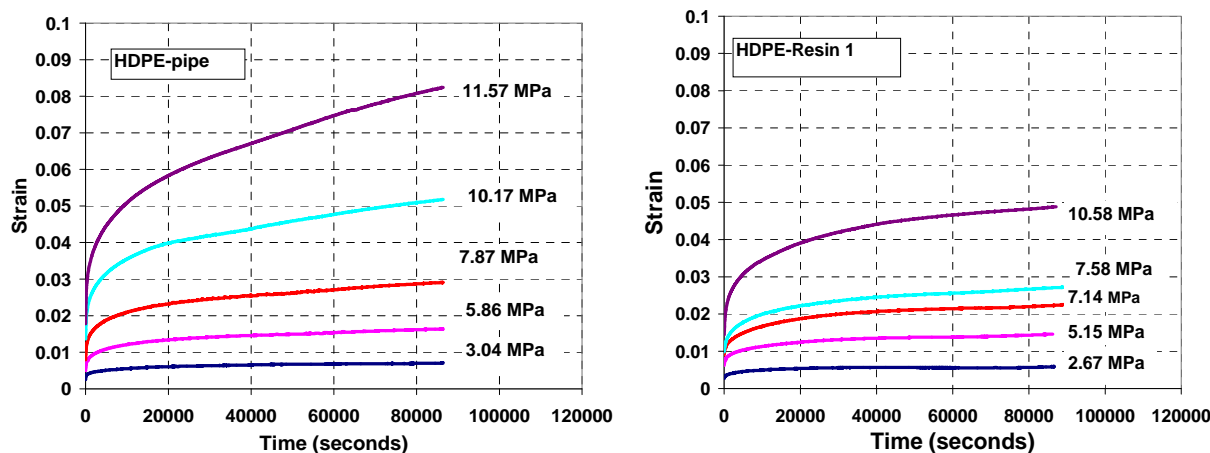


**Figure 6: Strain-time curves for 24-hour creep tests on HDPE-pipe (left), and HDPE-resin (right) (Liu, 2007)**

Both the material nonlinearity analysis and geometric nonlinearity analysis are of researchers' interest. The linearity corresponds to the small or infinitesimal deformation theory, while the nonlinearity follows the theory of large or finite deformation. Linearity in polymers is the result of the displacements of the material particles assumed to be much smaller than any relevant dimension of the body. With this assumption, the geometry and the constitutive properties of the material such as density and stiffness at each point of space can be assumed to be unchanged by the deformation. This results in simplification of the Lagrangian and Eulerian strain equations. Although a lot of work has been done on large deformation analysis of polymers (see, for instance, (Drozdov, 1998), (Drozdov, 1992), (Drozdov, 2007) & (Drozdov, et al., 2003)), infinitesimal behaviour has limited applications in polymers (see (Cernocky, et al., 1980)).

### 2.1.3 Experimental considerations

The main reason for performing experiments is to determine material characteristics. Creep test involves recording the strain due to application of constant stress, while relaxation test yields the resultant stress when the material is subjected to constant strain. In some cases, shear stress or strain experiments are done. Observations which show that deformations in viscoelastic materials such as polymers are more related to changes of shape than changes of volume, suggest that shear tests may be

more valuable than the traditional uniaxial tests. The main material classifications which form the basis of mathematical modelling of polymers are as follows:

**Viscoelastic and viscoplastic materials:** The first level of material classification is determining if the material is described best by a viscoelastic or a viscoplastic model. A viscoelastic material shows a significant amount of delayed recovery upon unloading, whereas there remains a permanent residual ‘plastic’ strain for viscoplastic materials. Even though either model can be used to describe the time dependent “creep” of materials under uniaxial loading, viscoplastic models are generally used to describe high temperature creep of metals, while viscoelastic models are used to describe creep of ductile polymers (Krishnaswamy, et al., 1992).

**Linear and nonlinear materials:** By performing creep tests at several constant stress levels, a series of strain vs. time curves are obtained. A plot of the compliance " $X = \varepsilon(t)/\sigma$ " vs. time can be used to determine if the material response at various stresses is linear or nonlinear. If the compliance is independent of the stress, meaning that a single curve is obtained for the compliance under different levels of constant stress, then the material is said to be ‘linear’. Otherwise, the compliance is a function of stress, the material is known as ‘nonlinear’, and a nonlinear model must be used to represent its creep behaviour (Krishnaswamy, et al., 1992).

**Nonlinear materials-separable and non-separable:** Nonlinear materials can be categorized taking into account whether the effects of stress ( $\sigma$ ) and time ( $t$ ) on strain ( $\varepsilon$ ) are separable or not. If all compliance curves for nonlinear materials have the same ‘shape’, the material needs a nonlinear-separable model, i.e., same function for all stresses.  $\varepsilon$  is given by the following Eq. (7)

$$\varepsilon = h(\sigma)f(t) \quad (7)$$

Otherwise, if the shape of the compliance curves at all stress levels is not similar, then  $\varepsilon$  must be represented by a different function of time at each stress level. In this case, the material can only be described by a nonlinear non-separable model given by Eq. (8)

$$\varepsilon = g(\sigma, t) \quad (8)$$

### 2.1.3.1 Polymer material testing at the University of Waterloo

Polymer studies have been a major research area at the University of Waterloo. Material testing has included creep and tensile testing of a variety of polyethylene and polyfluoroethylene. Mechanical

testing was supplemented by detailed analysis of polymer micromolecular properties (Cheng, et al., 2008) (Sardashti, et al., 2012) and (Sardashti, et al., 2014). This section outlines the testing done and the rationale behind it.

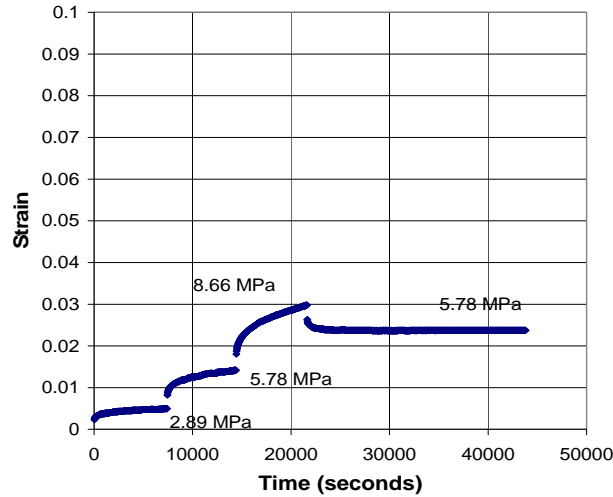


**Figure 7: Strain versus time tests (Liu, et al., 2008)**

Liu (Liu, 2007) and Liu et al. (Liu, et al., 2008) have done experiments on high density and medium density polyethylene (PE) materials. Testing was done on seven types of PEs and included short term tensile creep (3 and 24 hours), long-term creep (7 days and 14 days), creep with step loading, constant stress rate, constant strain rate, and complex load history tests. The specimens were produced from resins by melting them and machining, and from pipes by cutting out the samples. 24-hour creep testing was done at different stress levels to examine time dependent and nonlinear behaviour of the materials. The testing showed clear differences in the behaviour of different HDPEs; examples of the results of HDPE 24 hour creep curves for two different materials are shown in Figure 6. Based on the measured strain values under different stress levels and observing creep compliance  $D(t) = \varepsilon(t)/\sigma$  diagrams versus time (Liu, et al., 2008), it can be inferred that polyethylenes show high degree of material nonlinearity and time dependency. Comparing the compliance curves in terms of similarity reveals that they cannot be separated by two stress dependent and time dependent terms. This leads to the conclusion that the final constitutive equation of polyethylene is a non-linear-non-separable relationship.

The long term, step loading, complex stress and strain history, and tensile tests, were all conducted to provide experimental data for mathematical modelling of the behaviour of the materials. Some of



the creep tests were later used for parameter estimation, while others served for model verification. Tensile rate tests were conducted with the stress rate equal to 1.0, 0.1, 0.05, and 0.01 (MPa/s), and also with the constant strain rates of 0.05, 0.01 and 0.005 (/s). The step loading tests involved tests where a material first creeps for a period of time under a constant stress and then creeps for a period of time at another (increased or decreased) constant stress level. An example of a strain–time curve for stepped loading creep tests of HDPE-Pipe is shown in Figure 7. For increasing stress, progressive strain growth can be observed; for decreasing stress, strain reduction under sustained loading can be observed.

Behjat (Behjat, 2009) and Behjat et al. (Behjat, et al., 2014) performed further experiments on six different HDPEs obtained from various industrial sources and designed for a variety of applications. These PEs had a wide range of environmental stress crack resistance (ESCR) values, determined by prior microstructural analysis testing of the resins performed by Cheng (Cheng, 2008). Two blow-molding resins (PE1 and PE4) had low ESCR and unimodal narrow molecular weight distribution (MWD). These were compared to pipe resins (PE 7-10) with high ESCR and broad or bimodal MWD. The differences in the short and long-term behaviour of the two groups of resins provided meaningful information on the link between molecular structure and mechanical properties of PEs. The mechanical testing included short and long-term creep tests and strain rate controlled tests at 7 (mm/min) strain rate based on ASTM D638-03 standard recommendation.

ESCR in PE resins occurs through a slow crack growth mechanism under low applied stresses and long periods of time. This property is usually assessed by unreliable and time consuming testing methods, such as the notch constant load test (NCLT) on notched PE specimens in the presence of an aggressive fluid at elevated temperatures. Cheng et al. (Cheng, et al., 2008), (Cheng, et al., 2009) and (Cheng, et al., 2009)) performed tests on PE resins to determine their average molecular weights (MW), molecular weight distribution (MWD), short chain branching content, crystallinity, crystalline lamella thickness and area, ESCR by notch contact load test (NCLT) and hardening stiffness (HS) from short-term tensile strain hardening tests (i.e., the slope of the stress-strain curve during the strain hardening phase). They found that HS can be related to ESCR of PE. Following this, Behjat et al. (Behjat, et al., 2014) investigated the relationship of short term creep strain (8 hr at 10 MPa) and ESCR. In Figure 8 the hardening stiffness (HS) at a 7mm/min deformation rate is plotted against short-term creep strain at 10 MPa for all resins. The 8-hour strain (elastic plus creep strain) was chosen as an indicator of short term creep straining level. The graph indicates a relationship of increasing HS (and thus ESCR) with

an increase in short-term creep strain, meaning that short-term creep is inversely related to the long-term creep behaviour in environmental stress cracking.

Short chain branches (SCB) are well known to affect ESCR of PE (Cheng, 2008). A general trend of increasing SCB content is associated with an increase in creep strain. SCB interferes with the formation of crystalline lamellae, and hence, makes the PE more malleable.

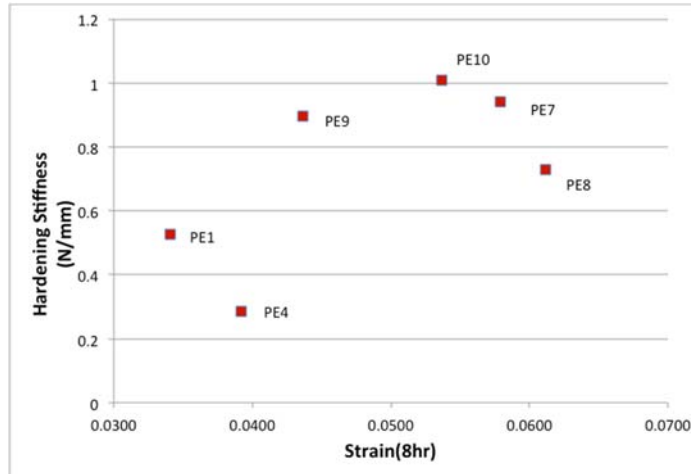


**Figure 8: Strain after 8 hours of creep test at 10 MPa versus hardening stiffness (Behjat, et al., 2014)**

The long-term mechanical behaviour of polyethylene (PE) is of great importance especially in cases where structural integrity is required. In order to predict characteristics of the mechanical behaviour of PE, it is necessary to fully understand the molecular structure of the employed resins. Sardashti et al. (Sardashti, et al., 2012) evaluated several micromolecular properties of PE. These properties influence an important performance indicator of PE for structural applications, namely, the environmental stress cracking resistance (ESCR). In (Sardashti, et al., 2012), relationships between molecular structure and material response characteristics, mainly between molecular weight properties and short chain branching content in relation to strain hardening behaviour of PE resins, were investigated based on results from tensile experiments.

Charbonneau (Charbonneau, 2011) and Charbonneau et al. (Charbonneau, et al., 2014) conducted tests on ethylene tetrafluoroethylene (ETFE) films. ETFE is used for producing films used in the construction industry for tensile cushions used for roofs and wall cladding, e.g, China's National Aquatics Centre, commonly known as the Water Cube, which hosted aquatic events during the 2008

summer Olympic Games was built using ETFE. The test program included a series of 24-hour uniaxial creep, 7-day creep, and stress-strain tests; all performed in the controlled temperature of 23C. Three film grades with varying thicknesses were tested. The 24 hour creep tests were done at stress levels of 2, 8, 12 and 14 MPa. All films were tested in both the longitudinal (the direction of extrusion) and transverse directions. A minimum of two independent replications were done on each film type, at each stress level and in each direction.

All of the films were tested at all stress levels in both the longitudinal and transverse directions of the material, and in nearly every case, more strain was observed in the transverse direction than the longitudinal direction. The stress-strain curves in Figure 9 show the same trend. The extrusion process by which ETFE film is created could be responsible for this anisotropic behaviour because it causes the molecules to be stretched in the direction of extrusion such that they are aligned in the longitudinal direction. It could also be due to the crystal structure of the molecule, i.e., the degree of crystallinity, the location of the crystalline regions and the orientation of the crystals, or to thermally activated relaxation processes that occur during film processing.

Same phenomenon is expected to happen in polyethylene material. The response of polyethylene material is not fully isotropic, due to the extrusion process or the non-uniform molding process. Also, due to the crystal structure of the molecule, i.e., the degree of crystallinity, the location of the crystalline regions and the orientation of the crystals, material response would not be same in different directions. one of the assumptions made through this research is that the material shows isotropic behavior, as in the practical applications of polyethylene, the applied stress is expected to be much smaller than the yield point. Therefore, it is assumed that at small stresses the material can be modelled as isotropic and the developed formulations and finite element procedure is applicable for isotropic analysis.

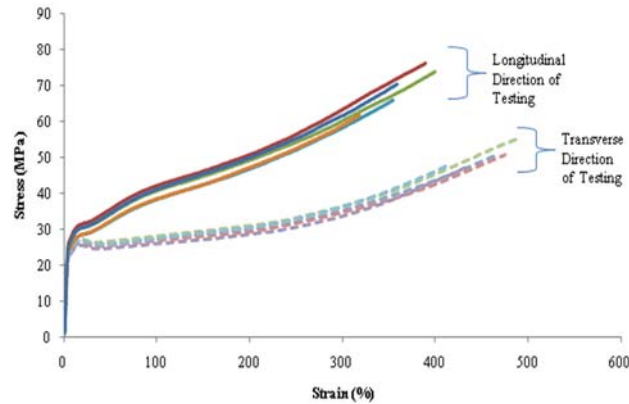


**Figure 9: Sample stress-strain curves for ETFE film tested in tension in both directions (Charbonneau, 2011)**

## 2.2 Constitutive modelling

Also known as anelasticity, viscoelasticity is the study of materials that exhibit both viscous and elastic characteristics when undergoing deformation. Viscous materials, like honey, resist shear flow and strain linearly with time when stress is applied. Elastic materials strain instantaneously when stretched and return to their original state once the stress is removed. Viscoelastic materials have elements of both of these properties and, as such, exhibit time-dependent strain. Whereas elasticity is usually the result of bond stretching along crystallographic planes in an ordered solid, viscoelasticity is the result of the diffusion of atoms or molecules inside of an amorphous material.

Another approach is based on viscoplasticity, which is a theory in continuum mechanics that describes the rate-dependent inelastic behaviour of solids. Rate-dependence in this context means that the deformation of the material depends on the rate at which loads are applied. The inelastic behaviour that is the subject of viscoplasticity is plastic deformation, which means that the material undergoes unrecoverable deformations when a load level is reached. Rate-dependent plasticity is important for transient plasticity calculations. The main difference between rate-independent plastic and viscoplastic material models is that the latter exhibit not only permanent deformations after the application of loads but continue to undergo a creep flow as a function of time under the influence of the applied load. The constitutive equations of these materials may be either linear or nonlinear.

The usefulness of a numerical model depends largely on three features (Zhang, et al., 1997): 1) physically, the constitutive model should be able to predict material response well for a wide range of

loading histories; 2) mathematically, the constitutive formulation should be simple and suitable for easy implementation in computer algorithms; and 3) the parameters in the model should be easily evaluated from experimental data.

In this section, different methods are discussed and constitutive models are developed which are useful for implementation in numerical procedures (e.g., finite elements).

### **2.2.1 Micro- and macro-scale modelling**

Two approaches are usually taken to develop constitutive models for polymeric materials. They are molecular and macroscopic in nature (Budiński, 1983). Micromechanical models emphasize the relation between the macroscopic properties of materials and their microstructure. The mechanical performance of polyethylene materials depends on loading and temperature conditions but also on phenomena occurring at the microscopic level (e.g., (G'Sell, et al., 1994), (Lin, et al., 1994), (Schrauwen, 2003) & (G'Sell, et al., 2002)). In recent years, there has been a considerable interest in developing reliable experimental and mathematical models to study polymeric materials at different scales. Understanding the nonlinear behaviour of semicrystalline polyethylene by relating microstructure with macroscopic performance under both small ( (Nikolov, et al., 2000), (Nikolov, et al., 2002)) and large ( (Lin, et al., 1994), (Cowking, et al., 1968)) deformations has been the focus of many studies.

Alvarado-Contreras et al., (Alvarado-Contreras, et al., 2007) and (Alvarado-Contreras, et al., 2008), proposed coupling a damage mechanics formulation for the crystalline phase and its amorphous counterpart in polyethylene. The study involved modelling degradation processes taking place in the microstructure due to loading effects. The mechanical properties were studied considering not only the original microstructure but also the particular mechanisms activated at various deformation steps. The microscopic deterioration was modeled considering an isotropic damage variable. The evolution of this variable was linked to the deformation evolution and the changes in tie-molecule density. This resulted in a damage-coupled model for semicrystalline polyethylene, which effectively incorporated the developed constitutive equations for the crystalline and amorphous phases.

For predicting mechanical response of polymers for structural analysis, the macroscopic approach is usually employed. Examples include the work of Zhang and Moore (Zhang, et al., 1997) and (Zhang, et al., 1997) and Drozdov et al. (Drozdov, et al., 1996), (Drozdov, 1995), (Drozdov, et al., 2006) and (Drozdov, 1998). The finite element programs developed for simulating viscoelastic or viscoplastic

analysis use formulations similar to those of the incremental theory of plasticity, in which the total strain rate is separable into elastic and inelastic components ( (Krishnaswamy, et al., 1990), (Zienkiewicz, 1977) and (Hughes, et al., 1978)).

In viscoelastic theory, constitutive equations are usually formulated using one of the differential or integral forms (Lockett, 1972). In contrast to the differential formulation (simulating the behaviour by spring and dash-pot element configurations) which involves only the current values of stress and strain and their current time rates, the integral form takes into account the history of loading and it is more accurate and strict in nonlinear modelling. The viscoplastic formulation is usually an extension of viscoelastic theory which considers permanent residual strain by assuming the rate of total strain as summation of elastic and plastic strain rates. These forms of the constitutive equation in linear viscoelasticity are described in the following sections.

### 2.2.2 Viscoelastic modelling

Two explanations can be offered for viscoelastic modelling. The first is defining the material response as a mixture of two simple cases: elastic and viscous. In the elastic behaviour, the material acts as a spring in which the length increases by a certain amount  $u$  or  $\varepsilon$ , in proportion to the applied load  $f$  or  $\sigma$ . When the force is removed, the spring returns to its original length. Assuming linear-elastic behaviour, Hooke's law,  $\sigma = E\varepsilon$ , is used to describe the stress-strain relation for the spring. In viscous behaviour, a piston cylinder (dash-pot) system is used to describe the time-dependent behaviour of viscous materials. In this case, the deformation rate is proportional to the applied force. Considering a linear relationship, the applied load is related to the rate of change of displacement by  $\sigma = \mu\dot{\varepsilon}$ . There are many possible spring and dash-pot configurations that describe viscoelastic material behaviour. *Maxwell Fluid* uses a spring and a dash-pot model in a series configuration and is suitable generally for viscoelastic fluid modelling. *Kelvin Solid* or *Voigt Solid* uses a spring and a dash-pot model in a parallel configuration and is suitable for modelling viscoelastic solid materials.

Direct use of spring and dash-pot elements and their combination in modelling of the material behaviour leads to the following constitutive equation and the method is referred as differential formulation,

$$P(D)\sigma(t) = Q(D)\varepsilon(t) \quad (9)$$

where the operators  $P$  and  $Q$  are polynomials in  $D$  such that  $D^n$  is interpreted as  $d^n/dt^n$ . Due to the complicated configurations of these two elements, one of the most useful methods to reach the final governing equation is Laplace Transformation. The second approach to the definition of linear viscoelastic behaviour is the hereditary integral form of the constitutive equations which takes into account the history of loading, described as:

$$\varepsilon(t) = \int_{-\infty}^t \psi(t - \tau) \dot{\sigma}(\tau) d\tau \quad (10)$$

$$\sigma(t) = \int_{-\infty}^t \phi(t - \tau) \dot{\varepsilon}(\tau) d\tau \quad (11)$$

where  $\phi(t)$  is known as the stress relaxation function for the material, and  $\psi(t)$  is known as the strain compliance function. They must be determined either by experiments or from the physics of the material structure. It is possible to consider the material to be linear at first and use the rule of linear superposition to calculate the strain produced by the common action of several loads (creep phase) or stress caused by the application of several strain constraints (relaxation phase). This is what makes this method special for non-linear modelling by means of linear superposition. The procedures for both creep and relaxation are the same. For any additional strain (stress), time is measured by a clock that starts at  $t = \tau$ . The total strain for  $t > \tau$  is (Flugge, 1967):

$$\varepsilon(t) = \int_{\tau=-\infty}^{\tau=+\infty} \psi(t - \tau) d\sigma(\tau) \quad (\text{creep phase}) \quad (12)$$

$$\sigma(t) = \int_{\tau=-\infty}^{\tau=+\infty} \phi(t - \tau) d\varepsilon(\tau) \quad (\text{relaxation phase}) \quad (13)$$

This form plays a significant role in linear and non-linear modelling of viscoelastic and viscoplastic materials. Either Eq. (12) or Eq. (13) can be used for defining the material response. Creep functions are easier to obtain from experiments. In the linear modelling case, the stress in the experiment is kept constant and the strain is recorded with time. For a constant applied stress, Eq. (12) becomes:

$$\varepsilon(t) = \sigma_c \psi(t) \quad (14)$$

The material modelling task is to find an approximation function  $\psi(t)$  that best fits test results. This is what one may get from the differential approach to viscoelasticity mentioned before in this section. In linear viscoelastic theory, Christensen (Christensen, 1971) introduced the concept of fading memory,

which states that the material response depends more on recent history than earlier events. Based on this, an assumption was made for the relaxation modulus and/or creep compliance:

$$A(t) = A_{\infty} - \sum_{i=1}^N A_i e^{-t/\tau_i} \quad (15)$$

In order to find the unknown parameters involved in A (assumed  $\psi$  and/or  $\phi$ ), the Prony series approximation is used. Based on what Christensen (Christensen, 1971) stated as fading memory, the best alternative for the Prony series is a multi-Kelvin approach model, since it considers the instantaneous elastic strain,  $\varepsilon^e$ , and consequently the instantaneous elastic modulus,  $E_0$  (or elastic compliance,  $\psi_0$ ). The strain growth rate decreases with time and it becomes constant at a certain time. Therefore, the linear viscoelastic material behaviour under constant stress can be described as Eq. (14), in which (Liu, et al., 2008):

$$\psi(t) = \psi_e + \psi_v(t) = \psi_0 + \sum_{i=1}^N \psi_i \left\{ 1 - \exp\left(-\frac{t}{\tau_i}\right) \right\} \quad (16)$$

Or, similarly, for constant strain by substituting  $\psi$  by  $\phi$  in which  $\psi_0 = 1/E_0$  or  $\phi_0 = E_0 = 1/\psi_0$ . Material constants are  $E_0$  and  $A_i$  (having same units as stress) with corresponding relaxation times  $\tau_i$ . One can obtain parameter values by fitting the material response (Eq. (16)) to experimental data.

### 2.2.3 Viscoplastic modelling

The plasticity in semicrystalline polymers like polyethylene starts to develop at small strain and the material behaves with both viscoelastic and viscoplastic characteristics. Yield (the development of permanent deformation) occurs gradually with a steady transition from linear to nonlinear response. Thus, it is difficult to identify exactly where yielding commences. For this reason, classical plastic potential theory (Zienkiewicz, 1977), (Bodner, et al., 1972) and (Bodner, et al., 1975) which employs a yield surface is unsuitable for characterizing rate effects. Instead, unified theories, (Bodner, 1984), (Liu, et al., 1979), (Bodner, et al., 1972) and (Bodner, et al., 1975), which do not separate creep strains and plastic strains and which consider inelastic deformation to be rate dependent, are a better alternative.

Based on a yield criterion, the total strain rate is considered to be decomposable into elastic and inelastic components:



$$\dot{\varepsilon}_{ij} = \dot{\varepsilon}_{ij}^e + \dot{\varepsilon}_{ij}^p \quad (17)$$

Based on what Krishnaswamy et al. (Krishnaswamy, et al., 1992) have suggested, a power law function can describe the linear viscoplastic creep behaviour. This function is able to model the growing deformation (strain) at decreasing rate, which doesn't approach an asymptotic value and the material remains time-dependent. In this model the compliance is expressed as a power law function (Liu, et al., 2008)

$$\psi(t) = \psi_e + \psi_v(t) = \frac{1}{E_0} + C_0 t^{C_1} \quad (18)$$

where  $\psi_e$  is the instantaneous elastic component,  $\psi_v(t)$  the time-dependent component, and  $E_0$  (same unit as stress),  $C_0$  (same unit as compliance) and  $C_1$  (no unit) are material constants. Similar to viscoelastic modelling, the formulation constants are obtained by least squares. Substituting Eq. (18) into Eq. (14), results in the final constitutive equation for linear viscoplasticity:

$$\varepsilon(t) = \frac{\sigma_n}{E_0} + \sigma_n C_0 t^{C_1} \quad (19)$$

### 2.3 Parameter estimation for linear modelling

Any configuration of spring and dash-pot obeys the following differential formula:

$$\sigma + p_1 \dot{\sigma} + p_2 \ddot{\sigma} + \dots = q_0 \varepsilon + q_1 \dot{\varepsilon} + q_2 \ddot{\varepsilon} + \dots \quad (20)$$

and the material properties are represented by an expression consisting of multiplication of a constant and a time-dependent term. In the development of linear viscoelasticity models, it is necessary to perform stress-strain experiments involving time as an independent variable. Thereafter, the experimental results are represented by a constitutive equation obtained by means of theoretical approaches. The relation is fitted to data and an error function has to be minimized.

The other way to construct constitutive equations is approximating a creep compliance or a relaxation modulus using an appropriate function. The function, then, is fitted to experimental data, and unknown parameters associated with the material response are obtained. Researchers use different methods of minimization along with approximation functions. One of the most common functions is called Prony's series, which uses an exponential basis function. The Prony series is the most used mathematical curve to represent viscoelastic materials properties, which many researches have proved to be a representative

and computationally efficient function for such materials. However, the procedure to obtain the Prony series unknown constants from experimental data is not trivial, involving many numerical tasks. Another notable point regarding this method is the complexity of viscoelastic time functions related to material properties, which involves complex mathematical relations that are easy to overcome using Prony's series.

**Prony series method:** Since the material properties are independent of the testing procedure, Eq. (12)~ Eq. (14) uniquely define the material response. Creep functions are easier to obtain from experiments. The material modelling task is to find an approximation function  $\psi(t)$  and/or  $\varphi(t)$  that best fits test results (see Eq. (15)).

The equation representing the viscoelastic material is obtained by a mechanical model consisting of linear springs and dashpots (as discussed in previous sections). The alternative representation of the relation can be of the form of Eq. (16), which can be rewritten as:

$$A(t) = A_0 + \sum_{i=1}^N A_i (1 - \exp(-t/\tau_i)) \quad (21)$$

where  $A_0 = A_\infty + \sum_{i=1}^N A_i$ . The terms  $A_\infty$  and  $A_0$  are called independent terms. The exponential terms  $\tau_i$  are known as time constants because they appear in association with the time variable  $t$ . The set of terms  $A_i$  are the dependent terms of the Prony series and the number of terms  $N$  is determined according to the experimental data. Usually, one must use around 8 to 15 terms in the Prony series in order to have a satisfactory mathematical model based on experimental data.

The objective is to determine the constants  $A_i$  and  $\tau_i$  from measured values of  $A(t)$  at fixed moments in time. The problem is particularly difficult in that the  $\tau_i$  appear non-linearly in the expression. Further the appropriate number  $N$  is also unknown. Collocation or least squares approaches are used for obtaining the unknown constants of Prony's series approximation function.

**Prony-collocation method:** let's say  $f(t) = A(t)$ . We suppose that experimental values of  $f(t)$  are specified on a set of  $N$  equally spaced points. Therefore from experimental results we have the values for  $f(0)$ ,  $f(\Delta t)$ ,  $f(2\Delta t)$ , ... . For simplicity we set  $f_k = f(k\Delta t)$ .

In Prony's method we will first find  $\alpha_i = \exp(-\Delta t/\tau_i)$  (from which  $\tau_i = -\Delta t/\ln(\alpha_i)$ ) and then we will find  $A_i$ , which are positive values. The procedure is to first note that

$$f_k = f(k\Delta t) = \sum A_i \alpha_i^k \quad (k = 0, 1, 2, \dots) \quad (22)$$

which is particular for Eq. (15), and that the  $\alpha_j$  can be considered the roots of the polynomial

$$p(\alpha) = \prod_{i=1}^N (\alpha - \alpha_i) = \alpha^N + c_{N-1}\alpha^{N-1} + \dots + c_0 \quad (23)$$

With these relations one can observe that

$$\begin{aligned} f_0 c_0 + f_1 c_1 + \dots + f_{N-1} c_{N-1} + f_N &= 0 \\ f_1 c_0 + f_2 c_1 + \dots + f_N c_{N-1} + f_{N+1} &= 0 \\ \dots & \\ f_k c_0 + f_{k+1} c_1 + \dots + f_{k+N-1} c_{N-1} + f_{k+N} &= 0 \end{aligned} \quad (24)$$

The first of these follows easily by expansion and noting that each  $\alpha_j$  is a root of  $p(\alpha) = 0$ ; the second follows by introducing  $\bar{A}_i = A_i \alpha_i$ , expanding, and using the root property again; the third follows by a similar procedure. Rewriting in matrix vector form, we have:

$$\left[ \begin{pmatrix} f_0 & f_1 & \dots & f_{N-1} \\ f_1 & f_2 & & f_N \\ \vdots & \vdots & \ddots & \vdots \\ f_{N-1} & f_N & \dots & f_{2N-2} \end{pmatrix} \right] \begin{pmatrix} c_0 \\ c_1 \\ \vdots \\ c_{N-1} \end{pmatrix} = - \begin{pmatrix} f_N \\ f_{N+1} \\ \vdots \\ f_{2N-1} \end{pmatrix} \quad (25)$$

With these equations we have a set of linear equations that we can solve for  $c_i$ . One can use only the number of equations needed to uniquely determine  $c_i$  (as shown) or one can use more equations and over-determine the system – thus leading to a least squares solution. Once the  $c_i$  are known, the roots  $\alpha_j$  of  $p(\alpha) = 0$  can be determined. Once these are known one can solve the system

$$\left[ \begin{pmatrix} 1 & 1 & \dots & 1 \\ \alpha_1^1 & \alpha_2^1 & & \alpha_N^1 \\ \vdots & \vdots & \ddots & \vdots \\ \alpha_1^{N-1} & \alpha_2^{N-1} & \dots & \alpha_N^{N-1} \end{pmatrix} \right] \begin{pmatrix} A_1 \\ A_2 \\ \vdots \\ A_N \end{pmatrix} = - \begin{pmatrix} f_0 \\ f_1 \\ \vdots \\ f_{N-1} \end{pmatrix} \quad (26)$$

for the  $A_i$ . These relations are the first  $N$  equations from Eq. (24). Note that in this procedure one needs to select  $N$  ahead of time.

**Prony-least squares method:** A linear least squares fitting is used by assuming values for the relaxation times  $\tau_j$  in Eqs. (15) & (21). We define the squared error as

$$F(t_j) = \sum_{i=1}^p (f(t_i) - \bar{f}(t_i))^2 \quad (27)$$

where  $p$  is the number of data (measurements),  $\bar{f}(t_i)$  is a data measurement at time  $t_i$ , and  $f(t_i)$  is the corresponding theoretical value (Eqs. (15) & (21)). By setting  $dF/dt_j = 0$  for  $j = 1 \dots N$  ( $N$  is the number of terms in Prony series), to minimize  $F(t_j)$ , a set of linear simultaneous equations with respect to the material parameters  $t_j$  is obtained.

$$[T]_{N \times N} \{A\}_{N \times 1} = \{B\}_{N \times 1} \quad (28)$$

where for Eq. (15)

$$T_{ij} = \sum_{k=1}^p (e^{-t_k/\tau_i})(e^{-t_k/\tau_j}) \quad (29)$$

$$B_i = \sum_{k=1}^p (\bar{f}(t_k) - A_\infty)(e^{-t_k/\tau_j})$$

and for Eq. (21)

$$T_{ij} = \sum_{k=1}^p (1 - e^{-t_k/\tau_i})(1 - e^{-t_k/\tau_j}) \quad (30)$$

$$B_i = \sum_{k=1}^p (\bar{f}(t_k) - A_0)(1 - e^{-t_k/\tau_j})$$

For this approach, see (Liu, et al., 2008) and (Cheng, et al., 2011).

## 2.4 Nonlinear modelling

This section deals with nonlinear constitutive relations for polymers. Polyethylene is time dependent with a high degree of nonlinearity.

In the linear approach, the compliance is a function of time which means that for a constant applied stress a resultant strain is obtained and the constitutive equation has a separable nature of Eq. (7). In the other hand, the nonlinear constitutive equation obeys the non-separable format of Eq. (8).

There are generally two methods of nonlinearization of model parameters. The classic method of nonlinearization and the optimized method of nonlinearization. In the former one, which has been used by Liu (Liu, 2007), model parameters (usually compliances and relaxation times) are obtained in several stress levels. Then model parameters for unexamined stress levels, let's say stress  $\sigma_a$  in which  $\sigma_n < \sigma_a < \sigma_m$ , are obtained by interpolating model parameters for two other stress levels  $\sigma_n$ , and  $\sigma_m$ .

In optimized method of nonlinearization, model parameters (usually compliances and relaxation times) are approximated by functions of stress. Obviously this method is much more accurate and more reliable than the classic method (presented by Liu), and is more complex and time consuming. In the following sections these methods are presented in detail.

#### 2.4.1 Classic method of nonlinearization by Liu (Liu, 2007)

Liu et al. (Liu, et al., 2008) obtained a separate set of material parameters for each stress level. The sets of constants for all creep tests created an array of material constants. The material parameters for stresses other than the tested stresses were obtained by linear interpolation. Thus, piece-wise linear functions were assumed for the material functions. The expressions for the linear interpolation of material parameters for non-linear viscoelastic modelling were the following:

$$\begin{aligned} E_0(\sigma) &= E_0(\sigma_m) + \frac{\sigma - \sigma_m}{\sigma_n - \sigma_m} [E_0(\sigma_n) - E_0(\sigma_m)] \\ \psi_i(\sigma) &= \psi_i(\sigma_m) + \frac{\sigma - \sigma_m}{\sigma_n - \sigma_m} [\psi_i(\sigma_n) - \psi_i(\sigma_m)] \end{aligned} \quad (31)$$

where  $\sigma_m$  and  $\sigma_n$  are stresses used for model development by considering  $\sigma_m < \sigma < \sigma_n$ . Similarly, for non-linear viscoplastic modelling:

$$\begin{aligned} C_0(\sigma) &= C_0(\sigma_m) + \frac{\sigma - \sigma_m}{\sigma_n - \sigma_m} [C_0(\sigma_n) - C_0(\sigma_m)] \\ C_1(\sigma) &= C_1(\sigma_m) + \frac{\sigma - \sigma_m}{\sigma_n - \sigma_m} [C_1(\sigma_n) - C_1(\sigma_m)] \end{aligned} \quad (32)$$

and the interpolation of the instantaneous elastic parameter,  $E_0(\sigma)$ , is the same as in the viscoelastic case, Eq. (31). The presented two-step curve-fitting approach works well at a given stress for a material for which the model is developed. However, since each polyethylene behaves differently under a creep test, the model compliance-stress relationship should theoretically be redefined for each specific

material. This means that for each specific material new compliance functions of stress representing material parameters should be created.

#### 2.4.2 Optimized method of nonlinearization (present research)

In our recent published work (Sepiani, et al., 2017), continuous functions for the ‘nonlinearizations’ of model parameters for the case of viscoelasticity were proposed. The process of developing a non-linear model starts with a linear model for the material under constant stress (separable form) and then it is extended to the nonlinear one by considering effects of stress on the stress dependent part (non-separable form). Thus, the following stress-strain relationship is defined for predicting the response of the material under constant applied stress:

$$\varepsilon(t) = \sigma X(t) \quad (33)$$

In this formulation,  $X(t)$  describes the creep compliance of the material and is based on the spring and dash-pot method of modelling described previously. According to the concept of fading memory, the material response depends more on recent history than on earlier events. Accordingly, this theory considers the following formulation for creep compliance:

$$X(t) = X_0 + \sum_{i=1}^N X_i (1 - e^{-t/\tau_i}) \quad (34)$$

where  $X_0$  is the elastic time-independent compliance at time  $t_0 = 0$ , and  $X_i$  and  $\tau_i$  are creep compliance and relaxation time, respectively, for the  $i^{th}$  Kelvin element.  $N$  indicates the number of Kelvin elements in the model.

Most finite element implementations of this form assume that the creep compliance and relaxation modulus have the exponential form of Eq. (34), which is a form of a Prony series approximation, with  $2 \times N$  unknown material properties ( $X_i$  and  $\tau_i$ ). The term  $X_0 = 1/E_0$  is called an independent term. One can obtain parameter values by means of least squares estimation by fitting the Prony series to experimental data by fixing a set of  $\tau_i$  or by pre-setting  $X_i$  and  $\tau_i$  as power law functions of  $t$ .

$X_i$  and  $\tau_i$  can be expressed as power-law functions of stress. To reduce the number of material functions, which is equal to  $2 \times N$ , all values of  $X_i$  and  $\tau_i$  are obtained using four parameters  $X_1$ ,  $\tau_1$ ,  $m$  and  $\alpha$  following the formulation presented by Zhang and Moore (Zhang, et al., 1997).

$$X_i = m^{1-i} \times X_1, \quad \tau_i = \alpha^{i-1} \times \tau_1 \quad (35)$$

$m$  and  $\alpha$  have no units of measurement. The determination of the material functions proceeds in two steps. In the first step, and for a particular creep stress, Eqs. (33)~(35) are used to fit the corresponding experimental creep curve and find the specific unknown parameters by means of least squares (linear modelling). Then, in the second step, curve fitting is used to produce stress-dependent parameters  $X_1(\sigma_n)$  and  $\tau_1(\sigma_n)$  based on the values from linear modelling. This is referred to as ‘nonlinearizing the constants’ by assuming that they are functions of stress and obey the non-separable form of the kinematic relation (Krishnaswamy, et al., 1992).

For simplicity, constants  $m$  and  $\alpha$  are considered to be stress-independent (Zhang, et al., 1997). In recent unpublished work of ours, the curve fitting of the two parameters  $X_1$  and  $\tau_1$  showed that the parameter distributions versus applied stress  $\sigma_n$  obeyed the following:

$$\begin{aligned} X_1^{-1} &= b_0 + b_1 \exp(b_2 - b_3 \sigma_n - b_4 / \sigma_n) \\ \tau_1 &= c_0 \exp(-c_1 + c_2 \sigma_n + c_3 \sigma_n^2 - c_4 \sigma_n^3) \end{aligned} \quad (36)$$

where  $X_0$  is a constant that is obtained from experimental results for each test and it is assumed to vary with respect to stress. The constants  $b_i$ ,  $c_i$ ,  $m$  and  $\alpha$  are obtained via least squares for each examined material. It can be seen that  $X_0$  is approximately constant for all stress levels, and the variation versus stress is trivial and therefore negligible. These material properties are used to plot the response of HDPE resin versus experiments in Figure 10.  $b_0$  and  $b_1$  have stress unit,  $b_2$  has no unit,  $b_3$  has inverse unit of stress and  $b_4$  has unit of stress.  $c_0$  has unit of time,  $c_1$  has no unit,  $c_2$  has unit of inverse of stress,  $c_3$  has unit of inverse of squared stress, and  $c_4$  has unit of inverse of cubic stress.

The nonlinearization for viscoelasticity starts with the assumption that the plastic flow starts to develop when there is a small strain and the material behaves in both viscoelastic and viscoplastic fashion. Since yield occurs gradually with a steady transition from a linear to a nonlinear response, unified theories, which do not separate creep strains and plastic strains, are a better alternative than those that consider creep and plasticity as separate phenomena (Zhang, et al., 1997). Here is the non-separable viscoplastic model that has been discussed in this chapter:

$$\varepsilon = \varepsilon^e + \varepsilon^v = \frac{\sigma}{E_0} + \sigma C_0 \left(\frac{t}{T}\right)^{C_1} \quad (37)$$

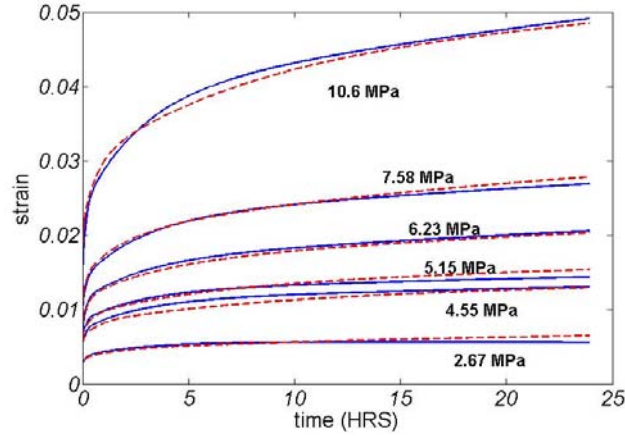


**Figure 10: Experimental (continuous line) (Liu, 2007), and non-linear viscoelastic model (dashed line) results for 24-hour creep tests for an HDPE resin**

Here,  $C_0$  has unit of inverse of stress,  $T$  has time unit and  $C_1$  has no unit. Similar to viscoelastic modelling, the determination of the material constants proceeds in two steps. In the first step, for a particular constant creep stress, Eq. (37) is used to fit the corresponding experimental creep curve and determine the unknown parameters (linear modelling). Then, in the second step, ‘nonlinearizing’ curve fitting is used to find the distribution of parameters,  $C_0(\sigma)$  and  $C_1(\sigma)$  with respect to stress.  $E_0$  is also obtained from the experimental data at each stress level.



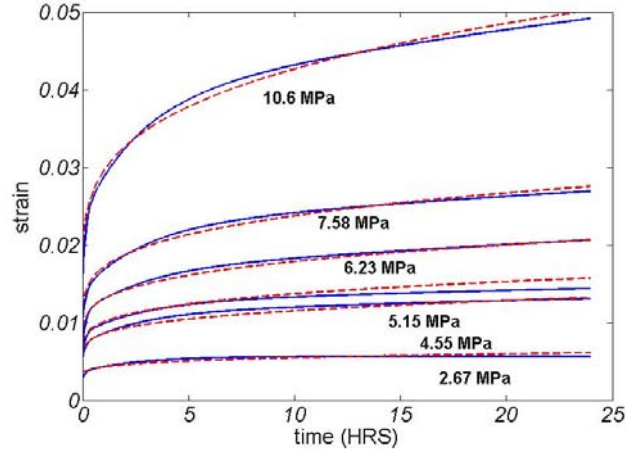


**Figure 11: Experimental (continuous line) (Liu, 2007), and non-linear viscoplastic model (dashed line) results for 24-hour creep tests for an HDPE resin**

The first step leads to the material constants, and corresponding plots of model and experiments are shown in Figure 11 for HDPE resin. Based on the variation of the constants versus stress, the following equations can be fitted:

$$\begin{aligned}
 C_0 &= (b_1 + b_2 \hat{\sigma} + b_3 \hat{\sigma}^2) \left( \frac{\sigma_n}{\bar{\sigma}} \right)^{(b_4 + b_5 \hat{\sigma} + b_6 \hat{\sigma}^2)} \\
 C_1 &= m_1 + m_2 \left( 1 + \frac{1}{2} \arctan \left( \frac{\hat{\sigma} - s_a}{\bar{\sigma}} \right) \right) \\
 T &= T_1 \left( \frac{\sigma_n}{\bar{\sigma}} \right)^{d_0}
 \end{aligned} \tag{38}$$

$\bar{\sigma}$  is introduced for dimensional consistency (in this research we have  $\bar{\sigma} = 1 \text{ MPa}$ ). Here,  $b_1$  has unit of compliance (inverse of stress),  $b_2$  has unit of inverse of squared stress and  $b_3$  has unit of inverse of cubic stress.  $b_4$  has no unit,  $b_5$  has unit of inverse of stress and  $b_6$  has unit of inverse of squared stress.  $m_1$ ,  $m_2$  and  $d_0$  have no units. Unit of  $s_a$  is same as stress and  $T_1$  is time.

## 2.5 Extending the material parameters to longer times frames

In order to realistically model the service life-time for polymeric structures, long-term prediction methods are needed within the developed constitutive law. The constitutive laws are normally formulated based on available short-term tests. One of the most popular methods for predicting long

term properties of polymers is ‘time temperature superposition’, which is based on short term behaviour and uses the information from short duration tests. The method uses the similarity between the variation of relaxation modulus (creep compliance) with time and temperature. The variation of time and temperature of the moduli (compliances) of a polymer is often said to be related or even equivalent (Barbero, 2011) & (Luo, et al., 2012). There are also several test methods for evaluating long-term properties of materials, including creep test ASTM-D2990, stress relaxation test D2991, hydrostatic test D1598, D2837, and DMA (Dynamic Mechanical Analysis).

A nonlinear approach has been proposed by recent work of ours and an overview is given in the following section.

### 2.5.1 Using short term testing for predictions at longer time frames

The important point of constructing a mathematical model is predicting the response of creep behaviour over extended operating time. Using the material properties and modelling constants, as described in section 4, resulted in good agreement during the test time interval which was 24 hours (creep test time, Figure 10 and Figure 11). To examine the validity of the model for extended times, the method proposed herein is to observe the trend of material constants with respect to test time. First, the curve fitting is done for all materials in different test times, namely: 10, 14, 18, 20, 22 and 24 hours. This allows one to observe how the modelling constants are dependent on test time ( $\lambda$ ). It is proposed that the material parameter change over test time can be represented by the following equations for the viscoelastic case:

$$\begin{aligned}
 b_i(\lambda) &= b'_i (\lambda/\lambda')^{d_i} \quad \text{for } i = 0, 1, 2 \\
 b_i(\lambda) &= b'_i / (\lambda/\lambda')^{d_i} \quad \text{for } i = 3, 4 \\
 c_0(\lambda) &= c'_0 (\lambda/\lambda')^{d_5}
 \end{aligned} \tag{39}$$

$\lambda$  stands for test time and  $\lambda'$  is introduced for dimensional consistency (in this research we have  $\lambda' = 1 \text{ hour}$ ).  $c'_0$ ,  $b'_i$  and  $d_i$  are constants independent of the test time used to develop the model. Here,  $b'_i$  and  $c'_0$  have same units as  $b_i$  and  $c_0$ , respectively and  $d_i$  have no units.

Similarly, when the same method is applied to viscoplastic modelling, the following equations for the dependency of constants on  $\lambda$  are obtained:

$$b_i(\lambda) = b'_i (\lambda/\lambda')^{d_i} \quad \text{for } i = 0 \sim 6 \tag{40}$$

$$m_j(\lambda) = m'_j (\lambda/\lambda')^{n_j} \quad \text{for } i = 1, 2$$

$$s_a(\lambda) = s'_a (\lambda/\lambda')^a$$

$$T_1(\lambda) = T'_1 (\lambda/\lambda')^{T_2}$$

Here,  $b'_i$ ,  $m'_j$ ,  $s'_a$  and  $T'_1$  have same units as  $b_i$ ,  $m_j$ ,  $s_a$  and  $T_1$ , respectively and  $s$ ,  $d_i$ ,  $n_j$ , and  $T_2$  have no units.

### 2.5.2 Viscoelastic (NVE) and viscoplastic (NVP) long term responses

The parameter identification procedure is based on a minimization of the total error between experimental data and model predictions. The models have been developed using the data from 24 hour creep testing (using 10, 12, 14... hour time frames). Then the model was verified using experimental data for long-term creep of polyethylene (Liu, et al., 2008). The model showed the ability to predict well the independent data from long-term testing; it sufficiently describes the variation of strain in time for the loading history. The long-term scheme was validated by tests on PIPE material and other HDPE resins. Creep tests were conducted under three different stress levels of 4.42 MPa, 6.08 MPa and 8.15 MPa over 40 hours (Liu, et al., 2008). In addition, creep strain measurements on a pipe material were conducted under 6.89 MPa in a seven-day test (Liu, et al., 2008).

Both NVE and NVP models have been applied to the experimental data. According to the definition, the parameter  $\lambda$  is set to be 40 and 168 for case I and case II, respectively. The theoretical results are depicted in Figure 12~Figure 15 and compared with experimental ones.

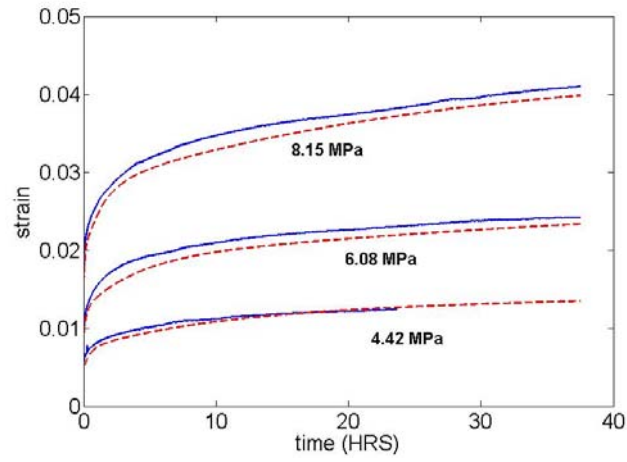


**Figure 12: Experimental (continuous line) (Liu, 2007), and present NVE model prediction (dashed line) in 40 hours test time (pipe material)**

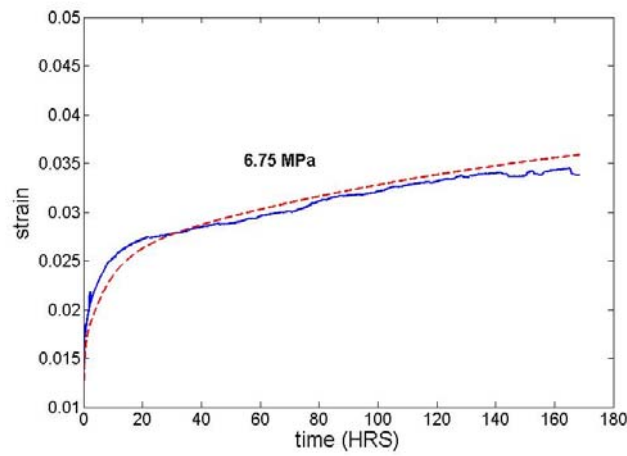


**Figure 13: Experimental (continuous line) (Liu, 2007), and present NVE model prediction (dashed line) in 7 days test time (pipe material)**

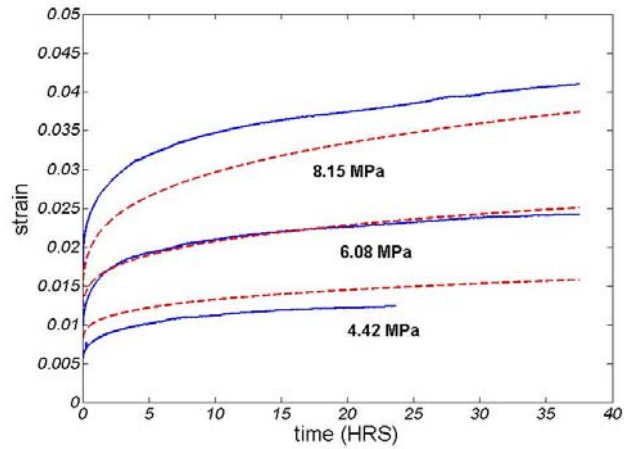


**Figure 14: Experimental (continuous line) (Liu, 2007), and present NVP model prediction (dashed line) in 40 hours test time (pipe material)**

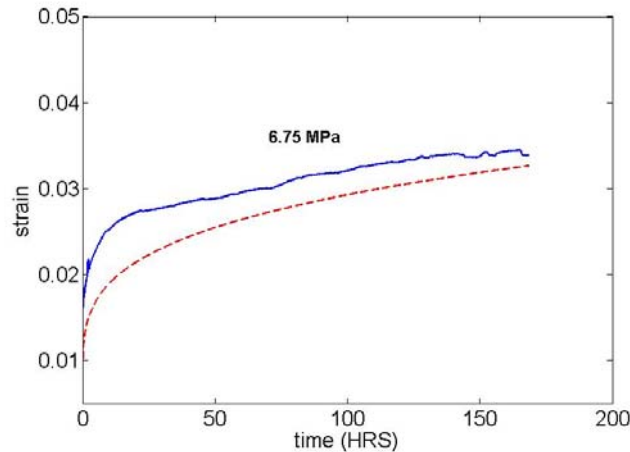


**Figure 15: Experimental (continuous line) (Liu, 2007), and present NVP model prediction (dashed line) in 7 days test time (pipe material)**

Looking at Figure 12 to Figure 15, it can visually be inferred that the NVE model results in smaller fitting error for the long-term strain response prediction compared to the NVP model. The NVE model seems more capable in modelling polymer behaviour in extended time. The most important reason for this is that the NVP model has only two parameters to adjust during fitting, while NVE has more, resulting in more accurate curve fitting. The other difference is that based on the nature of the governing

equation for each model, viscoplastic materials tend to extend under continuing applied load, while viscoelastic strain reaches an upper limit after a while.

## 2.6 Modelling the response under varying stress

The modified superposition principle (Findley 1967) employs the assumption that the strain response after any abrupt change of stress is the sum of the strain due to the first loading and the strain response due to each change of stress. This approach makes use of the equations from the multiple functions for constant stress (linear models) to describe the nonlinear yet synergistic characteristics of creep behaviour. In this method, the modification of the superposition principle consists of relaxing the requirement of linearity in stress and treating nonlinearity as discussed in this section.

### 2.6.1 Modified superposition principle (MSP)

The stress-strain equation for viscoelastic and viscoplastic materials consists of time-independent and time-dependent parts:

$$\varepsilon = \varepsilon^e + \varepsilon^v = f^e(\sigma) + f^v(\sigma, t) \quad (41)$$

where  $f^e(\sigma)$  denotes the elastic strain  $\varepsilon^e$ , and  $f^v(\sigma, t)$  denotes the time dependent strain  $\varepsilon^v$ , caused by applied constant stress.

The superposition method can be described as follows. When the state of stress is abruptly changed from  $\sigma_1$  to  $\sigma_2$  at time  $t_1$ , the creep behaviour can be considered as if, at this instant, stresses  $\sigma_1$  are removed and at the same time stresses  $\sigma_2$  are applied to the specimen, both being considered as independent actions. The recovery strain  $\varepsilon'$  resulting from removal of  $\sigma_1$  after loading time  $t_1$  is given by:

$$\begin{aligned} \varepsilon' &= f^e(\sigma_1) - f^e(\sigma_1) + f^v(\sigma_1, t) - f^v(\sigma_1, (t - t_1)) \\ \varepsilon' &= f^v(\sigma_1, t) - f^v(\sigma_1, (t - t_1)) \end{aligned} \quad (42)$$

The creep behaviour due to  $\sigma_2$  applied at  $t_1$ , denoted by  $\varepsilon''$ , is

$$\varepsilon'' = f^e(\sigma_2) + f^v(\sigma_2, (t - t_1)) \quad (43)$$

The total strain is the sum of  $\varepsilon'$  and  $\varepsilon''$  and equal to

$$\varepsilon = f^v(\sigma_1, t) - f^v(\sigma_1, (t - t_1)) + f^e(\sigma_2) + f^v(\sigma_2, (t - t_1)) \quad (44)$$

In this theory, the time-independent part of the strain response depends only on the final state of stress applied to the specimen. The time-independent part of the strain on loading and unloading follows the same path. Thus, when the stress state changes from  $\sigma_1$  to  $\sigma_n$ , the total strain response after the  $n^{th}$  stress change will be as follows:

$$\varepsilon = f^e(\sigma_n) + \sum_{p=1}^n \left[ f^v(\sigma_p, (t - t_{p-1})) - f^v(\sigma_{p-1}, (t - t_{p-1})) \right] \quad (45)$$

For example, consider a  $2N + 1$ -parameter ( $N$  Kelvin units) spring and dash-pot model. The stress-strain relationship under constant stress for the  $k^{th}$  step is as follows:

$$\begin{aligned} \varepsilon(t) &= f^e(\sigma_i) + f^v(\sigma_i, t) \\ \Rightarrow \varepsilon_k(t) &= X_{0,k}(\sigma, \lambda) \sigma_k \\ &+ \sum_{j=1}^k \left\{ \sum_{i=1}^N X_{i,j}(\sigma, \lambda) \left[ 1 - \exp\left(-\frac{t_k - t_{j-1}}{\tau_i(\sigma, \lambda)}\right) \right] \sigma_j \right. \\ &\left. - \sum_{i=1}^N X_{i,j-1}(\sigma, \lambda) \left[ 1 - \exp\left(-\frac{t_k - t_{j-1}}{\tau_i(\sigma, \lambda)}\right) \right] \sigma_{j-1} \right\} \end{aligned} \quad (46)$$

If the stress state changes from  $\sigma_1$  to  $\sigma_2$ , the total strain response for each step is:

$$0 \leq t < t_1 \quad \varepsilon_1(t) = X_{0,1} \sigma_1 + \sum_{i=1}^N X_{i,1} \left[ 1 - \exp\left(-\frac{t_1 - t_0}{\tau_i}\right) \right] \sigma_1 \quad (47)$$

$$\begin{aligned} \varepsilon_2(t) &= X_{0,2} \sigma_2 + \left\{ \sum_{i=1}^N X_{i,1} \left[ 1 - \exp\left(-\frac{t_2 - t_0}{\tau_i}\right) \right] \sigma_1 \right\} \\ t_1 \leq t < \infty &+ \left\{ \sum_{i=1}^N X_{i,2} \left[ 1 - \exp\left(-\frac{t_2 - t_1}{\tau_i}\right) \right] \sigma_2 \right. \\ &\left. - \sum_{i=1}^N X_{i,1} \left[ 1 - \exp\left(-\frac{t_2 - t_1}{\tau_i}\right) \right] \sigma_1 \right\} \end{aligned} \quad (48)$$

The theoretical and experimental results for a high density PE resin (HDPE) subjected to various load histories are compared and discussed next. The material was tested subject to multi-stress levels by (Liu, 2007).

Figure 16 shows three steps change in applied stress. The resin was tested under 2.9 MPa, 5.8 MPa and 8.7 MPa stresses which lasted 2 hours each. Very good correlation can be seen between two data sets. In Figure 17, the material was tested under five different time step loadings starting from smaller stress values. 1.46 MPa, 2.92 MPa, 4.38 MPa, 5.84 MPa and 7.30 MPa stresses were applied.

MSP can also be applied on viscoplastic formulations. The corresponding relation is:

$$\varepsilon_k = X_{0,\sigma_k} \sigma_k + \sum_{j=1}^k \left\{ \left[ C_{0,\sigma_j} \times (t_k - t_{j-1})^{C_{1,\sigma_j}} \right] \sigma_j - \left[ C_{0,\sigma_{j-1}} \times (t_k - t_{j-1})^{C_{1,\sigma_{j-1}}} \right] \sigma_{j-1} \right\} \quad (49)$$

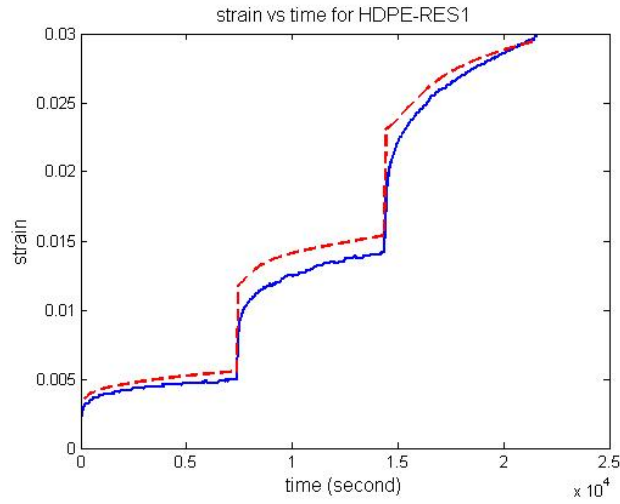


**Figure 16: Strain vs time for HDPE resin. Stress level 1 = 2.90 MPa, stress level 2 = 5.80 MPa, stress level 3 = 8.70 MPa, (blue continuous line: experimental data (Liu, 2007), red dashed line: present model)**



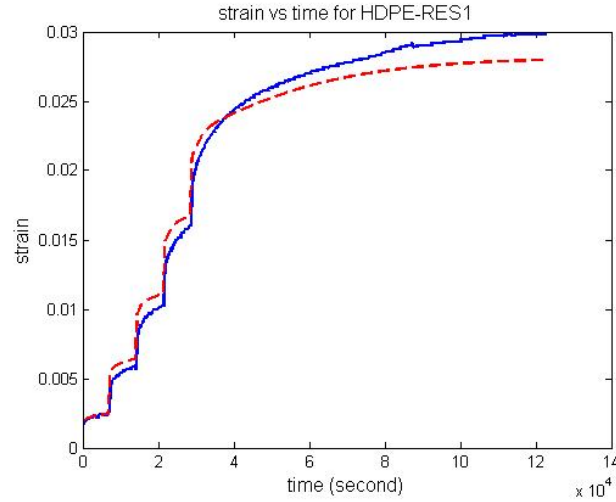


**Figure 17: Strain vs time for HDPE pipe. Stress level 1 = 1.50 MPa, stress level 2 = 2.90 MPa, stress level 3 = 4.38 MPa, stress level 4 = 5.84 MPa, stress level 5 = 7.30 MPa, (blue continuous line: experimental data (Liu, 2007), red dashed line: present model)**

For the first time-step the stress-strain relationship under constant stress is:

$$\varepsilon_1 = \{X_{0,\sigma_1} + C_{0,\sigma_1} \times t^{C_{1,\sigma_1}}\} \sigma_1 \quad (50)$$

If the stress state changes from  $\sigma_1$  to  $\sigma_2$ , the total strain response after the second stress change is:

$$\begin{aligned} 0 \leq t \leq t_1 & \quad \varepsilon_1 = \{X_{0,\sigma_1} + C_{0,\sigma_1} \times t^{C_{1,\sigma_1}}\} \sigma_1 \\ t_1 \leq t \leq \infty & \quad \varepsilon_2 = X_{0,\sigma_1} \sigma_1 + \{C_{0,\sigma_1} \times (t_2 - t_0)^{C_{1,\sigma_1}}\} \sigma_1 \\ & \quad + \{[C_{0,\sigma_2} \times (t_2 - t_1)^{C_{1,\sigma_2}}] \sigma_2 \\ & \quad - [C_{0,\sigma_1} \times (t_2 - t_1)^{C_{1,\sigma_2}}] \sigma_1\} \end{aligned} \quad (51)$$

## 2.7 Modelling Methodology

Modelling of viscous materials requires material properties. Finding material properties have basis in experimental data. These tests can be one dimensional tension/compression creep or relaxation or biaxial creep and/or relaxation. Many researchers (e. g. Findley (Findley, et al., 1976) and Aklonis

(Aklonis, et al., 1983)) have introduced methods on how to use these tests for extracting material properties. In this research, one dimensional creep tests on polyethylene materials are used for developing the methods and finding material properties.

**Material Properties:** Different methods can be used for finding modelling material properties. Two classes of models exist. The first consists of the so called “mechanical analogues” which, is a differential method of formulation. These are combinations of spring and dash-pot elements that are assembled to reproduce the viscoelastic or viscoplastic response of the real system. The right combinations of the elements must be chosen to match the real behaviour of a material. For example, the Multi Kelvin solid configuration best describes the viscoelastic behaviour of the materials, while the Multi Maxwell Fluid is more suitable for materials with high degree of plasticity or those that show fluidic behaviour (Flugge, 1967). The second method is called “hereditary integral”, method which is an integral formulation. This method is based on the approximation of the material properties. In this research, the first class of formulation, based on multi kelvin solid configuration, is used for finding the material properties for the viscoelastic behaviour of polyethylene, while the second class of formulation, using power law approximation function is used for viscoplastic behaviour. Both methods, result in a series of model constants, which are Prony series and power law constants, respectively. These constants (fitting parameters) are found by fitting the models to the experimental data. For this either a linear curve fitting method or nonlinear optimization technique can be used. For more details on the material properties refer to the next chapter. The resultant properties will be used for the finite element investigation.

**Finite Element Formulation:** Two methods can be used for developing a finite element procedure. The first is Multiple integral representation for three-dimensional behaviour, which is an extension of linear superposition to the nonlinear range, and the second one is a Schapery's single integral constitutive law, which is a simplified linear representation of multiple integral formulation.

**Multiple integral representation:** Multiple integral approach is very useful in modelling materials which are nonlinearly viscoelastic/viscoplastic. Many constitutive equations have been developed for nonlinear viscoelasticity from multiple integral formulation (Findley, et al., 1976). This method is an extension of linear superposition in the nonlinear range. The method is based on the small strain assumption, but it is extended to large deformation for materials in which the stress-strain relation is nonlinear. For small strains one can write  $\varepsilon_{ij} = \sigma_{ij} \chi(t)$ . where  $\chi(t)$  is time dependent relaxation

compliance. Discretizing for small changes of strain due to a constant stress in a small time interval yields the following formula which represents the resultant strain shown in Figure 18.

$$\varepsilon_i(t) = (\Delta\sigma_i) \chi(t) \quad (52)$$

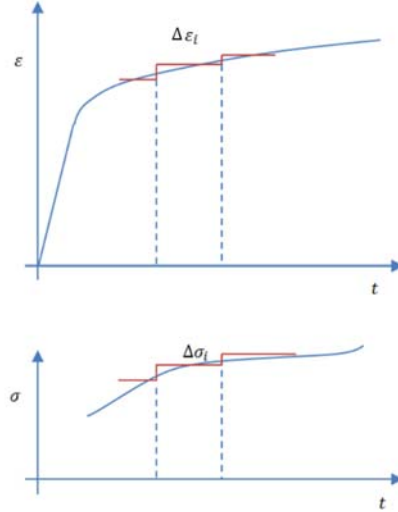


**Figure 18: Strain resultant due to the assumed constant stress increments; representation of superposition principle.**

Here  $\varepsilon_0$  is resulting constant strain due to small change in constant stress,  $\Delta\sigma_i$ . Eq. (52) is representation of Hooke's law. If a nonlinear material is stretched beyond its elastic limit, a plastic deformation contributes in the resultant response, meaning that the material doesn't return to its original shape when the applied force is removed. It will permanently deform and will no longer obey Hooke's law. Not all materials, especially polymers, obey Hooke's law when they are deformed. With reference to the Boltzmann's superposition principle which states that the sum of the strain outputs resulting from each component of stress input is the same as the strain output resulting from the combined stress input, in discretized model, the time-dependent strain resulting from a nonlinear constant stress may be represented by a polynomial as (Findley, et al., 1976)

$$\varepsilon_i(t) = (\Delta\sigma_i)\chi_1(t) + (\Delta\sigma_i)^2 \chi_2(t) + (\Delta\sigma_i)^3 \chi_3(t) + \dots \quad (53)$$

Eq. (53) is a multi-order discrete constitutive equation and  $\chi_j$  are time dependent material functions. By increasing the order of the equation in RHS, the accuracy increases. The integral form of total

resultant strain at current time,  $\varepsilon(t)$ , for the case of varying stress,  $\sigma$ , for time  $t$  would be (Findley, et al., 1976):

$$\begin{aligned} \varepsilon(t) = & \int_0^t \chi_1(t - \xi_1) \dot{\sigma}(\xi_1) d\xi_1 + \int_0^t \int_0^t \chi_2(t - \xi_1) \chi_2(t - \xi_2) \dot{\sigma}(\xi_1) \dot{\sigma}(\xi_2) d\xi_1 d\xi_2 \\ & + \int_0^t \int_0^t \int_0^t \chi_3(t - \xi_1) \chi_3(t - \xi_2) \chi_3(t - \xi_3) \dot{\sigma}(\xi_1) \dot{\sigma}(\xi_2) \dot{\sigma}(\xi_3) d\xi_1 d\xi_2 d\xi_3 + \dots \end{aligned} \quad (54)$$

which is so-called multi integral representation of the constitutive equation. Here  $\xi_1, \xi_2, \xi_3, \dots$  are integration variables,  $\dot{\sigma}(\xi) d\xi$  introduced instead of  $d\sigma(\xi)$  and  $\chi_j$  are kernel functions. This approach is used in chapter 4 for developing the finite element procedure.

**Schapery's single integral constitutive law:** Due to the complexity of the multiple integral formulation, the single integral representations have been the most widely applied theories. Especially the thermodynamic based theory of non-linear viscoelasticity developed by Schapery (Schapery, 1969) & (Schapery, 1997) has been found a convenient one, see for example (Smart, et al., 1972). Schapery's model utilizes the same structure as the linear integral model, in which just one term in RHS of the Eq. (53) is considered.

$$\varepsilon_i(t) = (\Delta\sigma_i) \chi_1(t) \quad (55)$$

so, the Eq. (54) is simplified to

$$\varepsilon(t) = \int_0^t \chi_1(t - \xi_1) \dot{\sigma}(\xi_1) d\xi_1 \quad (56)$$

Schapery presented a nonlinear constitutive equation based on the linear viscoelastic representation. Schapery's model utilizes the same structure as the linear integral model. In addition, several nonlinear models, such as the Leaderman model and the free volume approach by Knauss and Emri (Knauss, et al., 1981), can be interpreted as a special case of the Schapery model. Schapery's nonlinear viscoelastic model is given by

$$\varepsilon(t) = g_0 \sigma(t) D_0 + g_1 \int_0^t \Delta D (\psi^t - \psi^\tau) \frac{d}{d\tau} [g_2 \sigma(\tau)] d\tau \quad (57)$$

This approach is used in chapters 5 & 6 for developing the finite element procedures for viscoelastic behaviour.

**Determination of material functions:** For modelling the behaviour of materials reliably, the material functions in the constitutive equation must be accurately determined. For a linearly viscoelastic material, either the creep compliance or relaxation modulus must be determined. For the displacement based FE-method, it is convenient to use the relaxation-based constitutive equation. However, the creep test is easier to perform than the relaxation test. To develop the FE procedure, the material properties from experiments are used. The multi integral approach is difficult to use for finite element development. For this, some assumptions will be made in this research. These are 1) full incompressibility of a material and 2) simplifications of material functions. Exponential and power law functions are used for approximating material properties for nonlinear viscoelastic and viscoplastic behaviours, respectively (see chapter 4). The single integral method is easier to use for finite element model development. Chapters 5 & 6 in this research use this approach for modelling the viscoelastic linear and nonlinear behaviours, respectively.

## **2.8 Practical applications of the present work**

The purpose of this research is to provide a tool for predicting the viscoelastic and viscoplastic behaviour of polymers over time. The tool is intended to be user friendly and accurate enough to be applicable for practical applications.

Two steps are required to be taken for this purpose. First, the material properties need to be obtained from experiments. A code is developed in Matlab workspace. The code is able to read uniaxial tensile creep tests on samples of material. These data provide measured creep strains versus time for material samples under several constant stresses. The outcome of this analysis would be model parameters for either viscoelastic or viscoplastic behaviours which define the material properties. These material properties are suitable for studying the material response in a wide range of stresses and longer time frames beyond the test time.

The next step is foreseeing the viscoelastic and viscoplastic behaviours of polymers using a finite element (FE) method. The developed formulations are implemented into a finite element procedure through a user defined material subroutine (UMAT). The developed UMAT subroutine is linked to the commercial software ABAQUS, makes users able to investigate the creep and relaxation responses of 3D solid material models made in Graphic User Interface (GUI). The inputs to this step are the boundary conditions (which are defined through GUI) and material properties (which are obtained in step 1 as material model parameters).

By knowing the strain energy storage limit (resilience factor) of the material, the provided FE tool is also able to predict the time to failure of the material. Basic information, like resilience factor is obtained from stress rupture testing on the sample materials. Based on this data, a safe stress and a maximum value of stored strain energy can be determined below which it is safe to operate.

An instruction on how to use the developed Matlab and UMAT codes for practical applications are presented in Appendix A.

From practical application point of view, for a desired lifetime, that defines a maximum time, there is one maximum level of stress which satisfies the maximum strain. So the design is all about defining the priority (among three factors of maximum stress, time and strain) which depends on the specific application. In some situations, strain or deformation is more critical, which requires design for stiffness. Meaning that by limiting the strain to a certain small amount, the maximum allowable applied stress decreases and the life time increases. If the dimension precision of the component under discussion is not so important, design for strength is then used accordingly. Which means increase in maximum allowable applied stress, and consequently increase in deformation and decrease in life time. For complicated structures, like in nuclear industry, commercial buildings, infrastructures and pipelines, both can be used for design criteria to ensure successful material performance during service time. The presented tool (combination of material model and FE model) provided us with information on stress and strain vs. time and the ultimate limits.

It should be noted that some assumptions are made for developing the tool under discussion, like isotropic behaviour of material and isothermal condition. Also some simplifications are made on the formations to make them easy for finite element implementation. Also just one mechanism of failure is considered which is delayed failure due to stored strain energy. The comparison between results on experiments and the present model shows an acceptable prediction of material behaviour in long time.

## **2.9 Conclusion**

This chapter presents an overview of polymer material research including testing and modelling. Modelling techniques for short term, long-term and time-history cases are discussed.

The experimental results show a high degree of nonlinearity in polyethylene behaviour which requires simulations based on coupled non-separable formulations. Viscoelastic and viscoplastic

models were developed based on differential formulations, suitable for implementation in finite element procedures.

## **Chapter 3**

# **Modelling Short and Long Term Time-dependent Nonlinear Behaviour of Polyethylene**

Contents of this chapter is based on a paper which has been published in the journal of “Mechanics of Advanced Materials and Structures”. A new methodology for developing macromechanical constitutive formulations for time-dependent materials is presented in this chapter. In particular, two phenomenological constitutive models for polymer materials are illustrated, describing time-dependent and nonlinear mechanical behaviour. In this new approach, short term creep test data (done by Liu (Liu, 2007)) are used for modelling both short term and long term responses. The differential form of a model is used to simulate typical Nonlinear Viscoelastic (NVE) polymeric behaviour using a combination of springs and dashpots. Unified plasticity theory is then used to develop the second model, which is a Nonlinear Viscoplastic (NVP) one. Least squares fitting is applied for determination of material parameters for both models; based on experimental results. Due to practical constraints, experimental data are usually available for short term time-frames. In the presented proposed formulation, the material parameters determined from short term testing are used to obtain material parameter relationships for predicting the long term material response. This is done by extending short term information for longer time frames. Finally, theoretical and experimental results of tensile tests on polyethylene subjected to various load levels and test times are compared and discussed. Very good agreement of the modelling results with experimental data shows that the developed formulation provides a flexible and reliable framework for predicting load responses of polymers.

### **3.1 Introduction**

Polymers are increasingly used in many aspects of our lives, including infrastructure, building and pipeline construction. Thermoplastic polyethylene (PE) and unplasticized polyvinyl chloride (PVC or UPVC) are the predominant materials used for water and sewer pipes (Polak, et al., 2004). Other plastics for pipe production are polypropylene (PP), polybutylene (PB) and acrylonitrile-butadiene-styrene (ABS); which are all thermoplastics (Janson, 2003). The pipeline installation procedures, for example by horizontal directional drilling, impose tensile and bending deformations on the pipes and often result in significant amount of scratching of the pipe’s outer surface. Subsequent utilization



subjects the pipe to internal and external hoop stresses, often variable over time. The 3-D stress and strain under normal utilization conditions is relatively low due to high safety factors, which generally protect the pipes from failure under short term conditions. However, adequate long term strength of the PE pipes is a major concern in the design and construction of such pipeline systems. Therefore, theoretical and/or numerical modelling of the behaviour of these materials is essential to complement experimental data and to allow for structural analysis of polymeric elements and structures.

The primary goal of this chapter is to propose a practical formulation for nonlinear modelling of polymeric structures for short and long term time frames. Due to practical constraints, experimental data are usually available for short term testing. Extending this information for longer time frames is important for rational structural modelling. The proposed new theoretical approach for long term modelling, based on information from short-term testing, is presented in the chapter.

The models describing the behaviour of polymeric materials have basis in: 1) the physical concept of a network of macromolecular chains with cross-links, or 2) the phenomenological laws of viscoelastic solids. These are referred to as micromechanical modelling and macromechanical modelling, respectively. The work presented herein addresses the macromechanical approach, which is appropriate for the analysis of structures or structural components on the macroscale. This research is focused on development of constitutive formulations that are appropriate for subsequent implementation into such structural analysis platforms like, for instance, finite element modelling.

In the micromechanical approach time-dependent functions expressing breakage of links of macromolecule chains and deformations of crystalline phase are usually formulated and applied to characterize the development of stress and strain ( (Zehsaz, et al., 2014) to (Popa, et al., 2014)). Based on this approach, Alvarado et al. (Alvarado, et al., 2010) presented a novel damage-coupled constitutive formulation for the mechanical behaviour of semicrystalline polyethylene.

In the macromechanical modelling, phenomenological models of viscoelastic solids are often employed. The theoretical formulation results in the evolution equation of stress or strain, which is expressed generally as a linear or nonlinear differential equation. The equation can be function of either time, stress and strain rate (time hardening theory) or strain, stress and strain rate (strain hardening). Several constitutive models based on this methodology were developed in the past two decades. Several viscoelastic constitutive equations were developed by Bae and Cho (Bae, et al., 2015) to describe nonlinear viscoelastic behaviour. Zacharatos and Kontou (Zacharatos, et al., 2015) presented a one-

dimensional phenomenological constitutive model, representing nonlinear viscoelastic behaviour of polymers using a three element standard solid model. Hasanpour et al. (Hasanpour, et al., 2009) developed a finite element (FE) procedure for compressible viscoelastic materials. The work includes the formulation and constitutive equations of finite strain viscoelastic materials using multiplicative decomposition in a thermodynamically consistent manner. In a similar comprehensive research, a finite element algorithm was successfully developed by Krishnaswamy et al. (Krishnaswami, et al., 1992) to study nonlinear time-dependent problems. A practical simplified approach to nonlinear modelling of polyethylene, based on creep testing at different stress levels, was proposed by Liu et al. (Liu, et al., 2008). Cheng et al. (Cheng, et al., 2011) followed up on this work by presenting a rigorous statistical approach for modelling creep compliance of PE. In a work concerning a class of non-aging isotropic viscoelastic solids, Muliana et al. (Muliana, et al., 2015) proposed a model by developing a nonlinear integral formulation, which belongs to the class of quasi-linear viscoelastic models, for solid-like materials. A thermodynamics-based constitutive model was developed by Krairi and Doghri (Krairi, et al., 2014) for isotropic homogeneous thermoplastic polymers under arbitrary multiaxial and non-monotonic loadings. Chan and Ngan (Chan, et al., 2010) investigated polyethylene which is subjected to a tensile test with a jump in the loading rate. Muliana (Muliana, 2015) presented analyses of deformations in nonlinear viscoelastic beams that experience large displacements and rotations due to mechanical, thermal, and electrical stimuli. Nguyen et al. (Nguyen, et al., 2013) focused on viscoelasticity, as a predominant factor in the high cycle fatigue stress range. For this they derived an isothermal nonlinear viscoelastic model for small strains using a thermodynamics framework. An efficient method of fitting Prony series models to viscoelastic experimental data with power-law pre-smoothing was presented for the experimental data by Park and Kim (Park, et al., (2001). The same group also investigated and illustrated methods of interconversion between relaxation modulus and creep compliance for linear viscoelastic materials using data from asphalt concrete (Park, et al., 1999).

In modelling of polymers, experiments play an important role, since they offer insight into the material behaviour (namely, linearity and nonlinearity, and separable and non-separable form of equations), and they form the basis for model validation. The mechanical behaviour of polymeric materials depends on both time and temperature and several experimental techniques may be used to measure and quantify this behaviour. Drozdov and Christiansen reported their observations on uniaxial tensile tests with constant strain rates at moderate finite deformations, as well as in creep and relaxation tests on a thermoplastic elastomer (ethylene–octane copolymer) (Drozdof, et al., 2006) and

polyethylene (Drozdov, et al., 2003). Dusunceli and Colak (Dusunceli, et al., 2008), same as Liu et al. (Liu, et al., 2008), presented an approach for modelling the mechanical behaviour of polyethylene materials. They developed both viscoelastic and viscoplastic models and showed model corroboration with tensile, step-loading, and load-rate creep experimental results. They also presented creep numerical and experimental data for a medium density polyethylene (MDPE) pipe material and confirmed the efficiency of the macro- mechanical approach. Ayoub et al. (Ayoub, et al., 2010), Ellyin et al. (Ellyin, et al., 2007), Cao et al. (Cao, et al., 2010), Wendlandt et al. (Wendlandt, et al., 2010) and Pan et al. (Pan, et al., 2012) also used experimental results to validate proposed theoretical models.

Although viscoelastic and viscoplastic models of polymers have been developed by these aforementioned researchers, only limited work is available on the long term response prediction of material behaviour. The work that exists is limited to the demonstration of the well-known time-temperature superposition principle (Barbero (Barbero, 2011), Luo et al. (Luo, et al., 2012), Diani et al. (Diani, et al., 2015), Gnip et al. (Gnip, et al., 2008) & (Gnip, et al., 2010)). The research presented herein aims to propose a new empirical approach for long term modelling. For practical reasons, most creep testing of polymers is done using short term test frames. However, when constitutive modelling is applied to the analysis of real structural components, the long- term response is usually needed. The model presented herein has the capability of adjusting fitted parameters to the anticipated time interest. The long term material/parameter relationships are obtained based on the trends observed during short term testing. Experimental tensile short term creep tests (done by Liu (Liu, 2007)) are used for defining material properties of polyethylene to be used in nonlinear constitutive equations. Prony series and associated multi-Kelvin modelling are used to find viscoelastic (VE) material parameters, which is based on the work by Zhang and Moore (Zhang, et al., 1997), while plastic theory is used to determine the viscoplastic (VP) model parameters, based on research done by Krishnaswami (Krishnaswami, et al., 1992). The model considers time-dependent as well as nonlinear behaviour of the material. Theoretical and experimental results for polyethylene subjected to various load levels and test times are compared and discussed.

### **3.2 Problem Definition**

The primary target in this work is to develop nonlinear and time-dependent models using creep test results at different stress levels. These results, for any given material, are usually available in short time frames. The challenge is to use this short term creep test data for modelling longer time frames of

behaviour which is done by extending the short term models to long term ones. The responses of both short term and long term models are highly dependent on material characteristics as input data. Polymers, in particular polyethylene materials used in this work, show different material behaviour for different grades. Therefore, creep tests must be done for each material under investigation. Experimental results are used, as input information, for the development of constitutive models specific to a given material. This can be done using procedures described herein implemented into the Matlab platform. The computerized procedures for material model development allow for fast and efficient ways to create a customized model for a given polymeric material. The input for the model are creep curves, at short time frames (24 hours in this work), at different constant stress levels.

The development of the models proceeds as follows. The 24 hour creep tests, are used first for the creation of the viscoelastic and viscoplastic nonlinear models. The development is based on the premise that material parameters change with stress, as the models are nonlinear. Then, the stress- and time-dependent models are validated by comparing theoretical and experimental results for longer than 24 hour time frames.

### **3.3 Material characteristics**

The experimental tensile creep results used in this work have been reported by Liu (Liu, 2007). Five high density polyethylene (HDPE) sample materials tested in our laboratories by Liu (Liu, 2007) are used for defining material properties (Table 1). The samples are of two types: pipe materials and HDPE resins. The pipe materials were cut from pipe samples with length along the pipe axis and width along the radius of the pipe, while the resin specimens were made by melting the resins and then pressing into plates. The process includes heating up the material to 320 F in the mould and then cooling down to room temperature on a hot plate with the heater off, followed by hot pressing into 7 in square plates. Both specimen types were then machined down to the required dog-bone shape dimensions. All tested specimens have dimensions that conform to ASTM Standard Test Method for Tensile Properties of Plastics (2002).

Material characteristics are tabulated in Table 1. Among those, Resin1 and Resin2 are blow molding resins, Resin4 is injection molding resin and PE80 is a pipe grade resin. These are cited to show differences in microstructural properties of the sample materials. These properties are not directly used in the modelling presented herein, as macromechanical model development uses creep tests for material characterization. The cited micromolecular properties are weight-average molecular weight,  $M_w$ ,

number-average molecular weight,  $M_n$ , and the environmental stress crack resistance (ESCR) values of resins. Environmental stress cracking (ESC) is one of the important factors affecting failure of polyethylene.

The creep test results allow classification of the polyethylene materials. The first level of material classification is determining if the material is described best by a viscoelastic or viscoplastic model. A viscoelastic material shows a significant amount of delayed recovery upon unloading, whereas there remains a permanent residual ‘plastic’ strain for viscoplastic materials. By performing creep tests at several constant stress levels, a series of strain vs. time curves are obtained. The compliance plot, " $\varepsilon/\sigma$ " vs. time, provides information if the compliance is independent of the stress level; if a single curve is obtained for the compliance under different levels of constant stress, then the material is said to be ‘linear’. Otherwise, the compliance is a function of stress and the material is known as ‘nonlinear’ and a nonlinear model must be used to represent its creep behaviour. Nonlinear materials can be categorized by considering whether the effects of stress ( $\sigma$ ) and time ( $t$ ) on strain ( $\varepsilon$ ) are separable or not. If all plotted compliance curves for nonlinear materials have the same ‘shape’, the material can be described as nonlinear-separable, i. e., the same type of time function can be used for compliance at all stresses. Strain ( $\varepsilon$ ) is then given by (Krishnaswami, et al., 1992):

$$\varepsilon = h(\sigma)f(t) \quad (58)$$

where  $h$  is a function of applied stress  $\sigma$  and  $f$  a function of time  $t$ . If the shape of the compliance curves at different stress levels is not similar, then strain ( $\varepsilon$ ) must be represented by a different function of time at each stress level. In this case, the material can only be described by a nonlinear non-separable model given by (Krishnaswami, et al., 1992):

$$\varepsilon = g(\sigma, t) \quad (59)$$

where  $g$  is a function of both variables, stress and time.

### 3.4 Non-linear Viscoelastic (NVE) Model Development

Based on test results for the materials listed in Table 1, conducted by Liu et al. (Liu, et al., 2008) and (Liu, 2007)) and briefly described in the previous section, a strong nonlinearity was observed in material responses, because different time-dependent compliance curves were seen for different applied stresses (Liu, et al., 2008) and (Zhang, et al., 1997)). Subsequent to these test results, a suggested process of developing a non-linear model (Zhang, et al., 1997)) is to start with a linear model for the

material under constant stress (separable form) and then extend it to the nonlinear one by considering effects of stress on the stress-dependent part (non-separable form).

For the first step which is linear modelling, the following stress-strain relationship is defined for predicting the linear response of the material under a particular constant applied stress:

$$\varepsilon(t) = \sigma X(t) \quad (60)$$

In this formulation,  $X(t)$  describes the creep compliance of the material and is based on the spring and dash-pot method of modelling described by Flugge (Flugge, 1967). According to the concept of fading memory (Christensen, 1971), the material response depends more on recent history than on earlier events. Accordingly, this theory considers the following formulation for creep compliance for a solid multi Kelvin configuration of spring and dash-pot, and is one of the most useful forms of creep compliance for finite element implementations

$$X(t) = \frac{1}{E_0} + \sum_{i=1}^N X_i (1 - e^{-t/\tau_i}) \quad (61)$$

Eq. (61) is a form of a Prony series approximation, with  $2 \times N$  unknown material properties ( $X_i$  and  $\tau_i$ ).  $X_i$  and  $\tau_i$  are creep compliance and relaxation time, respectively, for the  $i^{th}$  Kelvin element.  $N$  indicates the number of Kelvin elements in the model.  $E_0$  is the instantaneous elastic time-independent modulus and equals to  $1/X_0$ , which  $X_0$  is measured creep compliance at  $t_0 = 0$ , and is called an independent term.

One can obtain parameter values ( $X_i$  and  $\tau_i$ ) by fitting the Prony series to experimental data by means of an optimization technique or by classical simplified technique. For optimization Baumgaertal and Winter, (Baumgaertel, et al.) presented a regression technique in which  $X_i$  and  $\tau_i$  are all variables. Fernanda et. al (Fernanda, et al., 2011) also used same optimization technique to find constitutive parameters for viscoelastic materials. However, the more common practice is to avoid the optimization technique by estimating (fixing) the relaxation times,  $\tau_i$ , from the total range of time domain and finding the compliance values. Once this simplified method of estimating relaxation times is chosen, a classical technique to build the linear system must be defined. Using one of the most useful methods of curve fitting, which is the least squares method, results in the following linear system

$$T_{ij}X_i = B_j \quad (62)$$

Schapery (Schapery, 1961) and Liu et. al (Liu, et al., 2008), used this technique to fit a linear viscoelastic model to test data. In this equation  $X_i$  is the unknown compliance for each Kelvin element (Eq. (61)) and

$$\begin{aligned}
 T_{ij} &= \sum_{k=1}^{N_t} (1 - e^{-t_k/\tau_i})(1 - e^{-t_k/\tau_j}) \\
 B_i &= \sum_{k=1}^{N_t} (\hat{X}(t_k) - X_0)(1 - e^{-t_k/\tau_i})
 \end{aligned}
 \tag{63}$$

where  $\hat{X}(t_k)$  is the measured compliance at time  $t_k$  that from Eq. (60) is equal to  $\hat{\epsilon}_i/\sigma$ .  $N_t$  is the number of experimental points or equivalently number of measured  $\hat{\epsilon}_i$  for a particular stress.

Using either optimization or classical technique, one can find a set of  $2 \times N$  values ( $N$  values of  $X_i$  and  $N$  values of  $\tau_i$ ) for each particular stress. If  $n$  stress levels creep curves are used for modelling, this provides  $n$  sets of  $X_i$  and  $\tau_i$  values corresponding to the creep curves for  $n$  stress levels.

After the above first step is completed, the modelling progresses to the second step, which is non-linearization. For this, curve fitting is used to produce stress dependent parameters  $X_i(\sigma)$  and  $\tau_i(\sigma)$ . This can be done by fitting chosen approximation functions of stress to those  $n$  sets of parameters from linear step. Zhang and Moore (Zhang, et al., 1997) used exponential approximation functions to find stress dependent parameters by fitting the approximation functions to strain-time curves for eight stress levels.

In our work, the optimization method is chosen out of two described methods for linear modelling step. For the non-linearization step, parameters are approximated by the chosen exponential functions of stress. This results in a combined (step one and step two described above) step of nonlinear optimization, which aims to find stress dependent parameters by fitting the model to test data. The nonlinear optimization technique is generally referred to as ‘‘unconstrained nonlinear optimization’’. This is a method of either minimization or maximization. For this, one of the numerical methods, out of many available (Derivative-free method, Descent method, Line search, Gradient descent method, Steepest descent method, Newton’s method, Quasi-Newton’s method, etc.) is used. In this chapter, the procedure works by finding the minimum of the error function of several variables (fitting parameters), starting at an initial estimate. In this method, the process starts at the point  $x_0$  and returns a value  $x$  that

is a local minimizer of the function. For this a code is developed in a MATLAB workspace which uses a built-in algorithm of Derivative-free Optimization method.  $x_0$  can be a scalar, vector, or matrix and the error function is a function handle (see section 3.7 for further discussion on the function).

It is known that when a local optimization technique is applied to minimize the error function it is sensible to the starting point,  $x_0$ , since the problem may have many local minima. To overcome this problem and to force the convergence to the global optimal set, different methods have been mentioned in the literature. Bower and Gunt (Bower, et al., April 1994), and Fernanda et al. (Fernanda, et al., 2011) suggested choosing the starting parameter set,  $x_0$ , close to global optimal set. However, this strategy is only possible when the range of the admissible parameters is known; otherwise the method requires multiple iterations of process by changing the first guess. The other suggested method is the improvement of the quality of the initial guess,  $x_0$ . For this Robert (Robert, 1997) proposed a strategy to begin with just a few Prony terms in Eq. (61). This is equivalent to simplifying the function (model) by removing the parameters that have less effect on the behavior in the initial iteration and adding those parameters in latter ones. By using either of these two suggestions, convergence may not be fully attained with one execution of the optimization technique. Therefore, one may need multiple iterations to get proper accuracy in the outcome. This is what we have done here by examining multiple start parameters until we get the desired error value. The outcome of the calculations is a set of fitting parameters for nonlinear viscoelastic model. The program works by pre-setting  $X_i$  and  $\tau_i$  as exponential functions of  $\sigma$ . Using such an approach, it is possible to effectively estimate values for  $\tau_i$  and  $X_i$ , with a relatively high degree of accuracy, compared to the classical technique.

In this work, to reduce the number of material parameters for a particular stress curve, which is equal to  $2 \times N$ , all values of  $X_i$  and  $\tau_i$  are obtained using four parameters, namely  $X_1$ ,  $\tau_1$ ,  $m$  and  $\alpha$ , following the formulation suggested in literature (Zhang, et al., 1997).

$$X_i = m^{1-i} X_1 \quad , \quad \tau_i = \alpha^{i-1} \tau_1 \quad (64)$$

Here,  $\alpha$  and  $m$  are approximation parameters with no units of measurement, which constrain the selection of higher order relaxation times/compliances to an optimized increasing/decreasing power law trend. For simplicity, parameters  $m$  and  $\alpha$  are considered to be stress-independent. Based on the analyses done using the developed MATLAB program the curve fitting of the two parameters  $X_1$  and  $\tau_1$  showed that the parameter distributions versus applied stress  $\sigma$  can be best described by approximation functions similar to those suggested in the literature (Zhang, et al., 1997), as following



$$X_0 = (a_0 + a_1 e^{(-a_2 \hat{\sigma}^3)})^{-1} \quad (65)$$

$$(a) \quad X_1^{-1} = b_0 + b_1 \exp(b_2 - b_3 \hat{\sigma} - b_4 / \hat{\sigma}) \quad (66)$$

$$(b) \quad \tau_1 = c_0 \exp(-c_1 + c_2 \hat{\sigma} + c_3 \hat{\sigma}^2 - c_4 \hat{\sigma}^3)$$

Here  $\hat{\sigma} = \sigma \times 10^{-6}$ , and  $\sigma$  is the applied stress for a given creep curve.  $E_0 = 1/X_0$  is obtained from experimental results for each test and varies with respect to stress. Eq. (65) is used to simulate this variation. The fitting parameters  $a_0$ ,  $a_1$  and  $a_2$  are obtained by fitting Eq. (65) to experimental readings and are tabulated in Table 2, while  $b_i$  and  $c_i$  will be discussed shortly below. Here,  $a_0$  and  $a_1$  have unit of compliance and  $a_2$  has unit of inverse of cubic stress.  $b_0$  and  $b_1$  have stress unit,  $b_2$  has no unit,  $b_3$  has inverse unit of stress and  $b_4$  has unit of stress.  $c_0$  has unit of time,  $c_1$  has no unit,  $c_2$  has unit of inverse of stress,  $c_3$  has unit of inverse of squared stress, and  $c_4$  has unit of inverse of cubic stress.

In this chapter, and for the sake of brevity, only the PIPE and Resin 1 materials are used as examples of material modelling. When considering  $N = 6$  (6 Kelvin elements chosen for NVE material modelling in Eq. (61)), the fitting parameters ( $m$ ,  $\alpha$ ,  $b_i$  and  $c_i$ ) for PIPE and Resin 1 are listed in Table 3. The corresponding material parameters ( $X_i$  and  $\tau_i$ ) for these two materials can be obtained using Eq. (66), which are tabulated in Table 4 and Table 5. In these tables, only  $X_1^{-1}$  and  $\tau_1$  are listed and  $\alpha$  and  $m$  are used to determine the remaining  $X_i^{-1}$  and  $\tau_i$  using Eq. (64). The material parameters of Table 4 and Table 5 (for  $N = 6$ ) are used to plot the material nonlinear response in Figure 19 and Figure 20, for PIPE and Resin1, respectively, and at the stress levels used for the development of the model (Eq. (60)).

### 3.5 Non-linear Viscoplastic ( NVP) Model Development

Plastic flow in PE starts to develop at small strain and the material behaves in both viscoelastic and viscoplastic fashion. Since yield occurs gradually with a steady transition from a linear to a nonlinear response, the unified theories, which do not separate creep strains and plastic strains, are a better alternative than those that consider creep and plasticity as separate phenomena (Krishnaswami, et al., 1992). One of the main points of using these theories is that there is no need to perform the unloading experiment, since they do not distinguish between elastic and plastic deformations. Following non-separable viscoplastic model, Eq. (67), has been suggested by Krishnaswamy et al. (Krishnaswami, et al., 1992). Although it includes both elastic and plastic terms, the model doesn't make use of each portion separately, meaning that the combination of two strains in a single equation is always valid

through the entire process of deformation. Hence, there is no need to specify the point at which plastic deformation starts.

$$\begin{aligned}
 (a) \quad & \varepsilon(t) = \sigma X(t) \\
 (b) \quad & X(t) = \frac{1}{E_0} + C_0 \left(\frac{t}{T}\right)^{C_1}
 \end{aligned} \tag{67}$$

Here,  $1/E_0 = X_0$  is the elastic compliance at  $t_0 = 0$ , explained by Eq. (65), and the rest of Equation (67)(b) represents the plastic portion of the time dependent creep compliance, and  $T$ ,  $C_0$  and  $C_1$  are material parameters.  $C_0$  has unit of inverse of stress,  $T$  has time unit and  $C_1$  has no unit.

Similarly, to viscoelastic modelling, the determination of the material parameters proceeds with nonlinear optimization method. For this, the curve fitting of the Eq. (67) is done on experimental data, using the least squares criterion. For nonlinearization, parameters are approximated by functions of stress, similar to those suggested in the literature (Krishnaswami, et al., 1992), as follows:

$$\begin{aligned}
 (a) \quad & C_0 = (b_1 + b_2 \hat{\sigma} + b_3 \hat{\sigma}^2) \left(\frac{\sigma_n}{\bar{\sigma}}\right)^{(b_4 + b_5 \hat{\sigma} + b_6 \hat{\sigma}^2)} \\
 (b) \quad & C_1 = m_1 + m_2 \left(1 + \frac{1}{2} \arctan\left(\frac{\hat{\sigma} - s_a}{\bar{\sigma}}\right)\right) \\
 (c) \quad & T = T_1 \left(\frac{\sigma_n}{\bar{\sigma}}\right)^{d_0}
 \end{aligned} \tag{68}$$

Again  $\hat{\sigma}$  is  $\sigma_n \times 10^{-6}$  for simplicity and  $\bar{\sigma}$  is introduced for dimensional consistency (in this research we have  $\bar{\sigma} = 1 \text{ MPa}$ ). Table 6 shows the compilation of fitting parameters  $b_i$ ,  $d_0$ ,  $m_i$ ,  $s_a$  and  $T_1$  for all examined materials. Here,  $b_1$  has unit of compliance (inverse of stress),  $b_2$  has unit of inverse of squared stress and  $b_3$  has unit of inverse of cubic stress.  $b_4$  has no unit,  $b_5$  has unit of inverse of stress and  $b_6$  has unit of inverse of squared stress.  $m_1$ ,  $m_2$ ,  $s$  and  $d_0$  have no units. Unit of  $s_a$  is same as stress and  $T_1$  is time.

Using fitting parameters and Eq. (68) material parameters  $T$ ,  $C_0$  and  $C_1$  are obtained which are listed in Table 7 and Table 8 for two materials, “PIPE” and “Resin1”, respectively. The corresponding plots (model and the experimental results used for model development) are shown in Figure 21 and Figure 22 .

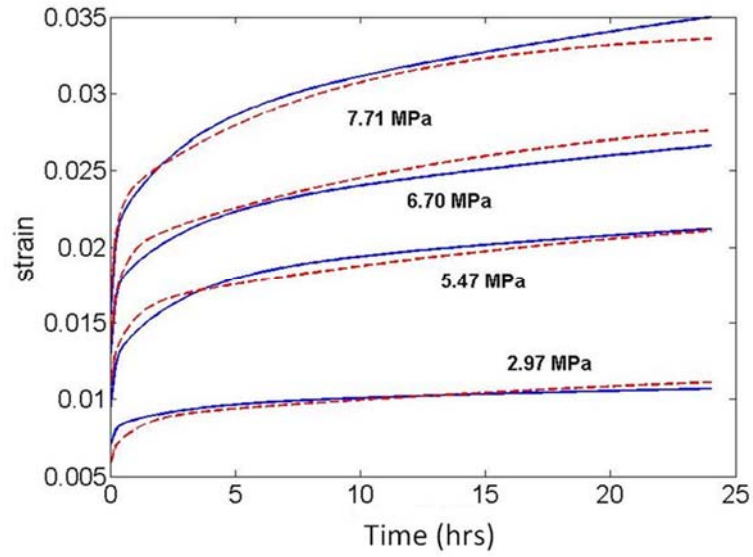


**Figure 19: Experimental (continuous line) (Liu, 2007), and nonlinear viscoelastic model (dashed line) results for 24 hour creep tests (PIPE) using Eqs. (61), (64) and (66) . (Material properties and fitting parameters are cited in Table 3 and Table 4, respectively)**

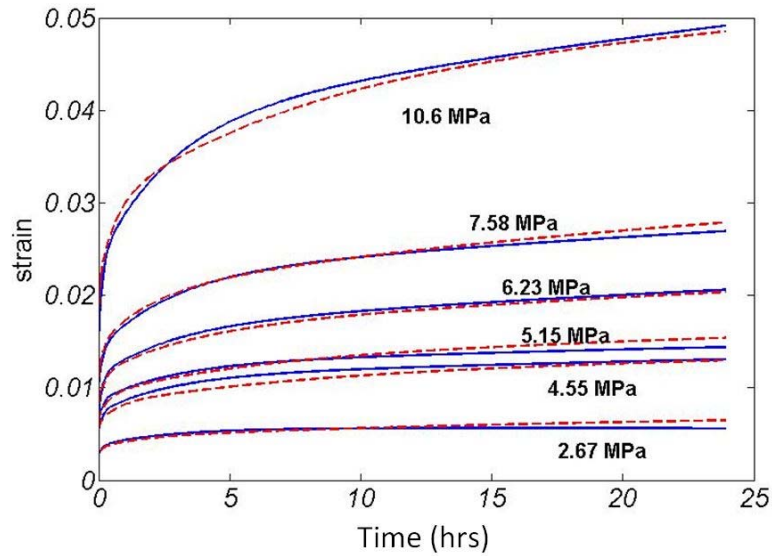


**Figure 20 Experimental (continuous line) (Liu, 2007), and nonlinear viscoelastic model (dashed line) results for 24 hour creep tests (Resin1) using Eqs. (61), (64) and (66) . (Material properties and fitting parameters are cited in Table 3 and Table 5, respectively)**

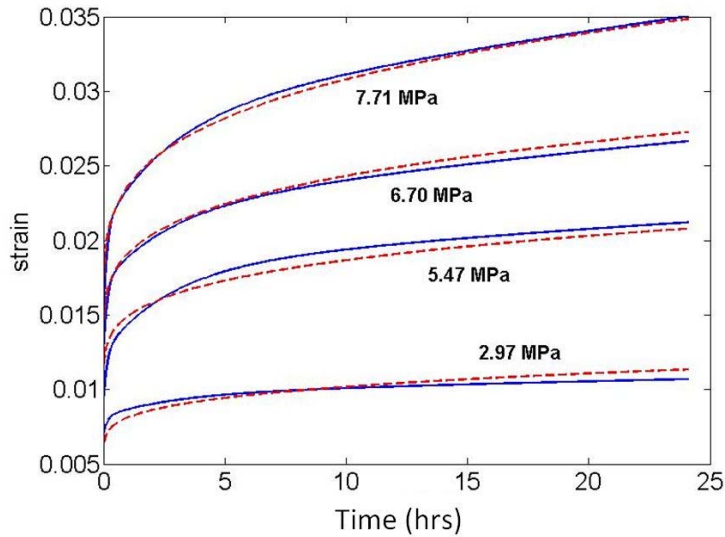


**Figure 21 Experimental (continuous line) (Liu, 2007) and nonlinear viscoplastic model (dashed line) results for 24 hour creep tests (PIPE) using Eqs. (67) and (68). (Material properties and fitting parameters are cited in Table 6 and Table 7, respectively)**

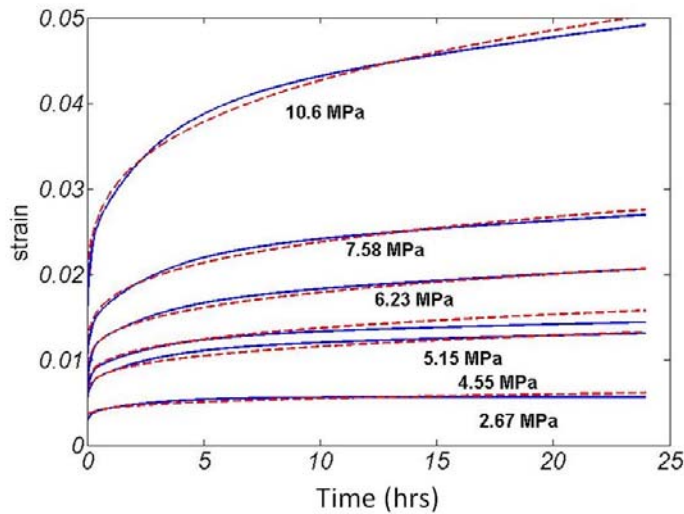


**Figure 22 Experimental (continuous line) (Liu, 2007), and nonlinear viscoplastic model (dashed line) results for 24 hour creep tests (Resin1) using Eqs. (67) and (68). (Material properties and fitting parameters are cited in Table 6 and Table 8, respectively)**

### 3.6 Modelling Long term Behaviour

The nonlinear models described in sections 3.4 and 3.5 are able to represent the response of the material within the test time-frame. It is well known that beyond the test time, the response of the viscoelastic model (described in Eq. (61)) approaches to an asymptotic value equal to  $X_0 + \sum_{i=1}^N X_i$  and the response of the viscoplastic model (described in Eq. (67)) increases continuously with a time dependent slope equal to  $C_0 C_1 T^{-C_1} t^{C_1-1}$ . This difference in the two modelling approaches clearly suggests that the models are most likely not valid beyond the curve fitting time period.

In this section an empirical solution to this problem is proposed, in view of the fact predicting the response of creep behaviour over extended time periods is very important for practical application of modelling real structures and elements. In this section, we propose a new method for obtaining the long term material parameter functions, based on the material parameters and creep testing done for the short term response. Using the discussion provided in sections 3.4 and 3.5, material parameters and fitting parameters (Table 4-Table 6) are obtained for 24 hour test periods. To examine the validity of the model for an extended time, the proposed method is to observe the trend of fitting parameters with respect to the test time. First, the curve fitting is done for all materials in different test times, namely: 10, 14, 18, 20, 22 and 24 hours. This allows observing how the fitting parameters are dependent on test time ( $\lambda$ ). We then propose that the parameter change over test time can be represented by the following equations for the viscoelastic case:

$$\begin{aligned}
 \text{(a)} \quad & b_i(\lambda) = b'_i (\lambda/\lambda')^{d_i} \quad \text{for } i = 0, 1, 2 \\
 \text{(b)} \quad & b_i(\lambda) = b'_i/(\lambda/\lambda')^{d_i} \quad \text{for } i = 3, 4 \\
 \text{(c)} \quad & c_0(\lambda) = c'_0 (\lambda/\lambda')^{d_5}
 \end{aligned} \tag{69}$$

Where  $\lambda$  stands for test time and  $\lambda'$  is introduced for dimensional consistency (in this research we have  $\lambda' = 1 \text{ hour}$ ).  $b_i(\lambda)$  and  $c_0(\lambda)$  are parameters used to define  $X_i$  and  $\tau_i$  as in Eq. (66), and  $b'_i$ ,  $c'_0$  and  $d_i$  are fitting parameters independent of the test time and used to extend the short term model response to a long term one. Here,  $b'_i$  and  $c'_0$  have same units as  $b_i$  and  $c_0$ , respectively and  $d_i$  have no units.

Similarly, when the same method is applied to viscoplastic modelling, the following equations for the dependency of parameters form Eq. (68) on  $\lambda$  are obtained:

$$\begin{aligned}
\text{(a)} \quad & b_i(\lambda) = b'_i (\lambda/\lambda')^{d_i} \quad \text{for } i = 1 - 6 \\
\text{(b)} \quad & m_j(\lambda) = m'_j (\lambda/\lambda')^{n_j} \quad \text{for } j = 1, 2 \\
\text{(c)} \quad & sa(\lambda) = s'_a (\lambda/\lambda')^s \\
\text{(d)} \quad & T_1(\lambda) = T'_1 (\lambda/\lambda')^{T_2}
\end{aligned} \tag{70}$$

These parameters obtained using nonlinear optimization technique by least squares fitting of the proposed formulation on the short term experimental results and are listed in Table 9 and Table 10 for the examined materials. Here,  $b'_i$ ,  $m'_j$ ,  $s'_a$  and  $T'_1$  have same units as  $b_i$ ,  $m_j$ ,  $s_a$  and  $T_1$ , respectively and  $d_i$ ,  $n_j$ , and  $T_2$  have no units.

### 3.7 Error Analysis

To examine the validity of the method, a criterion should be chosen for the convergence of the least squares fitting method. The test strain convergence criterion is adopted:

$$\left( \frac{\sum_{i=1}^{N_t} \left( \frac{\hat{\varepsilon}_i - \varepsilon_i}{\hat{\varepsilon}_i} \right)^2}{N_t} \right)^{1/2} = e \tag{71}$$

Eq. (71) is the Least Squares Error criterion which is the root mean square of deviation (RMSD) between the predicted values  $\varepsilon_i$ , and the measured  $\hat{\varepsilon}_i$  data and indicates the average scatter of the data points about the least squares fit curve. In recent years, it has become regarded as one of the most informative fit indices (Hooper, et al., 2008) and many researchers have used this criterion for validating the theory versus experiments. From those are Liu et. al (Liu, et al., 2008), Cantrell (Cantrell, 2008) and Fernanda et. al (Fernanda, et al., 2011). In Eq. (71)  $N_t$  is the number of strain measurements used for curve fitting.

The curve fitting procedure is applied on PIPE and Resin1 materials for NVE (nonlinear viscoelastic) and NVP (nonlinear viscoplastic) modelling (Figure 19-Figure 22). For this task, a code was developed in MATLAB. Material testing for PIPE includes four creep curves, each pertaining to different stress levels. The tests are done within 24 hours. Strain measurements are recorded every 30 seconds, which yields  $N_t = 2880$ , for each curve. Furthermore, to account for the long term prediction, the fitting procedure needs to be done for multiple test times,  $\lambda$ , other than 24 hours. As discussed in previous section, 10, 14, 18, 20 and 22 hours are considered, which yields in  $N_t = 1200, 1680, 2160, 2400$  and

2640, respectively. Four stress levels and six test times, result in  $4 \times 6 = 24$  error values obtained using Eq. (71). The purpose of the developed code is to minimize the average of the errors using local optimization technique. The mean fitting error (MFE) is defined for each material, which is the average of fitting errors associated with  $n$  stress levels and  $m$  test times. Same procedure is followed for material Resin1 considering  $n = m = 6$ .

$$MFE = \frac{1}{n \times m} \sum_{i=1}^n \sum_{j=1}^m e_{ij} \quad (72)$$

Here  $e_{ij}$  is error related to stress level  $i^{th}$  and  $j^{th}$  test time. To obtain the best fit, MFE in the code, is set to an optimum value. It is well known that if a smaller value is chosen, a more correlated estimation to test data is achieved, although it is also more probable that the calculations could diverge. Thus, the choice of MFE is an important issue for the success of the nonlinear optimization technique. Different values are suggested in literatures for the goodness of fit. MacCallum et. al (MacCallum, et al., 1996) used 0.01, 0.05 and 0.08 to indicate excellent, good, and acceptable fit, respectively. However, others have suggested 0.1 as the cut-off for poor fitting models (Hooper, et al., 2008). Here in our research we choose MFE to be equal to 0.05 (5%).

The other important choice is  $N$ , the number of Kelvin elements in viscoelastic modelling (Eq. (61)). This doesn't apply to viscoplastic modelling as we are using one single term for inelastic portion of the response (Eq. (67)). In NVE modelling, as the number of Kelvin elements increases, the accuracy of the fitting increases (Flugge, 1967), while in viscoplastic analysis, one term approximation formula yields enough accuracy in relatively short term behaviours (see discussions in (Findley, et al., 1976)). Since the MFE (Eq. 12) for each material should satisfy the convergence criterion ( $MFE \leq 0.05$ ), six Kelvin elements ( $N = 6$ ) are considered in this chapter which result in  $2 \times 6$  unknown material constants (fitting parameters). Although further increase in the number of Kelvin elements is expected to result in more accurate calculations of strains, the observations show that the results are essentially the same as for  $N = 6$ . For  $MFE = 0.05$  and test time  $\lambda = 24$  error values are recorded for both viscoelastic (Table 4 and Table 5) and viscoplastic (Table 7 and Table 8) models. As observed from recorded values, the average of least squares errors for both materials are less than the criterion. This shows that both models are valid for short term (24 hour) analysis.

### 3.8 Results

The first example presented is to show how the developed models can be used to predict creep behaviour at another stress level. Figure 23 and Figure 24 show the viscoelastic and viscoplastic behaviour predictions, using the developed formulation, for a test under 5.97 MPa constant stress for the PIPE material. This creep test result, which was obtained previously by Liu (Liu, 2007), has clearly a different shape than the other creep curves for the same materials (see Figure 19 and Figure 21) due to possible test errors. When the experimental results of the creep at 5.97 MPa are used to fit both the NVE and NVP models, the average of errors for 24 hour ( $\lambda = 1$ ) curve fitting, significantly increases by 3.5%. Also, as seen, the model does not fit well to these inaccurate creep test data (for 24 hour test frame the theoretical results should be in close agreement with the test). The error for this curve only is 8.6% and 8.1% for viscoelastic and viscoplastic modelling, respectively, which, as per MacCallum et. al (MacCallum, et al., 1996), are not within the acceptable range of goodness of fit. This is an interesting ‘counter-example’ with a problematic creep test data set. One can thus do effective process ‘trouble-shooting’ and ‘detect’ a potential abnormality in the data. In other words, the developed formulation, through the estimation of material parameters that should follow predetermined trends, can also be used to eliminate erroneous experimental data sets from constitutive modelling.

The next examples are used to corroborate the accuracy of the developed long term modelling approach. A separate set of tests (separate from the 24 hour creep tests used to estimate the material parameters) is used to predict the material responses over a longer term time frames. Two kinds of tests are considered for the PIPE material. One is a creep test that is done under three different stress levels, namely, 4.42 MPa, 6.08 MPa and 8.15 MPa, and the time frame of 40 hours, *Case I*. The second test is creep strain measurements of the PIPE material under 6.75 MPa, for seven days, *Case II* (Liu, 2007). Both NVE and NVP models are used in the model verification study. Accordingly,  $\lambda$  is set to 40 hours and 170 hours for *Case I* and *Case II*, respectively. The results are shown in Figure 25-Figure 28, which show a comparison between experimental data (continuous lines) and model predictions (dashed lines). Figure 25 and Figure 26 show the long term viscoelastic response of PIPE for 40 hours and 7 days, respectively. Long term viscoplastic responses are shown in Figure 27 and Figure 28 for 40 hours and 7 days, respectively. The errors (per Eq. (71)) associated with each stress level, case and model are tabulated in Table 11 and Table 12. Table 11 cites the errors obtained for  $\lambda = 40$ , while Table 12 shows the errors for longer test times ( $\lambda = 170$ ). The observed errors in both tables are not greater than 9% and 16% for both cases of long term analyses, for NVE and NVP, respectively. Scrutinizing the error



levels for both cases and model types, one can infer that NVE yields more accurate results compared to NVP. The differences between experiments and model prediction seen in both Figure 27 and Figure 28 indicate that the proposed NVP model is not as rigorous as the presented NVE model. This is due to the number of fitting parameters, which is less in NVP compared to NVE. Furthermore, the ability to set the number of Kelvin units ( $N$ ), allows for more flexibility in fitting process, which leads in more accurate and reliable prediction of response in NVE. The presented results show the usefulness of the present approach in forecasting the response over extended test times-frames

### 3.9 Conclusions

A new approach including integrated macromechanical constitutive models is proposed, which makes it possible to predict the long term behaviour of polymeric materials. Short term (24 hour) experimental tensile creep tests were used for determining material properties of polyethylene to be used in nonlinear constitutive equations and predicting the response of the material in the long term. Molecular properties were not considered in the model development, as ESCR affects just the failure mechanism, and effects of molecular weight averages and density are inherent in mechanical properties without appearing directly in macromechanical formulations.

Prony's series and associated multi-Kelvin modelling are used to determine viscoelastic material parameters, while plastic theory was used to determine viscoplastic model parameters. The models consider time-dependent and nonlinear behaviour of the material. Theoretical and experimental results for polyethylene subjected to various load levels and test times were compared and discussed. The NVE model in comparison with the NVP model results in smaller fitting errors for long term strain response predictions. Both models can be used in computational methods for predictions of long term material behaviour.

The developed modelling approach, implemented into the computational Matlab platform, allows for effective and fast parameter optimization and development of constitutive modelling for time-dependent and nonlinear polymeric materials. In this particular case, the formulation was used for modelling different grades of polyethylene. Since each grade behaves differently under stress, such a constitutive modelling approach is needed for analysis of polymeric structures and structural components.

Based on the research conducted in this chapter and summarized above, the following specific findings and contributions can be mentioned:

A nonlinear optimization method of finding material parameters has been used in this research. To construct the material models, a theoretical optimization method of finding material properties using experimental uniaxial creep test results developed for short term investigation. Differential formulation as well as unified plasticity theory is used for development of 1-D nonlinear viscoelastic and viscoplastic models, respectively. Material models are then extended to long terms. Materials parameters are obtained using nonlinear optimization technique, which is a minimization technique of error function. For this a code was developed in MATLAB workspace.

Here are the conclusions:

- 1- The Prony's series approach, and the associated multi-Kelvin solid modelling, is able to determine viscoelastic material parameters, while plastic theory is able to determine viscoplastic model parameters. The developed nonlinear optimization method allows for effective and fast parameter optimization and the development of constitutive modelling for time-dependent and nonlinear polymeric materials, and it is more efficient than linear methods.
- 2- Beyond the short term test time, the response of the viscoelastic model (exponential formulation) approaches an asymptotic value and the response of the viscoplastic model (power law formulation) increases continuously with a time dependent slope. This difference in the two modelling approaches clearly suggests that the models are most likely not valid beyond the curve fitting time period. The result of the proposed long term formulation (which simulates the long term behaviour), lies between the curves which are the extension of viscoelastic and viscoplastic models beyond the short term period.
- 3- The proposed material models are able to detect erroneous creep test curve. It is because the developed material models are able to predict creep behaviour at another stress level, meaning that the models give an estimation of the creep curve which its applied stress level is between the two available ones. One can thus do effective process "trouble-shooting" and "detect" a potential abnormality in the data. In other words, the developed formulation, through the estimation of material parameters that should follow predetermined trends, can also be used to eliminate erroneous experimental data sets from constitutive modelling.
- 4- The comparisons show that the proposed constitutive model can satisfactorily represent the time-dependent mechanical behaviour of polymers in short term analysis. Both theoretically

presented models are able to predict short term responses with less than 5% error (in most cases).

- 5- Fitting results for both viscoelastic and viscoplastic material models show that the viscoelastic one yields a better fit for both short and long term modelling, and the reason is that the former one has more fitting parameters compared to viscoplastic one which results in more flexible fitting to the short term test data, so more accurate short term and long term response prediction.

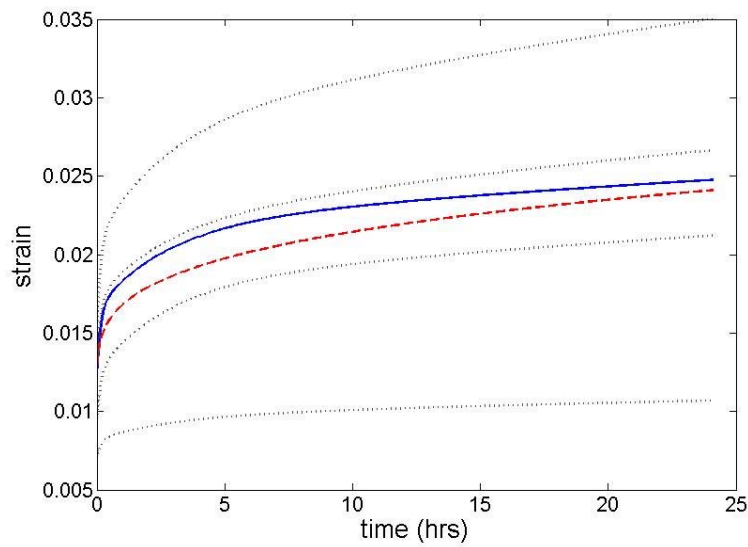


**Figure 23: Experimental (continuous line) (Liu, 2007), and present nonlinear viscoelastic model (dashed line) results for 24 hour creep test showing erroneous behaviour at 5.97 MPa (PIPE) using Eqs. (61), (64) and (66). Other stress levels are shown in grey (dotted lines)**

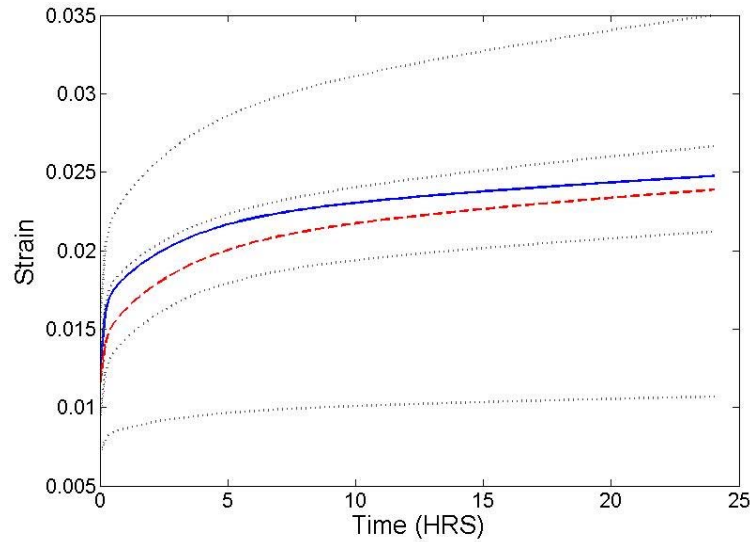


**Figure 24: Experimental (continuous line) (Liu, 2007), and present nonlinear viscoplastic model (dashed line) results for 24 hour creep test showing erroneous behaviour at 5.97 MPa (PIPE) using Eqs. (67) and (68). Other stress levels are shown in grey (dotted lines)**

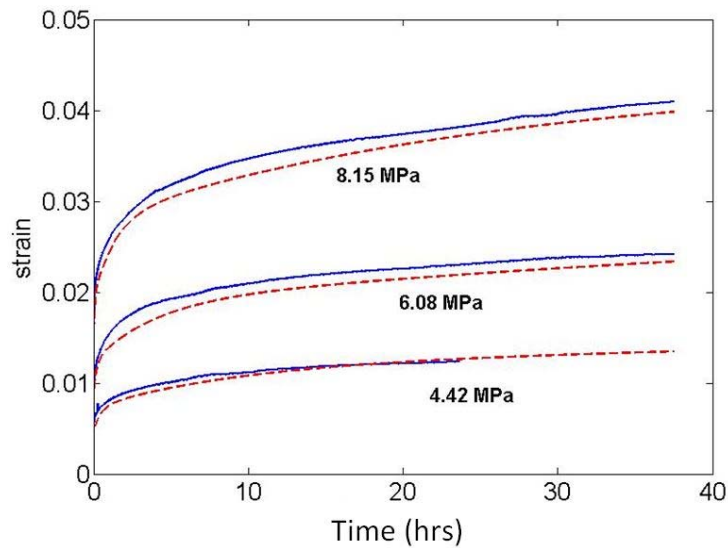


**Figure 25: Experimental (continuous line) (Liu, 2007), and present nonlinear viscoelastic model prediction (dashed line) in 40 hours test time (PIPE) using Eqs. (61), (64), (66) and (69). (Material properties and fitting parameters are cited in Table 4 and Table 9, respectively)**

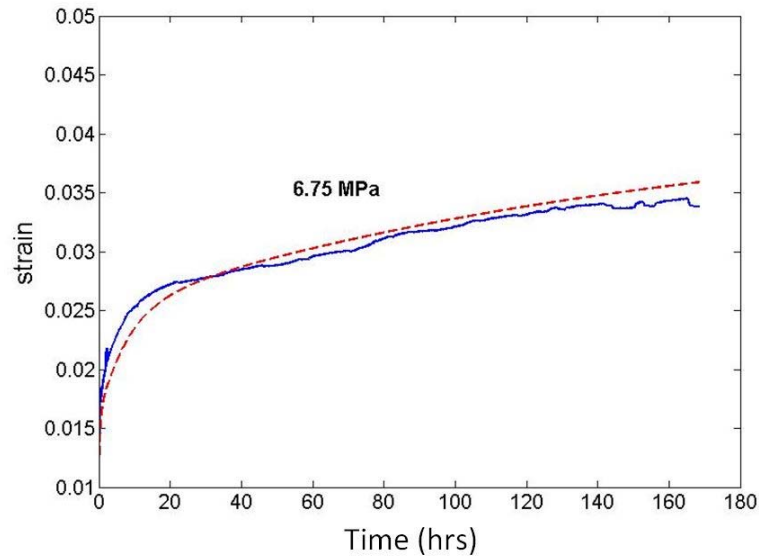


**Figure 26: Experimental (continuous line) (Liu, 2007), and present nonlinear viscoelastic model prediction (dashed line) in 7 days (170 hours) test time (PIPE) using Eqs. (61), (64), (66) and (69). (Material properties and fitting parameters are cited in Table 4 and Table 9, respectively)**

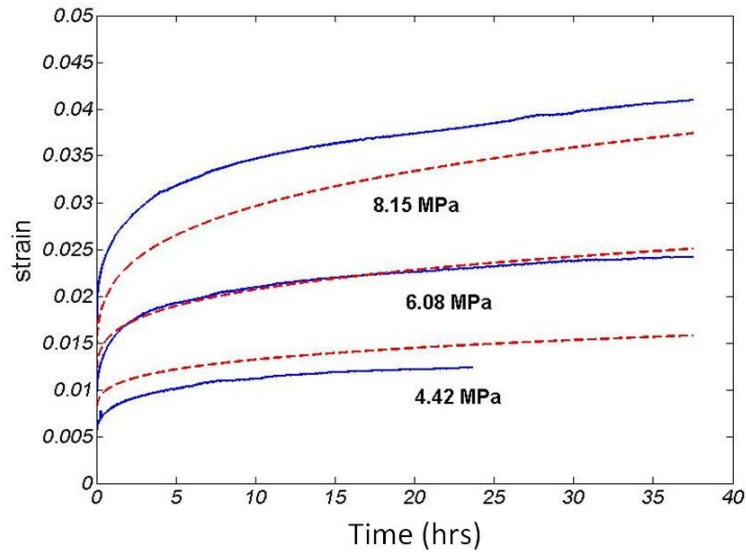


**Figure 27: Experimental (continuous line) (Liu, 2007), and present nonlinear viscoplastic model prediction (dashed line) in 40 hours test time (PIPE) using Eqs. (67), (68) and (70). (Material properties and fitting parameters are cited in Table 8 and Table 10, respectively)**

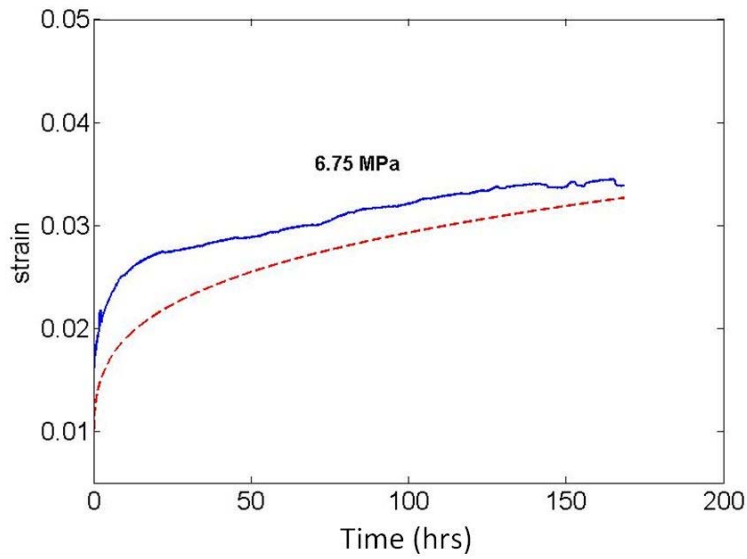


**Figure 28: Experimental (continuous line) (Liu, 2007), and present nonlinear viscoplastic model prediction (dashed line) in 7 days (170 hours) test time (PIPE) using Eqs. (67), (68) and (70). (Material properties and fitting parameters are cited in Table 8 and Table 10, respectively)**

No.	Material	Type	Thickness* (mm)	Width* (mm)	Code	$M_w$ (kg/mol)	$M_n$ (kg/mol)	ESCR (h)
1	HDPE-PIPE	pipe	5.00	13.05	PIPE	Data not available		
2	HDPE-Resin1	resin	5.80	12.76	RES1	127.5	16.3	4.8
3	HDPE-Resin2	resin	5.65	12.89	RES2	118.5	15.7	1.2
4	HDPE-Resin4	resin	6.27	12.42	RES4	79.4	19.7	3.6
5	MDPE-PE80	resin	5.04	12.76	PE80	202.1	14.0	198.3

\* These represent dogbone dimensions; allowance for thickness is  $\pm 0.03$ , and  $\pm 0.05$  for width

Table 2: Fitting parameters for  $X_0$

Material	$a_0$ (MPa <sup>-1</sup> )	$a_1$ (MPa <sup>-1</sup> )	$a_2$ (MPa <sup>-2</sup> )
PIPE	5.33e8	1.36e4	0.1864
RES1	7.25e8	2.31e8	0.0029
RES2	-5.82e13	5.82e13	4.7e-9
RES4	-3.83e13	3.83e13	1.9e-9
PE80	-5.07e8	1.25e8	4.3e-4

Table 3: Fitting parameters for NVE model								
	<b>m</b>	<b><math>\alpha</math></b>	<b><math>b_0</math> (MPa)</b>	<b><math>b_2</math></b>	<b><math>b_4</math> (MPa)</b>	<b><math>c_0</math> (s)</b>	<b><math>c_2</math></b> <b>(MPa<sup>-1</sup>)</b>	<b><math>c_4</math></b> <b>(MPa<sup>-3</sup>)</b>
			<b><math>b_1</math> (MPa)</b>	<b><math>b_3</math> (MPa<sup>-1</sup>)</b>		<b><math>c_1</math></b>	<b><math>c_3</math> (MPa<sup>-2</sup>)</b>	
<b>PIPE</b>	0.6816	15.78	-6224	3.24	49.9	2.04e-6	-0.606	0.0006
			329	0.798		-22.4	0.0118	
<b>RES1</b>	0.5563	16.83	7.486	7.702	423	1.7e-6	-0.584	0.00024
			0.2886	1.546		-18.23	0.0103	

Table 4: Material parameters for “PIPE” (Viscoelastic)				
<b><i>Stress (MPa)</i></b>	<b><i>Error (%)</i></b>	<b><i>E<sub>0</sub> (GPa)</i></b>	<b><i>X<sub>1</sub><sup>-1</sup> (GPa)</i></b>	<b><i><math>\tau_1</math> (s)</i></b>
<b>2.97</b>	7.2%	0.5469	2.571	294
<b>5.47</b>	2.9%	0.5418	2.645	90
<b>6.7</b>	3.9%	0.5368	2.662	55
<b>7.71</b>	5.1%	0.5310	2.671	39

Table 5: Material parameters for “Resin1” (Viscoelastic)				
<b><i>Stress (MPa)</i></b>	<b><i>Error (%)</i></b>	<b><i>E<sub>0</sub> (GPa)</i></b>	<b><i>X<sub>1</sub><sup>-1</sup> (GPa)</i></b>	<b><i><math>\tau_1</math> (s)</i></b>
<b>2.67</b>	5.3%	0.9445	3.967	337
<b>4.55</b>	7.1%	0.9010	3.997	127
<b>5.15</b>	2.6%	0.8804	4.002	94
<b>6.23</b>	4.2%	0.8392	4.009	55
<b>7.58</b>	1.7%	0.7898	4.015	29
<b>10.60</b>	3.1%	0.7325	4.022	7



Table 6: Fitting parameters for NVP model

Material	$b_1$ (MPa <sup>-1</sup> )	$b_3$ (MPa <sup>-3</sup> )	$b_5$ (MPa <sup>-1</sup> )	$m_1$	$s_a$ (MPa)	$d_0$
	$b_2$ (MPa <sup>-2</sup> )	$b_4$	$b_6$ (MPa <sup>-2</sup> )	$m_2$	$T_1$ (s)	
PIPE	-4.84E-04	-1.57E-05	-0.223	0.171	-0.015	-0.0236
	3.10E-04	0.052	0.020	0.053	39.5	
RES1	1.38E-03	1.47E-05	0.048	0.037	-0.108	-0.0483
	-2.86E-04	-0.007	0.022	0.140	-15162	

Table 7: Material parameters for “PIPE” (Viscoplastic)

<i>Stress (MPa)</i>	<i>Error (%)</i>	<i>E<sub>0</sub> (GPa)</i>	<i>C<sub>0</sub> (MPa<sup>-1</sup>)</i>	<i>T (s)</i>	<i>C<sub>1</sub></i>
<b>2.97</b>	1.8%	0.4302	0.00033	313.1	0.2472
<b>5.47</b>	4.3%	0.5332	0.00048	300.7	0.2585
<b>6.7</b>	5.9%	0.5332	0.00054	296.7	0.2610
<b>7.71</b>	6.4%	0.5332	0.00061	293.9	0.2626

Table 8: Material parameters for “Resin1” (Viscoplastic)

<i>Stress (MPa)</i>	<i>Error (%)</i>	<i>E<sub>0</sub> (GPa)</i>	<i>C<sub>0</sub> (MPa<sup>-1</sup>)</i>	<i>T (s)</i>	<i>C<sub>1</sub></i>
<b>2.67</b>	5.0%	0.9445	0.00073	10406.0	0.2392
<b>4.55</b>	3.7%	0.9010	0.00108	11506.2	0.2572
<b>5.15</b>	3.4%	0.8804	0.00114	11778.1	0.2601
<b>6.23</b>	7.2%	0.8392	0.00124	12208.5	0.2641
<b>7.58</b>	4.4%	0.7898	0.00139	12668.4	0.2674
<b>10.60</b>	3.4%	0.7325	0.00208	13495.2	0.2717

Table 9: Fitting parameters for NVE long term model						
Material	$b'_0$ (MPa)	$b'_1$ (MPa)	$b'_2$	$b'_3$ (MPa <sup>-1</sup> )	$b'_4$ (MPa)	$c'_0$ (s)
<b>PIPE</b>	-19972	72.7	6.772	0.5435	22.0	2.318e-06
<b>RES1</b>	9782	128.9	6.151	3.8827	272.7	3.414e-06
<b>RES2</b>	-4231	660.7	2.315	3.5057	-118.1	2.621e-06
<b>RES4</b>	5130	-331.6	28.539	0.5392	-378.2	1.1338e-06
<b>PE80</b>	-35906	445.1	6.044	0.6635	222.4	1.6682e-06

Table 9 (cont'd): Fitting parameters for NVE long term model						
Material	$d_0$	$d_1$	$d_2$	$d_3$	$d_4$	$d_5$
<b>PIPE</b>	0.8735	0.4802	-1.0359	2.7954	1.9781	-0.2065
<b>RES1</b>	-2.2412	0.6736	-0.2153	15.7128	-0.4458	-2.5547
<b>RES2</b>	-0.8276	-0.95436	0.21306	10.1362	3.7429	-0.1288
<b>RES4</b>	0.1035	0.8721	-1.5122	0.7342	7.4731	2.3958
<b>PE80</b>	-2.1686	-0.5946	-0.1970	0.5938	1.8661	0.4858

Table 10: Fitting parameters for NVP long term model										
Material	$b'_1$ MPa <sup>-1</sup>	$b'_2$ MPa <sup>-2</sup>	$b'_3$ MPa <sup>-3</sup>	$b'_4$	$b'_5$ MPa <sup>-1</sup>	$b'_6$ MPa <sup>-2</sup>	$m'_1$	$m'_2$	$s'_a$ MPa	$T'_1$ (s)
<b>PIPE</b>	-4.48E-04	3.08E-04	-1.67E-05	0.0521	- 0.2289	0.0210	0.1730	0.0510	- 0.015	43
<b>RES1</b>	1.31E-03	-2.73E-04	1.41E-05	- 0.0068	0.0507	0.0222	0.0365	0.1444	- 0.101	- 17679
<b>RES2</b>	7.05E-05	1.35E-04	-3.67E-07	- 0.0236	- 0.0078	0.0010	0.0211	0.1675	- 0.183	6538
<b>RES4</b>	1.22E-05	-1.83E-06	8.78E-08	- 0.0255	0.0274	0.0041	- 0.2245	0.3114	- 0.003	0
<b>PE80</b>	-2.17E-03	-7.89E-04	9.75E-04	- 0.0616	- 0.3767	0.0267	0.0836	0.0736	0.020	10635

Table 10 (cont'd): Fitting parameters for NVP long term model										
Material	$d_1$	$d_2$	$d_3$	$d_4$	$d_5$	$d_6$	$n_1$	$n_2$	$s$	$T_2$
<b>PIPE</b>	-0.024	0.025	0.002	-0.018	-0.002	-0.008	-0.018	-0.004	0.010	0.008
<b>RES1</b>	-0.048	0.014	0.014	0.014	0.008	-0.018	-0.006	0.006	-0.010	0.022
<b>RES2</b>	0.043	0.004	-0.045	-0.024	0.089	-0.009	0.036	0.002	-0.014	-0.032
<b>RES4</b>	0.048	-0.012	0.011	-0.004	-0.021	-0.042	-0.017	0.004	0.013	0.027
<b>PE80</b>	0.099	0.082	0.069	0.041	-0.035	0.009	-0.023	-0.029	0.060	-0.037

Table 11: Fitting error, PIPE material (test time of 40 hours, case I) per Eq. (71)			
<b>Stress</b>	<b>4.42 MPa</b>	<b>6.08 MPa</b>	<b>8.15 MPa</b>
<b>Error-NVE</b>	0.0896	0.0571	0.0367
<b>Error-NVP</b>	0.1600	0.0249	0.1247

Table 12: Fitting error, PIPE material (test time of 7 days, case II) per Eq. (71)	
<b>Stress</b>	<b>6.75 MPa</b>
<b>Error-NVE</b>	0.0287
<b>Error-NVP</b>	0.1308

## **Chapter 4**

### **Finite Element Implementation of Viscoelastic and Viscoplastic Models based on Multi-Integral Formulation**

This chapter presents finite element (FE) implementation of phenomenological three-dimensional viscoelastic and viscoplastic constitutive models for long term behaviour prediction of polymers. Multiple integral representation for three-dimensional behaviour, which is an extension of linear superposition to the nonlinear range, is employed. The method is based on the small strain assumption, but is extended to large deformation for materials in which the stress-strain relation is nonlinear and the concept of incompressibility is governing. An empirical approach is employed for determination of material parameters in the constitutive equations, based on measured material properties. The modelling process uses a spring and dash-pot, and a power-law approximation function method for viscoelastic and viscoplastic nonlinear behaviour, respectively. The model improvement for long term behaviour prediction is done by modifying the material parameters in such a way that they account for the current test time. The determination of material properties has its basis on the non-separable type of relations for nonlinear materials in which the material properties change with stress coupled with time. The proposed viscoelastic and viscoplastic models are implemented in a user material algorithm of the FE general purpose program ABAQUS and the validity of the models is assessed by comparisons with experimental observations from tests on HDPE samples in one-dimensional tensile loading (done by Liu (Liu, 2007)). Comparisons show that the proposed constitutive model can satisfactorily represent the time-dependent mechanical behaviour of polymers even for long term predictions.

#### **4.1 Introduction**

Modelling of polymeric materials can proceed with two general approaches: micro- and macro-mechanical. Micromechanical models emphasize the relation between the properties of materials and their microstructure. Examples of such models are works by Alvarado et al. (Alvarado, et al., 2010), Zehsaz et al. (Zehsaz, et al., 2014), Behzadfar et al. (Behzadfar, et al., 2013) and Popa et al. (Popa, et al., 2014). Such modelling can provide an excellent insight into what elements of molecular structure affect macro-scale behaviour and as such can guide in material manufacturing, processing and development.

In this chapter a macromechanical approach is presented. Such approach must be employed for predicting the mechanical response of polymers for structural analysis. In this approach, which is applied herein to semicrystalline polymers, the phenomenological models of viscoelastic/viscoplastic solids and/or irreversible thermodynamics with internal variables are employed. The theoretical formulation results in the evolution equation of stress or strain, which is formulated as a linear or nonlinear differential equation. The equation can be a function of time, stress or strain rate (time hardening theory) or strain, stress and strain rate (strain hardening theory).

Many researchers have carried out macromechanical investigations on polymers in the past two decades. Cheng, Polak and Penlidis (Cheng, et al., 2011) presented a rigorous statistical approach for modelling creep compliance of polyethylene (PE). They examined linear viscoelastic modelling using the multi-Kelvin element theory and compared test data with this theory in two forms: model linear in parameters and model nonlinear in parameters. In this work, and other similar theoretical investigations, experimental results play an important role, since they give insights into the material behaviour, and form the basis for model validation. Zhang and Moore performed extensive experimental work to characterize the nonlinear time-dependent response of the material tested under uniaxial compression (Zhang, et al., 1997). Drozdov and Christiansen reported their observations on uniaxial tensile tests with constant strain rates at moderate finite deformations, as well as in creep and relaxation tests on a thermoplastic elastomer (ethylene–octane copolymer) (Drozdof, et al., 2006) and polyethylene (Drozdov, et al., 2003). Liu et al. (Liu, et al., 2008) presented an approach for modelling mechanical behaviour of polyethylene materials where both viscoelastic and viscoplastic models were developed based on one-dimensional creep tests. The model corroboration was done by comparing results of tensile, step-loading, and load-rate creep with experimental ones. Ayoub et al. (Ayoub, et al., 2010), Ellyin et al. (Ellyin, et al., 2007), Cao et al. (Cao, et al., 2010), Wendlandt et al. (Wendlandt, et al., 2010) and Pan et al. (Pan, et al., 2012) also used experimental results for material parameters determination.

Rigorous numerical methods for predicting the material behaviour are necessary for analysis of materials and structural components. Generally, three features of usefulness of a numerical model can be described (Zhang, et al., 1997) as: 1) the constitutive model should be able to predict material response well for a wide range of loading histories; 2) the constitutive formulation should be simple and suitable for easy implementation in computer algorithms; and 3) the parameters in the model should be easily evaluated from experimental data.

Finite element implementation of constitutive equations, as a rigorous numerical method, has been researched in recent years. Kim et al. (Kim, et al., 2004) proposed a FE formulation for rubber under small oscillatory loads superimposed on large static deformations. Using a three-dimensional mixed finite element method with a nonlocal pressure field, Areias and Matous (Areias, et al., 2008) modeled nonlinear viscoelastic response of reinforced elastomers. Hasanpour and Ziaei-Rad ( (Hasanpour, et al., 2008) and (Hasanpour, et al., 2009)) also proposed constitutive equations and developed a finite element (FE) procedure implemented in a code to predict the response of elastomer bushings. Naghdabadi et al. (Naghdabadi, et al., 2012) also investigated the same material by developing a phenomenological finite strain viscoelastic constitutive model, within the framework of irreversible thermodynamics with internal variables. They implemented the proposed procedure into a user-defined subroutine UMAT in the nonlinear finite element software ABAQUS/Standard, which is applicable for compressible polymers and elastomers. These materials properties obey the Ogden hyperelastic model (Naghdabadi, et al., 2012). Some other works that used finite element programs for simulating viscoelastic or viscoplastic analysis can be found in (Krishnaswamy, et al., 1990), (Zienkiewicz, 1977) and (Hughes, et al., 1978).

The above presented models give satisfactory predictions within the short term. One of the most known methods for predicting long term behaviour of polymers is based on the Time Temperature Superposition Principle (TTSP), which is in its turn based on short term behaviour and uses the information from short duration tests at different temperatures. The method uses the similarity of the variation of relaxation modulus (creep compliance) with time and temperature. The variations in time and temperature of the moduli (compliances) of a polymer are related (Brinson, et al., 2008). This method provides a master curve, which is shifted to longer term using a shift factor. Numerous works have been done on predicting long term response of polymers and characterizing the shift factor. Gupta et al. (Gupta, et al., 2012) extended an effective time framework to successfully demonstrate a time-temperature superposition of creep and stress relaxation data of a soft glassy system comprised of a clay suspension. Diani et. al (Diani, et al., 2015) characterized the time-temperature superposition property of an amorphous polymer acrylate network. Tajvidi et. al (Tajvidi, et al., 2005) applied the method to viscoelastic properties of a high-density polyethylene (HDPE) composite, and tested its validity. Other sample works are from Li (Li, 2000), Nguyen et. al (Nguyen, et al., 2013) and Naya et. al (Naya, et al., 2013).

Although many works have been done on the TTSP method for predicting the long term behaviour of polymers, to the best of our knowledge, no work is available on methods other than TTSP, and this research aims to fill this gap by providing an efficient empirical approach considering that one means of generating relevant design data is to investigate prototype structures.

In this chapter a finite element implementation of phenomenological three-dimensional viscoelastic and viscoplastic constitutive models are presented for polymeric materials. This procedure can be used to predict the nonlinear response of material for long term problems, which is beyond the experimental time-frame. For this the following steps are taken:

- 1- Model definition is done based on Multi Integral approach (section 4.2)
- 2- Constitutive equations are simplified based on the following assumptions (section 4.2):
  - Full incompressibility
  - Superposition of small to large deformation (Boltzmann's superposition)
  - Simplification of material functions
- 3- Material/kernel functions ( $K_2$ ,  $K_6$ , and  $K_{12}$ ) are approximated as follows (section 4.3):
  - Exponential form of equations for Viscoelastic behaviour
  - Power law form of equations for Viscoplastic behaviour
- 4- Empirical approach is used for defining the fitting parameters (section 4.3)
- 5- Model parameters are optimized for long term prediction (section 4.4)
- 6- Models are implemented in FE user subroutine (section 4.5)
- 7- The presented models results are validated (section 4.6)

In section 4.2 (steps 1 and 2), a multiple integral approach, which in a sense is an extension of Boltzmann's linear superposition principle to the nonlinear range (Findley, et al., 1976), will be employed for three-dimensional behaviour of viscoelastic and viscoplastic materials. Boltzmann's superposition principle states that the sum of the strain outputs resulting from each component of stress input is the same as the strain output resulting from the combined stress input (Figure 18). This principle is widely used in viscoelastic, viscoplastic and plasticity descriptions of materials' behaviour (Findley, et al., 1976). The current research benefits from some simplifications of the constitutive equations,



namely the assumption of fully incompressible behaviour, the superposition of small time dependent deformation on large deformation, and finally the simplification of the material functions (see section 4.3).

The resulting constitutive equations include unknown kernel functions (material functions), which are defined in section 4.3. First, the estimation process (step 3) uses the spring and dash-pot, exponential form, and plasticity power-law function methods for viscoelastic and viscoplastic modelling, respectively. The determination of material properties is based on the non-separable nature of relations for nonlinear materials in which the material properties change with stress coupled with time. Then, the equations describing material behaviour are modified based on the measured material properties (tests done by Liu (Liu, 2007)) through an empirical approach (step 4). For this, the resulting equations are fitted to experimental data and fitting parameters are obtained.

In section 4.4, the models are optimized for predicting long term responses, which is beyond the test time (step 5). The resulting models are able to predict the behaviour of both viscoelastic and viscoplastic materials for extended times and can be implemented in finite element procedures (step 6). The procedure is presented in section 4.5 which is the implementation of the developed material models into a user-defined material algorithm in Abaqus (UMAT).

Steps 3, 4 and 5 (sections 4.3 and 4.4), in which deal with material model functions and parameters and nonlinearization for long term prediction, use the information provided in Chapter 3, and the formulations, graphs and parameters in tables associated with this concept are all repetitions from Chapter 3. The repetitions are intentionally, as the author intends to keep this chapter independently conveyer of the proposed concept in the chapter.

The current version of the commercial software Abaqus allows only linear viscoelastic modelling, which can be used for both small and large strain problems. It has to be used in conjunction with linear elastic behaviour or hyperelastic behaviour. Material properties are defined either by a specification of Prony series parameters, or by an inclusion of creep, relaxation or frequency test data. The built-in procedure in Abaqus software is not able to analyze the nonlinear behaviour of viscoelastic and viscoplastic materials. Noting that nonlinear time domain analysis requires application of time- and stress-dependent material properties, a specific procedure needs to be defined, which justifies the application of user generated subroutines for material definition in this work.

The validity of the models is assessed by comparison with experimental observations on high density polyethylene (HDPE) specimens under uniaxial loading (done by Liu (Liu, 2007)), in section 6 (step 7). The comparisons show that the proposed constitutive model can satisfactorily represent the time-dependent mechanical behaviour of polymers.

## 4.2 The Constitutive Model

Polymeric materials exhibit remarkable time dependent viscous behaviour. It is therefore difficult to distinguish an elastic deformation regime from a viscous regime simply from the stress–strain, creep or relaxation curves. Part of the elastic deformation is recoverable during and after the unloading while some parts are permanent. Experimental observations show that the mechanical behaviour can be decomposed into two parts: an elastic and a rate-dependent response (Hasanpour, et al., 2009). In other words, the material can be modelled as a combination of elements representing both elastic (spring) and viscous (dash-pot) responses. In general, the three-dimensional behaviour of both viscoelastic and viscoplastic materials can be described by:

$$\dot{\varepsilon}_{ij} = \beta_{ij}(\sigma_{kl}, \varepsilon_{kl}) \quad (73)$$

which has its basis on the strain hardening phenomenon, and can also be equivalently described by the following:

$$\dot{\varepsilon}_{ij} = g_{ij}(\sigma_{kl}, t) \quad (74)$$

Where Eq. (74) indicates the time hardening phenomenon. Here  $\dot{\varepsilon}_{ij}$  is the strain rate and  $\beta_{ij}$  and  $g_{ij}$  are functions of stress,  $\sigma_{kl}$ , and strain  $\varepsilon_{kl}$  or time,  $t$ , respectively.

This constitutive model requires to define the field equations to analyze three-dimensional problems. For a viscoelastic domain,  $V$ , under a constant sustained load, the solution procedure involves finding the displacement and the stress tensor for each point of the domain ( $x_1, x_2 \in V$ ) in time  $t$ . The displacement vector  $u_i(x_1, x_2, t)$  and the stress tensor  $\sigma_{ij}(x_1, x_2, t)$  need to satisfy the kinematic relation between strains and displacements and equations of static equilibrium, respectively. The relationship between strains and stresses is governed by either Eq. (73) or Eq. (74), which is the constitutive relation for all times  $t$  and  $x_1, x_2 \in V$ . The solution must also satisfy the specified initial conditions at time  $t = 0$ , the traction boundary conditions, and the displacement boundary conditions (Krishnaswami, et al., 1992).

Nonlinear materials can be categorized by determining whether the effects of stress,  $\sigma$ , and time,  $t$ , on the strain,  $\varepsilon$ , are separable or not. If all observed compliance curves for nonlinear materials have the same shape, the material obeys nonlinear-separable model, i. e. same function for all stresses. In this case,  $\varepsilon$  is given by the following equation (Krishnaswamy, et al., 1992)

$$\varepsilon_{ij} = h_{ij}(\sigma_{kl})f(t) \quad (75)$$

where  $h_{ij}$  is a function of stress and is associated with  $\varepsilon_{ij}$ , and  $f(t)$  represents a function of time. Otherwise, if the shapes of compliance curves, at all stress levels, are not similar, then  $\varepsilon$  must be represented by a different function of time at each stress level. In this case, the material can only be described by the general form of nonlinear non-separable model given by Eq. (74) (Krishnaswamy, et al., 1992). For linear materials, the strain is linearly related to the stress. If the variation of the Poisson's ratio with time is negligible, as in the case of ductile polymers, Eq. (74) can be written as:

$$\varepsilon_{ij} = \sigma_{ik} \chi_{kj}(t) \quad (76)$$

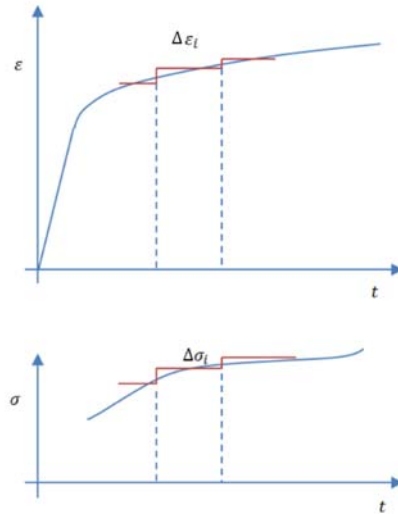


**Figure 29: Strain resultant due to the assumed constant stress increments. Representation of superposition Principle.**

where  $\chi(t)$  is time dependent relaxation compliance. Discretizing the above relation for small changes of strain due to a constant stress in a small time interval and for one-dimensional case, yields the following formula, which represents the resultant strain shown in Figure 18.

$$\Delta\varepsilon_i(t) = (\Delta\sigma_i) \chi(t) \quad (77)$$

Here  $\varepsilon_i$  is a resulting constant strain due to small change in constant stress,  $\Delta\sigma_i$ .

Eq. (77) is a representation of Hooke's law. If a nonlinear material is stretched beyond its elastic limit, a plastic deformation contributes in the resultant response, meaning that the material doesn't return to its original shape when the applied force is removed. It will permanently deform and will no longer obey Hooke's law. Polymers do not obey Hooke's law when they are deformed. With reference to the Boltzmann's superposition principle, which states that the sum of the strain outputs resulting from each component of stress input is the same as the strain output resulting from the combined stress input, in discretized model, the time-dependent strain resulting from a nonlinear constant stress may be represented by a polynomial as: (Findley, et al., 1976)

$$\varepsilon_i(t) = (\Delta\sigma_i)\chi_1(t) + (\Delta\sigma_i)^2 \chi_2(t) + (\Delta\sigma_i)^3 \chi_3(t) + \dots \quad (78)$$

This equation is a multi-order discrete constitutive equation and  $\chi_i$  are time dependent material functions (with inverse stress unit). By increasing the order of the equation in RHS, the accuracy increases. The Eq. (78) can be further expanded to  $N$  steps of stress change, as follows:

$$\begin{aligned} \varepsilon(t) = & \sum_{i=0}^N (\Delta\sigma_i)\chi_1(t - t_i) + \sum_{i=0}^N \sum_{j=0}^N (\Delta\sigma_i)(\Delta\sigma_j)\chi_2(t - t_i, t - t_j) \\ & + \sum_{i=0}^N \sum_{j=0}^N \sum_{k=0}^N (\Delta\sigma_i)(\Delta\sigma_j)(\Delta\sigma_k)\chi_3(t - t_i, t - t_j, t - t_k) + \dots \end{aligned} \quad (79)$$

If all  $\chi_i$ , except  $\chi_1$ , vanish for all time arguments, Eq. (79) becomes the Boltzmann linear superposition principle. This equation can be considered as an extension of the linear superposition principle by adding the nonlinear effect (Findley, et al., 1976). Eq. (79) models only a limited number of stress changes, thus the integral form of total resultant strain at current time,  $\varepsilon(t)$ , for the case of varying stress,  $\sigma$ , for time  $t$ , would be (Findley, et al., 1976):

$$\begin{aligned} \varepsilon(t) = & \int_0^t \chi_1(t - \xi_1) \dot{\sigma}(\xi_1) d\xi_1 + \int_0^t \int_0^t \chi_2(t - \xi_1) \chi_2(t - \xi_2) \dot{\sigma}(\xi_1) \dot{\sigma}(\xi_2) d\xi_1 d\xi_2 \\ & + \int_0^t \int_0^t \int_0^t \chi_3(t - \xi_1) \chi_3(t - \xi_2) \chi_3(t - \xi_3) \dot{\sigma}(\xi_1) \dot{\sigma}(\xi_2) \dot{\sigma}(\xi_3) d\xi_1 d\xi_2 d\xi_3 \\ & + \dots \end{aligned} \quad (80)$$

which is a multi-integral representation of the constitutive equation (Eq. (76)) in one-dimension (uniaxial). Here  $\xi$  is an integration variable (has time unit), and  $\dot{\sigma}(\xi)d\xi$  is introduced instead of  $d\sigma(\xi)$ .

The resulting uniaxial nonlinear constitutive relation can be extended to a three-dimensional stress state by representing the stress tensor as summation of a volumetric stress,  $\sigma_v$ , and the deviatoric stress,  $s_{ij}$ , which is  $\sigma_{ij} = \sigma_v\delta_{ij} + s_{ij}$ . Therefore, all possible terms of the strain for isotropic materials can be expressed as volumetric and deviatoric effects. After some mathematical manipulations, the resulting relation will be a  $N$ -order constitutive equation for creep strain in terms of stress history (see (Findley, et al., 1976) for details).

When a state of stress (or strain) is applied abruptly at time  $t = 0$ , and is held constant for a time period, then within that period, all time parameters in the kernel functions reduce to  $t$  instead of  $(t - \xi_i)$  and the integrals may be evaluated by means of the Dirac delta function  $\delta(t)$  for which  $\dot{\sigma}(\xi) = \sigma\delta(\xi)$  for creep (with constant stress) and  $\dot{\epsilon}(\xi) = \epsilon\delta(\xi)$  for relaxation (with constant strain). Applying these relations, the following nonlinear relation for creep at multi-dimensional constant stress can be derived (Findley, et al., 1976):

$$\begin{aligned} \boldsymbol{\epsilon}(t) = & \mathbf{I} (K_1 \text{tr}(\boldsymbol{\sigma}) + K_3 \text{tr}(\boldsymbol{\sigma})\text{tr}(\boldsymbol{\sigma}) + K_4 \text{tr}(\boldsymbol{\sigma}\boldsymbol{\sigma}) + K_7 \text{tr}(\boldsymbol{\sigma}\boldsymbol{\sigma}\boldsymbol{\sigma}) + \\ & K_8 \text{tr}(\boldsymbol{\sigma}\boldsymbol{\sigma})\text{tr}(\boldsymbol{\sigma})) + \boldsymbol{\sigma}(K_2 + K_5 \text{tr}(\boldsymbol{\sigma}) + K_9 \text{tr}(\boldsymbol{\sigma})\text{tr}(\boldsymbol{\sigma}) + K_{10} \text{tr}(\boldsymbol{\sigma}\boldsymbol{\sigma})) + \boldsymbol{\sigma}^2(K_6 + \\ & K_{11} \text{tr}(\boldsymbol{\sigma})) + \boldsymbol{\sigma}^3 K_{12} + \dots \end{aligned} \quad (81)$$

where  $\text{tr}(\boldsymbol{\sigma})$  is the trace of the tensor  $\boldsymbol{\sigma}$  and the bold notation indicates three-dimensional tensors. Eq. (81) consists of  $N(N + 1)$  unknown kernel functions,  $K_i$ , where  $K_i$  are functions of time:

$$\begin{aligned} K_i = & K_i(t - \xi_1, t - \xi_2, t - \xi_3, \dots, t - \xi_n), \\ i = & n(n - 1) + 1 \sim n(n + 1) \end{aligned} \quad (82)$$

where  $n$  indicates the  $n^{\text{th}}$  term of the polynomial.  $K_i$  are material parameters, which are defined from experiments.

In the presented superposition model some assumptions are applied, namely the material is taken to be isotropic and the stress and strain are zero prior to time  $t = 0$ . In addition, the assumption of incompressibility is employed which simplifies the equations by decreasing the number of unknown Kernel functions,  $K_i$ . An incompressible material is defined as one whose response to stressing or straining is insensitive to volumetric type changes in strain or stress. This means the relation between the volumetric strain and stress is uncoupled. In the creep formulation, incompressibility implies that

1) a volumetric stress  $\sigma_v$  (mean normal stress or negative pressure) has no effect on the total strain, and  
 2) the total stress has no effect on volumetric type strain  $\varepsilon_v$ . The stress tensor  $\sigma(t)$  may be written in terms of the deviatoric stress tensor  $s(t)$  and the volumetric stress,  $\sigma_v(t)$ , which is  $\sigma_{ij} = \sigma_v \delta_{ij} + s_{ij}$ . Also  $tr s = 0$  and  $\sigma_v = \sigma_{kk}/3 = -p$  and  $p$  is the hydrostatic pressure. Therefore:

$$\begin{aligned}
 \boldsymbol{\sigma} &= \mathbf{s} + \mathbf{I}\sigma_v \\
 tr(\boldsymbol{\sigma}) &= tr(\mathbf{s}) + 3\sigma_v \\
 \boldsymbol{\sigma}^2 &= \mathbf{s}^2 + 2\mathbf{s}\sigma_v + \mathbf{I}\sigma_v^2 \\
 tr(\boldsymbol{\sigma}^2) &= tr(\mathbf{s}^2) + 3\sigma_v^2 \\
 \boldsymbol{\sigma}^3 &= \mathbf{s}^3 + 3\mathbf{s}^2\sigma_v + 3\mathbf{s}\sigma_v^2 + \mathbf{I}\sigma_v^3 \\
 tr(\boldsymbol{\sigma}^3) &= tr(\mathbf{s}^3) + 3tr(\mathbf{s}^2)\sigma_v + 3\sigma_v^3
 \end{aligned} \tag{83}$$

Substituting in Eq. (81) we have

$$\begin{aligned}
 \boldsymbol{\varepsilon}(t) &= \mathbf{I}\hat{\boldsymbol{\varepsilon}} + \mathbf{I}(3K_1 + K_2)\sigma_v + K_2\mathbf{s} + \mathbf{I}(9K_3 + 3K_4 + 3K_5 + K_6)\sigma_v^2 + (3K_5 + \\
 &2K_6)\mathbf{s}\sigma_v + \mathbf{I}K_4tr(\mathbf{s}^2) + K_6\mathbf{s}^2 + \mathbf{I}(3K_7 + 9K_8 + 9K_9 + 3K_{10} + 3K_{11} + \\
 &K_{12})\sigma_v^3 + (9K_9 + 3K_{10} + 6K_{11} + 3K_{12})\mathbf{s}\sigma_v^2 + \mathbf{I}(3K_7 + 3K_8 + K_{10})\mathbf{s}^2\sigma_v + \\
 &\mathbf{I}K_7tr(\mathbf{s}^3) + K_{10}\mathbf{s}tr(\mathbf{s}^2) + K_{12}\mathbf{s}^3
 \end{aligned} \tag{84}$$

where  $\hat{\boldsymbol{\varepsilon}}$  is any non-stress induced volumetric strain (Findley, et al., 1976). The incompressibility assumption requires the coefficients of terms containing  $\sigma_v$  to be zero. This removes all kernel functions except  $K_2$ ,  $K_6$ , and  $K_{12}$ . Therefore, the final nonlinear relation for constant stress reduces to a simplified form of:

$$\boldsymbol{\varepsilon}(t) = \boldsymbol{\sigma}(K_2) + \boldsymbol{\sigma}^2(K_6) + \boldsymbol{\sigma}^3K_{12} + \dots \tag{85}$$

Here it is rewritten as

$$\boldsymbol{\varepsilon}(t) = \boldsymbol{\sigma}\Psi_0(t) + \boldsymbol{\sigma}^2\Psi_1(t) + \boldsymbol{\sigma}^3\Psi_2(t) + \dots \tag{86}$$

This equation represents the contribution of elastic as well as inelastic portions of the behaviour of material to the final resultant strain. By removing the higher order terms, the relation simply reduces to the linear elastic Hook's relation  $\boldsymbol{\varepsilon}(t) = \boldsymbol{\sigma}\Psi_0$ .

The form given in Eq. (86) is the same as derived by a different method by Locket and Strafford (Spencer, et al., 1959). They also found three independent kernel functions are required for calculation of finite strain. By observing the trend of terms in Eq. (86) and considering higher orders of nonlinearity in Eq. (77), one can come up with the following general relation for incompressible viscoelastic/viscoplastic materials

$$\boldsymbol{\varepsilon}(t) = \boldsymbol{\sigma} \left( \Psi_0(t) + \sum_{n=1}^N \boldsymbol{\sigma}^n \Psi_n(t) \right) \quad (87)$$

$N$  is the order of the nonlinear part.

The next step is determination of unknown functions which is done by curve fitting of the model to one-dimensional creep tests. This yields the nonlinear one-dimensional form of a constitutive equation for constant stress. This form will then be used to construct 3-D constitutive equations, which is the final goal of this investigation. This procedure will be explained in the following.

### 4.3 Determination of material functions

A number of tests were done by Liu (Liu, 2007) at the University of Waterloo, on high density and medium density polyethylene materials. Experiments were performed on five types of PEs and included tests on: short term tensile creep (24 hours), long term creep (7 days and 14 days), creep with step loading, constant stress rate, constant strain rate, and complex load history tests (Liu, et al., 2008). The specimens were produced from resins by melting them and machining, and from pipes by cutting out the samples (Table 13). 24-hour creep testing was done at different stress levels to examine time dependent and nonlinear behaviour of the materials. The testing showed clear differences in the behaviour of different HDPEs. Based on the measured strain values under different stress levels and observing creep compliance  $D(t) = \boldsymbol{\varepsilon}(t)/\boldsymbol{\sigma}$  diagrams versus time (Liu, et al., 2008), it can be inferred that polyethylenes show high degree of material nonlinearity and time dependency. Comparing the compliance curves in terms of similarity reveals that they cannot be separated by two stress dependent and time dependent terms. This leads to the conclusion that the final constitutive equation of polyethylene is a nonlinear-non-separable relationship (Eq. (74)).

Such uniaxial creep tests provide a straightforward way to determine the material parameters. The method is to minimize the Least Squares Error by fitting Eq. (87) to the experimental results and

determining material functions  $\Psi_i$ . For this, a one-dimensional form needs to be extracted from Eq. (87) which is the following:

$$\varepsilon_{11}(t) = \sigma_{11} \left( \Psi_0(t) + \sum_{n=1}^N \sigma_{11}^n \Psi_n(t) \right) \quad (88)$$

Subscript “11” indicates the component of the tensor in the axial direction. The first step in determination of the material properties is finding a good approximation for the time functions,  $\Psi_i(t)$ .

Table 13: List of tested polyethylene (Liu, 2007)								
No.	Material	Type	Thickness* (mm)	Width** (mm)	Code	$M_w$ (kg/mol)	$M_n$ (kg/mol)	ESCR (h)
1	HDPE-PIPE	pipe	5.00	13.05	PIPE	Data not available		
2	HDPE-resin1	resin	5.80	12.76	RES1	127.5	16.3	4.8
3	HDPE-resin2	resin	5.65	12.89	RES2	118.5	15.7	1.2
4	HDPE-resin4	resin	6.27	12.42	RES4	79.4	19.7	3.6
5	MDPE-PE80	resin	5.04	12.76	PE80	202.1	14.0	198.3

\*  $\pm 0.03$

\*\*  $\pm 0.05$

The more the “time functions” make sense physically, the more realistic the model will be. Understanding the theory behind the behaviour of the investigated material is helpful. Below, viscoelastic and viscoplastic approaches are discussed. In viscoelastic theory, constitutive equations are usually formulated using one of the differential or integral forms (Lockett, 1972). In contrast to the differential formulation (simulating the behaviour by spring and dash-pot elements configuration), which involves only the current values of stress and strain and their current time rates, the integral form takes into account the history of loading and is more accurate and strict in nonlinear modelling. The most useful analysis in finite element applications is the spring and dash-pot method of modelling described by Flugge (Flugge, 1967). According to the concept of fading memory (Bodner, 1984), the material response depends more on recent history than on earlier events. Accordingly, this theory considers the exponential formulation for most nonlinear materials, such as HDPE, for which the effects of stress and time on the resulting strain are not separable.



Another approach is the viscoplastic theory with a nonlinear time dependent power-law function, which doesn't have an asymptote, in contrast to the viscoelastic model, which approaches an asymptotic limit. Both the viscoelastic and viscoplastic formulations are usually an extension of the theory, which considers permanent residual strain by assuming the rate of total strain as summation of elastic and plastic strain rates. In this research, the expressions shown in Eq. (89) and Eq. (90) are considered as  $\Psi_n(t)$  for both viscoelastic and viscoplastic models, respectively:

$$\Psi_0(t) = X_0 , \quad \Psi_n(t) = A_n(1 - e^{-t/\tau_n}) \quad (89)$$

$$\Psi_0(t) = X_0 , \quad \Psi_n(t) = B_n \left(\frac{t}{T}\right)^{C_n} \quad (90)$$

where  $A_n$ ,  $\tau_n$ ,  $B_n$  and  $C_n$  are material parameters.  $A_n$  and  $B_n$  have same unit as compliance, and  $\tau_n$  and  $T$  have time unit, and  $C_n$  has no unit.

Developing the model for viscoelastic behaviour is done by substituting Eq. (89) in Eq. (88) and then the viscoplastic modelling follows by the substitution of Eq. (90).

By substituting Eq. (89) in Eq. (88) one can find the following constitutive equation for viscoelastic uniaxial response.

$$\varepsilon(t) = \sigma \psi(t, \sigma) = \sigma \left[ X_0 + \sum_{n=1}^N X_n(\sigma)(1 - e^{-t/\tau_n}) \right] \quad (91)$$

which  $X_n = A_n \sigma^n$ . In this formulation  $\psi(t, \sigma)$  is the creep compliance,  $N$  is the number of approximation terms that is equivalent to the number of Kelvin units in spring and dash-pot modelling,  $X_0 = 1/E_0$  is the elastic time-independent compliance at time  $t_0 = 0$ , which is unknown and is obtained from experimental results, for each test.  $X_n$  and  $\tau_n$  are the equivalent creep compliance and the relaxation time, respectively, for the  $n^{th}$  Kelvin element (see (Flugge, 1967) for more detail).

For the uniaxial tension case, the stress in the entire deformation is constant and equal to the applied stress  $\sigma$ . Hence  $X_0$  and  $X_n$  are constant. In such a case the stress does not vary within the domain, the spatial gradients of stress and, hence, compatibility, are automatically satisfied and the stress does not redistribute within the domain for a uniaxial tensile specimen. For other geometries, wherein the gradients in stresses are small, redistribution of stresses with time may be negligible. However, in regions of high stress gradients there may be significant redistribution in stress. Use of the non-

separable form (where  $X_0$ ,  $X_n$  and  $\tau_n$  are functions of stress) in the constitutive model makes it possible to take high stress gradients into account. In the following, a procedure which defines the stress- and time-dependent fitting functions is presented.

Most finite element implementations of this form assume that the creep compliance has the exponential form of Eq. (91), which is a form of a Prony series approximation, with  $2 \times N$  unknown material properties ( $X_n$  and  $\tau_n$ ). The term  $E_0 = 1/X_0$  is called an independent term. One can obtain parameter values using least squares estimation by fitting the Prony series to experimental data by either fixing a set of  $\tau_n$  (Hildebrand, 1974) or pre-setting either  $X_n$  or  $\tau_n$  as power law functions of  $t$  (Liu, et al., 2008) & (Sepiani, et al., 2017)). Thus, it is possible to estimate values for  $\tau_n$  as well as  $X_n$  and at the same time secure high degree of accuracy in final governing equations.

In this research,  $X_n$  and  $\tau_n$  are approximated by power-law functions of stress. To reduce the number of material functions, which is equal to  $2 \times N$ , all values of  $X_n$  and  $\tau_n$  are obtained using four parameters  $X_1$ ,  $\tau_1$ ,  $m$  and  $\alpha$

$$A_n = \left(\frac{\sigma}{\tilde{m}}\right)^{n-1} A_1, \quad \tau_n = \alpha^{n-1} \tau_1 \quad (92)$$

Here  $\tilde{m}$  is set to be a function of stress,  $\tilde{m} = m\sigma$ , and for simplicity,  $\alpha$  and  $m$  are considered to be stress-independent parameters with no unit dimension. To account for high stress gradients,  $X_0$ ,  $X_1$  and  $\tau_1$  are considered to be in the following form of stress dependent approximation functions.

$$X_0 = (a_0 + a_1 e^{-a_2 \hat{\sigma}^3})^{-1} \quad (93)$$

$$(a) \quad A_1 = \sigma [b_0 + b_1 \exp(b_2 - b_3 \hat{\sigma} - b_4 / \hat{\sigma})]^{-1} \quad (94)$$

$$(b) \quad \tau_1 = c_0 \exp(-c_1 + c_2 \hat{\sigma} + c_3 \hat{\sigma}^2 - c_4 \hat{\sigma}^3)$$

Here  $\hat{\sigma}$  is  $\sigma \times 10^{-6}$  for simplicity.  $a_0$  and  $a_1$  have unit of compliance and  $a_2$  has unit of inverse of cubic stress.  $b_0$  and  $b_1$  have stress unit,  $b_2$  has no unit,  $b_3$  has inverse unit of stress and  $b_4$  has unit of stress.  $c_0$  has unit of time,  $c_1$  has no unit,  $c_2$  has unit of inverse of stress,  $c_3$  has unit of inverse of squared stress, and  $c_4$  has unit of inverse of cubic stress. The parameters  $a_i$ ,  $b_i$ ,  $c_i$ ,  $m$  and  $\alpha$  are obtained via minimizing the least squares error for the examined HDPE pipe sample material (Liu, 2007). For this a code is developed in MATLAB workspace, which allows fitting the model to the test data with an optimization technique, which estimates the fitting parameters from experimental data. The fitting parameters  $a_i$ ,  $b_i$ ,  $c_i$ ,  $m$  and  $\alpha$  are cited in Table 14 and Table 15, for all materials, considering  $N = 6$ .

Figure 30 and Figure 31 show examples of fitting the proposed model (Eq. (91)) to experimental data for PIPE and RES1.

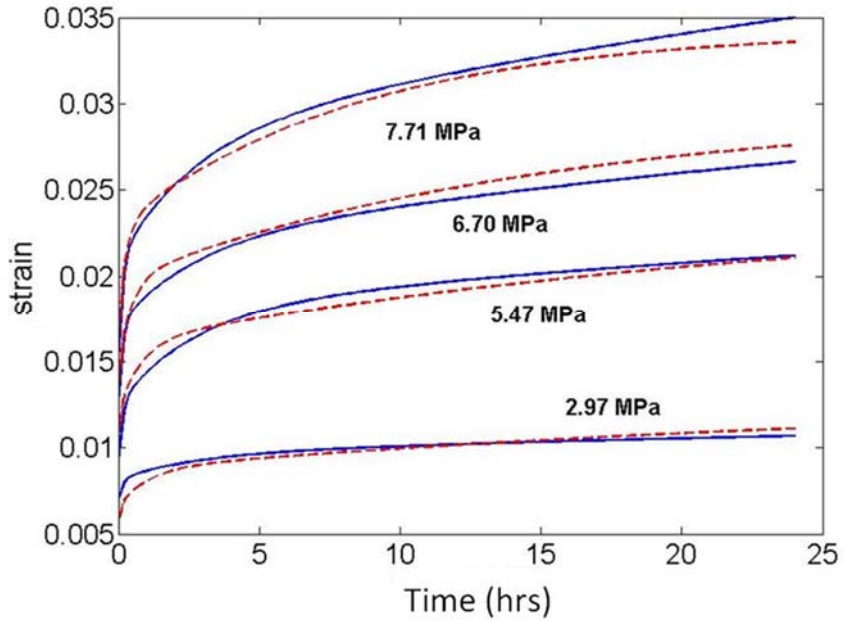


**Figure 30: Experimental (continuous line) (Liu, 2007), and nonlinear viscoelastic model (dashed line) results for 24 hour creep tests (PIPE)**

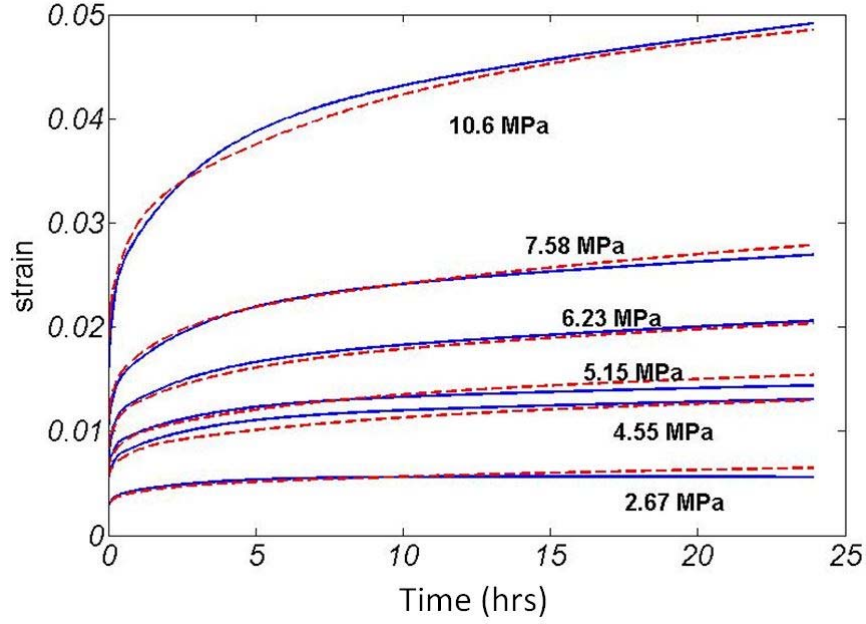


**Figure 31: Experimental (continuous line) (Liu, 2007), and nonlinear viscoelastic model (dashed line) results for 24 hour creep tests (RES1)**

Similar to viscoelasticity, in the theory of viscoplasticity, the total strain rate is considered to be decomposable into elastic and inelastic components, which matches our consideration for linear and nonlinear portions of behaviour in Eq. (86), which is  $\varepsilon_{ij} = \varepsilon_{ij}^e + \varepsilon_{ij}^p$ . From the literature (Krishnaswamy, et al., 1992), a power law function can describe the nonlinear viscoplastic creep behaviour. This function is able to model the growing deformation (strain) at decreasing rate, which doesn't approach an asymptotic value and the material remains time-dependent. Here we consider the following power-law relationship for resultant strain ( (Krishnaswamy, et al., 1992) & (Liu, et al., 2008)).

$$\varepsilon(t) = \sigma \psi(t, \sigma) = \sigma \left[ X_0 + \sum_{n=1}^N X_n(\sigma) \left( \frac{t}{T} \right)^{C_i} \right] \quad (95)$$

where  $X_n = B_n \sigma^n$ .

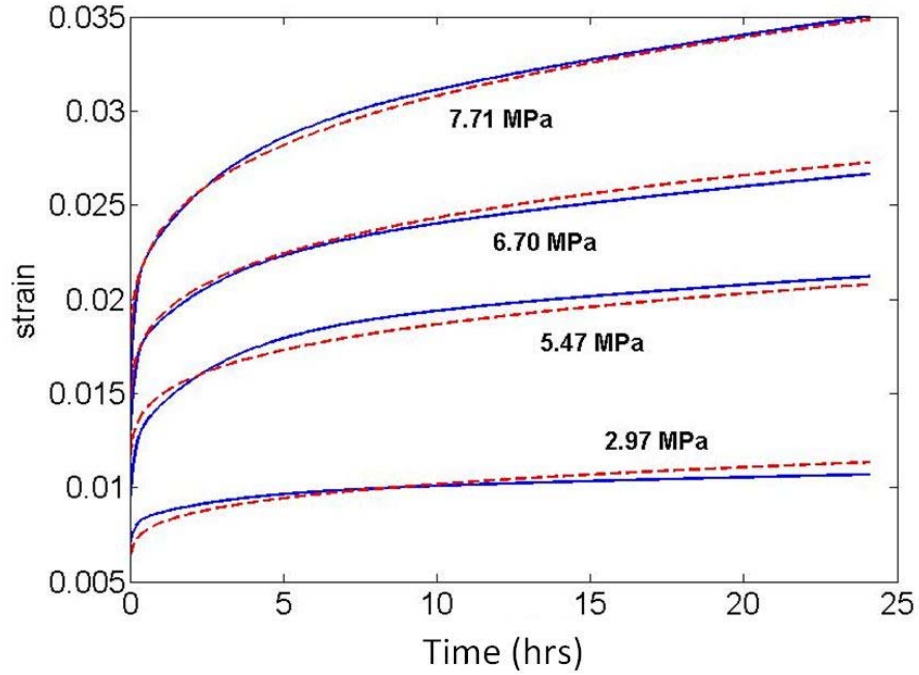


**Figure 32: Experimental (continuous line) (Liu, 2007), and nonlinear viscoplastic model (dashed line) results for 24 hour creep tests (PIPE)**

The formulation parameters are obtained by means of Least Squares approximation method through curve fitting process. Here it is considered that:

$$B_n = \left(\frac{\sigma}{\tilde{m}}\right)^{n-1} B_1, \quad C_n = \tilde{\alpha}^{n-1} C_1 \quad (96)$$

For simplicity, just two terms of polynomial ( $N = 1$ ) (Eq. (95)) are taken into account (thus, no need to find values for  $\alpha$  and  $\tilde{m}$ ). Through a nonlinearizing process of material parameters for stress gradient consideration, based on the experimental observations, the following equations are fitted:

$$B_1 = \sigma \left[ (b_1 + b_2 \hat{\sigma} + b_3 \hat{\sigma}^2) \left(\frac{\sigma_n}{\bar{\sigma}}\right)^{(b_4 + b_5 \hat{\sigma} + b_6 \hat{\sigma}^2)} \right]$$

$$C_1 = m_1 + m_2 \left( 1 + \frac{1}{2} \arctan \left( \frac{\hat{\sigma} - s_a}{\bar{\sigma}} \right) \right) \quad (97)$$

$$\text{And} \quad T = T_1 \left(\frac{\sigma_n}{\bar{\sigma}}\right)^{d_0}$$

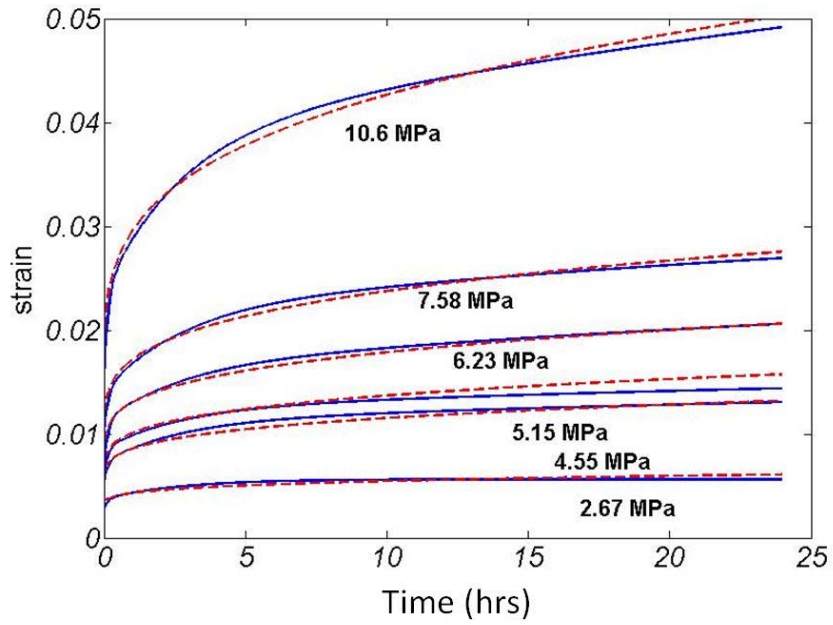


**Figure 33: Experimental (continuous line) (Liu, 2007), and nonlinear viscoplastic model (dashed line) results for 24 hour creep tests (RES1)**

Table 14: Material fitting parameters for  $X_0$  (Eq. (93))

Material	$a_0$ (MPa <sup>-1</sup> )	$a_1$ (MPa <sup>-1</sup> )	$a_2$ (MPa <sup>-2</sup> )
PIPE	5.33e8	1.36e4	0.1864
RES1	7.25e8	2.31e8	0.0029
RES2	-5.82e13	5.82e13	4.7e-9
RES4	-3.83e13	3.83e13	1.9e-9
PE80	-5.07e8	1.25e8	4.3e-4

Table 15: Material fitting parameters for NVE model (Eq. (92) & Eq. (94))								
	<b>m</b>	<b><math>\alpha</math></b>	<b><math>b_0</math> (MPa)</b>	<b><math>b_2</math></b>	<b><math>b_4</math> (MPa)</b>	<b><math>c_0</math> (s)</b>	<b><math>c_2</math> (MPa<sup>-1</sup>)</b>	<b><math>c_4</math> (MPa<sup>-3</sup>)</b>
			<b><math>b_1</math> (MPa)</b>	<b><math>b_3</math> (MPa<sup>-1</sup>)</b>		<b><math>c_1</math></b>	<b><math>c_3</math> (MPa<sup>-2</sup>)</b>	
<b>PIPE</b>	0.5534	18.57	167.6	0.98	0.055	1.78e-5	-0.778	0.00015
			668.6	2.6e-5		-21.0	0.0216	
<b>RES1</b>	0.4036	35.58	1838	0.00748	-3.43	6.87e-6	-0.249	0.00052
			484.9	-0.0168		-18.52	0.0018	
<b>RES2</b>	0.7504	18.72	-58.96	0.0245	-1.08	1.23e-7	-0.418	0.00157
			3061.3	0.111		-24.1	0.046	
<b>RES4</b>	0.1939	76.54	-194573	3.127	-0.025	0.00071	0.442	0.00325
			8647	-2.5e-10		-11.8	-0.014	
<b>PE80</b>	0.7231	44.41	-9.7e-5	0.275	-6e-27	1.18e-5	-0.46	0.00384
			572.1	0.0068		-20.1	0.026	

$C_0$  has unit of inverse of stress,  $T$  has time unit and  $C_1$  has no unit.  $\bar{\sigma}$  is introduced for dimensional consistency (in this research we have  $\bar{\sigma} = 1 \text{ MPa}$ ). Here,  $b_1$  has unit of compliance (inverse of stress),  $b_2$  has unit of inverse of squared stress and  $b_3$  has unit of inverse of cubic stress.  $b_4$  has no unit,  $b_5$  has unit of inverse of stress and  $b_6$  has unit of inverse of squared stress.  $m_1$ ,  $m_2$  and  $d_0$  have no units. Unit of  $s_a$  is same as stress and  $T_1$  is time.

$X_0$  is found directly from experiments and is the same for viscoelastic and viscoplastic modelling (Eq. (93) and Table 14). Fitting parameters for viscoplastic modelling are tabulated in Table 16 for all materials from Table 13. Examples of curve fitting of the presented formulation to experimental data is shown in Figure 32 and Figure 33.

Table 16: Material fitting parameters for NVP model (Eq. (97))

Material	$b_1$ (MPa <sup>-1</sup> )	$b_2$ (MPa <sup>-2</sup> )	$b_3$ (MPa <sup>-3</sup> )	$b_4$	$b_5$ (MPa <sup>-1</sup> )	$b_6$ (MPa <sup>-2</sup> )	$m_1$	$m_2$	$s_a$ (MPa)	$T_1$ (s)	$d_0$
PIPE	-4.84E-04	3.10E-04	-1.57E-05	0.052	-0.223	0.020	0.171	0.053	-0.015	39.5	-0.0236
RES1	1.38E-03	-2.86E-04	1.47E-05	-0.007	0.048	0.022	0.037	0.140	-0.108	-15162	-0.0483
RES2	7.14E-05	1.17E-04	-3.40E-07	-0.031	-0.008	0.001	0.021	0.160	-0.165	7503.3	0.0428
RES4	1.18E-05	-1.90E-06	8.67E-08	-0.024	0.024	0.004	-0.228	0.325	-0.003	0.0	0.0476
PE80	-2.82E-03	-9.82E-04	1.11E-03	-0.055	-0.388	0.025	0.084	0.074	0.018	14562.9	0.0989

#### 4.4 Extending the material parameters to longer times frames

In order to realistically model the service life-time for polymeric structures, long term prediction methods are needed within the developed constitutive law. The constitutive laws are normally formulated based on available short term tests.

The nonlinear models described in the previous section are able to represent the response of the material within the test time. It is well known that beyond the test time, the response of the viscoelastic model (described in Eq. (91)) approaches an asymptotic value equal to  $X_0 + \sum_{i=1}^N X_i$  and the response of the viscoplastic model (described in Eq. (95)) increases continuously with a time dependent slope equal to  $X_1 C_1 T^{-c_1} t^{c_1-1}$ . This divergent behaviour clearly suggests that defined models are most likely



not valid beyond the curve fitting time periods (which is 24 hours for the experimental data used to generate the models in Table 15 and Table 16).

One method of generating relevant design data is to investigate prototype structures, which in this case would be actual long term testing. Prototype testing can be expensive, or impractical, and therefore in the following, a solution to this problem is presented, considering that the important point of constructing a mathematical model is predicting the response of creep behaviour over extended time periods.

Using the material properties and material fitting parameters (Table 15 and Table 16) results in good agreement during the test time interval (24 hours). To examine the validity of the models for an extended time, the proposed method is to observe the trend of fitting parameters with respect to test time. First, the curve fitting is done for all experiments in different test times, namely: 10, 14, 18, 20, 22 and 24 hours. This allows one to observe how the material fitting parameters are dependent on test time ( $\lambda$ ). It is proposed that the parameter change over test time can be represented by the following equations for the viscoelastic case:

$$\begin{aligned}
 \text{(a)} \quad & b_i(\lambda) = b'_i (\lambda/\lambda')^{d_i} \quad \text{for } i = 0, 1, 2 \\
 \text{(b)} \quad & b_i(\lambda) = b'_i/(\lambda/\lambda')^{d_i} \quad \text{for } i = 3, 4 \\
 \text{(c)} \quad & c_0(\lambda) = c'_0 (\lambda/\lambda')^{d_5}
 \end{aligned} \tag{98}$$

$\lambda$  stands for test time and  $\lambda'$  is introduced for dimensional consistency (in this research we have  $\lambda' = 1 \text{ hour}$ ).  $c'_0$ ,  $b'_i$  and  $d_i$  are fitting parameters independent of the test time used to develop the model.  $b'_i$  and  $c'_0$  have same units as  $b_i$  and  $c_0$ , respectively and  $d_i$  have no units. Similarly, when the same method is applied to viscoplastic modelling, the following equations for the dependency of parameters on  $\lambda$  are obtained:

$$\begin{aligned}
 \text{(a)} \quad & b_i(\lambda) = b'_i (\lambda/\lambda')^{d_i} \quad \text{for } i = 1 - 6 \\
 \text{(b)} \quad & m_i(\lambda) = m'_j (\lambda/\lambda')^{n_j} \quad \text{for } i = 1, 2 \\
 \text{(c)} \quad & sa(\lambda) = s'_a (\lambda/\lambda')^s \\
 \text{(d)} \quad & T_1(\lambda) = T'_1(\lambda/\lambda')^{T_2}
 \end{aligned} \tag{99}$$

Here,  $b'_i$ ,  $m'_j$ ,  $s'_a$  and  $T'_1$  have same units as  $b_i$ ,  $m_j$ ,  $s_a$  and  $T_1$ , respectively and  $d_i$ ,  $n_j$ ,  $s$  and  $T_2$  have no units. These parameters are listed in Table 17 for the examined material “PIPE” as reference.

Table 17: Material fitting parameters for long term Viscoelastic (Eq. (98)) and Viscoplastic (Eq. (99)) models for “PIPE” material sample

VE	$b'_0$	$b'_1$	$b'_2$	$b'_3$	$b'_4$	$c'_0$	$d_0$	$d_1$	$d_2$	$d_3$	$d_4$	$d_5$
	MPa	MPa		MPa <sup>-1</sup>	MPa	s						
	-19972	72.7	6.772	0.543	22.0	2.3e-6	0.8735	0.4802	-1.03	2.795	1.9781	-0.206
VP	$b'_1$	$b'_2$	$b'_3$	$b'_4$	$b'_5$	$b'_6$	$m'_1$	$m'_2$	$s'_a$	$T'_1$		
	MPa <sup>-1</sup>	MPa <sup>-2</sup>	MPa <sup>-3</sup>		MPa <sup>-1</sup>	MPa <sup>-2</sup>			MPa			
	-4.5E-4	3E-4	-2E-5	0.052	-0.229	0.0210	0.1730	0.0510	-0.015	43		
	$d_1$	$d_2$	$d_3$	$d_4$	$d_5$	$d_6$	$n_1$	$n_2$	$s$	$T_2$		
-0.024	0.025	0.002	-0.018	-0.002	-0.008	-0.018	-0.004	0.010	0.008			

#### 4.5 Implementation in the Finite Element Program ABAQUS

The finite deformation constitutive model presented in the previous section was implemented in a User Subroutine UMAT. The ABAQUS 3-D modelling involves three stages: (1) pre-processing where the 3-D model is generated and finite element mesh, loads and boundary conditions are assigned, (2) analysis where displacements, stresses and strains are computed using material properties, which are defined as User Material, and (3) post-processing, where the results are graphically presented. ABAQUS user interface is used for defining the model and assigning meshes, loads and boundary conditions, while the user material subroutine was developed in Visual Studio workspace for material determination. This subroutine is compiled by Fortran software and is called at each increment and material calculation point. In the ABAQUS script the \*MATERIAL definition includes \*USER MATERIAL input expression. In each increment this expression invokes the viscoelastic and viscoplastic mechanical constitutive models, as described in the previous sections. The subroutine must perform two functions: first, it must update the stresses and the solution-dependent state variables to

their values at the end of the increment; second, it must provide the elasticity matrix or the so called “material Jacobian matrix”  $\partial\sigma_{ij}/\partial\varepsilon_{ij}$ .

The constitutive model is implemented in a three-dimensional formulation using the material parameters obtained by curve fitting and nonlinear optimization (Table 15 and Table 16). All material constants are obtained as a function of applied stress for one element, which in one-dimensional tension case is equal to  $\sigma_{33}$  with the other components of the stress tensor being zero. In one-dimensional analysis,  $\sigma_{33}$  could be interpreted as the maximum principal stress, von Mises stress or maximum stress component in the element. Since there are 6 stress components in the three-dimensional analysis, which change through the loading process, some assumptions have to be made. Here it is assumed that all time-dependent behaviour is restricted to the deviatoric response and that the dilatational behaviour is elastic (Krishnaswamy, et al., 1992). Furthermore, Poisson's ratio  $\nu$  is considered to be time independent and equal to 0.45 for HDPE, that is,  $\nu \rightarrow 0.5$ . This assumption results in a bulk modulus of about  $10^4 - 10^6$  which is recommended in the literature ( (Krishnaswamy, et al., 1992) & (Hinterhoelzl, et al., 2004)). Based on the assumption of incompressibility in the multiaxial formulation, it is obvious that  $\varepsilon_{kk} = 0$ . Therefore, the material properties ( $X_0$ ,  $X_i$ ,  $\tau_i$  and  $C_i$ ) in the three-dimensional form are considered to be functions of the effective stress, which is defined as

$$\begin{aligned} \sigma &= \sigma_{eff} \text{ and} \\ \sigma_{eff} &= \max. \{ \sigma_{11}, \sigma_{22}, \sigma_{33} \} \end{aligned} \tag{100}$$

In each increment the effective stress is calculated and updated. The full viscoelastic (or viscoplastic) boundary value problem is solved in each increment and for each integration point.

The constitutive equations must be written in an incremental algebraic form. First a fixed system of rectangular Cartesian coordinate  $(x_1, x_2, x_3)$  is considered in which the material point is denoted by  $(\bar{X}_1, \bar{X}_2, \bar{X}_3)$ . Through the deformation process the new material position is:  $x_i(\bar{X}_i, t)$ . The components of the displacement vector  $u = (u_1, u_2, u_3)$  are :  $u_i = x_i - \bar{X}_i$ , and the components of the velocity vector  $\bar{v} = (\bar{v}_1, \bar{v}_2, \bar{v}_3)$  are:  $\bar{v}_i = Du_i = \left. \frac{\partial u_i}{\partial t} \right|_{x_j=constant}$ , where  $D$  denotes the material time derivative.

In this system the equation of motion, which expresses the balance of linear and angular momentum, is:

$$\sigma_{ij,j} + F_j = \rho D^2 u_i = \rho D \bar{v}_i \tag{101}$$

which  $\rho$  is material density and  $\partial\rho/\partial t + (\rho\bar{v}_j)_{,j} = 0$ . For incompressible material  $\rho$  is constant, so  $\bar{v}_{j,j} = 0$ . In classical theory of infinitesimal linear elasticity, the additional relations connecting stress and displacement are provided through the intermediary of a strain tensor  $\varepsilon_{ij}$  which is defined as  $\varepsilon_{ij} = (u_{i,j} + u_{j,i})/2$ . In linearized theory involving small displacements, no distinction is made between the independent variables  $x_i$  and  $X_i$ . The constitutive relation for linear elastic material can now be written in the form of:

$$\varepsilon_{kl} = \mathbb{D}_{ijkl}\sigma_{ij} \quad (102)$$

where  $\mathbb{D}$  is the compliance matrix and inverse of the elastic moduli of the material,  $\mathbb{C}$ . Eq. (102) is a general representation of both viscoelastic and viscoplastic constitutive equations, Eq. (91) and Eq. (95), respectively. It takes on a special form since the material is considered isotropic and can be rewritten as

$$\mathbb{D} = \mathbb{C}^{-1} = \psi(t, \sigma) \begin{bmatrix} 1 & -\nu & -\nu & 0 & 0 & 0 \\ -\nu & 1 & -\nu & 0 & 0 & 0 \\ -\nu & -\nu & 1 & 0 & 0 & 0 \\ 0 & 0 & 0 & 2(1+\nu) & 0 & 0 \\ 0 & 0 & 0 & 0 & 2(1+\nu) & 0 \\ 0 & 0 & 0 & 0 & 0 & 2(1+\nu) \end{bmatrix} \quad (103)$$

in which the  $\psi(t, \sigma)$  terms are defined in Eq. (91) and Eq. (95). For simplicity in programming, stress components in Eq. (102), can be expressed as functions of time- and stress-dependent Lamé parameters,  $\lambda$  and  $\mu$ , as

$$\sigma_{ij} = \lambda\varepsilon_V\delta_{ij} + 2\mu\varepsilon_{ij} \quad (104)$$

These parameters are related to mechanical properties as:

$$\begin{aligned} \psi^{-1} &= \mu(3\lambda + 2\mu)/(\lambda + \mu) \\ \nu &= \lambda/2(\lambda + \mu) \\ K &= \lambda + \frac{2}{3}\mu \\ \mu &= G \end{aligned} \quad (105)$$

The rate of variation in co-rotational description (Jaumann) is

$$\dot{\sigma}_{ij} = \lambda \dot{\varepsilon}_V \delta_{ij} + 2\mu \dot{\varepsilon}_{ij} + \dot{\lambda} \varepsilon_V \delta_{ij} + 2\dot{\mu} \varepsilon_{ij} \quad (106)$$

Using a central difference operator as a stable integration operator for this equation we have

$$\begin{aligned} \dot{f}_{t+\Delta t/2} &= \frac{\Delta f}{\Delta t} \\ f_{t+\Delta t/2} &= f_t + \frac{\Delta f}{2} \end{aligned} \quad (107)$$

where  $f$  is any function.  $f_t$  is its value at the beginning of increment,  $\Delta f$  is the change in the function over the increment, and  $\Delta t$  is the time increment. Applying this to Eq. (106) we have:

$$\begin{aligned} \frac{\Delta \sigma_{ii}}{\Delta t} &= \left( \lambda(t) + \frac{\Delta \lambda(t)}{2} \right) \left( \frac{\Delta \varepsilon_V(t)}{\Delta t} \right) + 2 \left( \mu(t) + \frac{\Delta \mu(t)}{2} \right) \left( \frac{\Delta \varepsilon_{ii}(t)}{\Delta t} \right) \\ &+ \left( \frac{\Delta \lambda(t)}{\Delta t} \right) \left( \varepsilon_V(t) + \frac{\Delta \varepsilon_V(t)}{2} \right) + 2 \left( \frac{\Delta \mu(t)}{\Delta t} \right) \left( \varepsilon_{ii}(t) + \frac{\Delta \varepsilon_{ii}(t)}{2} \right) \end{aligned} \quad (108)$$

for  $i \in (x, y, z)$  and

$$\frac{\Delta \sigma_{ij}}{\Delta t} = 2 \left( \mu(t) + \frac{\Delta \mu(t)}{2} \right) \left( \frac{\Delta \varepsilon_{ij}(t)}{\Delta t} \right) + 2 \left( \frac{\Delta \mu(t)}{\Delta t} \right) \left( \varepsilon_{ij}(t) + \frac{\Delta \varepsilon_{ij}(t)}{2} \right) \quad (109)$$

for  $ij \in (xy, yz, zx)$ . Therefore:

$$\Delta \boldsymbol{\sigma} = \mathbb{C} \Delta \boldsymbol{\varepsilon} + \Delta \mathbb{C} \Delta \boldsymbol{\varepsilon} + \Delta \mathbb{C} \boldsymbol{\varepsilon} \quad (110)$$

and

$$\boldsymbol{\sigma}_t = \boldsymbol{\sigma}_{t-\Delta t} + \Delta \boldsymbol{\sigma}$$

and finally

$$\boldsymbol{\sigma}_t = \boldsymbol{\sigma}_{t-\Delta t} + \mathbb{C}_t \Delta \boldsymbol{\varepsilon} + \Delta \mathbb{C} \Delta \boldsymbol{\varepsilon} + \Delta \mathbb{C} \boldsymbol{\varepsilon}_t \quad (111)$$

Here, subscript  $(t - \Delta t)$  indicates the value at the beginning of the time increment and subscript  $t$  refers to the value at the end of the increment. In addition,  $\Delta \mathbb{C} = \mathbb{C}_t - \mathbb{C}_{t-\Delta t}$  and  $\Delta \boldsymbol{\varepsilon} = \boldsymbol{\varepsilon}_t - \boldsymbol{\varepsilon}_{t-\Delta t}$ .

## 4.6 Results and Discussion

To examine the validity of the proposed finite element procedure, the theoretical results are compared to test measurements (other than the tests used for calibration of material modelling) by considering

one of the materials under investigation (Table 13), the “PIPE” material. The material fitting parameters and resulting material constants are based on the creep curves shown in Figure 30 and Figure 32.

The material constants of the nonlinear viscoelastic and viscoplastic models are tabulated in Table 18 and Table 19 for three test measurements for different stress levels. These constants are obtained from curve fitting described in section 4.3. For this, fitting parameters in Table 15 and Table 16 are used in Eqs. (92)~(94) and (96)~(97). Figure 34 compares experimental and simulated data. It is shown that the simulated strain data fit well with experimental measurements for both viscoelastic and viscoplastic models. An offset in model prediction from actual response can be observed for stress level 2.97 MPa. This is due to the offset in approximating the measured instantaneous module of elasticity. Meaning that if the measured elastic modulus is not accurate, the approximation variation affects the whole prediction and shifts the prediction curve of the subject stress level up or down.

Table 18: Material constants (properties) for “PIPE” (Viscoelastic)							
<b><i>Stress (MPa)</i></b>	<b><i>E<sub>0</sub> (GPa)</i></b>	<b><i>E<sub>1</sub> (GPa)</i></b>	<b><i>E<sub>2</sub> (GPa)</i></b>	<b><i>E<sub>3</sub> (GPa)</i></b>	<b><i>τ<sub>1</sub> (s)</i></b>	<b><i>τ<sub>2</sub> (s)</i></b>	<b><i>τ<sub>3</sub> (s)</i></b>
<b>2.97</b>	0.4302	4.7932	2.6233	1.4357	118	1869	29469
<b>5.47</b>	0.5332	2.1201	1.1603	0.6350	582	9183	144755
<b>7.71</b>	0.5332	2.1180	1.1592	0.6344	200	3163	49865

Table 19: Material constants for “PIPE” (Viscoplastic)				
<b><i>Stress (MPa)</i></b>	<b><i>E<sub>0</sub> (GPa)</i></b>	<b><i>C<sub>0</sub> (MPa<sup>-1</sup>)</i></b>	<b><i>T (s)</i></b>	<b><i>C<sub>1</sub></i></b>
<b>2.97</b>	0.4302	0.00033	313.1	0.2472
<b>5.47</b>	0.5332	0.00048	300.7	0.2585
<b>7.71</b>	0.5332	0.00061	293.9	0.2626

To examine the validity of the method, a criterion should be chosen for the goodness of fit of the theoretical method. This creep curve validation criterion is the root mean square of deviation/error (RMSD/RMSE) which is a deviation between the predicted values  $\varepsilon_i$ , and the measured  $\hat{\varepsilon}_i$  data

$$\frac{\left(\sum_{i=1}^{N_t} \left(\frac{\varepsilon_i - \hat{\varepsilon}_i}{\hat{\varepsilon}_i}\right)^2\right)^{1/2}}{N_t} = RMSE \quad (112)$$

where  $N_t$  is the number of strain measurements recorded for each creep test. This is a criterion which is used to examine how well the FEM results are close to experimental ones. This is the same as the criterion used for curve fitting of the models to test data and finding the fitting parameters and material functions (see section 4.3). In the curve fitting procedure, least squares error (RMSE) was set to 0.05 (5%) which provides a “good” fit as per MacCallum et. al (MacCallum, et al., 1996).

For the information shown in Figure 34 the resulted fitting errors are 4.5%, 3.1% and 3.5% for viscoelastic modelling, and 4.3%, 2.1% and 3.2% for viscoplastic one, under 2.97 MPa, 5.47 MPa and 7.71 MPa, respectively. This states that the accuracy of the results meets the expected “acceptable” fitting error criterion (per MacCallum et. al (MacCallum, et al., 1996)).

To study the long term prediction capability of the models, FE results were recorded for 7 days analysis (in which  $\lambda = 180$ ). These results were calculated for the “PIPE” material for both viscoelastic and viscoplastic responses. A 3D unit cell was modeled in ABAQUS graphic interface and meshed with a single element quadratic hexahedron, C3D20R. Boundary conditions for the single unit geometrical model were chosen to be same as the tested sample materials under 6.75 Mpa and 6.89 Mpa applied constant stresses. In Figure 35, the long term behaviour of the model has been presented for viscoelastic and viscoplastic responses as described in this chapter. The models have been developed using the data from 24 hour creep testing. The models showed the ability to predict well the independent data from long term testing; they sufficiently describe the variation of strain with time for the loading history. The maximum Least Squares error of the model prediction from the experimental data is 3.5% for the nonlinear viscoelastic model and 5% for the nonlinear viscoplastic model for both loading cases.

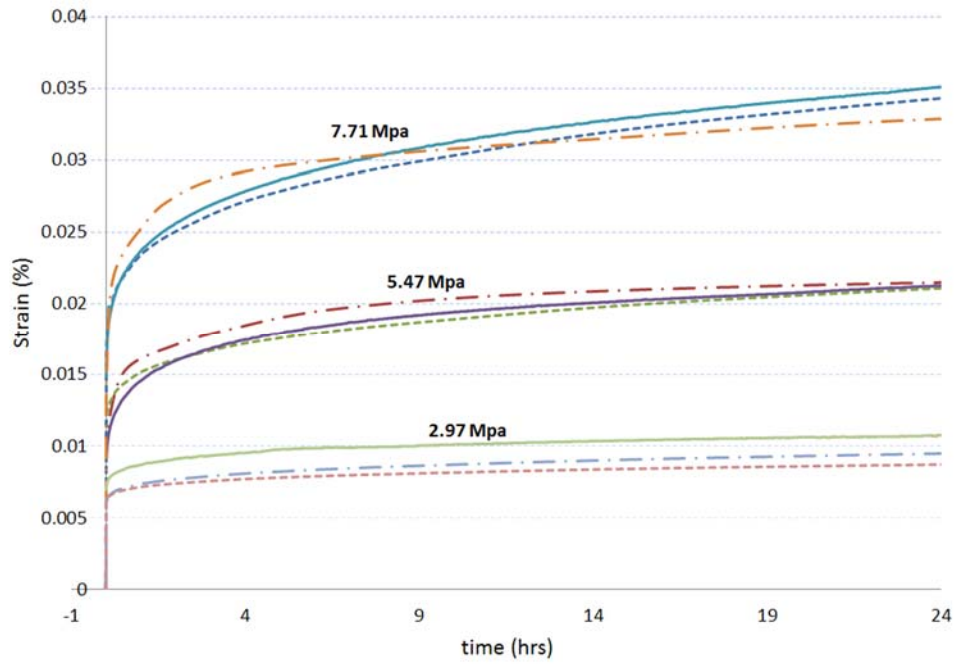


**Figure 34: Viscoelastic (dashed-dotted line -.-.) and viscoplastic (dashed line - - -) model responses compared to 24 HRS test data (solid line) (Liu, 2007), for PIPE material**

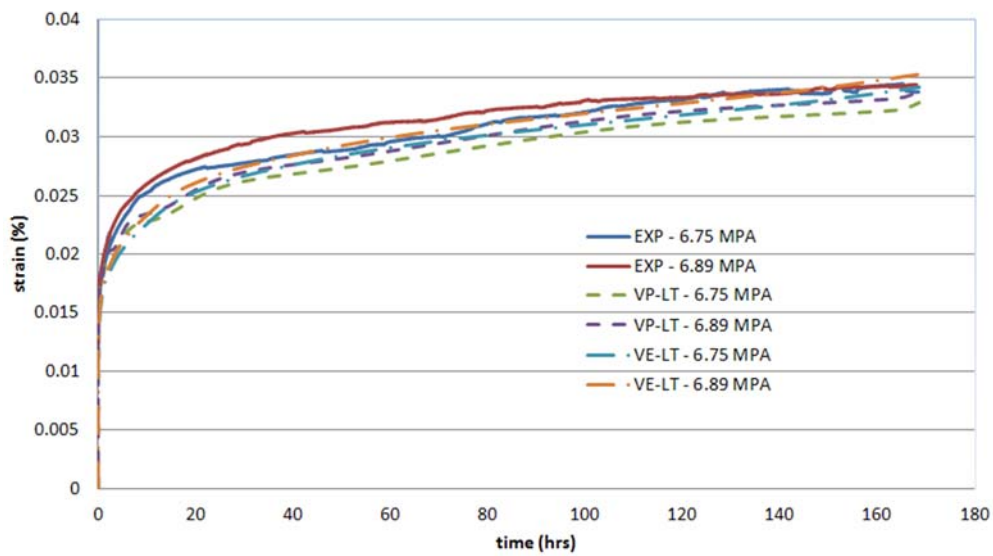


**Figure 35: One week (7 days) viscoelastic VE (dashed-dotted line -.-.) and viscoplastic VP (dashed line - - -) models responses compared to test data (solid line) (Liu, 2007), for PIPE material**



This is also illustrated in Figure 36 which compares long term viscoelastic and viscoplastic theoretical responses for 40 hours with experimental observations. Tests have been done on HDPE pipe materials under 4.42MPa, 6.08MPa and 8.15MPa applied loads. According to the definition, the parameter  $\lambda$  (Eq. (98) and Eq. (99)) is set to 40. The errors associated with these results are 2%, 3.0% and 7.5% for viscoelastic model, and 3.6%, 1.8% and 6.1% for viscoplastic model, for the aforementioned applied stresses, respectively.

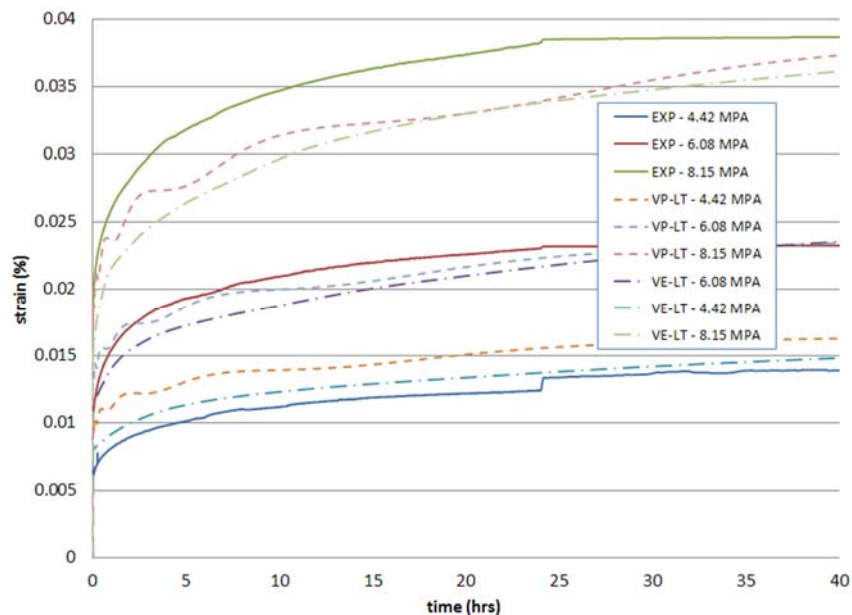


**Figure 36: Experimental (continuous line) (Liu, 2007), and viscoelastic VE (dotted dashed line) and viscoplastic VP (dashed line) models prediction (dashed line) in 40 hours test time (PIPE).**

**Analyses done using UMAT in Abaqus.**

Following the previous discussion, the observations for long term response (longer than test time: 24 hour) from Figure 35 and Figure 36 reveal that the viscoelastic model doesn't approach an asymptotic limit, which is to be expected, since the material properties are updated as the time increases. The viscoplastic response also doesn't obey fully the power-law relationship. These illustrate that the proposed viscoelastic long term model realistically predicts actual behaviour.

Another example is shown in Figure 37. This figure shows long term predicted responses using the developed formulation and also, another approach, where the theoretical 24 hour creep curves are directly extended to longer time frames (without adjustment of parameters proposed herein). As

expected, the unadjusted viscoelastic and viscoplastic responses obey the regular exponential and power-law relations used in material characterization (Eq. (91) and Eq. (95), respectively), as the time goes beyond 24 hours.

The proposed viscoelastic and viscoplastic long term methods lie between these two unadjusted curves. In this figure, the curves with rhombus and star markers are the adjusted viscoelastic and viscoplastic model predictions, respectively, and the dashed-dotted and dashed curves represent the unadjusted viscoelastic and viscoplastic models, respectively. As can be inferred, the unadjusted power law model (viscoplastic case) predicts higher values of creep strain than the adjusted model, while in contrast, the unadjusted exponential model (viscoelastic case) predicts smaller values of creep strain.

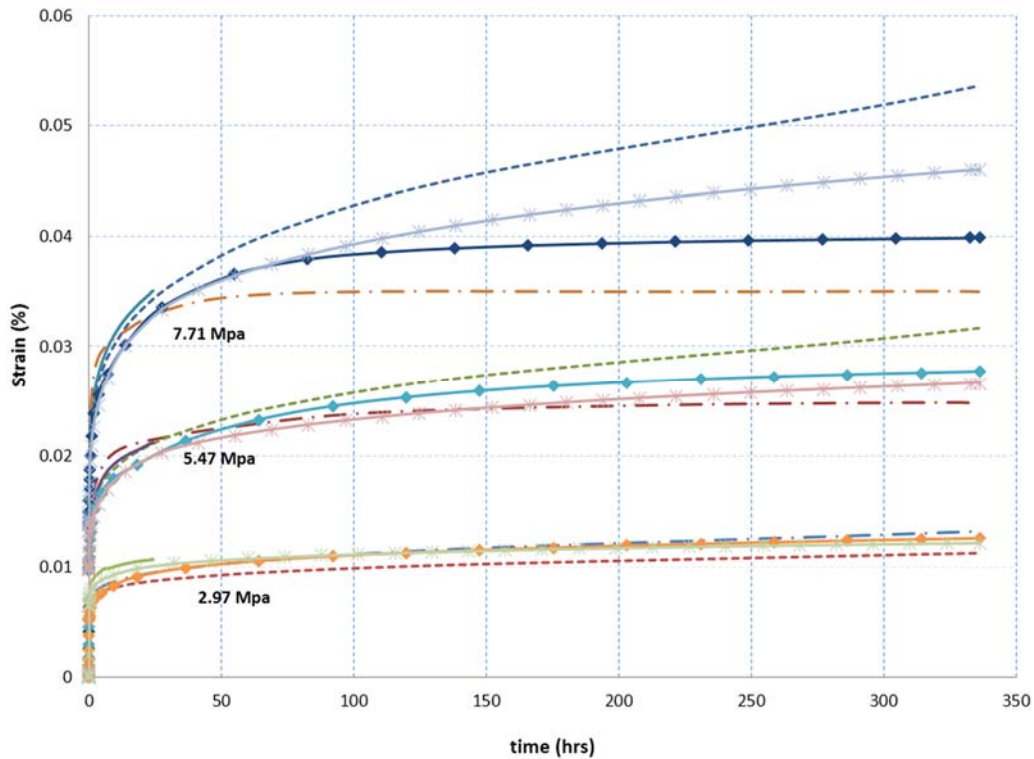


**Figure 37: Two weeks (14 days) unadjusted viscoelastic and viscoplastic (dashed-dotted lines -.-.- and dashed lines - - -, respectively) as well as adjusted viscoelastic and viscoplastic (rhombus marked lines -◇-◇- and star marked lines -\*-\*- , respectively) model responses compared to 24 HRS test data (solid line) (Liu, 2007), for PIPE material**

## 4.7 Conclusions

Finite element three-dimensional viscoelastic and viscoplastic models for polymers are presented herein. The models can be used to predict the response of a material beyond the experimental time period.

The proposed method utilizes simplification of the constitutive equations in order to obtain a rational theory, namely the incompressible behaviour assumption of the material, the superposition of small time dependent deformation on large deformation, and the simplifications of material functions. The equations are modified for long term time frames based on the measured material properties through an empirical approach. The proposed formulations are based on the spring and dash-pot concept, and plasticity power-law function for viscoelastic and viscoplastic behaviours, respectively. The determination of material properties is based on the non-separable nature of relations for nonlinear materials in which the material properties change by stress coupled with time. The validity of the models was assessed by comparing the results of the FE procedure with experimental observations (Liu, 2007) on high density polyethylene (HDPE) specimens under uniaxial loading. Comparisons showed that the proposed constitutive model can satisfactorily represent the time-dependent mechanical behaviour of polymers.

The proposed FE formulation has the potential for practical analysis of polymeric structures. The constitutive model can be developed based on few short term creep tests and through the proposed method of extension to longer time frames, the multi-integral FE implementation and 3-D assumptions, it can be used for the analysis of mechanical and structural components under a variety of loadings.

Based on the research conducted in this chapter and summarized above, the following specific findings and contributions can be mentioned:

The multiple integral approach, is employed for three-dimensional behaviour analysis. Some simplifications are done in order to obtain a particularly useful theory, which are the fully incompressible behaviour assumption of the material, the superposition of small time dependent deformation on large deformation, and finally the simplifications of the material functions. Differential formulation (exponential form), and unified plasticity (power-law function) approximations are used for viscoelastic and viscoplastic modellings, respectively. The models are optimized for long-term responses which are beyond the test time. Finite element procedures are implemented in the user-defined material algorithm in Abaqus (UMAT).

The developed finite element procedure, allows to model the long term as well as short term responses of polymers. For this a code was developed in Fortran workspace, which is linked to commercial software ABAQUS.

The inputs to the developed code include a structural model and a material model. The former is done through the ABAQUS user interface and includes 3D solid modelling, boundary conditions, loadings, meshing and time discretization. The latter is obtained from experiments and needs material analysis.

The validity of the models is assessed by comparison with experimental observations on high density polyethylene (HDPE) for single element specimens under uniaxial loading.

Here are the conclusions:

- 1- A superposition of small deformations can be used to model large deformations, and the multi-integral description can be simplified for finite element implementation, using the incompressibility assumption.
- 2- Both viscoelastic and viscoplastic formulations can be implemented in the finite element analysis using the linear superposition principle. The developed finite element procedure uses the proposed material definition based on experimental data.
- 3- Nonlinear Viscoelastic, NVE, and Nonlinear Viscoplastic, NVP, models can be used in computational (finite element) methods for predictions of long term material behaviour. In the long term, the NVE model in comparison with the NVP model results in smaller fitting errors for strain response predictions, and both results are in relatively good correlation with experiments (less than 10% error in most cases). Again, similar to material modelling, the reason is that the former one has more fitting parameters compared to viscoplastic one which results in more flexible fitting to the short term test data, so more accurate short term and long term response prediction. It is concluded that with proper material parameters to reflect the deformations involved in the mechanical tests, the behaviour observed experimentally can be satisfactorily predicted using the FEM simulation.
- 4- The proposed FE formulations have the potential for practical analysis of polymeric structures. The constitutive model can be developed based on few short term creep tests and through the proposed method of extension to longer time frames, the multi-integral FE implementation and

- 3-D assumptions, it can be used for the analysis of mechanical and structural components under variety of loadings.
- 5- A good correlation (less than 5% error) of model and experimental data is always achievable if proper material fitting parameters are obtained from test data. This requires accurate experimental measurements, as well as availability of numerous test results in each set of test data.

## Chapter 5

### Constitutive equations and finite element implementation of linear modelling for viscoelastic materials

This chapter presents phenomenological three-dimensional linear viscoelastic constitutive model for time dependent analysis. Based on Boltzmann linear superposition principle, a linear solution procedure has been provided to solve for viscoelastic behaviour. The process uses the Prony series material parameters and the constitutive relations are based on the non-separable form of equations. Based on the proposed constitutive equations, a finite element (FE) procedure is developed and implemented in a User Material FE code in ABAQUS commercial software. The validity of the model is assessed by comparison with experimental observations by Liu (Liu, 2007) on high density polyethylene (HDPE) for uniaxial loading cases. A reasonably good correlation was observed between these two sets of results and the research shows that the proposed FEM model can reproduce the experimental strain-time curves accurately.

#### 5.1 Introduction

Polymers are increasingly used in many aspects of our lives, including infrastructure, building and pipeline construction. Thermoplastic polyethylene (PE) and unplasticised polyvinyl chloride (PVC or UPVC) are the predominant materials used for water and sewer pipes (Polak, et al., 2004). Other plastics for pipe production are polypropylene (PP), polybutylene (PB) and acrylonitrile-butadiene-styrene (ABS), which are all thermoplastics (Janson, 2003). Polymeric pipe materials are subjected to tensile and bending stresses and deformations during the installation procedures. Furthermore, these materials will then be subjected to longer term persistent loadings from environmental conditions, which lead to the creep and relaxation phenomena. Although the applied stress and strain under normal conditions of application are way lower than the critical yield and ultimate stress and strain, long term application of loading causes permanent deformation and/or delayed failure. Hence, theoretical and/or numerical modelling of the behaviour of these materials is useful in predicting the material's response. In this research, a method is presented based on experimental data which allows for structural analysis of viscoelastic materials.

There are two approaches for modelling polymers: micromechanical and macromechanical. In the micromechanical approach, time-dependent functions expressing deformation and breakage of links of macromolecule chains and deformations of crystalline phase are usually formulated and applied to characterize the development of stress and strain ( (Zehsaz, et al., 2014), (Behzadfar, et al., 2013) and (Popa, et al., 2014)). Based on this approach, Alvarado et al. (Alvarado, et al., 2010) presented the description of a damage-coupled constitutive formulation for the mechanical behaviour of semicrystalline polyethylene.

In the macromechanical modelling, phenomenological models of viscoelastic solids and/or irreversible thermodynamics with internal variables are often employed. The theoretical formulation results in the evolution equation of stress or strain, which is formulated generally as a linear or nonlinear differential equation. The equation can be a function of either time, stress and strain rate (time hardening theory) or strain, stress and strain rate (strain hardening). Several constitutive models based on this methodology were developed in the past two decades. Various viscoelastic constitutive equations have been developed by Bae and Cho (Bae, et al., 2015) to describe nonlinear viscoelastic behaviour. Zacharatos and Kontou (Zacharatos, et al., 2015) presented a one-dimensional phenomenological constitutive model, representing a viscoelastic behaviour of polymers using a three element standard solid model. Hasapour et al. (Hasanpour, et al., 2009) developed a finite element (FE) procedure for compressible viscoelastic materials. The work is concerned with the formulation of constitutive equations for a finite strain viscoelastic material using multiplicative decomposition in a thermodynamically consistent manner. In a similar comprehensive research, a finite element algorithm was developed to study time-dependent problems by Krishnaswamy et al. (Krishnaswami, et al., 1992). In this research, nonlinear viscoelastic and viscoplastic models were used to study the time-dependent deformation and failure of high density polyethylene (HDPE). A practical simplified approach to linear and nonlinear modelling of polyethylene, based on creep testing at different stress levels, was proposed by Liu et al. (Liu, et al., 2008). Cheng et al. (Cheng, et al., 2011) followed the work by presenting a rigorous statistical approach for estimating parameters in modelling creep compliance of PE. In a work concerning a class of non-aging isotropic viscoelastic solids, Muliana et al. (Muliana, et al., 2015) proposed a model by developing a nonlinear integral formulation, which belongs to the class of quasi-linear viscoelastic models, for solid-like materials. A thermodynamically-based constitutive model was developed by Krairi and Doghri (Krairi, et al., 2014) for isotropic homogeneous thermoplastic polymers under arbitrary multiaxial and non-monotonic loadings. Chan and Ngan (Chan, et al., 2010)

demonstrated that, when polyethylene is subject to a tensile test with a jump in the loading rate, an elastic modulus, given as the ratio of the jump in stress rate to the resultant jump in strain rate, is invariant with respect to the magnitude of jump in the loading rate, at a given strain at which the jump is imposed. Muliana (Muliana, 2015) presented analyses of deformations in nonlinear viscoelastic beams that experience large displacements and rotations due to mechanical, thermal, and electrical stimuli. Nguyen et al. (Nguyen, et al., 2013) proposed a framework which focuses on viscoelasticity, as a predominant factor in the high cycle fatigue stress range. For this they derived an isothermal nonlinear viscoelastic model for small strains under an irreversible process thermodynamic framework. An efficient method of fitting Prony series models to viscoelastic experimental data with power-law presmoothing was presented for unsmoothed experimental data by Park and Kim (Park, et al., (2001)). The same group also investigated and illustrated methods of interconversion between relaxation modulus and creep compliance for linear viscoelastic materials using data from asphalt concrete (Park, et al., 1999).

In theoretical modelling of polymers, experimental tests play an important role in the investigation, since they offer insight into the material behaviour, namely: linearity and nonlinearity, best fit for separable and non-separable forms of equations, and a basis for model validation. The mechanical behaviour of polymeric materials depends on both time and temperature and several experimental techniques may be used to measure and quantify this behaviour. Zhang and Moore based their models on experimental data (Zhang, et al., 1997) and performed extensive experimental work to characterize the nonlinear time dependent response of HDPEs under uniaxial loading. Drozdov and Christiansen reported their observations on uniaxial tensile tests with constant strain rates at moderate finite deformations, as well as in creep and relaxation tests on a thermoplastic elastomer (ethylene–octane copolymer) (Drozdof, et al., 2006) and polyethylene (Drozdov, et al., 2003). Dusunceli and Colak (Dusunceli, et al., 2008) and Liu et al. (Liu, et al., 2008) presented an approach for modelling the mechanical behaviour of polyethylene materials. They developed both viscoelastic and viscoplastic models and showed model corroboration by comparing test results of tensile, step-loading, and load-rate creep with experimental ones. They also presented creep numerical and experimental data for a medium density polyethylene (MDPE) pipe material and confirmed the efficiency of the macromechanical approach by test results. Ayoub et al. (Ayoub, et al., 2010), Ellyin et al. (Ellyin, et al., 2007), Cao et al. (Cao, et al., 2010), Wendlandt et al. (Wendlandt, et al., 2010) and Pan et al. (Pan, et al., 2012) also used experimental results to validate proposed theoretical models.



This chapter presents a phenomenological three-dimensional viscoelastic constitutive model for polymers. The following steps are followed:

- 1- Multi Kelvin Solid representation of springs and dash-pots is employed for viscoelastic behaviour (section 5.2)
- 2- The differential constitutive equation is developed using energy method (section 5.2)
- 3- Inelastic creep compliance is estimated by Prony series function (section 5.2)
- 4- An integral form of constitutive equation is provided based on the superposition principle (section 5.3)
- 5- Finite element FE procedure is described (section 5.3)
- 6- FE procedure is extended to the multi-dimensional case (section 5.3)
- 7- The model is implemented in FE user subroutine (section 5.4)
- 8- The presented model results are validated for one dimensional loading of cubic unit cell sample materials (section 5.5)

The method in section 5.2 is based on the small strain assumption, but it is extended to large deformation for materials in which the stress-strain relation is time dependent. The constitutive equation governing the model response may be derived in a thermodynamically consistent way considering linear spring-dashpot elements. The main problem in generalizing constitutive models from small to finite deformations is to extend the theory in a thermodynamically consistent way, so that the second law of thermodynamics remains satisfied in every admissible step. This chapter presents the formulation and constitutive equations for a finite strain viscoelastic material using the superposition principle in a thermodynamically consistent manner.

Based on the proposed constitutive equations, a finite element (FE) procedure developed in section 5.3, is implemented in the User Material FE code (section 5.4).

In section 5.5, the previously estimated material parameters are used. The model is used to predict the response of sample materials and the results are compared to experimental ones (Liu, 2007). A reasonably good correlation was seen between these two sets of results.

## 5.2 Constitutive Equations

In viscoelastic theory, constitutive equations are usually formulated using either the differential or the integral forms (Lockett, 1972). In contrast to the differential formulation (simulating the behaviour by spring and dash-pot elements configuration), which involves only the current values of stress and strain and their current time rates, the integral form takes into account the history of loading and it is more accurate and strict in both linear and nonlinear modelling. In this section the integral approach is used by means of exponential description of kinematic relations of material properties. The most useful analysis in finite element applications is spring and dash-pot method of modelling described by Flugge (Flugge, 1967). According to the concept of fading memory (Christensen, 1971), the material response depends more on recent history than on earlier events. Accordingly, this theory considers exponential formulation for most nonlinear materials, such as HDPE, for which the effects of stress and time on the resulting strain are not separable. Similarly, the viscoplastic theory assumes a nonlinear time dependent power-law function which doesn't have an asymptote, in contrast to the viscoelastic model which approaches to an asymptotic limit (Brinson, 1973). Both the viscoelastic and viscoplastic formulations are usually an extension of the theory which considers permanent residual strain by assuming the rate of total strain as the summation of elastic and plastic strain rates.

$$\dot{\varepsilon}(t) = \dot{\varepsilon}^e(t) + \dot{\varepsilon}^i(t) \quad (113)$$

The dot over the variable shows the time rate. In this equation  $\varepsilon^e$  can be interpreted as the elastic strain, which is recoverable and  $\varepsilon^i$  denotes the inelastic strain, which results if the stress is infinitely fast unloaded from the actual state to the stress free state. This strain decomposition states that every linear viscoelastic and viscoplastic solid material is always associated with two moduli,  $E^e$  and  $E^i$ , which are the elastic modulus and the viscous one, respectively. This definition of strain may be seen to be in a natural way connected with the multi-Kelvin solid, comprising of multi spring and dash-pot elements. A 3-parameter configuration of Kelvin solid is illustrated in Figure 38 (Model A). The strains  $\varepsilon^e$  and  $\varepsilon^i$  belong to the spring with the modulus  $E_0 = E^e$  and the Kelvin unit with the modulus  $E_1$ , respectively.

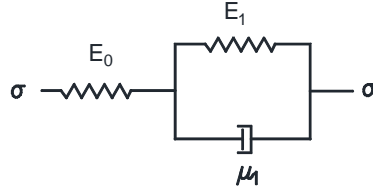


**Figure 38: A 3-parameter Model A**

The mechanical response of the Model A configuration is defined by the ordinary differential equation (Flügge, 1967)

$$\dot{\sigma} + \frac{1}{\mu_1} \frac{E_0^2}{E_0 - E_1} \sigma = E_0 \dot{\varepsilon} + \frac{E_1}{\mu_1} \frac{E_0^2}{E_0 - E_1} \varepsilon \quad (114)$$

where  $\mu_1$  is the coefficient of viscosity for the first Kelvin unit and  $\dot{\sigma}$  is the rate of change of total stress. The free energy function associated with Model A is given as summation of energies associated with two strains,  $\varepsilon_0$  and  $\varepsilon_1$ , which are  $\psi^e$  and  $\psi^i$ , respectively (Guedes, 2004)

$$\psi^A = \psi^e(\varepsilon^e) + \psi^i(\varepsilon^i) = \frac{1}{2} E_0 \varepsilon_0^2 + \frac{1}{2} E_1 \varepsilon_1^2 \quad (\varepsilon_0 = \varepsilon^e, \varepsilon_1 = \varepsilon^i) \quad (115)$$

which implies that the energy can only be stored in the two springs. Considering that the behaviour is adiabatic and the isothermal approximation makes the free internal energy  $\psi$  to coincide with energy, the Clausius-Planck inequality applies (Huber, et al., 2000)

$$\dot{\psi}^A \leq \sigma(t) \dot{\varepsilon}(t) \quad (116)$$

which guarantees that the second law of thermodynamics is satisfied. Consequently, using Eq. (113), Eq. (115) can be rewritten as

$$\left( \sigma - \frac{\partial \psi^e}{\partial \varepsilon^e} \right) \dot{\varepsilon} + \left( \frac{\partial \psi^e}{\partial \varepsilon^e} - \frac{\partial \psi^i}{\partial \varepsilon^i} \right) \dot{\varepsilon}^i \geq 0 \quad (117)$$

Since  $\dot{\varepsilon}$  may be chosen as arbitrary, the following are necessary and sufficient conditions for Eq. (117) to hold.

$$\sigma = \frac{\partial \psi^e}{\partial \varepsilon^e} = E_0 \varepsilon^e \quad (118)$$

$$\left(\frac{\partial\psi^e}{\partial\varepsilon^e} - \frac{\partial\psi^i}{\partial\varepsilon^i}\right)\dot{\varepsilon}^i = (\sigma - \sigma_1)\dot{\varepsilon}^i \geq 0 \quad (119)$$

Here  $\sigma$  is the total applied stress and  $\sigma_1$  is a part of stress affecting the elastic spring of the Kelvin unit. Thus

$$\sigma_1 = \frac{\partial\psi_i}{\partial\varepsilon_i} = E_1\varepsilon^i \quad (120)$$

$$\dot{\varepsilon}^i = \dot{\varepsilon}_1 = (\sigma - \sigma_1)/\mu_1 \quad (121)$$

The concept can be extended to a more general case by introducing a multi-Kelvin solid configuration, which is illustrated in Figure 39 (Model B). The configuration includes a spring and  $N$  Kelvin units in series. Similarly, the strains  $\varepsilon^e$  and  $\varepsilon^i = \sum_{n=1}^N \varepsilon_n$  belong to the spring with modulus  $E_0 = E^e$  and the Kelvin units, respectively. The free energy function associated with Model B is given by

$$\begin{aligned} \psi^B &= \psi^e(\varepsilon^e) + \psi^i(\varepsilon^i) = \psi^e(\varepsilon^e) + \sum_{n=1}^N \psi_n^i(\varepsilon_n) \\ &= \frac{1}{2}E_0\varepsilon_0^2 + \sum_{n=1}^N \frac{1}{2}E_n\varepsilon_n^2 \end{aligned} \quad (122)$$

Using the Clausius-Planck inequality (Eq. (116)) yields

$$\sigma = \frac{\partial\psi^e}{\partial\varepsilon^e} = E_0\varepsilon^e \quad (123)$$

$$\sigma_n = \frac{\partial\psi_n^i}{\partial\varepsilon_n} = E_n\varepsilon_n \quad (124)$$

$$\dot{\varepsilon}_n = (\sigma - \sigma_n)/\mu_n \quad (125)$$

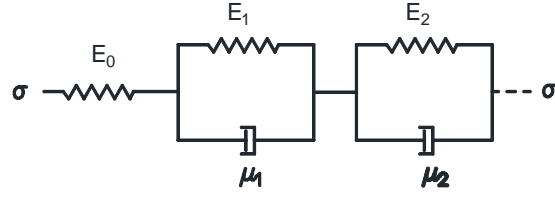


**Figure 39: Multi Kelvin Solid configuration Model B.**

Using Eq. (113) and considering,  $\varepsilon^i = \sum_{n=1}^N \varepsilon_n$ , and using Eqs. (123)~(125), one can come up with the following relations

$$\varepsilon = \varepsilon^e + \varepsilon^i = \varepsilon^e + \sum_{n=1}^N \left( \frac{\sigma_n}{E_n} \right) = \sigma D_0 + \sigma D(t) \quad (126)$$

so

$$\varepsilon = \sigma \frac{1}{E_0} + \sigma \sum_{n=1}^N \left[ \frac{1}{E_n} \left( 1 - \frac{\dot{\varepsilon}_n \mu_n}{E_0 \varepsilon_0} \right) \right] = \sigma D_0 + \sigma D(t) \quad (127)$$

which  $D_0$  is the instantaneous elastic compliance,  $1/E_0$ , and  $D(t)$  is the transient creep compliance function. Here  $\mu_n$  and  $E_0$  are properties of the material and  $\varepsilon_0$  and  $\dot{\varepsilon}_n$  change by stress and time. To simplify the resultant equation and make it ready for finite element implementation, boundary conditions are applied. Note that strain at  $t = 0$  equals to instantaneous elastic strain  $\varepsilon^e = \sigma/E_0$ , while at stable conditions ( $t \rightarrow \infty$ ) strain approaches to following

$$\sigma \frac{1}{E_0} + \sigma \sum_{n=1}^N \left[ \frac{1}{E_n} \right]$$

which states that the expression  $\left( \frac{\dot{\varepsilon}_n \mu_n}{E_0 \varepsilon_0} \right)$  can be approximated by a decreasing exponential function  $e^{-(t E_n)/\mu_n}$ , which in turn leads to an exponential form of a Prony series as

$$D(t) = \sum_n D_n [1 - e^{-t/\tau_n}] \quad (128)$$

where  $D_n$  and  $\tau_n$  are the  $n^{th}$  creep compliance and relaxation time, respectively, defined as  $\tau_n = E_n \mu_n$  and  $D_n = 1/E_n$  and,  $1 \leq n \leq N$ , where  $N$  equals to the order of the expression and represents the number of Kelvin units in the spring and dash-pot simulation of the material behaviour (for further discussion see (Flügge, 1967)).

### 5.3 Finite deformation formulation of Model B

As may be inferred from Eqs. (115) and (122), Model A is a special case of Model B in which  $n = 1$ . By increasing the number of Kelvin units in the configuration, the number of material parameters increases, and the fitting is improved. This is true in all approaches of viscoelastic modelling, in which the configuration consists of spring and dash-pot elements (Christensen, 1971).

The general theory of finite linear viscoelasticity is about finding an approximation function and material parameters that best match the test results. This is what one may get from the differential approach to viscoelasticity described by Christensen (Christensen, 1971) which introduced a concept of fading memory. This concept states that material response depends more on recent history than earlier events. In this theory, the stress is decomposed into an equilibrium stress that corresponds to the stress response at an infinite slow rate of deformation and a viscosity-induced overstress. The overstress is expressed as an integral over the deformation history and a relaxation function is specified as a measure for the materials memory.

Experimental results for PE show a high degree of deformability and strong nonlinearities, which states that the constitutive models need to be based on finite strain theories in consistence with the natural laws of thermodynamics. In the following, small deformation equations are extended to the cases of finite deformations. The approach corresponds to the finite deformation viscoelasticity within the framework of the superposition principle. It is aimed to derive the finite deformation viscoelasticity model by considering the satisfaction of the second law of thermodynamics in the form of the Clausius–Duhem inequality ( (Hasanpour, et al., 2009) & (Huber, et al., 2000)).

The strain produced by the common action of several loads can be calculated using the rule of linear superposition (Flügge, 1967) & (Reddy, 2013). If a stress is applied suddenly at time  $t = 0$  (a step load), it produces a strain  $\varepsilon = \sigma_0 D(t)$ , where  $D(t)$  is the time-dependent tensile creep compliance of the material (Figure 40). If the stress  $\sigma_0$  is kept constant, the relation  $\varepsilon = \sigma_0 D(t)$  will describe the strain for the entire duration of the step loading. However, if more stress is added at time  $t = t'$ , then for

$t > t'$  the material will experience additional strain which is proportional to the increase in stress  $\Delta\sigma'$ , which depends on the creep compliance  $D(t)$ ; time is measured from the start of the new stress loading at  $t = t'$ . The cumulative strain for any time  $t = t'$ , is

$$\varepsilon(t) = \sigma_0 D(t) + \Delta\sigma' D(t - t') \quad (129)$$

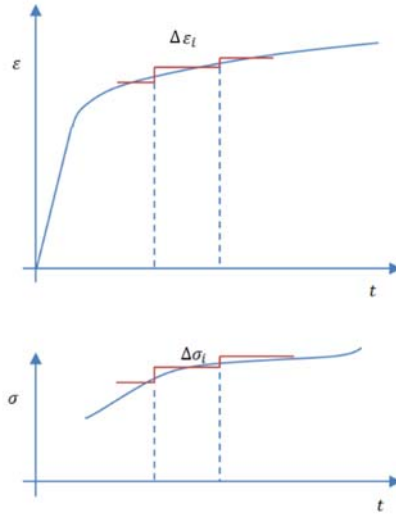


**Figure 40: Applied step-load stress history**

Any arbitrary stress history can now be divided into the initial stress state  $\sigma_0$  and a sequence of infinitesimal step functions as shown in Figure 40. The corresponding strain at time  $t$  is therefore the sum of all the incremental steps that have taken place at time  $t = t'$ , giving (Schapery, 1969)

$$\varepsilon(t) = \sigma_0 D(t) + \int_0^t D(t - t') \frac{d\sigma^{t'}}{dt'} dt' \quad (130)$$

The integral in Eq. (130) is referred to as a hereditary integral and is the governing equation for linear viscoelastic behaviour under uniaxial loading. This linearly viscoelastic constitutive equation can be written for an isotropic material undergoing uniaxial loading as (Roy, et al., 1988)

$$\varepsilon^t = \sigma^t D_0 + \int_0^t D(t - t') \frac{d\sigma^{t'}}{dt'} dt' \quad (131)$$

Here  $\varepsilon^t$  and  $\sigma^t$  represent uniaxial strain and the Cauchy stress, respectively, at current time  $t$ .  $D_0$  is the instantaneous elastic compliance and  $D(t)$  represents a transient creep compliance function (Eq. (128)). Substitution of Eq. (128) in Eq. (131) gives

$$\varepsilon^t = \sigma^t D_0 + \int_0^t \sum_n D_n \left[ 1 - e^{-\frac{(t-t')}{\tau_n}} \right] \frac{d\sigma^{t'}}{dt'} dt' \quad (132)$$

Simplifying yields

$$\varepsilon^t = \sigma^t D_0 + \sum_n D_n \int_0^t \frac{d\sigma^{t'}}{dt'} dt' - \sum_n D_n \int_0^t e^{-\frac{(t-t')}{\tau_n}} \frac{d\sigma^{t'}}{dt'} dt' \quad (133)$$

The second integral on the right hand side of the equation is now separated into two parts, the first part having limits from zero to  $(t - \Delta t)$ , and the second integral spanning only the current load step, that is, from  $(t - \Delta t)$  to  $t$ . The first can be written as (Roy, et al., 1988)

$$\int_0^{t-\Delta t} e^{-\frac{(t-t')}{\tau_n}} \frac{d\sigma^{t'}}{dt'} dt' = e^{-(\Delta t)/\tau_n} q_n^{t-\Delta t} \quad (134)$$

where

$$q_n^{t-\Delta t} = \int_0^{t-\Delta t} e^{-\frac{(t-\Delta t-t')}{\tau_n}} \frac{d\sigma^{t'}}{dt'} dt' \quad (135)$$

and the second integral is integrated by parts, as follows:

$$\begin{aligned} \int_{t-\Delta t}^t e^{-\frac{(t-t')}{\tau_n}} \frac{d\sigma^{t'}}{dt'} dt' &= \frac{d\sigma^{t'}}{dt'} \tau_n e^{-\frac{(t-t')}{\tau_n}} \Big|_{t-\Delta t}^t - \int_{t-\Delta t}^t e^{-\frac{(t-t')}{\tau_n}} \frac{d^2\sigma^{t'}}{dt'^2} dt' \\ &= \frac{d\sigma(t')}{dt'} \tau_n \left[ 1 - e^{-\frac{(t-t')}{\tau_n}} \right] \end{aligned} \quad (136)$$

In order to carry out the integration, it is assumed that  $\sigma$  varies linearly over the current time step  $\Delta t$  and its second derivative is zero. This leads to the following equation

$$\frac{d\sigma^t}{dt} = \frac{\sigma^t - \sigma^{t-\Delta t}}{\Delta t} \quad (137)$$

which simplifies Eq. (136) to



$$\int_{t-\Delta t}^t e^{-\frac{(t-t')}{\tau_n}} \frac{d\sigma^{t'}}{dt'} dt' = (\sigma^t - \sigma^{t-\Delta t})\beta_n^t \quad (138)$$

where

$$\beta_n^t = \frac{\tau_n}{\Delta t} \left( 1 - e^{-\frac{\Delta t}{\tau_n}} \right) \quad (139)$$

Substituting Eq. (134) and Eq. (138) back into Eq. (133), one obtains (Roy, et al., 1988)

$$\varepsilon^t = \left[ D_0 + \sum_n D_n (1 - \beta_n^t) \right] \sigma^t + \sum_n D_n \left( \beta_n^t \sigma^{t-\Delta t} - e^{-\frac{\Delta t}{\tau_n}} q_n^{t-\Delta t} \right) \quad (140)$$

or

$$\varepsilon^t = D_I^t \sigma^t + \bar{E}^t \quad (141)$$

where

$$D_I^t = D_0 + \sum_n D_n (1 - \beta_n^t) \quad (142)$$

$$\bar{E}^t = \sum_n D_n \left( \beta_n^t \sigma^{t-\Delta t} - e^{-\frac{\Delta t}{\tau_n}} q_n^{t-\Delta t} \right) \quad (143)$$

Here  $D_I^t$  is the instantaneous compliance multiplying the instantaneous stress  $\sigma^t$  and  $\bar{E}^t$  is the hereditary strains. The term  $q_n^{t-\Delta t}$  is the  $r^{th}$  component of the hereditary integral series at the end of the previous load step which is carried over to the current step and is defined as the following recurrence formula.

$$q_n^t = e^{-\frac{\Delta t}{\tau_n}} q_n^{t-\Delta t} + (\sigma^t - \sigma^{t-\Delta t})\beta_n^t \quad (144)$$

### 5.3.1 Extending to Three-Dimensional Viscoelastic Constitutive Relations

The formulation needs to be generalized to multiaxial stress state in order to be able to sustain a fully three-dimensional stress state. It can be shown that the constitutive law for a homogeneous isotropic viscoelastic material reduces to the form ( (Schapery, 1969) & (Schapery, 1969))

$$e_{ij}^t = \{J\}\{\sigma_{ij}^t\} + \{D - J\}\{\sigma_{mm}^t\}\delta_{ij} , \quad i, j = 1 \sim 3 \quad (145)$$

where  $J$  is shear creep compliance and the operator  $\{\cdot\}$  implies convolution integral as indicated below

$$\{J\}\{\sigma_{ij}^t\} = J_0\sigma_{ij}^t + \int_0^t J(t-t') \frac{\partial}{\partial t'}(\sigma_{ij}^{t'})dt' \quad (146)$$

$$\{D-J\}\{\sigma_{mm}^t\}\delta_{ij} = [D_0 - J_0]\sigma_{mm}^t + \int_0^t [D(t-t') - J(t-t')] \frac{\partial}{\partial t'}(\sigma_{ij}^{t'})dt' \quad (147)$$

Expanding Eq. (145) term by term for the strains

$$\begin{aligned} e_{11}^t &= \{D\}\{\sigma_{11}^t\} + \{D-J\}\{\sigma_{22}^t\} + \{D-J\}\{\sigma_{33}^t\} \\ e_{22}^t &= \{D-J\}\{\sigma_{11}^t\} + \{D\}\{\sigma_{22}^t\} + \{D-J\}\{\sigma_{33}^t\} \\ e_{33}^t &= \{D-J\}\{\sigma_{11}^t\} + \{D-J\}\{\sigma_{22}^t\} + \{D\}\{\sigma_{33}^t\} \\ \gamma_{12}^t &= 2\{J\}\{\sigma_{12}^t\}, \quad \gamma_{23}^t = 2\{J\}\{\sigma_{23}^t\}, \quad \gamma_{13}^t = 2\{J\}\{\sigma_{13}^t\} \end{aligned} \quad (148)$$

Similar to the transient components of the creep compliances, Eq. (128), the shear compliances can be written in the form of a Prony series as

$$J(t) = \sum_n J_n [1 - e^{-t/T_n}] \quad (149)$$

where  $T_n$  are the relaxation times in shear. Also  $J_0$  represents the elastic shear compliance at  $t = 0$ . The axial and shear terms of deformations into Eq. (148) are defined as follows (Roy, et al., 1988)

$$\{D\}\{\sigma_{ij}^t\} = D_I^t \sigma_{ij}^t + Q_{ij}^t \quad (150)$$

where  $D_I^t$  is the instantaneous creep compliance function and  $Q_{ij}^t$  represents the hereditary strain components due to tensile creep at time  $t$

$$D_I^t = D_0 + \sum_n D_n (1 - \beta_n^t) \quad (151)$$

$$Q_{ij}^t = \sum_n D_n \left( \beta_n^t \sigma_{ij}^{t-\Delta t} - e^{-\frac{\Delta t}{\tau_n}} q_{n,ij}^{t-\Delta t} \right) \quad (152)$$

and

$$q_{n,ij}^t = e^{-\frac{\Delta t}{\tau_n}} q_{n,ij}^{t-\Delta t} + (\sigma_{ij}^t - \sigma_{ij}^{t-\Delta t}) \beta_n^t \quad (153)$$

Similarly, expressions can be developed for  $\{J\}\{\sigma_{ij}^t\}$ . For a fully three-dimensional problem, substituting the resultant equations in Eqs. (148) and dropping superscripts, one obtains for the viscoelasticity problem the following matrix format (Roy, et al., 1988)

$$\mathbf{e} = \mathbf{N}\boldsymbol{\sigma} + \mathbf{H} \quad (154)$$

where  $\mathbf{H}$  is a vector of hereditary strains that contain the entire load history effect (Roy, et al., 1988). For a linear three-dimensional viscoelasticity problem note that the left-hand side of Eq. (154) is a vector containing the algebraic difference of kinematic strains  $\boldsymbol{\varepsilon}$  and dilatational strains  $\theta I$

$$\mathbf{e}^T = \{(\varepsilon_{11} - \theta), (\varepsilon_{11} - \theta), (\varepsilon_{11} - \theta), \gamma_{12}, \gamma_{23}, \gamma_{13}\} \quad (155)$$

while  $\boldsymbol{\sigma}$  contains the six components of the Cauchy stress tensor. The matrix  $\mathbf{N}$  is a  $6 \times 6$  matrix of coefficients given by

$$\mathbf{N} = \begin{bmatrix} D_I & (D_I - J_I)(D_I - J_I) & 0 & 0 & 0 \\ (D_I - J_I) & D_I & (D_I - J_I) & 0 & 0 & 0 \\ (D_I - J_I)(D_I - J_I) & D_I & 0 & 0 & 0 & 0 \\ 0 & 0 & 0 & 2J_I & 0 & 0 \\ 0 & 0 & 0 & 0 & 2J_I & 0 \\ 0 & 0 & 0 & 0 & 0 & 2J_I \end{bmatrix} \quad (156)$$

Multiplying Eq. (154) by  $\mathbf{N}^{-1}$ , an explicit expression for stresses in terms of strains is obtained

$$\boldsymbol{\sigma} = \mathbf{N}^{-1}(\mathbf{e} - \mathbf{H}) \quad (157)$$

Eq. (157) provides a general viscoelastic constitutive relation that can be applied to three-dimensional viscoelasticity problems. Note that the use of tensile creep and shear compliances as a material property input allows Poisson's ratio to change with time. Hence, the present formulation is applicable to any thermorheologically simple isotropic three-dimensional viscoelastic material over any length of time, unlike some other formulations that assume constant Poisson's ratio.

For the special case where Poisson's ratio is constant with time, then

$$J(t) = (1 + \nu)D(t) \quad (158)$$

which makes the relaxation times in tensile creep and shear to be identical. The matrix  $\mathbf{N}$  takes the simplified form

$$\mathbf{N} = D_I \times \mathbf{C} = D_I \begin{bmatrix} 1 & -\nu & -\nu & 0 & 0 & 0 \\ -\nu & 1 & -\nu & 0 & 0 & 0 \\ -\nu & -\nu & 1 & 0 & 0 & 0 \\ 0 & 0 & 0 & 2(1+\nu) & 0 & 0 \\ 0 & 0 & 0 & 0 & 2(1+\nu) & 0 \\ 0 & 0 & 0 & 0 & 0 & 2(1+\nu) \end{bmatrix} \quad (159)$$

## 5.4 FEM implementation

To perform finite element analysis, a subroutine is developed in Visual Studio workspace for material determination, which defines the viscoelastic mechanical constitutive behaviour of material. The subroutine is compiled by Fortran software which is linked to finite element software ABAQUS/Standard. The FE software ABAQUS/Standard calls the subroutine in each increment and each material calculation point for which the \*MATERIAL definition includes \*USER MATERIAL input expression. The model for which the material is defined by the aforementioned user defined material subroutine (UMAT) needs first to be defined in ABAQUS user interface where meshes, loads and boundary conditions are defined. Generally, the ABAQUS 3-D modelling involves three stages: (1) pre-processing, where the 3-D model is generated and finite element mesh, loads and boundary conditions are assigned, (2) analysis, where displacements, stresses and strains are computed by means of material properties, which have been defined as User Material in the first stage, and (3) post-processing, where the results are graphically presented.

For analyzing time-dependent behaviour of the materials under study by means of the finite element method, the three-dimensional finite deformation constitutive model for Model B is implemented in an FEM program through a User Subroutine. This model was presented in the previous section. Eq. (157) defines the behaviour of Model B. In this equation, the Cauchy stress,  $\sigma$ , indicates the stress at the end of increment and its components equal to  $\sigma_{ij}^{t-\Delta t} + \Delta\sigma_{ij}$ , which is the value at the beginning of the increment,  $\sigma_{ij}^{t-\Delta t}$ , plus the change due to  $\Delta t$ . The same applies to the strain tensor, in which  $\varepsilon_{ij} = \varepsilon_{ij}^{t-\Delta t} + \Delta\varepsilon_{ij}$ . Rewriting Eq. (140) in 1-D yields

$$\Delta\sigma = D_I^{-1}\varepsilon^{t-\Delta t} + D_I^{-1}\Delta\varepsilon - D_I^{-1} \sum_n D_n \left( \beta_n^t \sigma^{t-\Delta t} - e^{-\frac{\Delta t}{\tau_n}} q_n^{t-\Delta t} \right) - \sigma^{t-\Delta t} \quad (160)$$

Differentiating the stress increment,  $\Delta\sigma$ , versus strain increment,  $\Delta\varepsilon$ , provides

$$\frac{\Delta\sigma}{\Delta\varepsilon} = D_I^{-1} = E^t = \left[ D_0 + \sum_n D_n(1 - \beta_n^t) \right]^{-1} \quad (161)$$

which is the stiffness modulus and in three-dimensional form represents the elasticity matrix or the so called “material Jacobian matrix”,  $\partial\sigma_i/\partial\varepsilon_j$ . This matrix defines the change in the  $i^{th}$  stress component at the end of the time increment,  $\Delta t$ , caused by an infinitesimal perturbation of the  $j^{th}$  component of the strain increment array. As seen,  $E^t$ , is defined in each increment by means of the time dependent material parameters, as well as the time increment. This tensor has to be updated at the end of each increment, as one of two main functions performed by the subroutine. The second function, the is that subroutine must update the stresses and the solution-dependent state variables to their values at the end of the increment. With the use of Eq. (155), Eq. (157) can be rewritten as

$$\sigma^t = \sigma^{t-\Delta t} + \Delta\sigma = D_I^{-1}(\varepsilon^{t-\Delta t} - \theta - H) + D_I^{-1}\Delta\varepsilon \quad (162)$$

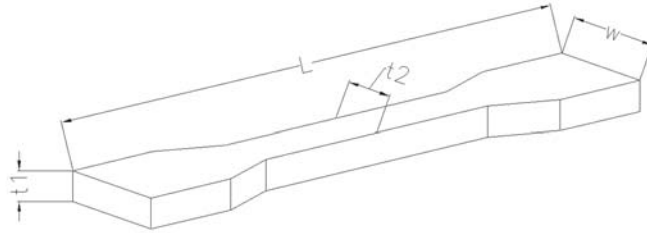
This expresses the Cauchy stress tensor at the end of the increment,  $\sigma^t$ , and this is passed forward at the beginning of the increment, as  $\sigma^{t-\Delta t}$ . Here, the array  $H$  is a function of material properties and stresses, as well as  $q_n^{t-\Delta t}$ , at the beginning of the increment. Values of  $q_n^{t-\Delta t}$  are passed forward in the from previous increment as a state variable and need to be calculated in each increment.

## 5.5 Results, materials and comparison

In this section, case studies are solved and compared to available experimental data. For this, the analysis is performed by concentrating on the multi-Kelvin linear viscoelastic model, which is a general configuration of spring and dash-pots (Model B) and is more accurate than the 3-parameter solid configuration (Model A, which is a special case ( $n = 1$ ) of the general one, Model B), because it has more material parameters, thus a more accurate fit.

In this case study, the analysis has been conducted on a single 3-D cubic element structure representing a beam in uniform tension. The FEM results for the beam under 1-D tension have been compared with the experimental ones. The uniaxial tension experiments have been done on dog-bone shape structures (Figure 41) by Liu (Liu, 2007), at the University of Waterloo, on high density and medium density polyethylene materials. Experiments were performed on numerous types of PEs and include tests on short term tensile creep (24 hours). Herein the comparisons are done on short term behaviour of three materials. The specimens were produced, from resins by melting them and

machining and from pipes by cutting out the samples (Table 20). 24-hour creep testing was done at different stress levels to examine time dependent and nonlinear behaviour of the materials. The testing showed clear differences in the behaviour of different HDPEs. Using these uniaxial creep tests is the easiest way to determine the material behaviour. Using the method of minimization of the Least Squares Error by fitting the model to the experimental results, the stiffness matrix parameters, Eq. (159), and material parameters were determined by Liu (Liu, 2007), and these were used as inputs to the FEM analysis. These parameters, which are Prony series parameters, for the sample materials (Table 20), are tabulated in Table 21. These parameters are obtained by considering  $N = 3$  in Model B, meaning that three Kelvin units are used in constructing the spring and dash-pot configuration. Relaxation times in all cases are considered to be fixed and equal to 500s, 10000s and 200000s for  $n = 1 \sim 3$ . Poisson's ratio  $\nu$  is considered to be time independent and equal to 0.45 for HDPE, that is,  $\nu \rightarrow 0.5$ . This assumption results in a bulk modulus about  $10^4 - 10^6$  which is recommended in the literature (Krishnaswami, et al., 1992).



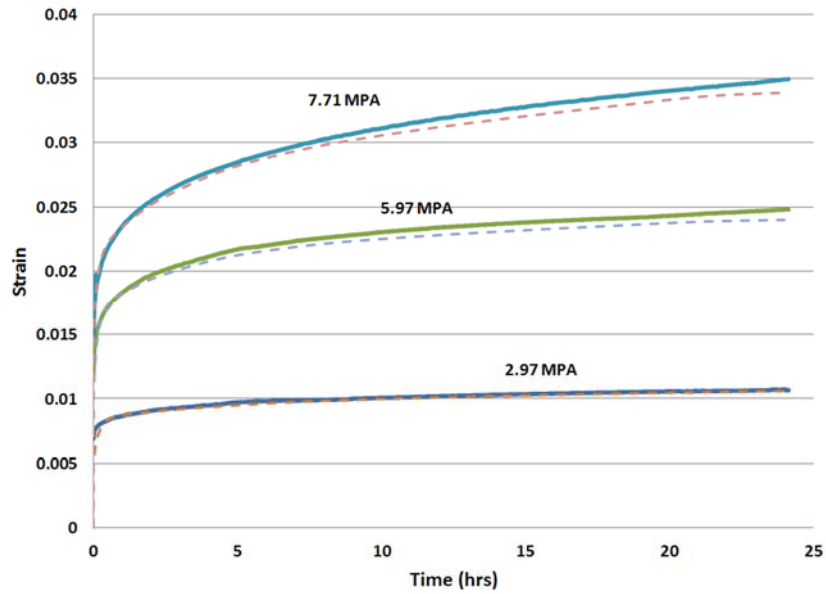
**Figure 41: Dog-bone shape material sample test used by Liu (Liu, 2007)**

Table 20: List of tested polyethylene (Liu, 2007)								
No.	Material	Type	Thickness* (mm)	Width** (mm)	Code	$M_w$ (kg/mol)	$M_n$ (kg/mol)	ESCR (h)
1	HDPE-PIPE	pipe	5.00	13.05	PIPE	Data not available		
2	HDPE-resin1	resin	5.80	12.76	RES1	127.5	16.3	4.8
3	HDPE-resin2	resin	5.65	12.89	RES2	118.5	15.7	1.2

\*  $\pm 0.03$

\*\*  $\pm 0.05$

Table 21: Prony series parameters (material parameters) (Liu, 2007)								
Material	Stress (MPa)	$E_0$ (MPa)	$E_1$ (MPa)	$E_2$ (MPa)	$E_3$ (MPa)	$\tau_1$ (s)	$\tau_2$ (s)	$\tau_3$ (s)
HDPE-PIPE	2.97	650	797.3	2320. 3	925.1	500	1000 0	200000
	5.97	580	913.6	1212. 3	695.0	500	1000 0	200000
	7.71	520	1224. 8	1105. 0	385.9	500	1000 0	200000
HDPE-resin1	2.67	990	2473. 5	1434. 3	1.0e8	500	1000 0	200000
	5.15	830	2153. 6	1319. 8	949.4	500	1000 0	200000
	7.14	790	2614. 5	993.8	747.7	500	1000 0	200000
	7.58	770	1771. 7	959.6	537.9	500	1000 0	200000
	10.6	730	1153. 4	706.9	352.5	500	1000 0	200000
HDPE-resin2	2.68	2500	2848. 6	3650. 6	1053. 8	500	1000 0	200000
	5.58	2300	2125. 6	1811. 4	696.3	500	1000 0	200000
	7.28	1700	1515. 4	1537. 4	603.9	500	1000 0	200000
	10.6	1200	1180. 3	1111. 9	405.5	500	1000 0	200000
	13.7	1100	999.9	810.1	145.0	500	1000 0	200000



**Figure 42: Test results (continuous line) (Liu, 2007) vs. present FEA (dashed line) for HDPE-PIPE material**

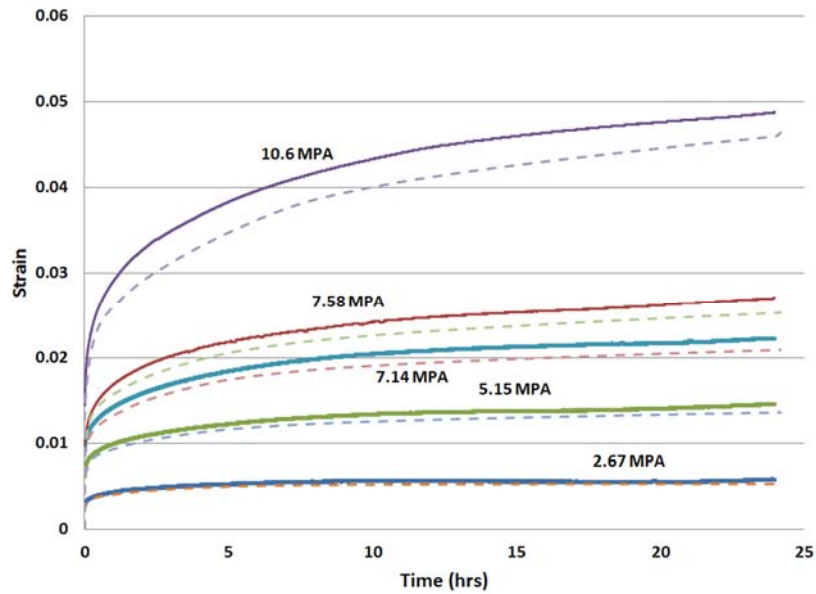


**Figure 43: Test results (continuous line) (Liu, 2007) vs. present FEA (dashed line) for HDPE-RES1 material**



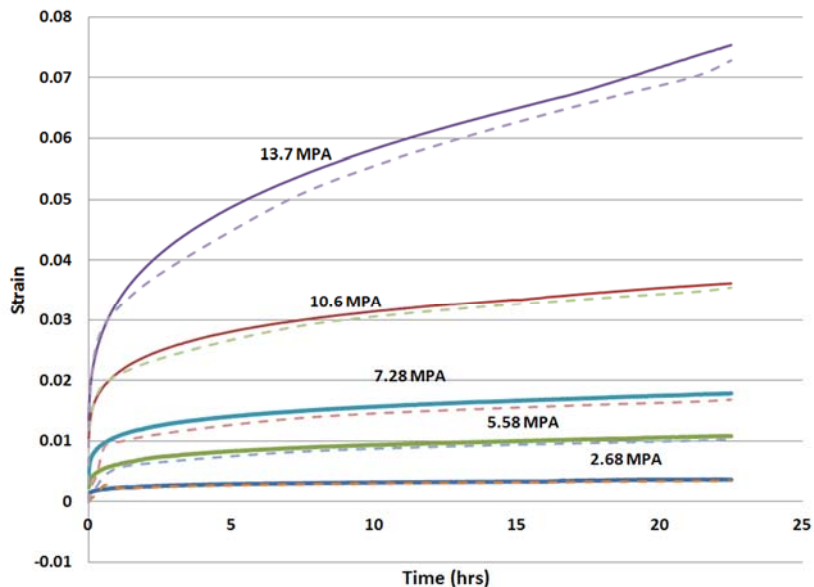


**Figure 44: Test results (continuous line) (Liu, 2007) vs. present FEA (dashed line) for HDPE-RES2 material**

Figure 42 to Figure 44 compare the experimental measurements of strain vs. time with results obtained from finite element analysis. The comparison shows relatively good correlation between these two sets of results, except in some cases that an offset is observed (like for stress levels 7.58 MPa and 10.6 MPa in Figure 43). The author believes that the reason of this offset is error in the first readings of the measurements. The first measurement indicates the instantaneous strain and/or compliance and plays an important role in predicting the material response in times greater than initial test time.

Here Model A will be compared to model B. As it was mentioned before, Model A is a simple case of Model B in which  $N = 1$ , meaning that just one Kelvin unit is considered. So, the number of associated moduli of elasticity and relaxation times decrease to one ( $E_1$  and  $\tau_1$ ). The method that is used by Liu (Liu, 2007) for obtaining the material parameters, is a method of pre-setting the relaxation time and finding the associated moduli of elasticity. For more information, readers are referred to Chapter 3. Before comparing the two mentioned models together, let's see how the pre-setting of relaxation times affect the results.

Here Model A is considered and PIPE material is chosen for analysis. To find the material parameters, in a similar method to Liu's, different relaxation times are set and related moduli are

obtained. These times are 1000s, 5000s, 15000s and 50000s for different cases of  $N=1$  (1), (2), (3) and (4), respectively. The corresponding moduli are 410 MPa, 391 MPa, 352 MPa and 239 MPa. These cases and the material parameters for each case are shown in Table 22. Using the developed finite element procedure, and setting  $N = 1$ , finite element results are obtained for PIPE material under 7.71 MPa uniaxial loading. The resultant strain curves are shown in Figure 45 for each simulation case. As one can see, comparison of FE results with the experimental ones, is not satisfactory. The Least Squares Errors (LSE) (see chapter 3 for more information) for each case in Figure 45 are tabulated in Table 22. As inferred, the shape of the curves, and the associated errors, are dependent on the choice of relaxation time. Therefore, it can be concluded that the model A is not satisfactory, as just one Kelvin unit is used and, furthermore, the method of pre-setting material parameters, are not reliable enough, as the results are very sensitive to the choice of relaxation times. For accurate results, the method of nonlinear optimization (Chapter 3) is highly recommended for  $N < 3$ .

Case	N=1 (1)	N=1 (2)	N=1 (3)	N=1 (4)
$E_1$ (MPa)	410	391	352	239
$\tau_1$ (s)	1000	5000	15000	50000
Error (%)	15.2	8.9	8.6	12.3

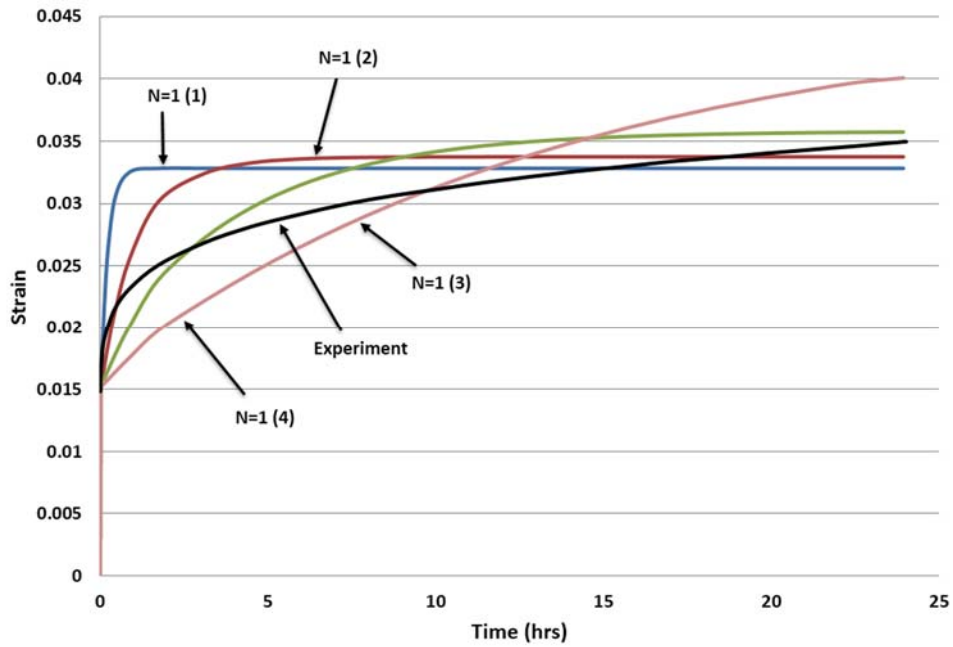
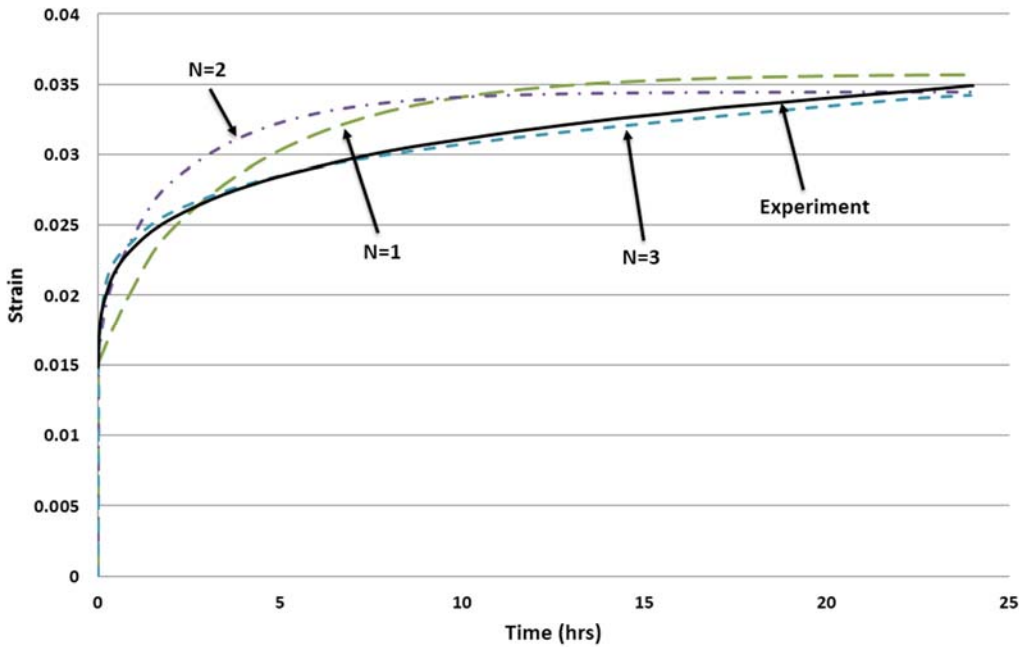


Figure 45: Finite element results for PIPE material under 7.71MPa, Model A (N=1) compared to experiments, see Table 22 for material parameters for each case

Table 23: Prony series parameters for PIPE under 7.71MPa uniaxial force

Case	Model A N=1 (3)	Model B N=2	Model B N=3 (Liu, 2007)
$E_1$ (MPa)	352	2297	1225
$E_2$ (MPa)		449	1105
$E_3$ (MPa)			386
$\tau_1$ (s)	15000	500	500
$\tau_2$ (s)		10000	10000
$\tau_3$ (s)			200000
Error (%)	8.6	6.7	2.7

To see how the number of Kelvin units affect the resultant strain curves, three cases are considered: Case I: Model A with  $\tau_1 = 15000s$ , and Case II and III: Model B, with  $N = 2$  and  $N = 3$ , respectively. The cases and material parameters are shown in Table 23. Figure 46 shows the resultant finite element curves using the material parameters for each case. As seen, by increasing the number of Kelvin units, the correlation between simulation and test data improves. This has been illustrated by LS errors calculated for each case (Table 23).



**Figure 46: Finite element results for PIPE material under 7.71MPa, using Model A (N=1), and Model B (N=2 & N=3) compared to experiments (Liu, 2007)**

## 5.6 Conclusion

A phenomenological three-dimensional linear viscoelastic constitutive model for time dependent analysis was presented. The model was based on Boltzmann linear superposition principle, and provided a linear solution procedure to solve viscoelastic behaviour. The Prony series material parameters used in the process and the constitutive relations were based on the separable form of equations. It was shown that the presented model is suitable for development of a unified computer code that can handle linear viscoelastic material behaviour. Based on the proposed constitutive equations, a finite element (FE) procedure was developed and implemented in a User Material FE code

in ABAQUS. The validity of the model was assessed by comparison with experimental observations on high density polyethylene (HDPE) for uniaxial loading cases. For this, the code was used to predict the response of a single cubic element sample material. A reasonably good correlation was seen between these two sets of results and it is concluded that the proposed FEM model can reproduce the experimental strain-time curves quite accurately.

Based on the research conducted in this chapter and summarized above, the following specific findings and contributions can be mentioned:

The developed finite element procedure, allows to model the long term as well as short term responses of polymers. For this a code was developed in Fortran workspace, which is linked to commercial software ABAQUS.

The inputs to the developed code include a structural model and a material model. The former is done through the ABAQUS user interface and includes 3D solid modelling, boundary conditions, loadings, meshing and time discretization. The latter is obtained from experiments and needs material analysis.

## Chapter 6

# Constitutive equations and finite element implementation of isochronous nonlinear viscoelastic behaviour

Contents of this chapter is based on a paper which will be submitted to the peer reviewed journals. This chapter presents phenomenological three-dimensional nonlinear viscoelastic constitutive model for time dependent analysis. Based on Schapery's single integral constitutive law, a solution procedure has been provided to solve nonlinear viscoelastic behaviour. This procedure is applicable to three dimensional problems and uses time- and stress-dependent material properties to characterize the nonlinear behaviour of material. The equations describing material behaviour are chosen based on the measured material properties in a short test time frame. This estimation process uses the Prony series material parameters and the constitutive relations are based on the non-separable form of equations. Material properties are then modified to include the long term response of material. The presented model is suitable for development of a unified computer code that can handle both linear as well as nonlinear viscoelastic material behaviour. The proposed viscoelastic model is implemented in a user-defined material algorithm in ABAQUS (UMAT) and the model validity is assessed by comparison with experimental observations on polyethylene for three uniaxial loading cases, namely, short term loading, long term loading, and step loading. A part of experiments are done by Liu (Liu, 2007), while the rest are provided by ExxonMobil, a division of Imperial Oil. The research shows that the proposed FEM model can reproduce the experimental strain-time curves accurately, and concludes that with proper material properties to reflect the deformation involved in the mechanical tests, the deformation behaviour observed experimentally can be accurately predicted using the FEM simulation.

### 6.1 Introduction

Within the context of the development of nonlinear viscoelastic constitutive models, three general approaches can be distinguished (Xia, et al., 2006): 1) rheological models in a differential form, 2) non-equilibrium thermodynamics, and 3) free volume models in an integral formulation. The first class is based on a certain configuration of mechanical elements, i.e. springs and dashpots, which reproduce the viscoelastic response of real material systems. The most popular combinations are the Burgers, the generalized Maxwell and the generalized Kelvin models. (Flugge, 1967). Non-equilibrium

thermodynamics approach has been found helpful in constructing constitutive relations and was investigated by several researchers, namely, Schapery (Schapery, 1969); Lustig et al. (Lustig, et al., 1996) and Weitsman (Weitsman, 1990). The free energy is expressed as a function of current values of strain (stress), temperature and other variables such as moisture and physical aging, which could be incorporated through a shift factor in reduced time. The nonlinear free volume approach is based on the concept of “free volume”, and the linear viscoelastic behaviour for small strains, except that the time scale is adjusted to the current free volume state, thereby introducing nonlinearity into the constitutive equations. Constitutive models based on this approach can be found in references by Mlekusch (Mlekusch, 2001) and Popelar and Liechi (Popelar, et al., 2003), among others.

In the present study, the focus is on the single integral thermodynamic approach, which is a simplified case of the multiple integral method and belongs to the second class of the above mentioned methodologies (non-equilibrium thermodynamics). One of the best known nonlinear theories of viscoelasticity was proposed by Green and Rivlin (Green, et al., 1957) for homogenous isotropic nonlinear viscoelastic materials with memory. It is a multiple integral constitutive law with multiple argument functions. These multiple argument functions require a large number of tests, which would be costly and unjustifiable. Lockett (Lockett, 1972) proposed constitutive models that uses only a single integral and do not require a large experimental effort. It should be noted that this simpler model is limited, and it should not be expected that such a theory can be adequate for all situations, like materials with high degree of nonlinearity. Alternately, a thermodynamically consistent theory for a single integral representation of nonlinear viscoelasticity was first proposed by Schapery (Schapery, 1969) & (Schapery, 1969). The law can be derived from fundamental principles using the concepts of irreversible thermodynamics. A comprehensive review of the thermodynamics basis of Schapery's theory has been presented by Hiel et al. (Hiel, et al., 1983) and Findley et al. (Findley, et al., 1976).

In contrast to the linear viscoelastic behaviour of a solid, in which the viscoelastic material parameters are independent of the state of deformation (or loading), in nonlinear behaviour, viscoelastic creep and relaxation depends not only on time but also on the stress (or strain) imposed on the material. Hence, the modelling becomes inherently nonlinear because changes in the strain (or stress) alter the viscoelastic material properties which, in turn, modify the resultant strain (or stress). Therefore, in this work, a three-dimensional finite element model is presented for isochronous nonlinear viscoelastic behaviour. The modelling proceeds with the following steps.

- 1- Model definition is done based on Schapery's single integral constitutive law (section 6.2)
- 2- Multi Kelvin solid representation of viscoelastic behaviour is employed (section 6.2)
- 3- Constitutive equations are extended to the three-dimensional case. (section 6.3)
- 4- Material/kernel functions ( $g_0^t$ ,  $g_1^t$  and  $g_2^t$ ) are defined for long term responses (section 6.4)
- 5- An empirical approach is used for defining the fitting parameters (section 6.4)
- 6- Model is implemented in FE user subroutine (section 0)
- 7- The presented model results are validated for: (section 6.6)
  - Short term behaviour
  - Long term behaviour
  - Step loading

A nonlinear solution procedure is developed (step 1) which uses Schapery's single integral constitutive law (Schapery, 1969) & (Schapery, 1969). A multi Kelvin solid configuration of spring and dash-pot elements is used to construct the constitutive equations (step 2). The procedure is based on the work done by Roy and Reddy (Roy, et al., 1988), in which the time- and stress dependent material properties (based on a generalized multi Kelvin simulation) are used to characterize the nonlinear behaviour.

A three-dimensional formulation is developed next (step 3), whereas for the implementation in finite element analysis Kernel functions ( $g_0^t$ ,  $g_1^t$  and  $g_2^t$ ) are subsequently defined and the material properties are modified to include the long term response of the material (step 4). The equations describing material behaviour are modified based on the measured material properties through an empirical approach (step 5).

The presented model is suitable for the development of a unified computer code that can handle both linear as well as nonlinear viscoelastic material behaviour. For simplicity, the model doesn't consider the geometric (kinematic) nonlinearity. For more details, readers are referred to Roy and Reddy (Roy, et al., 1988) & (Roy, et al., 1988), in which the formulation of a coupled geometrically nonlinear (i.e.,



including large deflection and rotation of the structure), and nonlinear viscoelastic behaviour can be found.

The proposed viscoelastic model is implemented in a user-defined material algorithm in Abaqus (UMAT) (step 6). The current version of the commercial software ABAQUS allows only linear viscoelastic modelling and lacks the nonlinear analysis of viscous materials. The validity of the models is assessed (step 7) by comparison with experimental observations on polyethylene specimens under uniaxial loading. A part of experiments are done by Liu (Liu, 2007), while the rest are provided by ExxonMobil, a division of Imperial Oil. The comparisons in section 6 show that the proposed constitutive model can satisfactorily represent the time-dependent mechanical behaviour of polymers.

Steps 2, 4 and 5 (sections 4.36.26.4 and 0), in which deal with constitutive equations and material model functions and parameters and nonlinearization for long term prediction, use the information provided in Chapter 5 and Chapter 3, respectively, and some formulations, graphs and parameters in tables associated with this concept might be repetitions. The repetitions are intentionally, as the author intends to keep this chapter independently conveyer of the proposed concept in the chapter.

## 6.2 Constitutive Equations

The uniaxial nonlinear viscoelastic constitutive equation of Schapery (Schapery, 1969) & (Schapery, 1969) can be written for an isotropic material as

$$\varepsilon^t = g_0^t \sigma^t D_0 + g_1^t \int_0^t \Delta D(\zeta^t - \zeta^{t'}) \frac{d}{dt'} [g_2^{t'} \sigma^{t'}] dt' \quad (163)$$

Here  $\varepsilon^t$  and  $\sigma^t$  represent uniaxial kinematic strain and the Cauchy stress, respectively, at current time  $t$ .  $D_0$  is the instantaneous elastic compliance and  $\Delta D(t)$  represents a transient creep compliance function. Superscript  $t$  denotes the value at current time. The nonlinear factor  $g_0^t$  defines stress and temperature effects on the instantaneous elastic compliance and is a measure of state dependent reduction (or increase) in stiffness,  $g_0^t = g_0(\sigma, T)$ . Transient (or creep) compliance factor  $g_1^t$  has a similar meaning, operating on the creep compliance component. The factor  $g_2^t$  accounts for the influence of load rate on creep, and depends on stress and temperature. The function  $\zeta^t$  represents a reduced time scale parameter defined by:

$$\zeta^t = \int_0^t \frac{1}{(a_{\sigma T}^t)} dt' \quad (164)$$

where  $a_{\sigma T}^t$  is a time scale shift factor. Generally,  $a_{\sigma T}^t = a_{\sigma T}^t(T, \sigma)$ , could be a function of stress and temperature at time  $t'$ , but for thermorheologically simple materials, is a function of temperature,  $T$ , only. Mathematically,  $a_{\sigma T}^t$ , shifts the creep data parallel to the time axis relative to a master curve for creep strain versus time. This technique is called time-temperature superpositioning and indicates that as the temperature increases, the polymer becomes more sensitive to the applied load and reacts sooner than at room temperature. Williams, Landal and Ferry (Williams, et al., 1955) applied it to a large number of polymers and found the following expression for the shift factor,

$$\log_{10} a_{\sigma T}^t = \frac{-\bar{C}_1(T - T_0)}{\bar{C}_2 + (T - T_0)} \quad (165)$$

where the constants  $\bar{C}_1$  and  $\bar{C}_2$  have the values of 17.44 and 51.6, respectively if the glass transition temperature  $T_g$  is used as the reference temperature  $T_0$ . The mentioned equation is known to be only valid above the  $T_g$ , because below this temperature the material can no longer be considered a super cooled liquid (Williams, et al., 1955). A shift factor below the  $T_g$  has been developed using the Arrhenius activation energy equation, which is (Ferry, 1980)

$$\log_{10} a_{\sigma T}^t = \frac{E_a}{2.303 R} \left( \frac{1}{T} - \frac{1}{T_g} \right) \quad (166)$$

Here an isochronous analysis is assumed, which defines  $a_{\sigma T}^t = 1$  and consequently,  $\psi^t = t$ .

In this model, the three material functions ( $g_0^t$ ,  $g_1^t$  and  $g_2^t$ ) are used to characterize the nonlinear behaviour (Findley, et al., 1976). These so called kernel functions are obtained by curve fitting of the theoretical modelling solution to the test data

It was shown by Schapery (Schapery, 1969) that the strain, Eq. (73), may be represented schematically as a mechanical analogue consisting of nonlinear springs and dashpots, as illustrated in Figure 47 (generalized configuration of a multi-Kelvin solid), with the following stress-strain relationship

$$\varepsilon = \varepsilon^e + \varepsilon^l = \sigma D_0 + \sigma D(t) \quad (167)$$

where  $\varepsilon^e$  is the elastic strain component and  $\varepsilon^i = \sum_{n=1}^N \varepsilon_n$  is the inelastic one. Here  $\varepsilon_n$  is the strain associated with each Kelvin unit and  $D_0$  represents instantaneous elastic compliance,  $1/E_0$ . The associated transient creep compliance function, is defined as the following Prony series

$$D(t) = \sum_n D_n [1 - e^{-t/\tau_n}] \quad (168)$$

where  $D_n$  and  $\tau_n$  are  $n^{th}$  equivalent creep compliance and relaxation time for  $n^{th}$  Kelvin unit, respectively, and,  $1 \leq n \leq N$ , which  $N$  equals to the order of expression and represents the number of Kelvin units in the spring and dash-pot simulation of material behaviour, Figure 39 (for further discussion see (Flugge, 1967)).

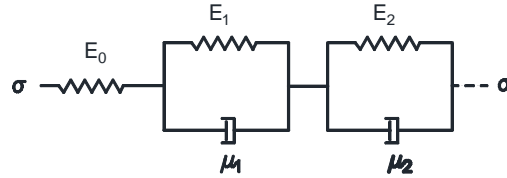


**Figure 47: Multi Kelvin Solid configuration**

Substituting in Eq. (73) yields

$$\varepsilon^t = g_0^t \sigma^t D_0 + g_1^t \int_0^t \sum_n D_n [1 - e^{-(t-t')/\tau_n}] \frac{d}{dt'} [g_2^t \sigma^{t'}] dt' \quad (169)$$

and then

$$\varepsilon^t = \sigma^t g_0^t D_0 + g_1^t \sum_n D_n(\sigma) \int_0^t \frac{d[g_2^t \sigma^{t'}]}{dt'} dt' - g_1^t \sum_n D_n(\sigma) \int_0^t e^{(-\frac{t-t'}{\tau_n})} \frac{d[g_2^t \sigma^{t'}]}{dt'} dt' \quad (170)$$

The second integral on the right hand side of the equation is now separated into two parts, the first part having limits from zero to  $(t - \Delta t)$ , and the second integral spanning only the current load step, that is, from  $(t - \Delta t)$  to  $t$

$$\int_0^t e^{(-\frac{t-t'}{\tau_n})} \frac{d[g_2^t \sigma^{t'}]}{dt'} dt' = \int_0^{t-\Delta t} e^{(-\frac{t-t'}{\tau_n})} \frac{d[g_2^t \sigma^{t'}]}{dt'} dt' + \int_{t-\Delta t}^t e^{(-\frac{t-t'}{\tau_n})} \frac{d[g_2^t \sigma^{t'}]}{dt'} dt' \quad (171)$$

The first integral can be written as (Findley, et al., 1976)

$$\int_0^{t-\Delta t} e^{\left(-\frac{t-t'}{\tau_n}\right)} \frac{d[g_2^t \sigma^{t'}]}{dt'} dt' = e^{\left(-\frac{\Delta t}{\tau_n}\right)} q_n^{t-\Delta t} \quad (172)$$

where

$$q_n^{t-\Delta t} = \int_0^{t-\Delta t} e^{\frac{-(t-\Delta t-t')}{\tau_n}} \frac{d[g_2^t \sigma^{t'}]}{dt'} dt' \quad (173)$$

and the second integral is integrated by parts: (Findley, et al., 1976)

$$\begin{aligned} \int_{t-\Delta t}^t e^{\frac{-(t-t')}{\tau_n}} \frac{d[g_2^t \sigma^{t'}]}{dt'} dt' &= \frac{d[g_2^t \sigma^{t'}]}{dt'} \tau_n e^{\frac{-(t-t')}{\tau_n}} \Big|_{t-\Delta t}^t - \int_{t-\Delta t}^t e^{\frac{-(t-t')}{\tau_n}} \frac{d^2[g_2^t \sigma^{t'}]}{dt'^2} dt' \\ &= \frac{d[g_2^t \sigma^t]}{dt} \tau_n \left[ 1 - e^{-\frac{t}{\tau_n}} \right] \end{aligned} \quad (174)$$

In order to carry out the integration, it is assumed that  $g_2^t \sigma^t$  varies linearly over the current time step  $\Delta t$  and its second derivative is zero. In other words,  $g_2^t \sigma^t$  is assumed to be represented in a piecewise linear manner over the entire load history without any loss of generality (Findley, et al., 1976). This leads to the following equation

$$\frac{d[g_2^t \sigma^t]}{dt} = \frac{g_2^t \sigma^t - g_2^{t-\Delta t} \sigma^{t-\Delta t}}{\Delta t} \quad (175)$$

which simplifies Eq. (136) to

$$\int_{t-\Delta t}^t e^{\frac{-(t-t')}{\tau_n}} \frac{d[g_2^t \sigma^{t'}]}{dt'} dt' = (g_2^t \sigma^t - g_2^{t-\Delta t} \sigma^{t-\Delta t}) \beta_n^t \quad (176)$$

where

$$\beta_n^t = \frac{\tau_n}{\Delta t} \left( 1 - e^{-\frac{\Delta t}{\tau_n}} \right) \quad (177)$$

Substituting Eq. (134) and Eq. (138) back into Eq. (133), one obtains the following single integral viscoelastic constitutive law in terms of a stress operator that includes instantaneous compliance and hereditary strains (Findley, et al., 1976)

$$\varepsilon^t = \left[ g_0^t D_0 + \sum_n g_1^t g_2^t D_n (1 - \beta_n^t) \right] \sigma^t + g_1^t \sum_n D_n \left( g_2^{t-\Delta t} \beta_n^t \sigma^{t-\Delta t} - e^{-\frac{\Delta t}{\tau_n}} q_n^{t-\Delta t} \right) \quad (178)$$

or

$$\varepsilon^t = D_I^t \sigma^t + \bar{E}^t \quad (179)$$

where

$$D_I^t = g_0^t D_0 + g_1^t g_2^t \sum_n D_n (1 - \beta_n^t) \quad (180)$$

$$\bar{E}^t = g_1^t \sum_n D_n \left( g_2^{t-\Delta t} \beta_n^t \sigma^{t-\Delta t} - e^{-\frac{\Delta t}{\tau_n}} q_n^{t-\Delta t} \right) \quad (181)$$

Here  $D_I^t$  is the instantaneous compliance multiplying the instantaneous stress  $\sigma^t$ , and  $\bar{E}^t$  is the hereditary strains. The term  $q_n^{t-\Delta t}$  is the  $r^{th}$  component of the hereditary integral series at the end of the previous load step which is carried over to the current step and is defined as the following recurrence formula.

$$q_n^t = e^{-\frac{\Delta t}{\tau_n}} q_n^{t-\Delta t} + (g_2^t \sigma^t - g_2^{t-\Delta t} \sigma^{t-\Delta t}) \beta_n^t \quad (182)$$

### 6.3 Extending to Multi-Dimensional Relations

The formulation needs to be generalized to multiaxial stress state in order to be able to sustain a fully three-dimensional stress state. The constitutive law for a homogeneous isotropic viscoelastic material can be expressed as ( (Schapery, 1969) & (Schapery, 1969))

$$e_{ij}^t = \{J\}\{g_2^t \sigma_{ij}^t\} + \{D - J\}\{g_2^t \sigma_{mm}^t\} \delta_{ij}, \quad i, j = 1 \sim 3 \quad (183)$$

where  $D$  and  $J$  are tensile and shear compliances, respectively, and the operator  $\{\cdot\}\{\cdot\}$  implies the convolution integral as indicated below:

$$\{J\}\{g_2^t \sigma_{ij}^t\} = J_0 \sigma_{ij}^t + \int_0^t J(t-t') \frac{\partial}{\partial t'} (g_2^t \sigma_{ij}^{t'}) dt' \quad (184)$$

$$\{D - J\}\{g_2^t \sigma_{mm}^t\} \delta_{ij} = [D_0 - J_0] \sigma_{mm}^t + \int_0^t [D(t-t') - J(t-t')] \frac{\partial}{\partial t'} (g_2^t \sigma_{ij}^{t'}) dt' \quad (185)$$

Expanding Eq. (145) term by term for the strains, one obtains:

$$e_{11}^t = \{D\}\{g_2^t \sigma_{11}^t\} + \{D - J\}\{g_2^t \sigma_{22}^t\} + \{D - J\}\{g_2^t \sigma_{33}^t\} \quad (186)$$

$$\begin{aligned}
e_{22}^t &= \{D - J\}\{g_2^t \sigma_{11}^t\} + \{D\}\{g_2^t \sigma_{22}^t\} + \{D - J\}\{g_2^t \sigma_{33}^t\} \\
e_{33}^t &= \{D - J\}\{g_2^t \sigma_{11}^t\} + \{D - J\}\{g_2^t \sigma_{22}^t\} + \{D\}\{g_2^t \sigma_{33}^t\} \\
\gamma_{12}^t &= 2\{J\}\{g_2^t \sigma_{12}^t\}, \quad \gamma_{23}^t = 2\{J\}\{g_2^t \sigma_{23}^t\}, \quad \gamma_{13}^t = 2\{J\}\{g_2^t \sigma_{13}^t\}
\end{aligned}$$

Similar to the transient components of the creep compliances, Eq. (168), the shear compliances can be written in the form of a Prony series as:

$$J(t) = \sum_n J_n(\sigma) \left[ 1 - e^{\left(-\frac{t}{T_n}\right)} \right] \quad (187)$$

where  $T_n$  (like  $\tau_n$  in tensile) is the relaxation time for shear. Also  $J_0$  (like  $D_0$  in tensile) represents the shear compliance at  $t = 0$ . Then Eq. (148) can be simplified to

$$\{D\}\{g_2^t \sigma_{ij}^t\} = D_I^t \sigma_{ij}^t + Q_{ij}^t \quad (188)$$

where  $D_I^t$  is the instantaneous creep compliance function and  $Q_{ij}^t$  are the hereditary strain components due to tensile creep at time  $t$ :

$$D_I^t = g_0^t D_0 + g_1^t \sum_n D_n (1 - \beta_n^t) \quad (189)$$

$$Q_{ij}^t = g_1^t \sum_n D_n \left( g_2^t \beta_n^t \sigma_{ij}^{t-\Delta t} - e^{-\frac{\Delta t}{\tau_n}} q_{n,ij}^{t-\Delta t} \right) \quad (190)$$

and

$$q_{n,ij}^t = e^{-\frac{\Delta t}{\tau_n}} q_{n,ij}^{t-\Delta t} + (g_2^t \sigma_{ij}^t - g_2^{t-\Delta t} \sigma_{ij}^{t-\Delta t}) \beta_n^t \quad (191)$$

Similar expressions can be developed for  $\{J\}\{\sigma_{ij}^t\}$  (Schapery, 1969) & (Schapery, 1969)). For a fully three-dimensional problem, substituting the resultant relations in Eq. (148) and dropping superscripts, one obtains for the viscoelasticity problem the following relation in matrix format:

$$\mathbf{e} = \mathbf{N}\boldsymbol{\sigma} + \mathbf{H} \quad (192)$$

where  $\mathbf{H}$  is defined in (Schapery, 1969) & (Schapery, 1969). For a nonlinear three-dimensional viscoelasticity problem, the left-hand side of Eq. (192) is a vector containing the algebraic difference of kinematic strains  $\boldsymbol{\varepsilon}$  and dilatational strains  $\theta I$

$$\mathbf{e}^T = \{(\varepsilon_{11} - \theta), (\varepsilon_{11} - \theta), (\varepsilon_{11} - \theta), \gamma_{12}, \gamma_{23}, \gamma_{13}\} \quad (193)$$

while  $\sigma$  contains six components of Cauchy stress tensor and  $H$  is a vector of hereditary strains that contains the entire load history effect. The matrix  $\mathbf{N}$  is a  $6 \times 6$  coefficients matrix given by

$$\mathbf{N} = \begin{bmatrix} D_I & (D_I - J_I)(D_I - J_I) & 0 & 0 & 0 \\ (D_I - J_I) & D_I & (D_I - J_I) & 0 & 0 & 0 \\ (D_I - J_I)(D_I - J_I) & D_I & 0 & 0 & 0 & 0 \\ 0 & 0 & 0 & 2J_I & 0 & 0 \\ 0 & 0 & 0 & 0 & 2J_I & 0 \\ 0 & 0 & 0 & 0 & 0 & 2J_I \end{bmatrix} \quad (194)$$

Multiplying Eq. (192) by  $\mathbf{N}^{-1}$ , an explicit expression for stresses in terms of strains is obtained

$$\boldsymbol{\sigma} = \mathbf{N}^{-1}(\mathbf{e} - \mathbf{H}) \quad (195)$$

Eq. (195) provides a general viscoelastic constitutive relation that can be applied to fully three-dimensional viscoelasticity problems. Note that the use of tensile creep and shear compliances as a material property input allows Poisson's ratio to change with time. Hence, the present formulation is applicable to any thermorheologically simple isotropic three-dimensional viscoelastic material over any length of time.

For the special case where Poisson's ratio is a constant with time, then

$$J(t) = (1 + \nu)D(t) \quad (196)$$

which makes the relaxation times in tensile creep and shear to be identical. The matrix  $\mathbf{N}$  takes the simplified form

$$\mathbf{N} = D_I \times \mathbf{C} = D_I \begin{bmatrix} 1 & -\nu & -\nu & 0 & 0 & 0 \\ -\nu & 1 & -\nu & 0 & 0 & 0 \\ -\nu & -\nu & 1 & 0 & 0 & 0 \\ 0 & 0 & 0 & 2(1 + \nu) & 0 & 0 \\ 0 & 0 & 0 & 0 & 2(1 + \nu) & 0 \\ 0 & 0 & 0 & 0 & 0 & 2(1 + \nu) \end{bmatrix} \quad (197)$$

## 6.4 Material Properties

To find a solution for Eq. (195), material properties need to be defined. These properties are obtained from test data and include: instantaneous compliance, Poisson's ratio, and  $2 \times N$  unknown creep compliances and relaxation times ( $D_n$  and  $\tau_n$ ) associated with  $N$  Kelvin units (Figure 47). Kernel functions, ( $g_0^t$ ,  $g_1^t$  and  $g_2^t$ ), that change with respect to stress,  $\sigma$ , also need to be defined for the material

nonlinearity. Here,  $g_2^t$  is considered to be equal to one, for simplicity, meaning that the main source of nonlinearity would be the material itself, and most importantly, the stress change in the time discrete time interval  $\Delta t$  is considered to be linear. The relaxation times are also considered to be functions of stress; which puts more accuracy in the system and the change of material properties versus stress would be more precise.

As discussed, the strain may be represented schematically by a mechanical analogue consisting of nonlinear springs and dashpots. A generalized configuration of a multi-Kelvin solid, Figure 47, is chosen, with the following stress-strain relationship for the applied stress at current time,  $\sigma^t$

$$\varepsilon = \varepsilon^e + \varepsilon^i = \sigma^t \psi_0(\sigma) + \sigma^t \psi(\sigma, t) \quad (198)$$

The transient creep compliance function for this case would be

$$\psi(\sigma, t) = \sum_n X_n(\sigma) \left[ 1 - e^{-\left(\frac{t}{\tau_n}\right)} \right] \quad (199)$$

which is a nonlinear representation of Eq. (168).

The process of defining the unknown material properties and kernel functions is curve fitting of the developed model to experimental results. Using uniaxial creep results is the easiest way to determine the material behaviour, as it's the most convenient method of testing. Tests conducted by Liu (Liu, 2007) at the University of Waterloo, on high density and medium density polyethylene materials were used as the basis. Experiments were performed on five types of PEs and included tests on: short term tensile creep (24 hours), long term creep (7 days and 14 days) and creep with step loading. The specimens were produced from resins by melting them and machining, and from pipes by cutting out the samples (Table 24). 24-hour creep testing was done at different stress levels to examine time dependent and nonlinear behaviour of the materials. Furthermore, more creep tests have been performed by ExxonMobil Chemical Canada, a division of Canada Imperial Oil Limited. The materials are Low Density (LDPE), High Density (HDPE) and cross-linked (PEX) polyethylene (Table 25), all used in the rotomolding process. Each material is tested in three different temperatures, forming nine sets of uniaxial creep experiments, and each set contains strain measurements under four applied constant stresses. The test time duration is 1007 hours and just a short term portion of results (50 hours) is used for material parameters development. Thus, the method of material definition is to minimize the Least Squares Error by fitting Eq. (198) to the experimental results noting that:



$$\begin{aligned}
\psi_0 &= X_0 = g_0^t(\sigma) D_0 \\
X_n &= g_1^t(\sigma) D_n \\
g_2^t &= 1 \\
\tau_n &= \tau_n(\sigma)
\end{aligned} \tag{200}$$

Furthermore, the Poisson's ratio  $\nu$  is considered to be time independent and equal to 0.45 for HDPE, that is,  $\nu \rightarrow 0.5$ . This assumption results in a bulk modulus of about  $10^4 - 10^6$  which is recommended in the literature ( (Krishnaswamy, et al., 1992) & (Hinterhoelzl, et al., 2004)). Therefore, the aim is to find  $X_0$ ,  $X_n$  and  $\tau_n$ , where the first describes the elastic portion of the behaviour and the latter two are related to inelastic response.

Here  $X_0$ ,  $X_n$  and  $\tau_n$  are approximated by power-law functions of stress. This follows the formulation presented in (Sepiani, et al., 2017), To reduce the number of inelastic material functions, which are equal to  $2 \times N$ , all values of  $X_n$  and  $\tau_n$  are obtained using four parameters  $X_1$ ,  $\tau_1$ ,  $m$  and  $\alpha$

$$X_0 = (a_0 + a_1 e^{(-a_2 \hat{\sigma}^3)})^{-1} \tag{201}$$

$$X_1^{-1} = b_0 + b_1 \exp(b_2 - b_3 \hat{\sigma} - b_4 / \hat{\sigma}) \tag{202}$$

$$\tau_1 = c_0 \exp(-c_1 + c_2 \sigma + c_3 \sigma^2 - c_4 \sigma^3) \tag{203}$$

$$X_n = m^{1-n} X_1 \tag{204}$$

$$\tau_n = \alpha^{n-1} \tau_1 \tag{205}$$

Parameters  $m$  and  $\alpha$  are considered to be stress-independent, as are several other fitting parameters  $a_i$ ,  $b_i$  and  $c_i$ , and  $\hat{\sigma} = \sigma \times 10^{-6}$ , where  $\sigma$  is the applied stress for a given creep curve. Here,  $a_0$  and  $a_1$  have unit of compliance and  $a_2$  has unit of inverse of cubic stress, while  $\alpha$  and  $m$  have no units.  $b_0$  and  $b_1$  have stress unit,  $b_2$  has no unit,  $b_3$  has inverse unit of stress and  $b_4$  has unit of stress.  $c_0$  has unit of time,  $c_1$  has no unit,  $c_2$  has unit of inverse of stress,  $c_3$  has unit of inverse of squared stress, and  $c_4$  has unit of inverse of cubic stress.

The modelling fitting parameters are further updated to make the model able to predict the material behaviour in an extended time period. In order to realistically model the service life-time for polymeric structures, long term prediction methods are needed within the developed constitutive law. The proposed method is to observe the trend of material fitting parameters with respect to test time.

Table 24: List of tested polyethylene materials (dog-bone shape samples) by Liu (Liu, 2007)

No.	Material	Type	Thickness* (mm)	Width* (mm)	Code	$M_w$ (kg/mol)	$M_n$ (kg/mol)	ESCR (h)
1	HDPE-PIPE	pipe	5.00	13.05	PIPE	Data not available		
2	HDPE-resin1	resin	5.80	12.76	RES1	127.5	16.3	4.8
3	HDPE-resin2	resin	5.65	12.89	RES2	118.5	15.7	1.2
4	HDPE-resin4	resin	6.27	12.42	RES4	79.4	19.7	3.6
5	MDPE-PE80	resin	5.04	12.76	PE80	202.1	14.0	198.3

\* These represent dogbone dimensions; allowance for thickness is  $\pm 0.03$ , and  $\pm 0.05$  for width

Table 25: List of tested polyethylene\* (from ExxonMobil Chemical Canada)

No.	Material	Temperature (°C)	Code	Density (g/cc)
1	LLPE	23	LL8461-23	0.938
2	LLPE	50	LL8461-50	0.938
3	LLPE	60	LL8461-60	0.938
4	HDPE	23	HD8660-23	0.942
5	HDPE	50	HD8660-50	0.942
6	HDPE	60	HD8660-60	0.942
7	PEX	23	Paxon7004-23	-
8	PEX	50	Paxon7004-50	-
9	PEX	60	Paxon7004-60	-

\* All materials are used in rotomolding process

Table 26: Fitting parameters for materials listed in Table 24

Material	HDPE-PIPE	HDPE-RES1	HDPE-RES2	HDPE-RES4	MDPE-PE80
<b><i>N</i></b>	3	3	3	3	3
<b><i>v</i></b>	0.45	0.45	0.45	0.45	0.45
<b><i>a0</i></b> (MPa <sup>-1</sup> )	533.2325	725.6315	-7.2E+07	-3.7E+07	-507.715
<b><i>a1</i></b> (MPa <sup>-1</sup> )	0.0001	231.5424	72260542	37202291	1248.756
<b><i>a2</i></b> (MPa <sup>-2</sup> )	0.183892	0.002946	3.79E-09	1.23E-09	4.32E-04
<b><i>m</i></b>	0.540456	0.5467	0.387638	0.601929	0.406989
<b><i>a</i></b>	20.0403	29.98126	40.49517	24.46203	89.94696
<b><i>b0'</i></b> (MPa)	-14034.7	13460.95	6442.475	-15059.4	5130.081
<b><i>b1'</i></b> (MPa)	718.8153	1058.728	1891.629	2644.639	283.3042
<b><i>b2'</i></b>	3.690799	1.388991	-2.39479	4.860857	6.037886
<b><i>b3'</i></b> (MPa <sup>-1</sup> )	1.102456	0.135361	1.749268	1.555322	-0.16663
<b><i>b4'</i></b> (MPa)	47.36683	159.7381	105.288	1.47E-13	1.18E+02
<b><i>c0'</i></b> (s)	9.43E-07	5.67E-06	1.31E-10	8.09E-07	8.31E-06
<b><i>c1'</i></b>	-22.3282	-18.3079	-30.9412	-20.7033	-18.7169
<b><i>c2'</i></b>	-0.63894	0.117145	-0.38184	-0.22939	-0.56437
<b><i>c3'</i></b>	0.008102	-0.01922	-0.02906	-0.00517	0.019896
<b><i>c4'</i></b>	-1.62E-04	-0.0013	-0.00163	0.00035	0.005194
<b><i>d0'</i></b>	-0.73126	-3.0538	-0.79544	-1.73155	-1.26327
<b><i>d1'</i></b>	0.078264	0.176628	0.05793	-0.20256	0.107159
<b><i>d2'</i></b>	-0.33487	-0.14866	-1.20575	-1.8171	-2.08471
<b><i>d3'</i></b>	4.609743	0.017361	4.427899	6.860456	0.06555
<b><i>d4'</i></b>	2.817401	3.20358	3.040402	-8.06257	2.29108
<b><i>d5'</i></b>	0.391291	-0.28303	0.376139	0.471621	0.750257

Table 27: Fitting parameters for materials listed in Table 25

Material	LL-8461			HD-8660			Paxon-7004		
Temp	23°C	50°C	60°C	23°C	50°C	60°C	23°C	50°C	60°C
<b>N</b>	6	6	8	4	6	8	8	8	4
<b><math>\nu</math></b>	0.45	0.45	0.45	0.45	0.45	0.45	0.45	0.45	0.45
<b><math>\alpha_0</math></b> (MPa <sup>-1</sup> )	460.482 2	134.01 5	125.09 5	-9.E+6	-103	141.69 8	4.60E+ 2	65.948	128.1 7
<b><math>\alpha_1</math></b> (MPa <sup>-1</sup> )	486.482	175.8	66.399 6	9.5E+ 6	402.96	376.14	4.86E+ 2	344.81	94.54 9
<b><math>\alpha_2</math></b> (MPa <sup>-2</sup> )	0.2103	0.0933	0.0048	1.1E-7	0.0025	0.0925	2.10E-1	0.0088	0.030 1
<b>m</b>	0.8333	1.1724	0.248	0.005 1	1.2038	0.4282	0.8333	0.6166	0.005 7
<b>a</b>	8.7739	3.9807	8.7093	0.232	8.0545	6.1101	8.7739	21.631	0.037
<b><math>b_0'</math></b> (MPa)	1.43E+3	454.8	4.61E+ 6	1.7E+ 9	133.08	7.58E+ 4	1.43E+ 3	-1.8E+5	-2.E+8
<b><math>b_1'</math></b> (MPa)	5.81E+9	3.3E+1 0	4.94E+ 6	1.5E+ 7	3.0344	3.5E+1 1	5.81E+ 9	310.86 5	7.2E+ 8
<b><math>b_2'</math></b>	28.181	5.8534	-0.8744	8.654 4	2.9668	-80.675	28.181	9.106	1.315 3
<b><math>b_3'</math></b> (MPa <sup>-1</sup> )	15.3112	7.8408	0.3755	0.923 6	-0.3147	-13.434	15.311	0.6777	0.121 5
<b><math>b_4'</math></b> (MPa)	27.815	16.343 1	-1.9153	1.507	-1.8918	3.1907	27.815	3.8627	0.207 9
<b><math>c_0'</math></b> (s)	88.8217	1.8E-11	10.971 8	0.107 3	2.7E+0 3	76.265 8	8.88E+ 1	285.17 6	1.6E+ 4

$c1'$	-0.6786	-25.880	8.4374	-24.67	1.9927	11.625 2	-0.6786	21.302 7	-7.355
$c2'$	-1.2337	-2.4988	-3.9044	-10.57	0.193	5.306	-1.2337	0.1032	-1.852
$c3'$	0.9775	1.0777	1.1849	3.704 1	-0.043	-2.2016	0.9775	-0.2979	0.803 4
$c4'$	0.1482	0.1111	0.1051	0.395 3	-0.0045	-0.2721	0.1482	-0.0453	0.093 5
$d0'$	-0.034	-0.1527	-0.1114	-0.057	-0.0501	3.7E-11	-3.4E-2	-1.5841	-0.253
$d1'$	-0.0839	-0.0081	-0.0921	-0.178	-0.002	-2E-12	-8.E-02	-0.359	-0.113
$d2'$	0.0	0.0	0.0	0.0	0.0	0.0	0.0	0.0	0.0
$d3'$	0.0	0.0	0.0	0.0	0.0	0.0	0.0	0.0	0.0
$d4'$	0.0	0.0	0.0	0.0	0.0	0.0	0.0	0.0	0.0
$d5'$	0.1954	1.2002	0.7971	0.094 5	0.0779	6.0E-09	0.1954	1.8135	0.486 5

First, the curve fitting is done for all experiments in different test times, namely: 10, 14, 18, 20, 22 and 24 hours. This allows one to observe how the model fitting parameters are dependent on test time ( $\lambda$ ). It is proposed that the parameter change over test time can be represented by the following equations for the viscoelastic case (Sepiani, et al., 2017):

$$\begin{aligned}
 \text{(a)} \quad & b_i(\lambda) = b'_i (\lambda/\lambda')^{d_i} \quad \text{for } i = 0, 1, 2 \\
 \text{(b)} \quad & b_i(\lambda) = b'_i / (\lambda/\lambda')^{d_i} \quad \text{for } i = 3, 4 \\
 \text{(c)} \quad & c_0(\lambda) = c'_0 (\lambda/\lambda')^{d_5}
 \end{aligned} \tag{206}$$

$\lambda$  stands for test time and  $\lambda'$  is introduced for dimensional consistency (in this research we have  $\lambda' = 1 \text{ hour}$ ). Here,  $b'_i$  and  $c'_0$  have same units as  $b_i$  and  $c_0$ , respectively and  $d_i$  have no units.  $c'_0$ ,  $b'_i$  and  $d_i$  are fitting parameters independent of the test time. The results of this curve fitting method are tabulated in Table 26.

## 6.5 FEM implementation

For FEA analysis, the developed subroutine is implemented into the nonlinear finite element software ABAQUS/Standard using solid elements. The ABAQUS 3-D modelling starts with pre-processing

where the 3-D model is generated and finite element mesh, loads and boundary conditions are assigned, then analysis is done where displacements, stresses and strains are computed by means of material properties, which are defined as User Material; subsequently, the modelling continues with post-processing where the results are graphically presented. The model definition and assigning meshes, loads and boundary conditions, are done through the ABAQUS user interface while the user material subroutine is developed in Visual Studio workspace for material determination. The subroutine is compiled by Fortran software linked to ABAQUS software. ABAQUS invokes the subroutine at each increment and material calculation point, for which the \*MATERIAL definition includes \*USER MATERIAL input expression and includes the viscoelastic mechanical constitutive behaviour of material.

To perform the analysis of time-dependent behaviour of the materials under study via the finite element method, the three-dimensional finite deformation constitutive equations presented in the previous section are implemented in an FEM program through a User Material Subroutine. Eq. (157) defines the stress-strain relation. In Eq. (157) the Cauchy stress,  $\sigma$ , indicates the stress at the end of increment and its components are equal to  $\sigma_{ij}^{t-\Delta t} + \Delta\sigma_{ij}$ , which is the value at the beginning of the increment,  $\sigma_{ij}^{t-\Delta t}$ , plus the change due to  $\Delta t$ . The same happens to the strain tensor in which  $\varepsilon_{ij} = \varepsilon_{ij}^{t-\Delta t} + \Delta\varepsilon_{ij}$ . Rewriting Eq. (140) in 1-D yields:

$$\begin{aligned} \varepsilon^{t-\Delta t} + \Delta\varepsilon = & \left[ X_0 + \sum_n X_n(1 - \beta_n^t) \right] (\sigma^{t-\Delta t} + \Delta\sigma) \\ & + \sum_n X_n \left( \beta_n^t \sigma^{t-\Delta t} - e^{-\frac{\Delta t}{\tau_n}} q_n^{t-\Delta t} \right) \end{aligned} \quad (207)$$

One can simplify the equation as:

$$\Delta\sigma = E^t \varepsilon^{t-\Delta t} + E^t \Delta\varepsilon - E^t \sum_n \psi_n \left( \beta_n^t \sigma^{t-\Delta t} - e^{-\frac{\Delta t}{\tau_n}} q_n^{t-\Delta t} \right) - \sigma^{t-\Delta t} \quad (208)$$

Here  $E^t = D_I^{-1}$ . Differentiating the stress increment,  $\Delta\sigma$ , versus the strain increment,  $\Delta\varepsilon$ , provides:

$$\frac{\Delta\sigma}{\Delta\varepsilon} = D_I^{-1} = E^t = \left[ X_0 + \sum_n X_n(1 - \beta_n^t) \right]^{-1} \quad (209)$$

which is the stiffness modulus and in three-dimensional form represents the elasticity matrix or the so called “material Jacobian matrix”,  $\partial\sigma_i/\partial\varepsilon_j$ . This matrix defines the change in the  $i^{th}$  stress component at the end of the time increment,  $\Delta t$ , caused by an infinitesimal perturbation of the  $j^{th}$  component of the strain increment array. As it is seen,  $E^t$ , is defined in each increment by means of time dependent material properties, as well as the time increment. This tensor has to be updated at the end of each increment, as one of two main functions performed by the subroutine. As the second function, the subroutine must update the stresses and the solution-dependent state variables to their values at the end of the increment. With the use of Eq. (155), Eq. (157) can be rewritten as:

$$\boldsymbol{\sigma}^t = \boldsymbol{\sigma}^{t-\Delta t} + \Delta\boldsymbol{\sigma} = \mathbf{D}_I^{-1}(\boldsymbol{\varepsilon}^{t-\Delta t} - \boldsymbol{\theta} - \mathbf{H}) + \mathbf{D}_I^{-1}\Delta\boldsymbol{\varepsilon} \quad (210)$$

This expresses the Cauchy stress tensor at the end of the increment,  $\boldsymbol{\sigma}^t$ , and is passed forward to the beginning of the increment, as  $\boldsymbol{\sigma}^{t-\Delta t}$ . Here, the array  $H$  is a function of material properties and stresses, as well as  $q_n^{t-\Delta t}$ , at the beginning of the increment. Values of  $q_n^{t-\Delta t}$  are passed forward from previous increment as a state variable and needs to be calculated in each increment.

The modified Quasi-Newton, built-in ABAQUS/Standard numerical method, is used as a numerical technique for solving the nonlinear equilibrium equations. The convergence rate obtained by using this method is satisfactory.

## 6.6 Results and comparisons

In this section, FEA results are compared to the available experimental data. In the following paragraphs, comparisons are conducted with three different cases of loading on a single 3D element (Figure 48), namely, 1) short term axial tension, 2) long term axial tension and 3) step loading.

### 6.6.1 Case 1: Short term loading

In the first case study, the analysis has been conducted on a 3-D unit cell element structure representing a beam in tension. The study is performed to see how the finite element results match the short term test data. The materials from Liu (Liu, 2007) are chosen for this section. The dimensions and fitting parameters for the five materials are shown in Table 24 and Table 26, respectively. As expected, material properties change with respect to applied stress. The application of load lasts for 24 hours, which is a short term loading case. During the FEM analysis  $N$  is considered to be equal to 3. Figure 49 to Figure 53 show the comparison between test results and present work. Table 28 tabulates the least

squares error, associated with each applied constant stress. Also, the average error for each material is shown. As seen, material RES1 yields an error less than 3%, which is classified as “excellent” correlation with experiments. PIPE and RES2, have less than 5% error, which is said to be “good” correlation, and others (RES4 and PE80) result in “acceptable” correlation, which means less than 10% error. For more details on error classifications, refer to Chapter 3.

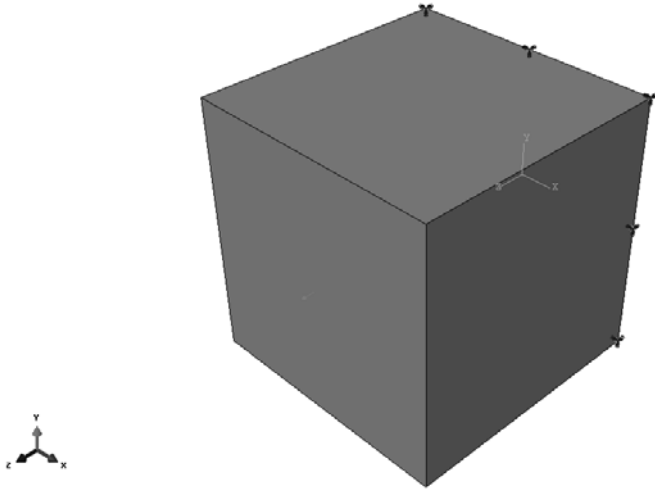


**Figure 48: Single 3D element made in ABAQUS and meshed by one quadratic hexahedron solid element, C3D20R**



Table 28: Error (%) for the readings of strain (FE model vs. experiment) for short term prediction

Material	PIPE	RES1	RES2	RES4	PE80
Error (%)/ Stress (MPa)	2.05 (2.97)	4.30 (2.67)	4.58 (2.68)	3.20 (2.59)	4.89 (3.05)
	5.11 (5.47)	1.52 (5.15)	4.54 (5.58)	4.81 (6.73)	4.34 (6.14)
	2.06 (6.70)	0.77 (7.14)	4.69 (7.28)	10.2 (9.71)	7.88 (8.37)
	4.90 (7.71)	0.85 (7.58)	2.74 (8.23)		10.11 (10.2)
		1.04 (10.6)	5.32 (10.6)		
<b>Average (%)</b>	<b>3.53</b>	<b>1.69</b>	<b>4.37</b>	<b>6.07</b>	<b>6.8</b>

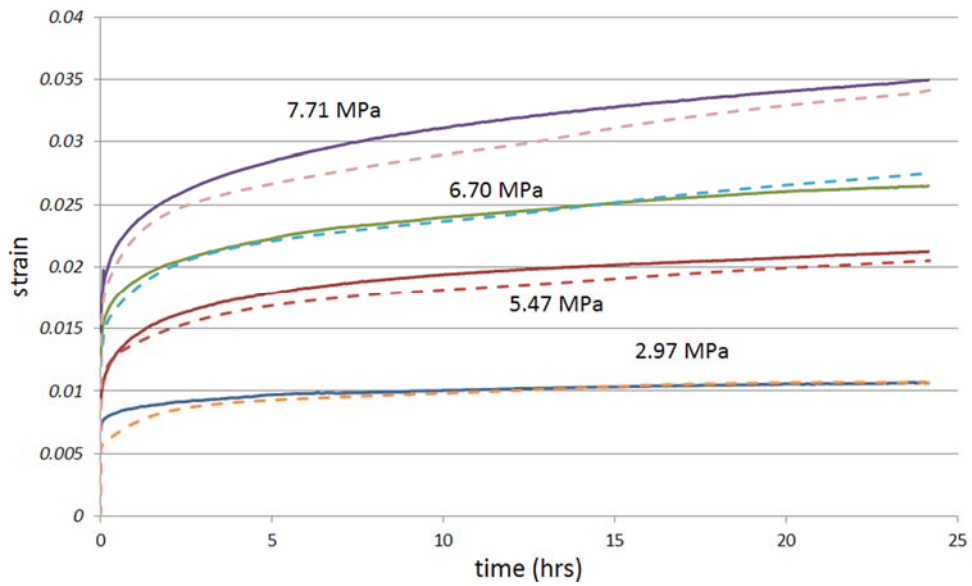
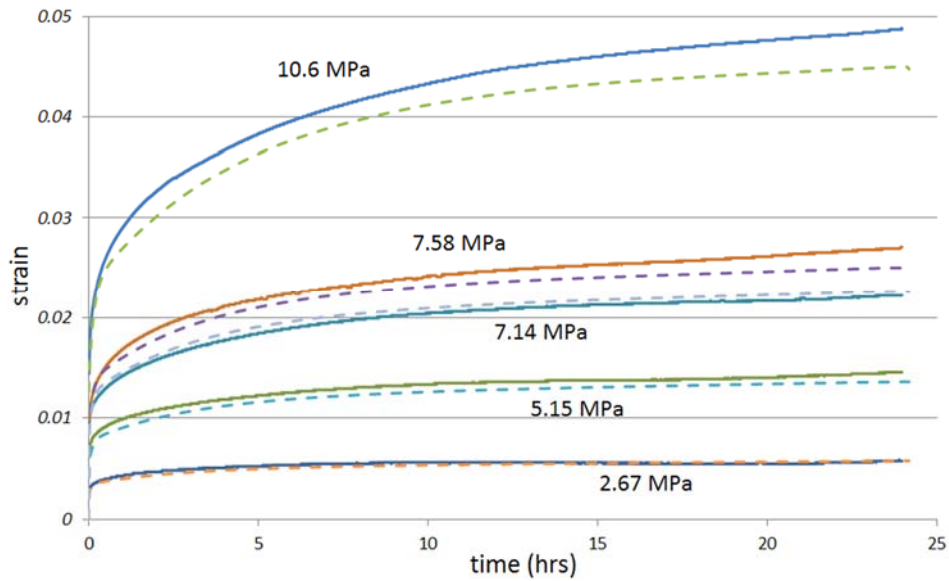
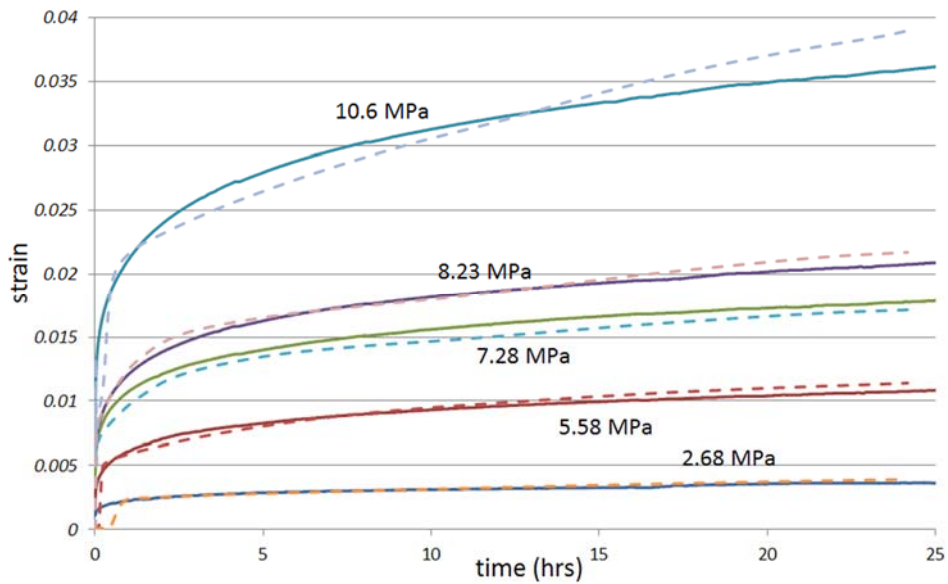


Figure 49: Short term (24 hour) results comparison for PIPE material between test data (solid lines) (Liu, 2007) and present FEA (dashed lines)



**Figure 50: Short term (24 hour) results comparison for RES1 material between test data (solid lines) (Liu, 2007) and present FEA (dashed lines)**



**Figure 51: Short term (24 hour) results comparison for RES2 material between test data (solid lines) (Liu, 2007) and present FEA (dashed lines)**

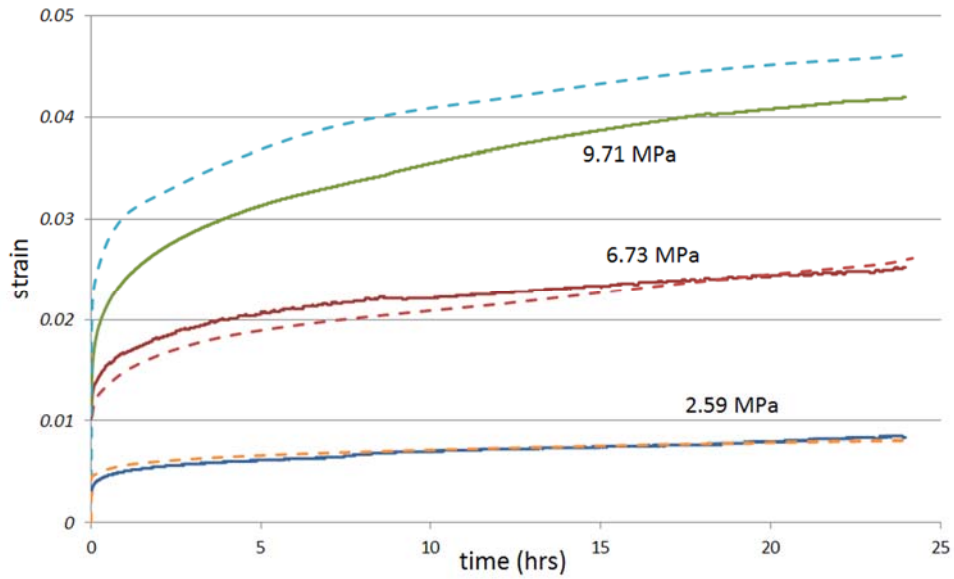


**Figure 52: Short term (24 hour) results comparison for RES4 material between test data (solid lines) (Liu, 2007) and present FEA (dashed lines)**

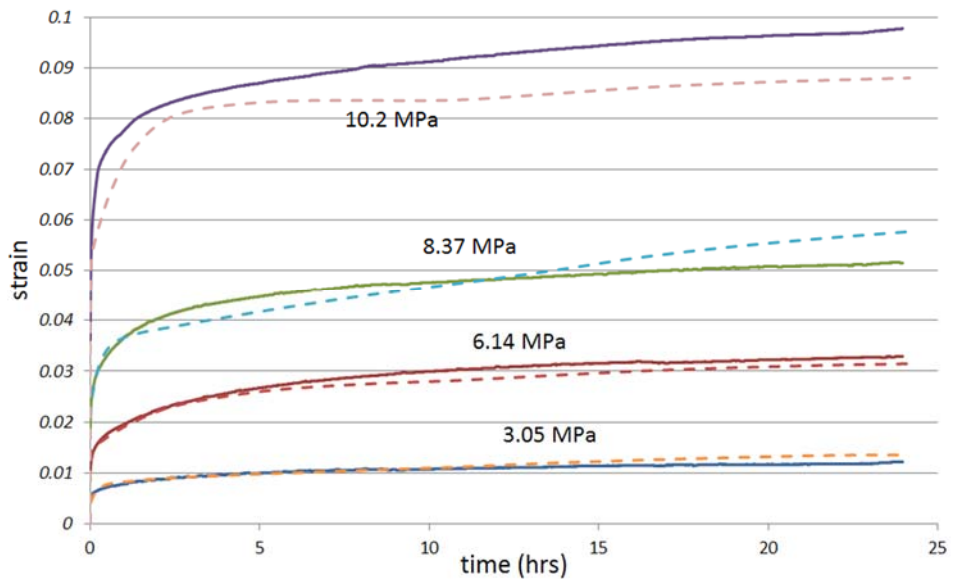


**Figure 53: Short term (24 hour) results comparison for PE80 material between test data (solid lines) (Liu, 2007) and present FEA (dashed lines)**

### 6.6.2 Case 2: Long term loading

In this case study, the long term response of the polyethylene is studied. Long term test data for PIPE material (Table 24) as well as for LL-8461, HD-8660 and Paxon-7004 are available (Table 25). The analysis is done in two steps:

- 1- The material model fitting parameters are obtained, for each material and test temperature, using the developed material model (results in Table 26 and Table 27).
- 2- The finite element long term responses are obtained for each test curve, using the fitting parameters from step 1, by means of the developed finite element procedure (Figure 54 to Figure 64).

First, the available test data for PIPE material (experiments conducted by Liu (Liu, 2007)) are used for the comparison with numerical predictions. These experiments investigated long term behaviour of high density polyethylene for two loading times which are 40 hours and 170 hours. Figure 54 shows the model prediction for 40 hours test time ( $\lambda = 40$ ) for three stress levels, 4.42 MPa, 6.08 MPa and 8.15 MPa. Similarly, Figure 55 depicts the same results for 170 hours test time ( $\lambda = 170$ ) for two stress levels 6.75 MPa and 6.89 MPa. Both figures show the validity of the modelling and its capability in predicting the long term responses of the nonlinear viscoelastic material.

Table 29 depicts the prediction errors for each test. The average error for 40 hour prediction is 10.44%, while the results for 170 hour prediction show 2.33% offset from experiments. In spite of our expectation, we see a smaller error for 170 hour test time, compared to 40 hour test time. Author believes that it might be because the tests in 40 hour are not as accurate and realistic as the 170 hour tests.

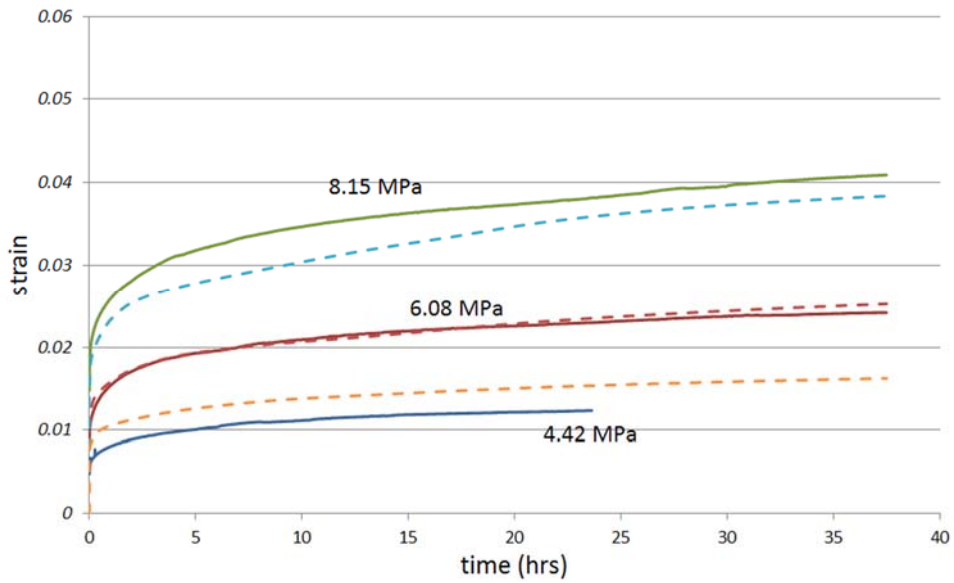


**Figure 54: Long term (40 hour) response prediction for PIPE material, test data (solid lines) (Liu, 2007) and present FEA (dashed lines)**

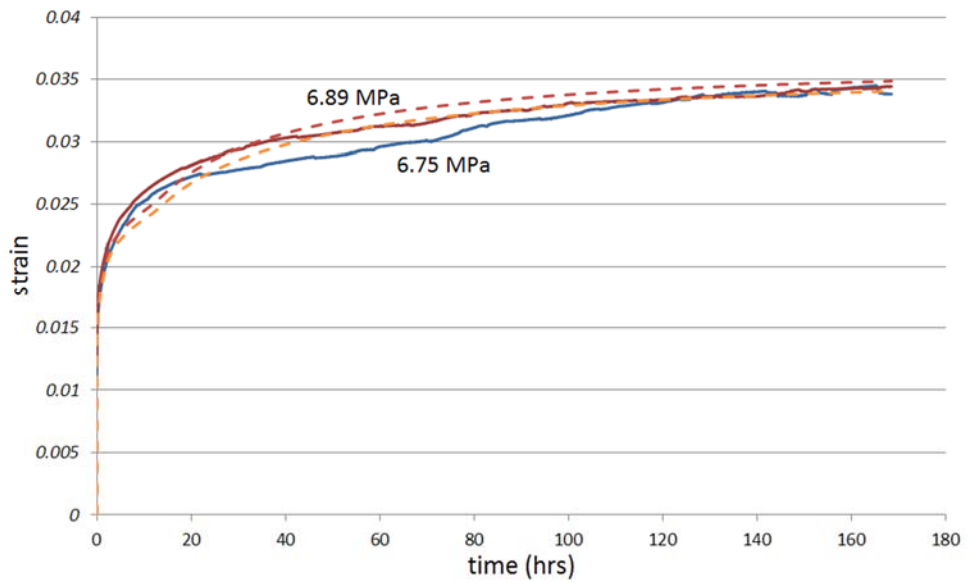


**Figure 55: Long term (170 hour) response prediction for PIPE material, test data (solid lines) (Liu, 2007) and present FEA (dashed lines)**

Table 29: Error (%) for the readings of strain (FE model vs. experiment) for long term predictions (40 hour and 170 hour) based on 24 hour material parameters for PIPE material						
	Test time, $\lambda$ (hr)		170		40	
	Error(%)/ Stress (MPa)		17.50 (4.42)		2.32 (6.75)	
			6.45 (6.08)		2.34 (6.89)	
			7.38 (8.15)			
	Average(%)		10.44		2.33	

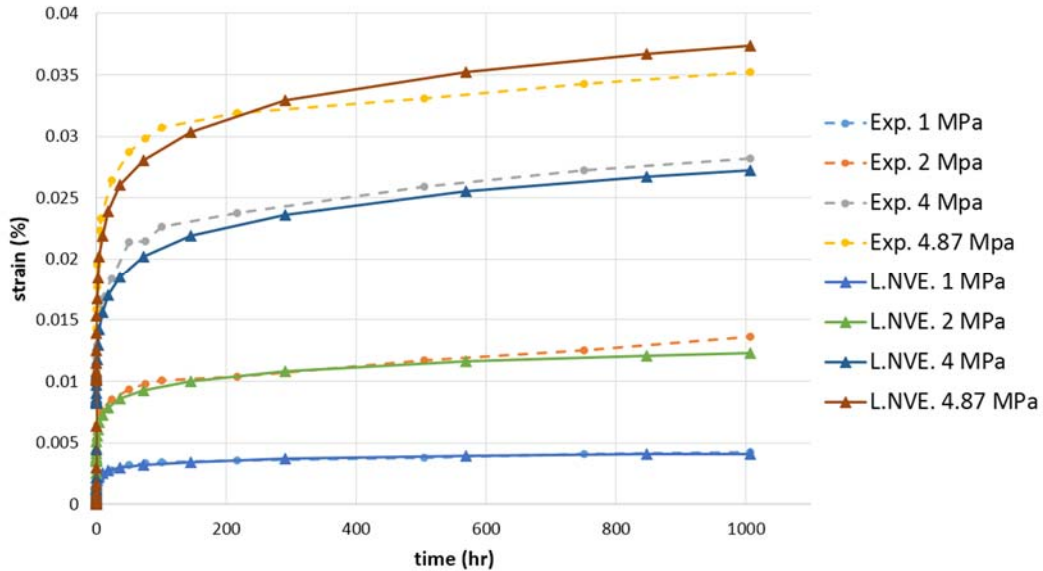
In the subsequent analysis, the long term Nonlinear Viscoelastic investigation proceeded with three different polyethylene materials from our industrial partner. The method is to look at short term 50 hour creep testing and observing the correlation to the longer term (1007 hour) creep data. Finite element analyses have been done and the results are compared to experimental observations. The experimental tests have been provided by ExxonMobil Chemical Canada, a division of Canada Imperial Oil Limited. The three materials under investigation, are shown in Table 25. Creep curves have been plotted by measuring the resultant strains versus time, for 1007 hours. Each material is tested in three different temperatures of 23°C, 50°C and 60°C. Thus, nine sets of experiments are available for analysis. Each set of experiment includes tests under four constant stresses, which are 1 MPa, 2 MPa, 4 MPa and 4.87 MPa. For the analysis, material fitting parameters from Table 27 are used as input to the finite element procedure.

Figure 56 to Figure 64 show the comparison between finite element results with experimental ones for 1007 hour test time. To see how the model is correlated to the test data, the errors associated to each test (creep curve) and the average error for each set of tests are tabulated in Table 30. Since the goal of

the research is to predict the strain at the end of the time duration, the values of strain at time = 1007 hour are considered for error calculation.

Looking at the average errors for each set of results (Table 30), it is seen that in one set (LL-8461 at 50°C) an error less than 5% (3.98%) is obtained, which shows a “good” forecast. In the other four sets (LL-8461 at 23°C, HD-8660 at 50°C, HD-8660 at 60°C and Paxon-7004 at 60°C) errors less than 8% (and more than 5%) are observed, which are “acceptable”. For the remaining sets, the errors are more than 8%, which are not “acceptable” (as per MacCallum et. al. see Chapter 3 for more details).

Scrutinizing the experimental measurements further, author believes that the two sets of test data (LL-8461 at 60°C and HD-8660 at 23°C) show unsmooth behaviour after about 100 hours test, which might be due to erroneous test process. since the prediction is based on short term observations, the proposed model is not able to predict that uneven behaviour, and we prefer removing these two sets of erroneous experiments from analysis. By ignoring these two sets of results, it can be concluded that the proposed Nonlinear Viscoelastic model is able to predict the long term behaviour of 5 sets of material test (out of 7 sets) with good correlation (which is more than 70%).



**Figure 56: Finite element (solid lines) vs. experimental (dashed lines) (by Imperial Oil), creep results for LL-8461 at 23°C**

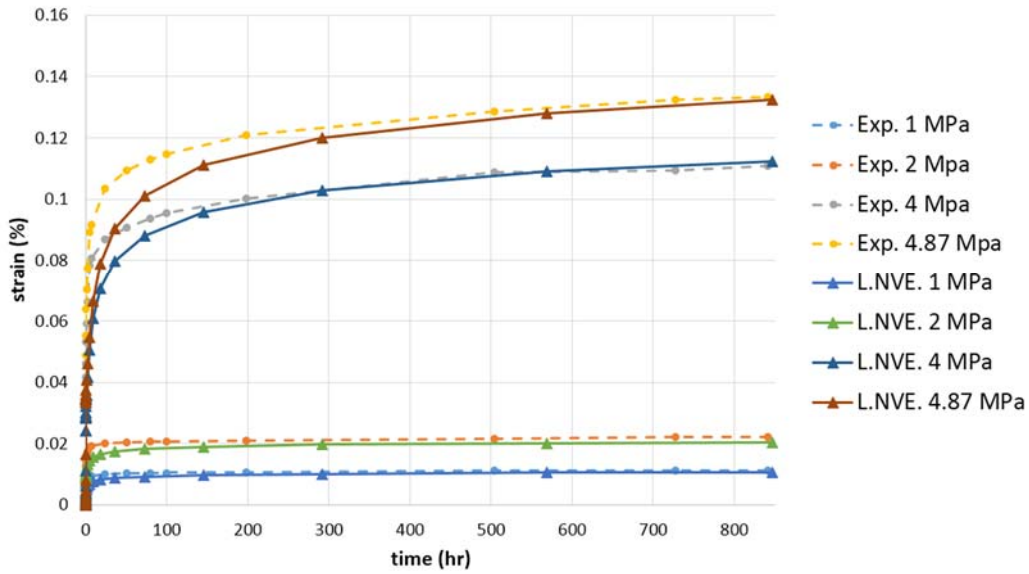


Figure 57: Finite element (solid lines) vs. experimental (dashed lines) (by Imperial Oil), creep results for LL-8461 at 50°C

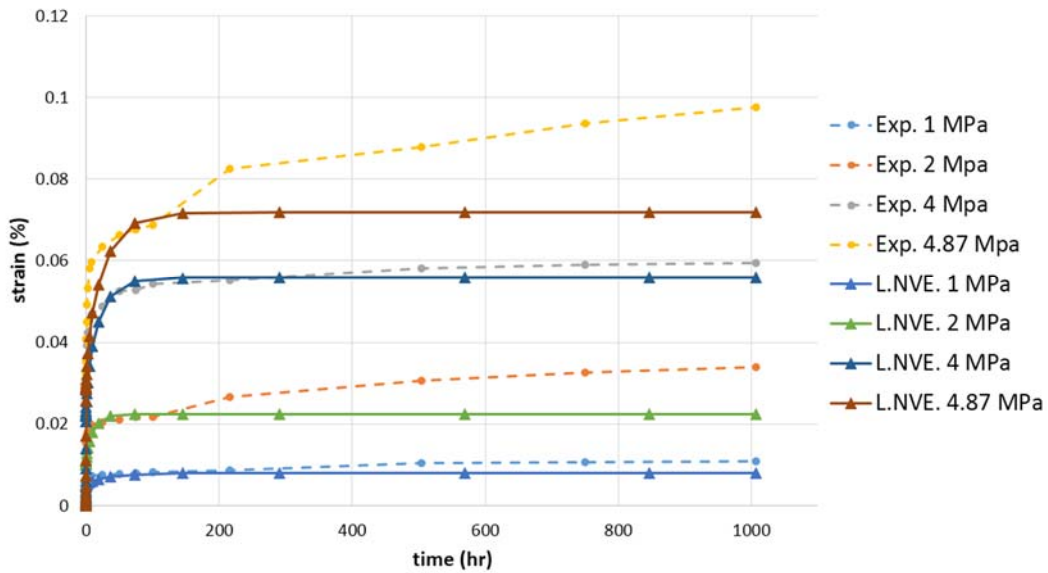
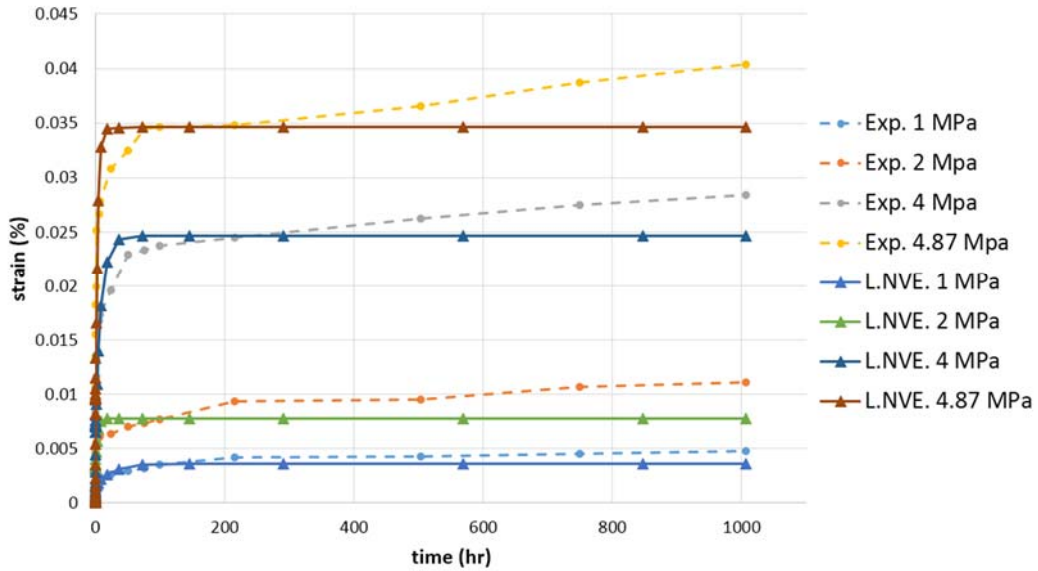
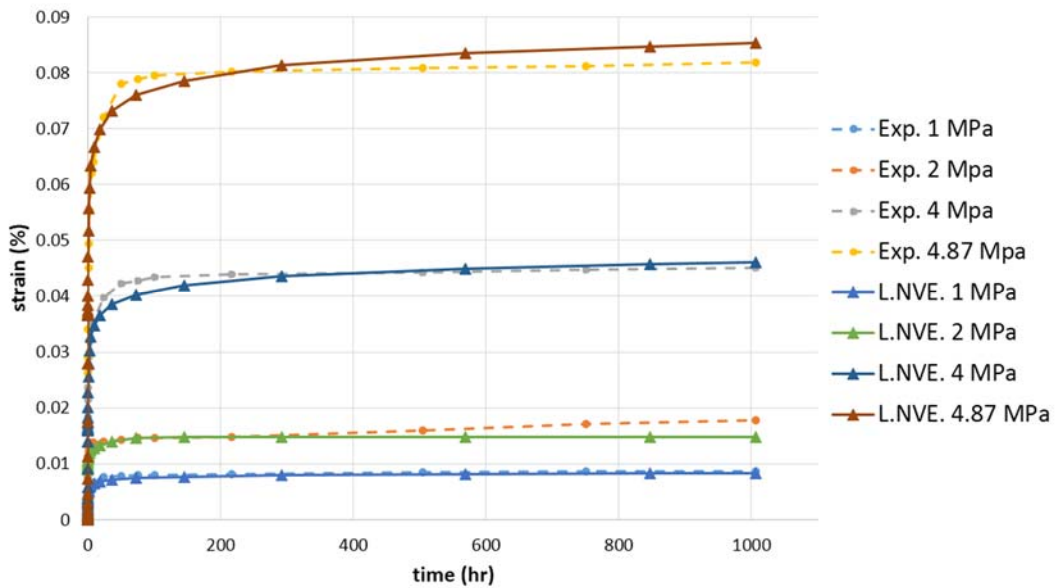


Figure 58: Finite element (solid lines) vs. experimental (dashed lines) (by Imperial Oil), creep results for LL-8461 at 60°C





**Figure 59: Finite element (solid lines) vs. experimental (dashed lines) (by Imperial Oil), creep results for HD-8660 at 23°C**



**Figure 60: Finite element (solid lines) vs. experimental (dashed lines) (by Imperial Oil), creep results for HD-8660 at 50°C**

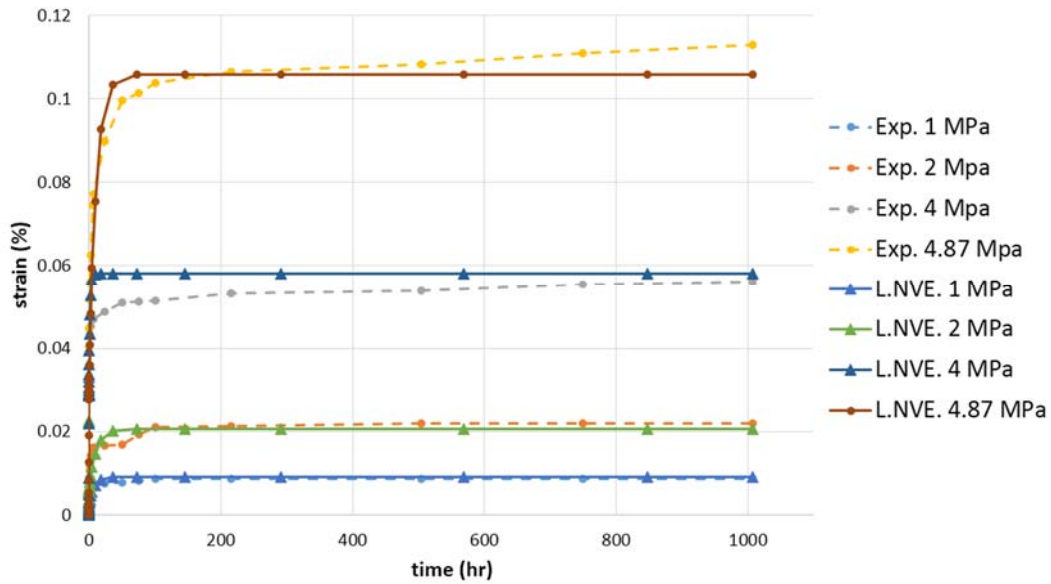


**Figure 61: Finite element (solid lines) vs. experimental (dashed lines) (by Imperial Oil), creep results for HD-8660 at 60°C**

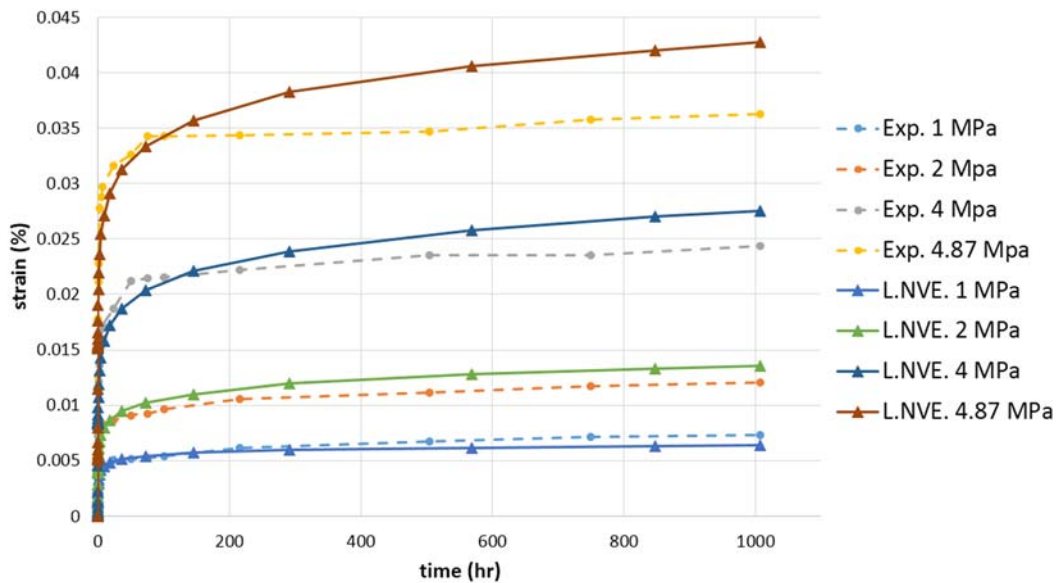


**Figure 62: Finite element (solid lines) vs. experimental (dashed lines) (by Imperial Oil), creep results for Paxon-7004 at 23°C**

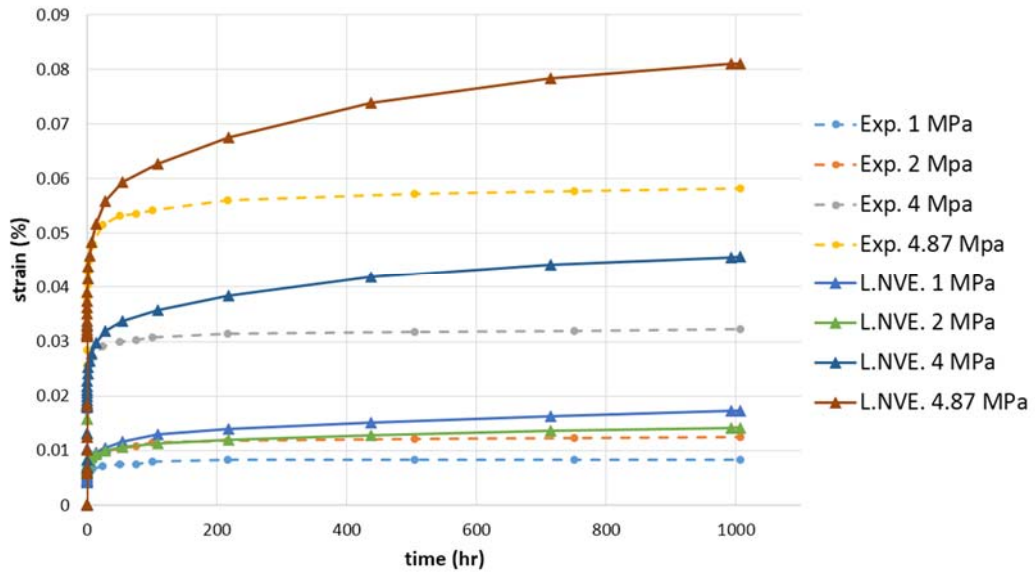


**Figure 63: Finite element (solid lines) vs. experimental (dashed lines) (by Imperial Oil), creep results for Paxon-7004 at 50°C**

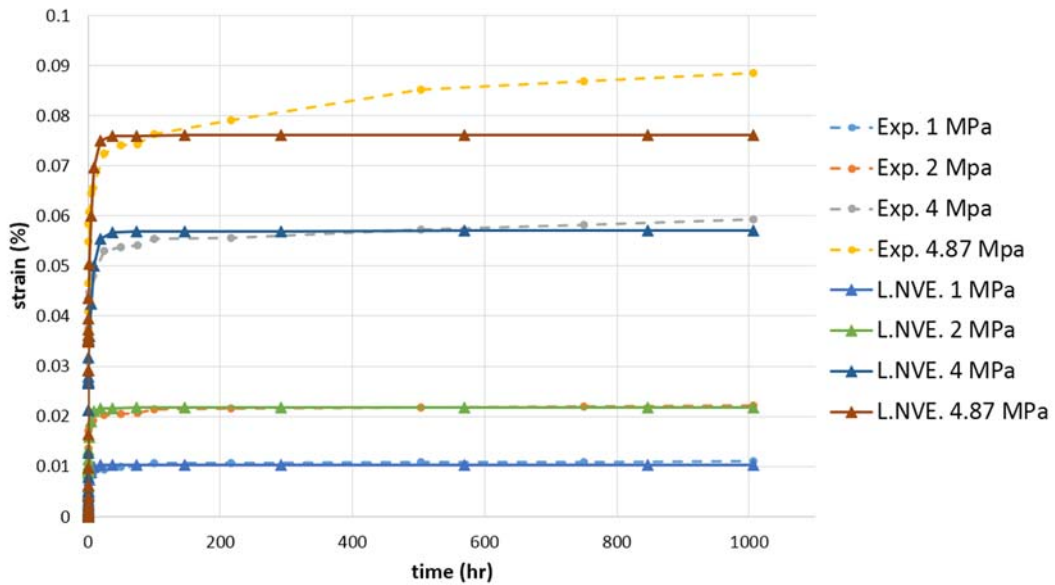


**Figure 64: Finite element (solid lines) vs. experimental (dashed lines) (by Imperial Oil), creep results for Paxon-7004 at 60°C**

Table 30: Error (%) for the readings of strain (FE model vs. experiment) at time = 1007 hr									
Material	LL-8461			HD-8660			Paxon-7004		
Temp.	23°C	50°C	60°C	23°C	50°C	60°C	23°C	50°C	60°C
<b>1 MPa</b>	4.42	4.73	27.00	24.38	3.58	4.82	13.05	106.73	5.99
<b>2 MPa</b>	9.71	7.66	34.05	30.12	16.64	6.30	12.29	13.95	1.98
<b>4 MPa</b>	3.21	2.72	5.98	13.01	2.11	3.56	12.93	41.64	3.78
<b>4.87 MPa</b>	6.07	0.81	26.21	14.24	4.10	6.30	17.74	39.05	13.99
<b>Average</b>	<b>5.85</b>	<b>3.98</b>	<b>23.31</b>	<b>20.44</b>	<b>6.61</b>	<b>5.24</b>	<b>14.00</b>	<b>50.34</b>	<b>6.43</b>

Another note which is worth mentioning here is that, looking at results for Paxon-7004 material (Table 30), one can infer that this material shows higher errors compared to other two materials. Noting that Paxon-7004 is a crosslinkable polyethylene while the other two (LL-8461 and HD-8660) are hexane copolymers, one may conclude that the present model is more accurate for hexane copolymers compared to crosslinkable polyethylene. This is a results that the author believes needs more experimental observations to be proved as a exactly determined outcome.

### 6.6.3 Case 3: Step loading

In the third case study by Liu (Liu, 2007), the material is subjected to abrupt stress changes. In Figure 65, HDPE-PIPE material is subjected to axial tension load of 5.33 MPa, which lasts for 5 hours and then by adding 2.98 MPa, the material deforms under 8.31 MPa for another 19 hours. Similarly, Figure 66 shows the same material behaviour under 2.9 MPa and 8.7 MPa, which last for one and four hours, respectively. In another study (Figure 67), the material experienced several abrupt changes in applied stress. The presented FEA model is compared with the experimental results, for all stress variation levels which start with 1.46 MPa. Following steps continue with the addition of 1.46 MPa applied stress to the previous step, which results in six loading steps. Each step lasts for almost two hours. Figure 68 also shows the stress change process by adding 2.89 MPa stress to the previous step. The last step shows

a process of unloading. In all figures, relatively good correlation can be seen between experimental and FEA results.

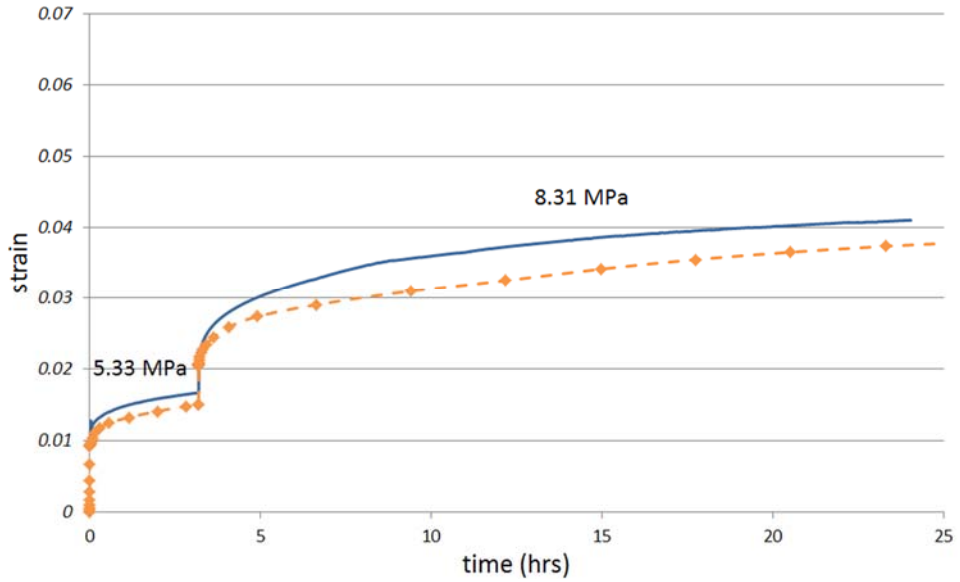


**Figure 65: Two step loading for PIPE material, test data (solid lines) (Liu, 2007) and present FEA (dashed lines)**

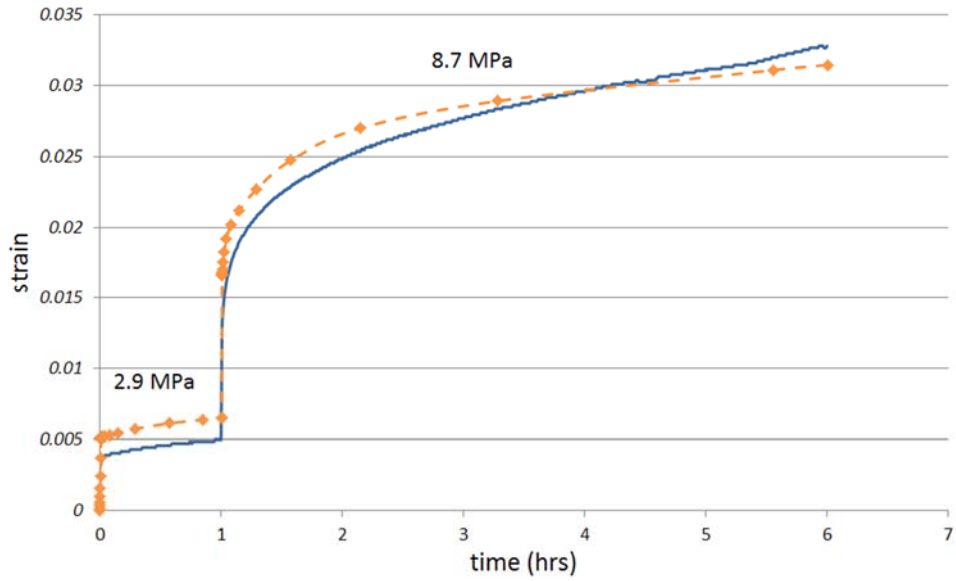


**Figure 66: Two step loading for PIPE material, test data (solid lines) (Liu, 2007) and present FEA (dashed lines)**

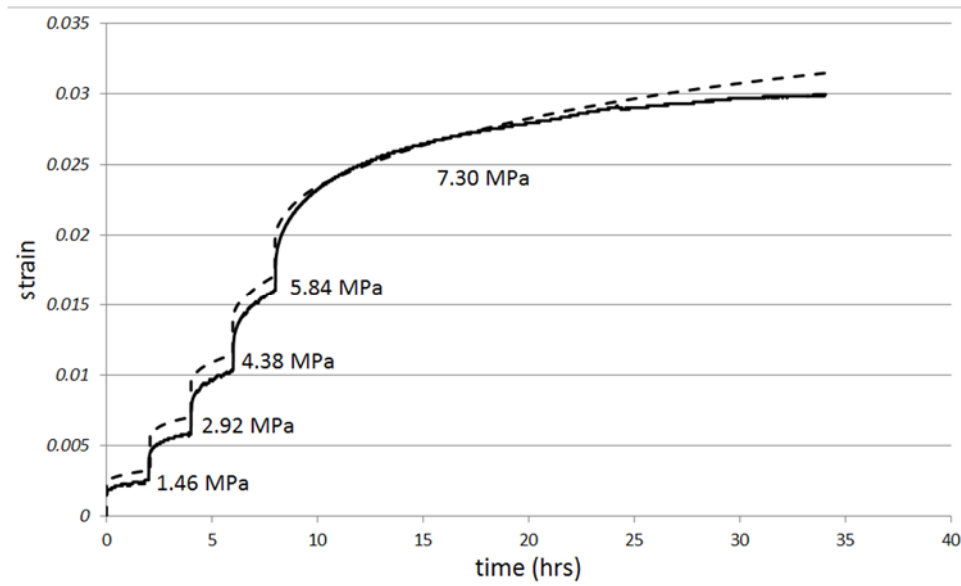


**Figure 67: Multi step loading for PIPE material, test data (solid lines) (Liu, 2007) and present FEA (dashed lines)**

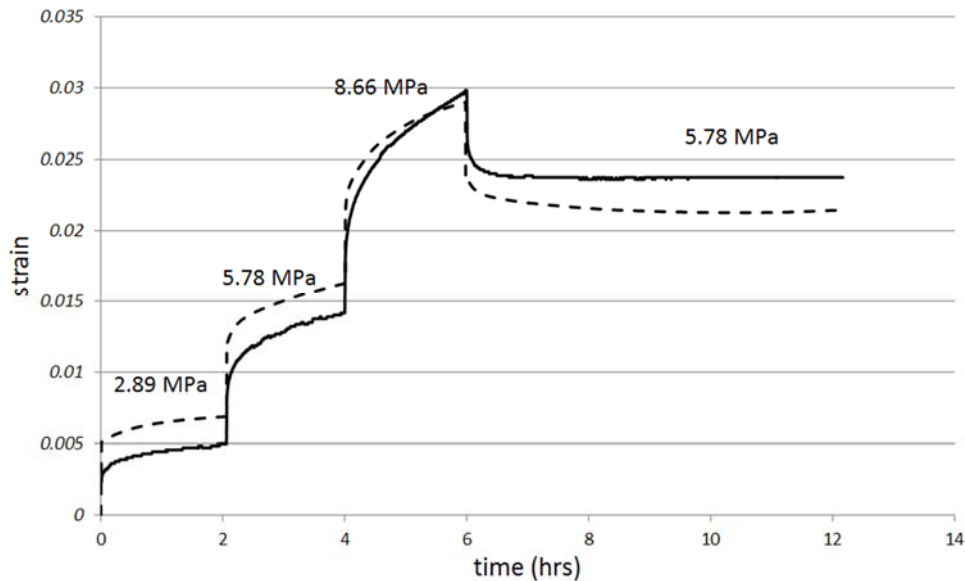


**Figure 68: Multi step loading and unloading for PIPE material, test data (solid lines) (Liu, 2007) and present FEA (dashed lines)**

## 6.7 Conclusions

Based on Schapery's single integral constitutive law, a nonlinear solution procedure was provided for viscoelastic materials to solve problems involving material nonlinearity. The procedure is based on the work done by Roy and Reddy (Roy, et al., 1988). The proposed procedure considers time- and stress-dependent material properties based on the generalized multi Kelvin simulation to characterize the nonlinear behaviour and it is applicable to three dimensional analysis. The material properties are also modified to include long term response of a material. The equations include material constants based on the measured material properties through an empirical fitting of the model to 24 hour uniaxial tension test results. These constitutive equations have exponential forms, which are adjustable to current time, meaning that they change as a function of current time. The material properties change with stress and time. The material functions obtained from short term test fittings are adjusted to predict the response of the material in longer time frames.

In order to conduct the proposed FEA, a unified computer code (user-defined material algorithm, UMAT) was generated. The validity of the models was assessed by comparison with experimental observations on polyethylenes for three uniaxial loading cases, which are short term loading, long term loading, and step loading.

24-hour test results for five different PE materials were used to predict the short term response of materials. Multiple strain-time curves were available for each material. For the long term, PIPE material test data for 40 hours and 170 hours as well as measurements on Low Density, High Density and Crossed-linked PE for 1007 hours duration, were used. The model can be used for prediction of the response with relatively good agreement to experimental results. The author believe that a good correlation (less than 5% average error) of model and experimental data is always achievable if proper material fitting parameters are obtained from test data. This requires accurate experimental measurements, as well as availability of numerous test results in each set of test data. Multiple step loading and unloading results were also compared with experimental data for the PIPE material. For all these theoretical results, a unit cell element sample model was created in Abaqus work space which invokes the developed UMAT code in each increment for material definition. The results showed that the proposed FEM model could reproduce the experimental results accurately, and it is concluded that with proper material properties to reflect the deformation involved in the mechanical tests, the deformation behaviour observed experimentally can be accurately predicted using the FEM simulation.

Based on the research conducted in this chapter and summarized above, the following specific findings and contributions can be mentioned:

Based on Schapery's single integral constitutive law a nonlinear solution procedure is used to solve problems involving material nonlinearity. To simulate the viscoelastic behaviour of materials, a multi Kelvin Solid configuration of spring and dash-pot elements is used to construct the constitutive equations. Time- and stress dependent material properties (based on generalized multi Kelvin simulation) are used to characterize the nonlinear behaviour of a material. The proposed viscoelastic model is implemented in a user-defined material algorithm in Abaqus (UMAT). The developed finite element procedure, allows to model the long term as well as short term responses of polymers. For this a code was developed in Fortran workspace, which is linked to commercial software ABAQUS.

The inputs to the developed code include a structural model and a material model. The former is done through the ABAQUS user interface and includes 3D solid modelling, boundary conditions, loadings, meshing and time discretization. The latter is obtained from experiments and needs material analysis.

The validity of the models is assessed by comparison with experimental observations.

Here are the conclusions:



- 1- The proposed single integral Nonlinear Viscoelastic model is able to predict the long term behaviour of material with “good” correlation (in more than 70% of the tested materials).
- 2- A good correlation (less than 5% error) of model and experimental data is always achievable if proper material fitting parameters are obtained from test data. This requires accurate experimental measurements, as well as availability of numerous test results in each set of test data.

## Chapter 7

### A Review on Failure Analysis of Viscoelastic Materials

#### 7.1 Introduction

One of the most important functions of engineering design is to be able to predict the performance of a structure over its design lifetime. Necessarily, mechanical behaviour of materials used in a structure must also be known over the intended life of the structure. For engineering design based upon linear elasticity, it is assumed that no intrinsic change in mechanical properties occurs over time. However, the molecular structure of polymers gives rise to mechanical properties that do change over time.

As engineering structures are often designed to last as long as 20 to 50 years (but often are then expected to last longer e.g. 100 years), there is a compelling reason to develop experimental and analytical approaches for polymer based materials that will allow the prediction of long term properties from relatively short term test data. Long term testing on the order of years to determine fundamental polymer properties, such as the relaxation modulus,  $E(t)$ , or creep compliance,  $D(t)$ , are quite impractical. Fortunately, the relationship between property changes of a polymer with time and property changes of a polymer with environmental effects like temperature, and environmental stress cracking can be utilized to develop accelerated test methods. These methods, like the one is discussed in this chapter, can assist in the difficult task of estimating life time of polymer-based materials from short term tests. In this chapter, an energy method based on delayed failure approach will be presented and then implemented in the finite element analysis for numerical applications.

It is worth mentioning that there are many other failure modes which take part in failure of polymeric materials, which are not the main concern of this chapter and can be further investigated for finite element implementation. One of them is Environmental Stress Cracking (ESC) which can occur after period of time when a polymer is subjected to stress below its yield point and is simultaneously exposed to a chemical medium. This will result in a reduction of the time to failure. The other mechanism is yield, which is failure due to exertion of limit load on the material. Polymers have a significant variation in the yield. As a result, various rate dependent plasticity theories have been developed for polymers that use yielding point as a reference point. The other mechanism is failure by rupture or separation rather than by yielding. For failures of this type, the fracture process begins at small microscopic defects

or flaws in the material. If a stress field around these flaws is increased to a certain limit, additional cracks will be produced near the tip of the flaw. There will be many of these micro-cracks and eventually one dominant crack will propagate and a tensile specimen will fail. This has led some researchers to consider the fracture process to be a stochastic event which resulted in development of statistical tools for the evaluation of viscoelastic fracture processes.

## 7.2 Delayed Failure

In contrast to an elastic material where all the energy of deformation is stored as strain energy, in viscoelastic materials, only a part of the total deformation energy is stored, and the rest of the energy is dissipated. Reiner and Weissenberg (Reiner, et al., 1939) showed that the main reason for the transition from viscoelastic response to yield in ductile materials or fracture in brittle ones is the time-dependent energy storage capacity. According to this theory, failure occurs when the stored deviatoric strain energy per unit volume in a body exceeds a certain maximum value called the resilience, which is a material property (Roy, et al., 1988). This theory may be used to predict failure in a nonlinearly viscoelastic material. When there is no dissipation, i.e., if the material is elastic, the Reiner-Weissenberg criterion becomes identical to the von Mises criterion.

The applicability of an energy criterion to model creep rupture of thermoplastics has been investigated by many researchers. In this regard, Bruller ( (Bruller, 1973), (Bruller, 1981) and (Bruller, 1978)) applied the Reiner–Weissenberg (R-W) theory with success to determine the failure in linear viscoelastic materials. They proposed a modification of the R–W theory for the prediction of fracture. This modification states that only the total time-dependent energy contributes for the creep rupture, provided the stress level is lower than the static rupture stress. Then failure occurs when this time-dependent energy reaches a limit value, which is considered a material property. They also established the conditions for creep and stress relaxation failure, demonstrated by experimental evidence. Theo et al. ( (Theo, 1990)- (Theoh, et al., 1992)) and Boey et al. (Boey, et al., 1990) also presented an application of the R–W criterion to a three-element mechanical model, to describe the creep rupture of polymers. The disadvantage of this theory is the uncoupling of the creep model and creep rupture model. Nevertheless, the predictions produced by such a creep rupture model were in good agreement with the experimental data for several tested polymers. Furthermore, the model appears to be able to determine the upper stress limit (immediate failure) and lower stress limit (no failure). More recently Brinson (Brinson, 1999) reviewed the state of the art regarding the time dependent failure of polymer

matrix composites. Brinson states that the R–W criterion could simplify the procedure to predict the delayed failures in structural polymers without losing the necessary accuracy.

Hiel (Hiel, et al., 1983) described the concepts of free energy using a generalized Kelvin model to describe the linear viscoelastic behaviour. In this case, free energy is defined as the sum of the energies stored in all springs. Using this simple concept and following the work developed by Bruller (Bruller, 1973), (Bruller, 1981) and (Bruller, 1978)), Hiel (Hiel, et al., 1983) determined the free energy accumulation during creep. The energy can be separated into a deviatoric and a dilatational part. The R–W theory (Reiner, et al., 1939) suggests the stored deviatoric free energy is responsible for failure. However, as Brinson (Brinson, 1999) cited, Bruller demonstrated that the deviatoric stored energy, assuming constant Poisson's ratio, represents 93% of the total free energy in a uniaxial tensile test. Nevertheless, in some 3D cases, the dilatational energy could be much more important than total free energy. Many polymers are very sensitive to properties like total free energy, as it shows the status of the material in general, for that reason Brinson (Brinson, 1999) assumes that the total free energy could be a better indicator for failure prediction.

Guedes (Guedes, 2004) has also done remarkable work on investigating the R-W method. He explored the time-dependent failure criteria for viscoelastic materials based on concepts proposed by Reiner and Weissenberg (Reiner, et al., 1939). This criterion is based on the stored energy and on the limit for this energy, which is considered a material constant (Guedes, 2004). Guedes used the methodology to predict delayed failure of multi-directional polymer matrix composites based on a non-linear viscoelastic model (Guedes, 2004). He also investigated the relationship between lifetime under creep and constant stress rate for polymer-matrix composites (Guedes, 2009). He analyzed the delayed fracture criterion for lifetime prediction of viscoelastic polymer materials by applying a multi-axial yield/failure model for viscoelastic/plastic materials and predicted long term creep rupture of polymers (Guedes, 2012) and (Guedes, 2012)). In a general review, Guedes proposed several theoretical approaches for lifetime predictions for polymer and polymer-based matrix composites. All those theories can be classified as global and homogenous approaches. He believed that, regarding engineering applications, the global and homogeneous analyses are more convenient. He presented fracture mechanics, damage mechanics and energy-based failure criteria and illustrated those with published experimental data.

Here, based on Schapery's single integral constitutive law (Schapery, 1969) & (Schapery, 1969), an energy based method of delayed failure, following the works by Hiel (Hiel, et al., 1983), and Roy and Reddy (Roy, et al., 1988) & (Roy, et al., 1988), is provided to solve polymer time to failure prediction involving material nonlinearity. This approach could also be applied to viscoplastic behaviour. The approach works with limiting the strain energy of the material to a boundary, which is the resilience limit. This limit is found from experimental results and observations for each material. Here a multi Kelvin solid model of viscoelastic material with exponential constitutive equation is considered for further investigation. For the power law constitutive equation describing a viscoplastic material, readers are referred to Guedes (Guedes, 2004). The resulting formulation is implemented in the developed finite element model presented in previous chapters. The presented failure results are then compared to the experimental results found in literature.

### 7.2.1 Uniaxial Delayed Failure

Several definitions and formulas for the free energy appear in the literature for viscoelastic materials. Here a solid Kelvin configuration of spring and dash-pot is shown in Figure 69.  $\varepsilon_0$  is the instantaneous strain while  $\varepsilon_n$  are strains associated with the  $n^{th}$  Kelvin unit. Under isothermal conditions and applied stress  $\sigma(t)$ , the total strain response  $\varepsilon(t)$  can be divided into two parts: the elastic instantaneous response  $\varepsilon_0 = \varepsilon^e$  and the inelastic transient response  $\varepsilon^i$ .

$$\varepsilon(t) = \varepsilon^e + \varepsilon^i = \varepsilon_0 + \sum_{n=1}^N \varepsilon_n \quad (211)$$

Here,  $1 \leq n \leq N$ , where  $N$  equals to the order of the expression and represents the number of Kelvin units in spring and dash-pot simulation of material behaviour, Figure 69.

The stress-strain representation of Eq. (211), which is a generalized configuration of a multi-Kelvin solid, would be

$$\varepsilon = \sigma D_0 + \sigma D(t) \quad (212)$$

where  $\sigma D_0$  is the elastic strain component and  $\sigma D(t)$  is the inelastic one.  $D_0$  represents the instantaneous elastic compliance,  $1/E_0$  and  $D(t)$  is the associated transient creep compliance function, which is defined by the following Prony series:

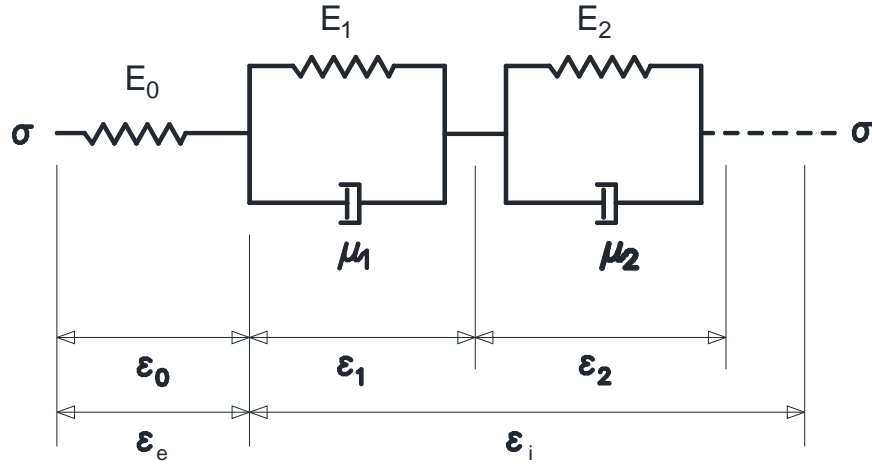


**Figure 69: Multi Kelvin Solid configuration subject to uniaxial stress.**

$$D(t) = \sum_n D_n [1 - e^{-t/\tau_n}] \quad (213)$$

where  $D_n$  and  $\tau_n$  are  $n^{th}$  creep compliance and relaxation time for  $n^{th}$  Kelvin unit, respectively (for further discussion see (Flügge, 1967)). In Eq. (211), the uniaxial stress using the representation of a unit step function  $H(t)$  is given as

$$\sigma(t) = \sigma_1 H(t) \quad (214)$$

where subscript 1 is associated with direction  $x_1$ .

Substituting Eq. (168) and Eq. (214) into Schapery's single integral representation of nonlinear viscoelastic constitutive equation for isotropic materials (Schapery, 1969) & (Schapery, 1969) (see Chapter 6), yields the following relation for isothermal condition ( $\psi^t = t$ ) in direction  $x_1$

$$\epsilon^t = g_0^t \sigma_1^t D_0 + g_1^t \int_0^t \sum_n D_n [1 - e^{-(t-t')/\tau_n}] \frac{d}{dt'} [g_2^t \sigma_1^t] dt' \quad (215)$$

Superscript  $t$  indicates the value at time  $t$ .  $g_i^t$  are material functions (see chapter 6 for details). Comparing with Eq. (211) yields that

$$\epsilon_0 = g_0^t \sigma_1^t D_0 \quad (216)$$

$$\varepsilon_n = \sigma_1^t g_1^t g_2^t D_n \left[ 1 - e^{-\left(\frac{t}{\tau_n}\right)} \right]$$

Consequently, the associated developed stress in each spring can be expressed as

$$\begin{aligned} \sigma_{10}^t &= \frac{\varepsilon_0}{g_0^t D_0} \\ \sigma_{1n}^t &= \frac{\varepsilon_n}{g_1^t D_n} = \sigma_{10}^t g_2^t \left[ 1 - e^{-\left(\frac{t}{\tau_n}\right)} \right] \end{aligned} \quad (217)$$

where second subscripts 0 and  $n$  denote the instantaneous elastic spring and springs associated with the  $n^{\text{th}}$  Kelvin unit. The first subscript denotes the uniaxial direction 1. It is obvious that  $\sigma_{10} = \sigma_1$ .

From Hiel et al (Hiel, et al., 1983), the total energy  $W^s$  stored in all springs is:

$$W^s = \int_0^{\varepsilon_0} \sigma_{10} d\varepsilon + \sum_{n=1}^N \int_0^t \sigma_{1n} \varepsilon_n dt = \frac{1}{2} g_0 D_0 \sigma_{10}^2 + \frac{1}{2} g_1 \sigma_{10}^2 g_2^2 \sum_{n=1}^N \left( D_n \left[ 1 - e^{-\left(\frac{t}{\tau_n}\right)} \right]^2 \right) \quad (218)$$

or

$$W^s = \frac{1}{2} \left[ g_0 D_0 + g_1 g_2^2 \sum_{n=1}^N \left( D_n \left[ 1 - e^{-\left(\frac{t}{\tau_n}\right)} \right]^2 \right) \right] \sigma_{10}^2 \quad (219)$$

According to the Reiner-Weissenberg hypothesis, failure occurs when the stored energy  $W^s$  equals or exceeds the resilience of the material. Denoting the resilience as  $R$ , the expression for the time dependent failure stress obtained from Eq. (219) for the uniaxial stress state is (Hiel, et al., 1983):

$$\sigma_f \geq \frac{\sqrt{2} \sqrt{R}}{\left[ g_0 D_0 + g_1 g_2^2 \sum_{n=1}^N \left( D_n \left[ 1 - e^{-\left(\frac{t}{\tau_n}\right)} \right]^2 \right) \right]^{1/2}} \quad (220)$$

## 7.2.2 Multi-axial Failure

The failure criterion for uniaxial loading is extended to the multi-axial one. Let's say the principal stresses at each point in an isotropic viscoelastic material are  $\sigma_1$ ,  $\sigma_2$  and  $\sigma_3$ . Then by definition, the shear stresses are zero on the principal planes. To construct the multi-axial configuration, it is assumed that the viscoelastic material is represented by a multi Kelvin solid model (Figure 69) in each principal

direction (Roy, et al., 1988). Then the applied multi-axial creep stresses in the material principal directions are given by

$$\begin{aligned}\sigma^{(1)} &= \sigma_1 H(t) \\ \sigma^{(2)} &= \sigma_2 H(t) \\ \sigma^{(3)} &= \sigma_3 H(t)\end{aligned}\tag{221}$$

$H$  are material parameters. Again, substituting into Schapery's single integral representation of the constitutive equation for a nonlinear viscoelastic isotropic material (Schapery, 1969) & (Schapery, 1969), and considering the shear effect of stress-strain relations in multi dimensions we have:

$$\begin{aligned}\varepsilon_{11} &= g_0 D_0 \left( \sigma_1 + \left(1 - \frac{G_0}{D_0}\right) \sigma_2 + \left(1 - \frac{G_0}{D_0}\right) \sigma_3 \right) + \\ &\sum_{n=1}^N g_1 D_n \left( \sigma_1 g_2 \left(1 - e^{-\left(\frac{t}{\tau_n}\right)}\right) + \sigma_2 g_2 \left[ \left(1 - e^{-\left(\frac{t}{\tau_n}\right)}\right) - \frac{G_1}{D_1} \left(1 - e^{-\left(\frac{t}{\gamma_n}\right)}\right) \right] \right. \\ &\quad \left. + \sigma_3 g_2 \left[ \left(1 - e^{-\left(\frac{t}{\tau_n}\right)}\right) - \frac{G_1}{D_1} \left(1 - e^{-\left(\frac{t}{\gamma_n}\right)}\right) \right] \right)\end{aligned}\tag{222}$$

Here  $G_0$  is the instantaneous shear compliance and  $G_i$  are shear compliances for the  $i^{th}$  Kelvin unit. Thus, the effective stresses developed in the spring with compliance  $D_0$ , and the nonlinear springs with compliance  $D_n$  acting in the principal direction 1, are given by

$$\begin{aligned}\sigma_{10}^e &= \sigma_1 g_2 + \left(1 - \frac{G_0}{D_0}\right) \sigma_2 g_2 + \left(1 - \frac{G_0}{D_0}\right) \sigma_3 g_2 \\ \sigma_{1n}^e &= \sigma_1 g_2 \left(1 - e^{-\left(\frac{t}{\tau_n}\right)}\right) + \sigma_2 g_2 \left[ \left(1 - e^{-\left(\frac{t}{\tau_n}\right)}\right) - \frac{G_n}{D_n} \left(1 - e^{-\left(\frac{t}{\gamma_n}\right)}\right) \right] \\ &\quad + \sigma_3 g_2 \left[ \left(1 - e^{-\left(\frac{t}{\tau_n}\right)}\right) - \frac{G_n}{D_n} \left(1 - e^{-\left(\frac{t}{\gamma_n}\right)}\right) \right]\end{aligned}\tag{223}$$

As before, on the left-hand side of Eqs. (223), the first subscript indicates the principal direction in which the effective stress acts, and the second subscript determines the spring number (associated with the Kelvin unit number). The total energy,  $W_1^S$ , stored in all springs in the material principal direction 1 over time  $t$ , can now be obtained by using Eq. (219) (Guedes, 2004)



$$W_j^s = \frac{1}{2} \tilde{D}_0 (\sigma_{j0}^e)^2 + \frac{1}{2} \sum_{n=1}^N (\tilde{D}_n (\sigma_{jn}^e)^2) \quad (224)$$

where  $\tilde{D}_0 = g_0 D_0$ ,  $\tilde{D}_n = g_1 D_n$ , and

$$\sigma_{j0}^e = \left(1 - \frac{G_0}{D_0}\right) (\sigma_1 + \sigma_2 + \sigma_3) g_2 + \frac{G_0}{D_0} g_2 \sigma_i \delta_{ij} \quad (225)$$

and

$$\sigma_{jn}^e = g_2 \left[ \left(1 - e^{-\left(\frac{t}{\tau_n}\right)}\right) - \frac{G_n}{D_n} \left(1 - e^{-\left(\frac{t}{\tau_n}\right)}\right) \right] (\sigma_1 + \sigma_2 + \sigma_3) + g_2 \frac{G_n}{D_n} \left(1 - e^{-\left(\frac{t}{\tau_n}\right)}\right) \sigma_i \delta_{ij} \quad (226)$$

In these equations, repeated indices imply summation, and  $\delta_{ij}$  is the Kronecker delta operator. Also, for computational convenience, the Prony series for the creep and shear compliance is assumed to have the same number of terms. Eq.s (224), (225), and (226) define the energy stored in the  $j^{th}$  principal direction in an isotropic viscoelastic material. Therefore, according to the Reiner-Weissenberg failure theory, the criterion for creep rupture in the  $j^{th}$  principal direction is given as (Guedes, 2004)

$$W_j^s \geq R \quad (227)$$

where  $R$  is the resilience of the isotropic nonlinear viscoelastic material under isothermal conditions. For a viscoelastic material with a constant Poisson's ratio  $\nu$ ,  $G(t)$  is given by

$$G(t) = (1 + \nu)D(t) \quad (228)$$

which simplifies Eq.s (225), and (226) to

$$\begin{aligned} \sigma_{j0} &= -\nu g_2 (\sigma_1 + \sigma_2 + \sigma_3) + (1 + \nu) g_2 \sigma_i \delta_{ij} \\ \sigma_{jn} &= -\nu g_2 (\sigma_1 + \sigma_2 + \sigma_3) \left(1 - e^{-\left(\frac{t}{\tau_n}\right)}\right) + (1 + \nu) g_2 \left(1 - e^{-\left(\frac{t}{\tau_n}\right)}\right) \sigma_i \delta_{ij} \end{aligned} \quad (229)$$

### 7.2.3 FEM implementation

The presented method is implemented in the finite element analysis. For this, principal stresses in each increment and each element and integration point are calculated. The model is developed for isothermally isotropic materials with constant Poisson's ratio  $\nu$  (see previous chapters). Thus, the effective stress in each time will be calculated using Eq. (229). Finally, the resultant deviatoric strain

energy in each principal plane is calculated based on Eq. (224). By means of the criterion defined in Eq. (227), energy strains in each principal direction are limited to the pre-set value of  $R$ . Failure happens once the criterion (Eq. (227)) is satisfied.

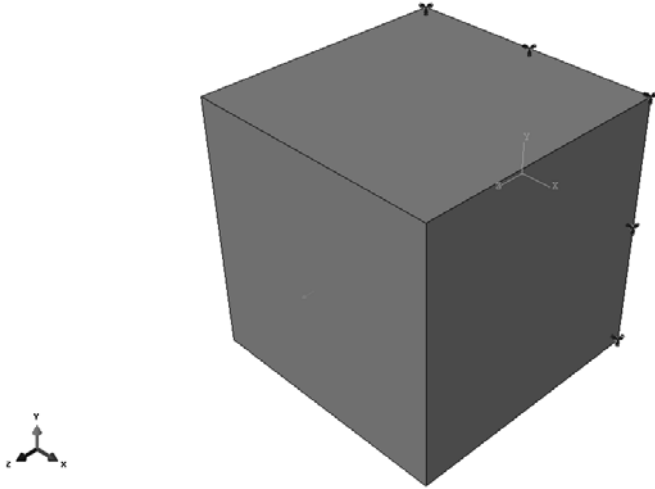


**Figure 70: A cubic single element solid model made in ABAQUS and meshed by one quadratic hexahedron solid element, C3D20R**

A cubic solid model is made and meshed by one quadratic hexahedron solid element, C3D20R, in the finite element software ABAQUS linked to pre-developed viscoelastic user material subroutine (see Chapter 6). The FE model is fixed at one end and constant uniaxial stress is applied to the other end (Figure 70). The software is run for 24 hours. Deviatoric strain energies in both axial and transverse directions are calculated in each time increment and are depicted in Figure 71 and Figure 72, respectively. As shown, deviatoric strain energy increases with time. It is also proportional to the applied stress, as expected. As the applied stress increases, the material is most likely to reach the maximum deviatoric energy,  $R$ , and fail. Thus, to obtain the “time to failure”, one needs to know the other side of Eq. (227), which is the resilience,  $R$ . This is a material property, which is obtained from experiments.

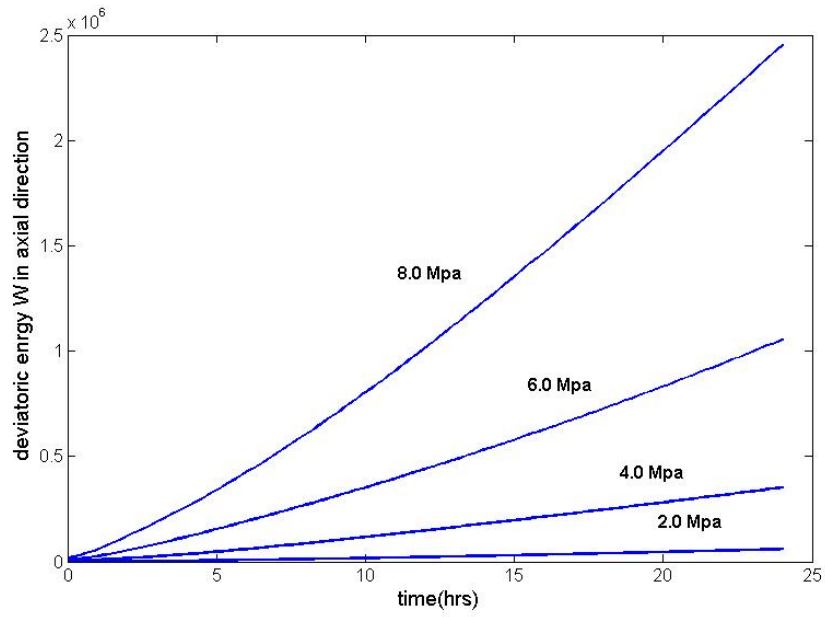


**Figure 71: Axial deviatoric free energy (W1) per time for PIPE material**

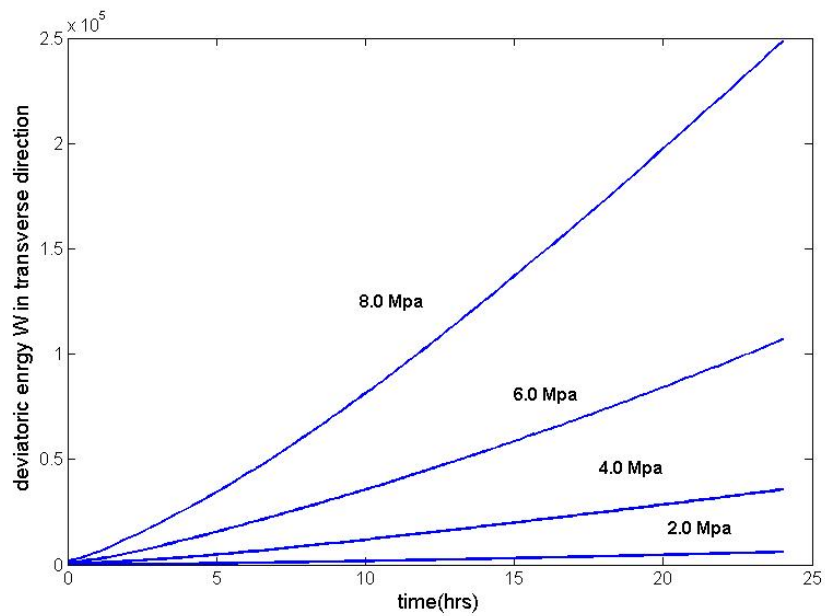


**Figure 72: Transverse deviatoric free energy (W2) per time for PIPE material**

McKenna and Pen have investigated the time dependent failure of polyethylene and polymethyl methacrylate (PMMA) by introducing a cumulative damage model (McKenna, et al., 1980). They compared their theory with experimental results and presented the time to failure of the discussed material versus applied stress. The results are depicted in Figure 73 in which shows a good correlation between these two sets of data. The polyethylene material tested by McKenna and Pen was a linear High Density Polyethylene (HDPE) with a number-average molecular weight of 15,600 and a weight-average molecular weight of 99,000. The material was moulded in a platen press at 160°C into 1.00 mm thick sheets which were then allowed to cool down to 90°C and subsequently removed from the mold. The material was allowed to lie in the laboratory for a minimum of one week prior to testing.

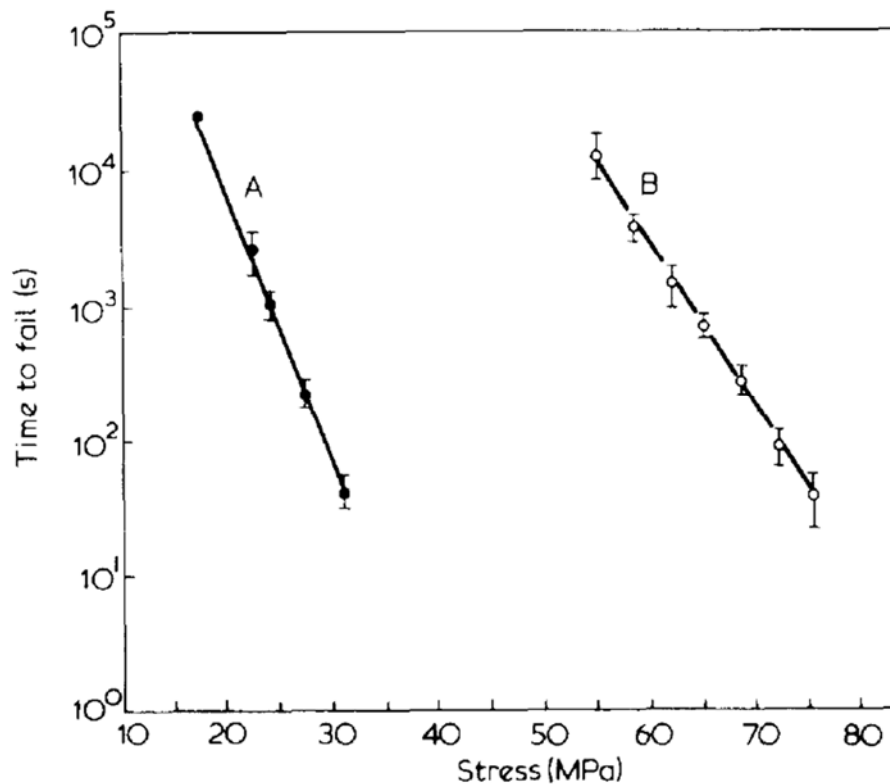


**Figure 73: Time to fail vs. stress for A) polyethylene, T=296K and B) polymethyl methacrylate (PMMA), T=297K (McKenna, et al., 1980)**

Here we are using the test results from McKenna et al (McKenna, et al., 1980) to find out the resilience factor for the polyethylene material that they have tested. Then this information will be used to predict the time to failure (TTF) of our polyethylene material sample. The chosen material sample

needs to have as close as possible material properties to the one that has been investigated by McKenna et al. The purpose is to show how the method works and how the resilient factor can be obtained from experimental observations and used for predicting the time to failure of same material. Thus, it is not suggested to use the test data from literature, unless it is exactly same material as what is under analysis for TTF.

For our investigation, a similar material was chosen. From those used in this research (see material list in chapter 3), Resin 2 can be considered similar to what McKenna and Pen have used. Although this similarity does not guarantee the accuracy of the outcome, it is just used for illustrating the methodology and the results are not reflecting the exact failure behaviour of the Resin 2 (as this requires accurate failure experiments on the material).

Considering this material and running some trial analysis it is found that, based on results in Figure 73, a resilient factor  $R$  is equal to 370500 MPa. To find this value, software was run in two cases of applied stresses, 11.7 MPa and 13.7 Mpa. Run time was set to 5000 hours. The reason these two stresses were chosen is that these two are closer to the range of stresses in Figure 73. The software was set to report the value of deviatoric energy in each time increment. From Figure 73, the material is expected to fail after  $335 \times 10^3$  s for 11.7 MPa and  $115 \times 10^3$  s for 13.7 MPa. Using Eq. (224) and Eq. (227), the resilience factor for 11.7 MPa at  $335 \times 10^3$  s found to be 370000 MPa and for 13.7 MPa at  $115 \times 10^3$  s found to be 371000 MPa. We chose the average of these two resilience factors as the limit value,  $R$ , for the material under investigation (Resin 2), which equals to 370500 MPa. This value was used to determine the “time to failure” for other stress levels and the results are shown in Table 31. Figure 74 and Figure 75, depict same result that is the failure time versus stress in normal scale and logarithmic scale, respectively.

Stress (MPa)	2.67	5.58	7.28	8.23	10.6	11.7	13.7
Time To Failure (s/hrs)	40.5E+6 /11263	8.6E+6 /2400	3.5E+6 /972	2.1E+6 /587	600E+3 /167	335E+3 /93	115E+3 /32

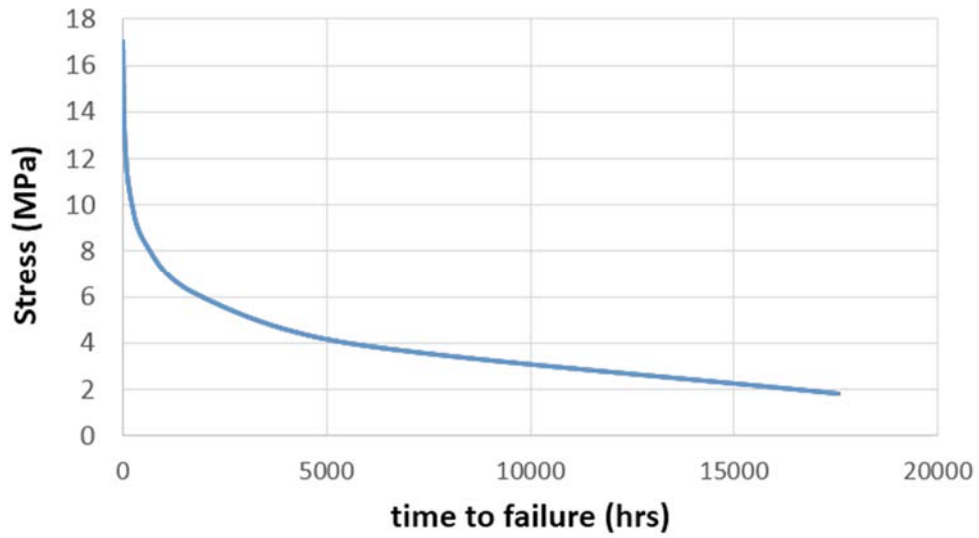


**Figure 74: Time to failure (hrs) vs. applied stress for material Resin 2, using the delayed failure approach**

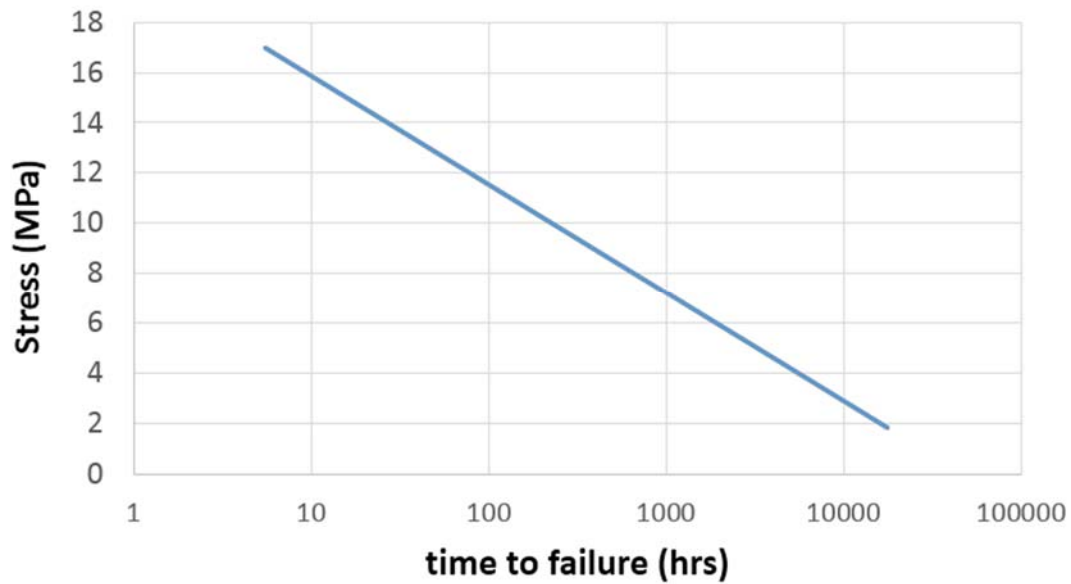


**Figure 75: Logarithmic time to failure (hrs) vs. applied stress for material Resin 2, using the delayed failure approach**

### 7.3 Conclusions

This chapter presents an approach (energy method based delayed failure) implemented in the finite element analysis for a numerical application.

The energy method based on Schapery's single integral constitutive law (Schapery, 1969) & (Schapery, 1969) was presented, and following the work by Hiel (Hiel, et al., 1983), and Roy and Reddy (Roy, et al., 1988) & (Roy, et al., 1988), an energy based method of delayed failure, was shown. The method was implemented in the previously developed FE procedure in Chapter 6. The principle stresses are obtained through the procedure and the strain energy in three principle directions are computed for each element at every time increment. Each strain energy is compared to the maximum limit (resilience factor,  $R$ ). If the strain energy is greater than the limit, the material is failing in that element and time. The time in which the strain energy gets greater than the resilience factor is called “time to failure”. The FE procedure is developed for nonlinear case (Chapter 6) meaning that the resultant “time to failure” prediction considers the nonlinearity of the material. This approach could be applied in viscoelastic situations. The approach works with limiting the strain energy of the material to a boundary which is the resilience limit.

Based on the research conducted in this chapter and summarized above, the following specific findings and contributions can be mentioned:

The developed code is able to predict the time to failure of materials based on delayed failure theorem. For failure analysis, a formulation is employed to develop the failure model. Out of many failure criteria, the maximum strain energy is chosen for finite element application. The method is implemented in developed material subroutine.

It was concluded that the delayed failure formulation can be implemented in the finite element analysis to find time to failure, and needs the resilience factor of the material (stored strain energy at time of failure), obtained from experiments.

## Chapter 8

### Conclusions and Future Work

#### 8.1 Conclusions

This study addresses a need to predict material behaviour response under multi-axial loadings for viscoelastic and/or viscoplastic materials. A finite element procedure was developed, which allows to model the long term as well as short term responses of polymers. A code was developed in Fortran workspace, which is linked to commercial software ABAQUS. Moreover, the code is able to predict the time to failure of materials based on delayed failure theorem.

The inputs to the developed code include a structural model and a material model. The former is done through the ABAQUS user interface and includes 3D solid modelling, boundary conditions, loadings, meshing and time discretization. The latter is obtained from experiments and needs material analysis. A nonlinear optimization method of finding material parameters has been used in this research.

The procedures are all detailed within the chapters of this dissertation. The manuscript starts with a description on the research significance and justification, as well as objectives and outline of the research. Later, a discussion on viscoelastic and viscoplastic materials, their application, and micromolecular and macromolecular characteristics, are provided. An introduction to the modelling methods is presented and the theoretical approaches adopted in the thesis are explained in detail. To construct the material models, a theoretical optimization method of finding material properties using experimental uniaxial creep test results developed for short term investigation. Differential formulation as well as unified plasticity theory is used for development of 1-D nonlinear viscoelastic and viscoplastic models, respectively. Material models are then extended to long terms. Materials parameters are obtained using nonlinear optimization technique, which is a minimization technique of error function. For this a code was developed in MATLAB workspace.

For the macromechanical modelling two approaches are employed. The first is the multi integral approach which is used for both nonlinear viscoelastic and viscoplastic modelling, and single integral approach which is used for nonlinear viscoelastic modelling. The multiple integral approach, is essentially an extension of the Boltzmann's linear superposition principle to nonlinear range, and is



employed for three-dimensional behaviour analysis. Some simplifications are done in order to obtain a particularly useful theory, which are the fully incompressible behaviour assumption of the material, the superposition of small time dependent deformation on large deformation, and finally the simplifications of the material functions. Differential formulation (exponential form), and unified plasticity (power-law function) approximations are used for viscoelastic and viscoplastic modellings, respectively. The models are optimized for long-term responses which are beyond the test time. Finite element procedures are implemented in the user-defined material algorithm in Abaqus (UMAT). The validity of the models is assessed by comparison with experimental observations on high density polyethylene (HDPE) for single element specimens under uniaxial loading. The single integral approach, in other hand, is developed by Schapery and is a simpler form of the multi integral one. based on Schapery's single integral constitutive law a nonlinear solution procedure is used to solve problems involving material nonlinearity. To simulate the viscoelastic behaviour of materials, a multi Kelvin Solid configuration of spring and dash-pot elements is used to construct the constitutive equations. Time- and stress dependent material properties (based on generalized multi Kelvin simulation) are used to characterize the nonlinear behaviour of a material. The proposed viscoelastic model is implemented in a user-defined material algorithm in Abaqus (UMAT). The validity of the models is assessed by comparison with experimental observations. For failure analysis, a formulation is employed to develop the failure model. Out of many failure criteria, the maximum strain energy is chosen for finite element application. The method is implemented in developed material subroutine.

Based on the research described in this thesis and summarized above, the following specific conclusions can be offered:

- 1- The Prony's series approach, and the associated multi-Kelvin solid modelling, is able to determine viscoelastic material parameters, while plastic theory is able to determine viscoplastic model parameters. The developed nonlinear optimization method allows for effective and fast parameter optimization and the development of constitutive modelling for time-dependent and nonlinear polymeric materials, and it is more efficient than linear methods.
- 2- Beyond the short term test time, the response of the viscoelastic model (exponential formulation) approaches an asymptotic value and the response of the viscoplastic model (power law formulation) increases continuously with a time dependent slope. This difference in the two modelling approaches clearly suggests that the models are most likely not valid beyond

the curve fitting time period. The result of the proposed long term formulation (which simulates the long term behaviour), lies between the curves which are the extension of viscoelastic and viscoplastic models beyond the short term period.

- 3- The proposed material models are able to detect erroneous creep test curve. It is because the developed material models are able to predict creep behaviour at another stress level, meaning that the models give an estimation of the creep curve which its applied stress level is between the two available ones. One can thus do effective process “trouble-shooting” and “detect” a potential abnormality in the data. In other words, the developed formulation, through the estimation of material parameters that should follow predetermined trends, can also be used to eliminate erroneous experimental data sets from constitutive modelling.
- 4- The comparisons show that the proposed constitutive model can satisfactorily represent the time-dependent mechanical behaviour of polymers in short term analysis. Both theoretically presented models are able to predict short term responses with less than 5% error (in most cases).
- 5- Fitting results for both viscoelastic and viscoplastic material models show that the viscoelastic one yields a better fit for both short and long term modelling, and the reason is that the former one has more fitting parameters compared to viscoplastic one which results in more flexible fitting to the short term test data, so more accurate short term and long term response prediction.
- 6- A superposition of small deformations can be used to model large deformations, and the multi-integral description can be simplified for finite element implementation, using the incompressibility assumption.
- 7- Both viscoelastic and viscoplastic formulations can be implemented in the finite element analysis using the linear superposition principle. The developed finite element procedure uses the proposed material definition based on experimental data.
- 8- Nonlinear Viscoelastic, NVE, and Nonlinear Viscoplastic, NVP, models can be used in computational (finite element) methods for predictions of long term material behaviour. In the long term, the NVE model in comparison with the NVP model results in smaller fitting errors for strain response predictions, and both results are in relatively good correlation with experiments (less than 10% error in most cases). Again, similar to material modelling, the

reason is that the former one has more fitting parameters compared to viscoplastic one which results in more flexible fitting to the short term test data, so more accurate short term and long term response prediction. It is concluded that with proper material parameters to reflect the deformations involved in the mechanical tests, the behaviour observed experimentally can be satisfactorily predicted using the FEM simulation.

- 9- The proposed FE formulations have the potential for practical analysis of polymeric structures. The constitutive model can be developed based on few short term creep tests and through the proposed method of extension to longer time frames, the multi-integral FE implementation and 3-D assumptions, it can be used for the analysis of mechanical and structural components under variety of loadings.
- 10- The proposed single integral Nonlinear Viscoelastic model is able to predict the long term behaviour of material with “good” correlation (in more than 70% of the tested materials).
- 11- A good correlation (less than 5% error) of model and experimental data is always achievable if proper material fitting parameters are obtained from test data. This requires accurate experimental measurements, as well as availability of numerous test results in each set of test data.
- 12- Delayed failure formulation can be implemented in the finite element analysis to find time to failure, and needs the resilience factor of the material (stored strain energy at time of failure), obtained from experiments.

## **8.2 Future Work**

It is believed that the present research topic is an area which can further be investigated. Although material model, macromechanical models, and failure model, are done within the framework of this research, more suggestions can be offered as future work. These suggestions can be categorized in two major classes of work which are: further improvement and optimization of proposed models and procedures, and filling the existent gaps in this area not covered in this work.

Since only polyethylene was used in material modelling, studying materials other than polyethylene can help further optimization of models. Using different materials, Like ETFE, Teflon, unplasticised polyvinyl chloride (PVC or UPVC), polypropylene (PP), Polybutylene (PB) and acrylonitrile-butadiene-styrene (ABS), can help to better understand the sensitivity of the proposed formulation to the material itself. Although the proposed formulation and procedure is generally applicable to all viscoelastic/viscoplastic materials, there might be some limitations which are not clear to the author.

In addition to the application of different materials, different methods of experiments can be employed. Although we have used one dimensional tensile tests for obtaining the material properties and validating the results, multi dimensional as well as compression tests are suggested. Uniaxial compression test would be useful to see how the material reacts to the compression versus tension. Generally, one dimensional tests are more common as they are easier to do and just a simple uniaxial test machine is sufficient. This type of test includes tension, compression and creep shear tests. On the other hand, multiaxial tests are very valuable but need more complicated test machines. In this category, biaxial tensile test is helpful in understanding the response of the material to applied forced in different direction. The most important benefit is that one can understand which stress is more effective in defining material properties, which leads to definition of effective (equivalent) stress for the material parameter dependency to the stress. In more complex and more accurate investigation, the three dimensional loading test would help also the understanding of the geometrical nonlinearities of the material and optimizing the three dimensional finite element model and theoretical formulations.

The nonlinear optimization method of model parameters, which has been used in material model development, has always been a challenging task for the researchers. This method requires a guess of first set of fitting parameters, and the outcome is highly sensitive to these values. Although it's been tried to use the best guesses for fitting parameters in this research, further optimization of these guessed values can be considered as an improvement to the model. It should be noted that a bad guess could even cause the optimization procedure to diverge. A built-in formulation of nonlinear optimization procedure in MATLAB (Derivative Free Method) is used to find a minimum to the fitting formulations. As another future work, other available numerical methods of minimization like: Descent method, Gradient descent method, Steepest descent method, Newton's method, etc., can be used and programmed for further investigation on improvement of efficiency of optimization.

Although multi-Kevin solid configuration of spring and dash-pots are used for viscoelastic modelling, other configurations can also be investigated. Multi-Kevin solid works well for polyethylene, but other configurations like: Elastic solid, Viscous fluid, Maxwell fluid, 3-parameter and 4-parameter solids and fluids, etc., might work better for other materials.

A one term approximation of power law function has been used for viscoplastic modelling. It can be further developed and optimized by increasing the terms using a repeatable form, similar to what is used in viscoelastic modelling.

Studying failure criteria other than the used delayed failure (such as Environment Stress Cracking Resistance (ESC), yield and rupture) and their implementation in the proposed finite element procedure, is another area which would be an improvement to the current work. Also, performing experimental failure test and studying the resilience factor (ultimate strain energy at time of failure) for polyethylene and other polymers, could be a future work which requires a vast elaboration.

In addition to the discussed items on the improvement of the proposed research, there are gaps which need to be filled as future work to the current one. One area is using the Modified Superposition Principle (MSP), instead of the used linear superposition principle. The implementation of the MSP approach into the modellings/formulations and then into the finite element procedure could be considered as a novel research. In addition, investigating the effects of temperature on the short and long term behaviour would be an interesting work. Introducing the temperature to the proposed modelling, could increase the capability of the finite element procedure in predicting the response of material. Comparing the outcome of this modification and comparing the results with those available on Time-Temperature Superposition Principle (TTSP) in the literature, could lead to an interesting area of study.

## Bibliography

- Lustiger A.** Understanding Environmental Stress Cracking in Polyethylene in Medical Plastics: Degradation, Resistance & Failure Analysis [Report]. - R. C. Portnoy, SPE : Plastic Design Library, 1998. - pp. 66-71.
- Aklonis John J. and MacKnight William J.** Introduction to Polymer Viscoelasticity [Book]. - New York : A Wiley-Interscience Publication, 1983.
- Alvarado J, Polak Maria A and Penlidis Alexander** Constitutive Modeling of Damage Evolution in Semicrystalline Polyethylene [Journal] // Journal of Engineering Materials and Technology. - 2010. - October : Vol. 132.
- Alvarado J., Polak M.A. and Penlidis A.** Constitutive Modeling of Damage Evolution in Semicrystalline Polyethylene [Journal] // Journal of Engineering Materials and Technology. - 2010. - 12 : Vol. 132.
- Alvarado-Contreras J., Polak M. A. and Penlidis A.** Computational Study on a Damage-Coupled Model for Crystalline Polyethylene [Journal] // Eng. Computations. - 2008. - Vol. 25. - pp. 612-636.
- Alvarado-Contreras J., Polak M. A. and Penlidis A.** Micromechanical Approach to Modeling Damage in Crystalline Polyethylene [Journal] // Polym. Eng. Sci.. - 2007. - Vol. 47. - pp. 410-420.
- Areias P. and Matous K.** Finite element formulation for modeling nonlinear viscoelastic elastomers [Journal] // Comput. Methods Appl. Mech. Engrg.. - 2008. - Vol. 197. - pp. 4702–4717.
- Ayoub G. [et al.]** Modelling large deformation behaviour under loading–unloading of semicrystalline polymers: Application to a high density polyethylene [Journal] // International Journal of Plasticity. - 2010. - Vol. 26. - pp. 329–347.
- Bae Jung-Eun and Cho Kwang Soo** Semianalytical methods for the determination of the nonlinear parameter of nonlinear viscoelastic constitutive equations from LAOS data [Journal]. - 2015. - pp. 525-555.
- Barbero E.J.** Time–temperature–age superposition principle for predicting long-term response of linear viscoelastic materials [Journal] // Creep and Fatigue in Polymer Matrix Composites. - 2011. - pp. 48-69.
- Baumgaertel M. and Winter H. H.** Determination of discrete relaxation and retardation time spectra from dynamic mechanical data [Journal] // Rheologica Acta. - Vol. 28. - pp. 511-519.

**Bauwens-Crowet C., Bauwens J. C. and Holmes G.** the Temperature Dependence of Yield of Polycarbonate in Uniaxial Compression and Tensile Tests [Journal] // Journal of Materials Science. - 1972. - Vol. 7. - pp. 176-183.

**Behjat Y. [et al.]** Influence of Micromolecular Structure on Environmental Stress Cracking Resistance of High Density Polyethylene [Journal] // ASCE Journal of Materials in Civill Engineering. - 2014.

**Behjat Y.** Relationship between Short-Term and Long-Term Creep, and the Molecular Structure of Polyethylene [Report]. - Waterloo, ON : M.A.Sc. Thesis, University of Waterloo, 2009. - p. 73.

**Behzadfar Ehsan and Hatzikiriakos Savaz** Viscoelastic properties and constitutive modelling of bitumen [Journal] // Fuel. - 2013. - Vol. 108. - pp. 391–399.

**Bodner S R and Partom Y** A Large Deformation Elastic-Viscoplastic Analysis of a Thick-Walled Spherical Shell [Journal] // Journal of Applied Mechanics. - 1972. - Vol. September. - pp. 751-757.

**Bodner S R and Partom Y** Constitutive Equations for Elastic-Viscoplastic Strain-Hardening Materials [Journal] // Journal of Applied Mechanics. - 1975. - Vol. June. - pp. 385-389.

**Bodner S. R. and Partom Y.** A Large Deformation Elastic-Viscoplastic Analysis of a Thick-Walled Spherical Shell [Journal] // Journal of Applied Mechanics. - 1972. - p. 571.

**Bodner S. R.** Review of a Unified Elastic-Viscoplastic Theory [Journal] // AFOSR-84-004. - 1984.

**Bodner S.R. and Partom Y.** Constitutive Equations for Elastic-Viscoplastic Strain-Hardening Materials [Journal] // Journal of Applied Mechanics. - June 1975. - pp. 385-389.

**Boey FYC. and Toeh S. H.** Bending creep rupture analysis using a nonlinear criterion approach [Journal] // Mater Sci Engng. - 1990. - 123 : Vol. A. - pp. 13-19.

**Bower M. V. and Gant S. F.** Stress relaxation Functions: Methods of Approximation [Report]. - April 1994. - NASA-CR-195830.

**Brinson H. F.** Matrix dominated time dependent failure predictions in polymer matrix composites [Journal] // Compos Struct. - 1999. - Vol. 47. - p. 445.

**Brinson H. F.** The Viscoelastic Behavior of a Ductile Polymer [Book Section] // Deformation and Fracture of High Polymers. - New York : Plenum Press, 1973.

**Brinson H. F., Griffith W. I. and Morris D. H.** Creep rupture of polymer matrix composites [Journal] // Experimental Mechanics. - 1981. - 9 : Vol. 21. - pp. 329-336.

- Brinson Hall F. and Brinson Catherine L.** Polymer Engineering Science and Viscoelasticity, An Introduction [Book]. - New York : Springer Science, 2008.
- Brunner O. S.** Energy-related failure criteria of thermoplastics [Journal] // Polym Engng Sci. - 1981. - 3 : Vol. 21. - p. 145.
- Brunner O. S.** On the damage energy of polymers in creep [Journal] // Polym Engng Sci. - 1978. - 42 : Vol. 18. - p. 4.
- Brunner O. S.** The energy balance of a viscoelastic material [Journal] // Int J Polym Mater. - 1973. - 137 : Vol. 2. - p. 48.
- Budianski B.** Micromechanics [Journal] // Computers and Structures. - 1983. - Vol. 16. - pp. 3-12.
- Cantrell C. A.** Technical Note: Review of methods for linear least-squares fitting of data and application to atmospheric chemistry problems [Journal] // Atmos. Chem. Phys.. - 2008. - Vol. 8. - pp. 5477–5487.
- Cao Kan [et al.]** Tensile behavior of polycarbonate over a wide range of strain rates [Journal] // Materials Science and Engineering A. - 2010. - Vol. 527. - pp. 4056–4061.
- Cernocky E P and Krempl E** A Theory of Viseoplastieity Based on Infinitesimal Total Strain [Journal] // Aeta Meehanica. - 1980. - Vol. 36. - pp. 263--289.
- Chan Y.L. and Ngan A.H.W.** Invariantelasticmodulusofviscoelasticmaterialsmeasuredby rate-jump tests [Journal] // PolymerTesting. - 2010. - Vol. 29. - pp. 558-564.
- Charbonneau L.** Tensile Time-Dependent Tensile Properties of ETFE Foils [Report]. - Waterloo, ON : Department of Civil Engineering, University of Waterloo, 2011.
- Charbonneau L., Polak M. A. and Penlidis A.** Mechanical Properties of ETFE Foils, Testing and Modelling, Construction and Building Materials [Journal] // Construction and Building Materials. - 2014. - Vol. 60. - pp. 63-72.
- Cheng J. J. [et al.]** Chain Entanglements and Mechanical Behaviour of High Density Polyethylene [Journal] // Journal of Engineering Materials and Technology - Transactions of the ASME. - 2010. - 1 : Vol. 132. - pp. 011-016.
- Cheng J. J.** Mechanical and Chemical Properties of High Density Polyethylene: Effects of Microstructure on Creep Characteristics [Report]. - Waterloo, ON : PhD Thesis, University of Waterloo, 2008.



**Cheng J. J., Polak M. A. and Penlidis A.** Phase interconnectivity and environmental stress cracking resistance of polyethylene: a crystalline phase investigation [Journal] // Journal of Macromolecular science: Pure and Applied Chemistry. - 2009. - 6 : Vol. 46. - pp. 572-583.

**Cheng J. J., Polak M. A. and Penlidis A.** Polymer Network Mobility and Environmental Stress Cracking Resistance of High Density Polyethylene [Journal] // Polymer-Plastics Technology and Engineering. - 2009. - 12 : Vol. 48. - pp. 1252-1261.

**Cheng J.J., Polak M.A. and Penlidis A.** An Alternative Approach to Estimating Parameters in Creep Models of High-Density Polyethylene [Journal] // Polymer Engineering and Science. - 2011. - Vol. 51. - pp. 1227-1235.

**Cheng Joy J, Polak Maria A and Penlidis Alexander** A Tensile Strain Hardening Test Indicator of Environmental Stress Cracking Resistance [Journal] // Journal of Macromolecular Science, Part A: Pure and Applied Chemistry. - 2008. - Vol. 45. - pp. 599–611.

**Cheng Joy J, Polak Maria A and Penlidis Alexander** Influence of micromolecular structure on environmental stress cracking resistance of high density polyethylene [Journal] // Tunnelling and Underground Space Technology. - 2011. - Vol. 26. - pp. 585-593.

**Christensen R.M.** Theory of Viscoelasticity [Book]. - [s.l.] : Academic Press, 1971.

**Cowie J. M. G., McEwen I. J. and McIntyre R.** Aging and Degradation of Polymer Blends (Polymer Blends Handbook) [Book]. - Dordrecht : Kluwer Academic Publishers, 2002. - Vol. 2 : pp. 977-1021.

**Cowking A. [et al.]** A Study on the Orientation Effects in Polyethylene in the Light of Crystalline Texture: Part 3 [Journal] // J. Mater. Sci.. - 1968. - Vol. 3. - pp. 646-654.

**Crochet M. J.** Symmetric Deformations of Viscoelastic-Plastic Cylinders [Journal] // J. of Applied Mechanics. - 1966. - Vol. 33. - p. 321.

**Denby E. F.** A note on the interconversion of creep, relaxation and recovery [Journal] // Rheologica Acta. - 1975. - Vol. 14. - pp. 591-593.

**Deng M. and Zhou J.** Effects of temperature and stress level on creep and tensile property of polypropylene sutures [Journal] // J Appl Polym Sci. - 2003. - Vol. 90. - pp. 3882-3888.

**Diani J., Gilormini P. and Arrieta J. S.** Direct experimental evidence of time-temperature superposition at finite strain for an amorphous polymer network [Journal] // Polymer. - 2015. - Vol. 58. - pp. 107-112.

- Diani J., Gilormini P. and Arrieta J.S.** Direct experimental evidence of time-temperature superposition at finite strain for an amorphous polymer network [Journal] // Polymer. - February 2015. - 10 : Vol. 58. - pp. 107-112.
- Drozdov A.D. and Christansen J.D.** Constitutive equations for the nonlinear viscoelastic and viscoplastic behavior of thermoplastic elastomers [Journal] // International Journal of Engineering Science. - 2006. - Vol. 44. - pp. 205-226.
- Drozdov A.D. and Christansen J.D.** Modelling the viscoplastic response of polyethylene in uniaxial loading–unloading tests [Journal] // Mechanics Research Communications. - 2003. - Vol. 30. - pp. 431–442.
- Drozdov Aleksey D** A Model for the Nonlinear Viscoelastic Response in Polymers at Finite Strains [Journal] // International Journal of Solids Structures. - 1998. - 18 : Vol. 35. - pp. 2315-2347.
- Drozdov Aleksey D** A New Model for an Aging Thermoviscoelastic Material [Journal] // Mechanics Research Communications. - 1995. - 5 : Vol. 22. - pp. 441-446.
- Drozdov Aleksey D and Kalamkarov A L** A Constitutive Model for Nonlinear Viscoelastic Behavior of Polymers [Journal] // Polymer Engineering and Science. - 1996. - 14 : Vol. 36. - p. July 1996.
- Drozdov Aleksey D** Constitutive equations in finite elasticity of rubbers [Journal] // International Journal of Solids and Structures. - 2007. - Vol. 44. - pp. 272-297.
- Drozdov Aleksey D** Constitutive Model of a Viscoelastic Material at Finite Strains [Journal] // Mechanics Research Communications. - 1992. - 6 : Vol. 19. - pp. 535-540.
- Drozdov Aleksey D** Creep rupture and viscoelastoplasticity of polypropylene [Journal] // Engineering Fracture Mechanics. - 2010. - Vol. 77. - pp. 2277-2293.
- Dusunceli Necmi and Colak Ozgen Umit** The effects of manufacturing techniques on viscoelastic and viscoplastic behavior of high density polyethylene (HDPE) [Journal] // Materials and Design. - 2008. - Vol. 29. - pp. 1117–1124.
- Ellyin F., Vaziri R. and Bigot L.** Predictions of Two Nonlinear Viscoelastic Constitutive Relations for Polymers under Multiaxial Loadings [Journal] // POLYMER ENGINEERING AND SCIENCE. - 2007.
- Eyring Henry** Viscosity, Plasticity, and Diffusion as Examples of Absolute Reaction Rates [Journal] // JOURNAL OF CHEMICAL PHYSICS. - 1936. - April : Vol. 4. - pp. 283-291.
- felbeck D. and Atkins A.** Strength and Fracture of Engineering Solids [Book]. - [s.l.] : Prentice Hall, 1996.

- Fernanda M., Costa P. and Ribeiro C.** Parameter Estimation of Viscoelastic Materials: A Test Case with Different Optimization Strategies [Conference] // ICNAAM 2011. - 2011. - pp. 771-774.
- Ferry J. D.** Viscoelastic Properties of Polymers [Book]. - New York : JW, 1980.
- Findley William N., Lai James S. and Onaran Kasif** Creep and Relaxation of Nonlinear Viscoelastic Materials [Book]. - [s.l.] : North-Holland Publishing, 1976. - Vol. 18.
- Flugge W.** Viscoelasticity [Book]. - [s.l.] : Blaisdell Publishing Company, 1967.
- Friedrich K.** Crazes and Shear Bands in Semi-Crystalline Thermoplastics [Journal] // Advances in Polymer Science. - 1983. - Vols. 52-53. - pp. 225-274.
- G'Sell C., Hiver J. M. and Dahoun A.** Experimental Characterization of Deformation Damage in Solid Polymers under Tension, and its Interrelation with Necking [Journal] // Int. J. Solids Struct.. - 2002. - Vol. 39. - pp. 3857-3872.
- Gnip I.Y. [et al.]** Experiments for the long-term prediction of creep strain of expanded polystyrene under compressive stress [Journal] // Polymer Testing. - September 2010. - 6 : Vol. 29. - pp. 693-700.
- Gnip I.Y. [et al.]** Long-term prediction of compressive creep development in expanded polystyrene [Journal] // Polymer Testing. - May 2008. - 3 : Vol. 27. - pp. 378-391.
- Green A. E. and Rivlin R. S.** The mechanics of non-linear materials with memory [Journal] // Archives of Rational Mechanics and Analysis. - 1957. - Vol. 1. - pp. 1-21.
- G'Sell C. and Dahoun A.** Evolution of Microstructure in Semi-crystalline Polymer under Large Plastic Deformation [Journal] // Mater. Sci. Eng. A. - 1994. - Vol. 175. - pp. 183-199.
- Guedes Rui Miranda** An energy criterion to predict delayed failure of multi-directional polymer matrix composites based on a non-linear viscoelastic model [Journal] // Composites: Part A. - 2004. - Vol. 35. - pp. 559-571.
- Guedes Rui Miranda** Analysis of a delayed fracture criterion for lifetime prediction of viscoelastic polymer materials [Journal] // Mech Time-Depend Mater. - 2012. - Vol. 16. - pp. 307-316.
- Guedes Rui Miranda** CREEP FAILURE CRITERIA FOR POLYMER BASED MATERIALS [Conference] // 15th International Conference on Experimental Mechanics (ICEM15). - 2012. - REF:3126.
- Guedes Rui Miranda** Mathematical Analysis of Energies for Viscoelastic Materials and Energy Based Failure Criteria for Creep Loading [Journal] // Mechanics of Time-Dependent Materials. - June 2004. - 2 : Vol. 8. - pp. 169-192.

**Guedes Rui Miranda** Relationship between lifetime under creep and constant stress rate for matrix composites [Journal] // Composites Science and Technology. - 2009. - Vol. 69. - pp. 1200–1205.

**Gupta R., Baldewa B. and Joshi Y. M.** Time temperature superposition in soft glassy materials [Journal] // Soft Matter. - 2012. - Vol. 8. - p. 4171.

**Hasanpour K. and Ziaei-Rad S.** Finite element simulation of polymer behaviour using a three-dimensional, finite deformation constitutive model [Journal] // Computers and Structures. - 2008. - Vol. 86. - pp. 1643–1655.

**Hasanpour K., Ziaei-Rad S. and Mahzoon M.** A large deformation framework for compressible viscoelastic materials: Constitutive equations and finite element implementation [Journal] // International Journal of Plasticity. - [s.l.] : International Journal of Plasticity, 2009. - Vol. 25. - pp. 1154-1176.

**Hiel C., Cardon A. H. and Brinson H. F.** The nonlinear viscoelastic response of resin matrix composite laminates [Report] / Department of Engineering Science and Mechanics, Virginia Polytechnic Institute and State University. - Blacksburg, VA : [s.n.], 1983. - Report No VPI-E-83-6.

**Hiel C., Crdon A. H. and Brinson H. F.** The nonlinear viscoelastic response of resin matrix composite laminates [Report] / Department of Engineering Science and Mechanics, Virginia Polytechnic Institute and State University. - Blacksburg, VA : [s.n.], 1983. - Report No VPI-E-83-6.

**Hildebrand F.B.** Introduction to Numerical Analysis [Book]. - New York : Dover Publications, Inc., 1974. - 2.

**Hinterhoelzl R M and Schapery R A** FEM Implementation of a Three-Dimensional Viscoelastic Constitutive Model for Particulate Composites with Damage Growth [Journal] // Mechanics of Time-Dependent Materials. - 2004. - Vol. 8. - pp. 65-94.

**Hittmair P. and Ullman R.** Environmental Stress Cracking of Polyethylene [Journal] // Journal of Applied Polymer Science. - 1962. - Vol. 6. - pp. 1-14.

**Hooper D., Coughlan J. and Mullen M.** Structural equation modelling: Guidelines for determining model fit [Report] / Dublin Institute of Technology. - 2008.

**Houshyar S. and Shanks R.A.** Tensile properties and creep response of polypropylene fibre composites with variation of fibre diameter [Journal] // Polym Int. - 2004. - Vol. 53. - pp. 1752-1759.

**Houshyar S., Shanks R.A. and Hodzic A.** Tensile creep behaviour of polypropylene fibre reinforced polypropylene composites [Journal] // Polym Test. - 2005. - Vol. 24. - pp. 257-264.

- Huber N and Tsakmakis C** Finite deformation viscoelasticity laws [Journal] // Mechanics of Materials. - 2000. - Vol. 32. - pp. 1-18.
- Hughes T. J. R. and Taylor R. L.** Unconditionally Stable Algorithms for Quasi-Static Elasto-Visco-Plastic Finite Element Analysis [Journal] // Computers & Structures. - 1978. - Vol. 8. - p. 169.
- Janson L.C.** Plastics pipes for water supply and sewage disposal [Book]. - [s.l.] : Borealis, 2003.
- Kaliske Michael, Nasdala Lutz and Rothert Heinrich** On damage modelling for elastic and viscoelastic materials at large strain [Journal] // Computers & Structures. - 2001. - Vol. 79. - pp. 2133-2141.
- Kim B., Youn S. and Lee W.** A constitutive model and FEA of rubber under small oscillatory load superimposed on large static deformat [Journal] // Archive of Applied Mechanics. - 2004. - Vol. 73. - pp. 781–798.
- Kinloch A. J. and Young R. J.** Fracture Behavior of Polymers [Book]. - London : Applied Science, 1983.
- Knauss W.G. and Emri I.** Non-linear viscoelasticity based on free volume consideration [Journal] // Computers and Structures. - 1981. - Vol. 13. - pp. 123-128.
- Kolarik J. [et al.]** Non-linear long-term tensile creep of poly(propylene)/cycloolefin copolymer blends with fibrous structure [Journal] // Macromol Mater Engng. - 2003. - Vol. 288. - pp. 629-641.
- Krairi Anouar and Doghri Issam** A thermodynamically-based constitutive model for thermoplastic polymers coupling viscoelasticity, viscoplasticity and ductile damage [Journal] // International Journal of Plasticity. - 2014. - Vol. 60. - pp. 163-181.
- Krishnaswami P., Tuttle M.E. and Emery A.F.** Finite Element Modeling of the Time-Dependent Behavior of Nonlinear Ductile Polymers [Journal] // Polymer Engineering and Science. - Aug 1992. - 16 : Vol. 32. - pp. 1086-1096.
- Krishnaswamy P, Tuttle M. E. and Emery A. F.** Finite element modelling of crack tip behaviour in viscoelastic materials. Part I: Linear behaviour [Journal] // International Journal of Numerical Methods and Engineering. - 1990. - Vol. 30. - pp. 371-387.
- Krishnaswamy P., Tuttle M. E. and Emery A. F.** Finite Element Modeling of the Time-Dependent Behavior of Nonlinear Ductile Polymers [Journal] // Polymer Engineering and Science. - 1992. - 16 : Vol. 32. - pp. 1086-1096.
- Lagaron J., Dixon N. M. and Kip B. J.** Cold-Drawn Material as Model Material for the Environmental Stress Cracking (ESC) Phenomenon in Polyethylene [Journal] // Macromolecules. - 1998. - Vol. 31. - pp. 5845-5852.

**Lagaron J., Pastor J. and Kip B.** Role of an active environment of use in an environmental stress crack resistance (ESCR) test in stretched polyethylene: A vibrational spectroscopy and a SEM study [Journal] // Polymer. - 1999. - Vol. 40. - pp. 1629-1636.

**Leaderman H.** Elastic and Creep Properties of Filamentous Materials and Other High Polymers [Book]. - Washington : The Textile Foundation, 1943.

**Li R.** Time-temperature superposition method for glass transition temperature of plastic mater [Journal] // Materials Science and Engineering. - 2000. - Vol. A278. - pp. 36-45.

**Lin L. and Argon A. S.** Review: Structure and Plastic Deformation of Polyethylene [Journal] // J. Mater. Sci.. - 1994. - Vol. 29. - pp. 294-323.

**Liu H.** Material Modelling for Structural Analysis of Polyethylene, MASC thesis [Report] / ept of Civil and Environmental Eng., University of Waterloo. - Waterloo : [s.n.], 2007.

**Liu H., Polak M.A. and Penlidis A.** A Practical Approach to Modeling Time-Dependant Nonlinear Creep Behavior of Polyethylene for Structural Applications [Journal] // Polymer Engineering and Science. - 2008. - 1 : Vol. 48. - pp. 159-167.

**Liu Hongtao** Material Modelling for Structural Analysis of Polyethylene [Report]. - Waterloo, ON, Canada : University of Waterloo, Civil & Environmental Department, 2007.

**Liu Hongtao, Polak Maria Anna and Penlidis Alexander** A Practical Approach to Modeling Time-Dependant Nonlinear Creep Behavior of Polyethylene for Structural Applications [Journal] // Polymer Engineering and Science. - 2008. - pp. 159-167.

**Liu M. C. M. and Krempl E.** A uniaxial viscoplastic model based on total strain and overstress [Journal] // Journal of Mechanics and Physics of Solids. - 1979. - 5 : Vol. 27. - pp. 377-391.

**Lockett F. J.** Nonlinear Viscoelastic Solids [Book]. - New York : Academic Press, 1972.

**Lu X. and Brown N.** The ductile-brittle transition in a polyethylene copolymer [Journal] // Journal of Materials science. - 1990. - Vol. 25. - pp. 29-34.

**Luo Wenbo [et al.]** Long-term creep assessment of viscoelastic polymer by time-temperature-stress superposition [Journal] // Acta Mechanica Solida Sinica. - December 2012. - 6 : Vol. 25. - pp. 571-578.

**Lustig S. R. and Shay R. M.** Thermodynamics constitutive equations for materials with memory on a material time scale [Journal] // J. Rheol.. - 1996. - Vol. 40. - pp. 69-106.

- Lustiger A. and Corneliussen R. D.** The Role of Crazes in the Crack Growth of Polyethylene [Journal] // Journal of Material Science. - 1987. - Vol. 22. - pp. 2470-2476.
- MacCallum R. C., Browne M. W. and Sugawara H. M.** Power Analysis and Determination of Sample Size for Covariance Structure Modeling [Journal] // Psychological Methods. - 1996. - 2 : Vol. 1. - pp. 130-149.
- McKenna G. B. and Penn R. W.** Time-dependent failure in poly(methyl methacrylate) and polyethylene [Journal] // Polymer. - 1980. - Vol. 21.
- Mlekusch B.** Calculation of residual stress development in injection moulding using a nonlinear viscoelastic model [Journal] // Mech. Time-Depend. Mat.. - 2001. - Vol. 5. - pp. 101-108.
- Muliana A., Rajagopal K.R. and Tscharnuter D.** A nonlinear integral model for describing responses of viscoelastic solids [Journal] // International Journal of Solids and Structures. - 2015. - Vol. 58. - pp. 146-156.
- Muliana Anastasia** Large deformations of nonlinear viscoelastic and multi-responsive beams [Journal] // International Journal of Non-Linear Mechanics. - 2015. - Vol. 71. - pp. 152-164.
- Nagdi P.M. and Murch S.A.** On the Mechanical Behavior of Viscoelastic-Plastic Solids [Journal] // J. of Applied Mechanics. - 1963. - Vol. 30. - p. 321.
- Naghdbadi R., Baghani M. and Arghavani J.** A viscoelastic constitutive model for compressible polymers based on logarithmic strain and its finite element implementation [Journal] // Finite Elements in Analysis and Design. - 2012. - Vol. 62. - pp. 18-27.
- Naya S. [et al.]** New method for estimating shift factors in time-temperature superposition models [Journal] // J Therm Anal Calorim. - 2013. - Vol. 113. - pp. 453-460.
- Nguyen M. [et al.]** Validation of the time-temperature superposition principle for crack propagation in bituminous mixtures [Journal] // Materials and Structures. - 2013. - Vol. 46. - pp. 1075-1087.
- Nguyen Song, Castagnet Sylvie and Grandidier Jean-Claude** Nonlinear viscoelastic contribution to the cyclic accommodation of high density polyethylene in tension: Experiments and modeling [Journal] // International Journal of Fatigue. - 2013. - Vol. 55. - pp. 166-177.
- Nikolov S and Doghri I** A micro/macro constitutive model for the small-deformation behavior of polyethylene [Journal] // Polymer. - 2000. - Vol. 41. - pp. 1883-1891.
- Nikolov S. [et al.]** Multi-scale Constitutive Modeling of the Small Deformations of Semi-crystalline Polymers [Journal] // J. Mech. Phys. Solids. - 2002. - Vol. 50. - pp. 2275-2302.

**Pan Douxing, Kang Guozheng and Jiang Han** Viscoelastic Constitutive Model for Uniaxial Time-Dependent Ratcheting of Polyetherimide Polymer [Journal] // POLYMER ENGINEERING AND SCIENCE. - 2012. - pp. 1874-1881.

**Park S.W. and Kim Y.R.** Fitting Prony-Series Viscoelastic Models with Power-Law Presmoothing [Journal] // Journal of Materials in Civil Engineering. - Jan/Feb (2001. - pp. 26-32.

**Park S.W. and Kim Y.R.** Interconversion between Relaxation Modulus and Creep Compliance for Viscoelastic Solids [Journal] // Journal of Materials in Civil Engineering. - Feb 1999. - pp. 76-82.

**Polak M., Duyvestin G. and Knight M.** Experimental Strain Analysis for Polyethylene Pipes Installed by Horizontal Directional Drilling [Journal] // Tunnelling and Underground Space Technology. - 2004. - Vol. 9. - pp. 205-216.

**Popa C.M. [et al.]** Formulation and implementation of a constitutive model for semicrystalline polymers [Journal] // International Journal of Plasticity. - 2014. - Vol. 61. - pp. 128–156.

**Popelar C. F. and Liechi K. M.** A distortion-modified free volume theory for nonlinear viscoelastic behavior [Journal] // Mech. Time-Depend. Mat.. - 2003. - Vol. 7. - pp. 89-141.

**Reddy J. N.** Introduction to Continuum Mechanics [Book] / ed. 2. - New York : Cambridge University Press, 2013.

**Reiner M. and Weissenberg K.** A thermodynamic theory of the strength of materials [Journal] // Rheology Leaflet. - 1939. - Vol. 10. - pp. 12-20.

**Reiner M. and Weissenberg K.** A thermodynamic theory of the strength of the materials [Journal] // Rheol Leaflet. - 1939. - 1 : Vol. 10. - pp. 12-20.

**Robert S. Chambers** RELFIT: A Program for Determining Prony Series Fits to Measured Relaxation Data [Report] / Sandia National Laboratories. - Albuquerque, New Mexico : [s.n.], 1997. - SAND97-0371.UC-706.

**Roy S. and Reddy J. N.** A finite element analysis of adhesively bonded composite joints with moisture diffusion and delayed failure [Journal] // Computers and Structures. - 1988. - 6 : Vol. 29. - pp. 1011-1031.

**Roy S. and Reddy J. N.** A FINITE ELEMENT ANALYSIS OF ADHESIVELY BONDED COMPOSITE JOINTS WITH MOISTURE DIFFUSION AND DELAYED FAILURE [Journal] // Computers and Structures. - 1988. - 6 : Vol. 29. - pp. 1011-1031.



**Roy S. and Reddy J. N.** Finite-element models of viscoelasticity and diffusion in adhesively bonded joints [Journal] // International Journal for Numerical Methods in Engineering. - 1988. - 11 : Vol. 26. - p. 2531-2546.

**Sardashti P. [et al.]** Effect of Temperature on Environmental Stress Cracking Resistance and Crystal Structure of Polyethylene [Journal]. - [s.l.] : J. Macromol. Sci. Pure & Appl. Chem., 2014. - 3 : Vol. 51. - pp. 1-14.

**Sardashti P. [et al.]** Improvement of Hardening Stiffness Test as an Indicator of Environmental Stress Cracking Resistance of Polyethylene [Journal]. - [s.l.] : J. Macromol. Sci., 2012. - 9 : Vol. 49. - pp. 689-698.

**Schapery R A** On the characterization of nonlinear viscoelastic materials [Journal] // Polymer Engineering Science. - 1969. - 4 : Vol. 9. - pp. 295-310.

**Schapery R. A.** A simple collocation method for fitting viscoelastic models to experimental data [Report] / California Institute of Technology. - Pasadena, USA : [s.n.], 1961. - GALCIT SM 61-23A.

**Schapery R. A.** Further development of a thermodynamic constitutive theory: stress formulation [Report] : A&S Report No. 69-2 / Purdue University, W. Lafayette, IN. - 1969.

**Schapery R.A.** Nonlinear Viscoelastic and Viscoplastic Constitutive Equations based on Thermodynamics [Journal] // Mechanics of Time-Dependent Materials. - 1997. - Vol. 1. - pp. 209-240.

**Scheirs J.** Compositional and Failure Analysis of Polymers [Book]. - Chichester : J. Wiley & Sons, 2000.

**Schmiedel H.** Handbook of Plastic Testing Audit [Book]. - München : Carl Hanser Verlag, 1992.

**Schrauwen B. A. G.** Deformation and Failure of Semicrystalline Polymer Systems: Influence of Micro and Molecular Structure [Report]. - [s.l.] : PhD dissertation, Eindhoven University of Technology, 2003.

**Sepiani Hossein, Polak Marria Anna and Penlidis Alexander** Modelling Short and Long Term Time Dependent Nonlinear Behaviour of Polyethylene [Journal] // Mechanics of Advanced Materials and Structures. - 2017.

**Smart J. and Williams J.G.** comparison of single-integral non-linear viscoelastic theories [Journal] // Journal of Mechanics and Physics of Solids. - 1972. - Vol. 20. - pp. 313-324.

**Spencer A. J. M. and Rivlin R. S.** The Theory of Matrix Polynomials and its Application to the Mechanics of Isotropic Continua" [Journal] // Arch. Rational Mech. Anal.. - 1959. - Vol. 2. - p. 21.

Standard Test Method for Tensile Properties of Plastics. - [s.l.] : ASTM International, 2002. - D638-02a.

**Tajvidi M., Falk R. H. and Hermanson J. C.** Time–Temperature Superposition Principle Applied to a Kenaf-Fiber/High-Density Polyethylene Composite [Journal] // Journal of Applied Polymer Science. - 2005. - Vol. 97. - pp. 1995-2004.

**Theo S. H.** Computational aspects in creep rupture modelling of polypropylene using an energy failure criterion in conjunction with a mechanical model [Journal] // Polymer. - 1990. - 2260 : Vol. 31. - p. 6.

**Theoh S. H., Cherry B. W. and Kaush H. H.** Creep rupture modelling of polymers [Journal] // Int J Damage Mech. - 1992. - 2 : Vol. 1. - p. 545.

**Weitsman Y.** A continuum diffusion model for viscoelastic materials [Journal] // J. Phys. Chem.. - 1990. - Vol. 94. - pp. 961-968.

**Wendlandt Michael, Tervoort Theo A. and Ulrich Suter W.** Strain-Hardening Modulus of Cross-Linked Glassy Poly(methyl methacrylate) [Journal] // Journal of Polymer Science: Part B: Polymer Physics. - 2010. - Vol. 48. - pp. 1464–1472.

**Williams M. L., Landel R. F. and Ferry J. D.** The Temperature Dependence of Relaxation Mechanisms in Amorphous Polymers and Other Glass Forming Liquids [Journal] // J. Am. Chem. Soc.. - 1955. - Vol. 77. - pp. 3701-3707.

**Wright D.** Environmental Stress Cracking of Plastics [Book]. - Shawbury : RAPRA Technology Ltd., 1996.

**Xia Z., Shen X. and Ellyin F.** An Assessment of Nonlinearly Viscoelastic Constitutive Models for Cyclic Loading: The Effect of a General Loading/Unloading Rule [Journal] // Mechanics of Time-Dependent Materials. - 2006. - Vol. 9. - pp. 281–300.

**Zacharatos Antonios and Kontou Evagelia** Nonlinear viscoelastic modeling of soft polymers [Journal] // Journal of Applied Polymer Science. - 2015.

**Zehsaz Mohammad, Vakili-Tahami Farid and Saemi-Sadigh Mohammad-Ali** Parametric study of the creep failure of double lap adhesively bonded joints [Journal] // Materials & Design. - 2014. - Vol. 64. - pp. 520-526.

**Zhang C. and Moore I.D.** Nonlinear Mechanical Response of High Density Polyethylene. Part I: Experimental Investigation and Model Evaluation [Journal] // Polymer Engineering and Science. - 1997. - 2 : Vol. 37. - pp. 404-413.

**Zhang C. and Moore I.D.** Nonlinear Mechanical Response of High Density Polyethylene. Part II: Uniaxial Constitutive Modeling [Journal] // Polymer Engineering and Science. - 1997. - 2 : Vol. 37. - pp. 414-420.

**Zhurkov S. N.** Kinetic Concept of the Strength of Solids [Journal] // Int. J. of Fracture Mech.. - 1965. - Vol. 1.

**Zienkiewicz O. C.** The Finite Element Method [Book]. - London : McGraw Hill, 1977.

## **Appendix A**

### **Viscous Material Analysis Instructions**

This analysis has two steps:

- 1- Finding material properties (constants/fitting parameters) based on experimental data using FITTEST program, a code developed in Matlab workspace
- 2- Finite element analysis of the material model in ABAQUS software, based on material properties obtained from the first step, using VISCOMAT, a user defined material subroutine, UMAT, developed in Fortran workspace

#### **Finding Material Properties using FITTEST**

Two steps have to be followed for obtaining the proper material constants. First material test results must be stored in an excel file. Let's call it testdata.xlsx. then FITTEST program must be run. Storing the data in the excel file are described following. Then FITTEST has to be run considering the tips that will be explained latter.

#### **Storing material test results in total.xlsx file.**

While performing one dimensional tension creep experiment on any polymeric material, the axial deformations are recorded in each time interval. For each constant stress level, the resultant axial strain is computed. Test information that will be stored in the file testdata.xlsx are:

- 1- number of creep tests (curves)
- 2- Applied constant stress for each test
- 3- Measurements of strain for each test
- 4- Time (in second) in which each strain is measured

A sample of test data storage is shown in the following figure.

	A	B	C	D	E	F
1	4	2970000	5470000	6700000	7710000	
2	30.102	0.006904	0.009026	0.01236	0.014819	
3	60.09	0.007174	0.00943	0.013471	0.015964	
4	90.02	0.007308	0.009699	0.014044	0.016671	
5	120.012	0.007409	0.009969	0.014414	0.017142	
6	180.102	0.007544	0.010137	0.014717	0.017513	
7	210.031	0.007578	0.010339	0.014953	0.017816	
8	240.082	0.007611	0.010474	0.015122	0.018085	
9	270.012	0.007645	0.010642	0.01529	0.018287	
10	330.102	0.007712	0.010743	0.015425	0.019769	
11	360.031	0.007746	0.010878	0.015559	0.018658	
12	390.082	0.007746	0.010979	0.015661	0.018826	
13	420.012	0.00778	0.01108	0.015762	0.018961	
14	450	0.007813	0.011148	0.015829	0.019096	
15	480.102	0.007813	0.011249	0.01593	0.019197	
16	510.043	0.007847	0.011316	0.015997	0.019331	
17	570.012	0.007881	0.011417	0.016098	0.019432	
18	600.063	0.007881	0.011484	0.016166	0.0195	

The first cell in testdata.xlsx (A1) indicates the number of creep tests on the material. Here the value of 4 means four creep test under constant stresses are being used. These stress values are mentioned in the remaining cells of first row. Here values in cells B1, C1, D1 and E1 show the stress values for each test. The first column (starting the second row, A2), contains the time intervals, and other columns, starting the second row, contain strain measurement. Each strain is associated with the time in the same row and first column, the stress at the first row of the same column. The number of data is not limited, meaning that any number of tests and time intervals can be entered.

If more than one material is tested, data for each material needs to be entered in a separate excel sheet.

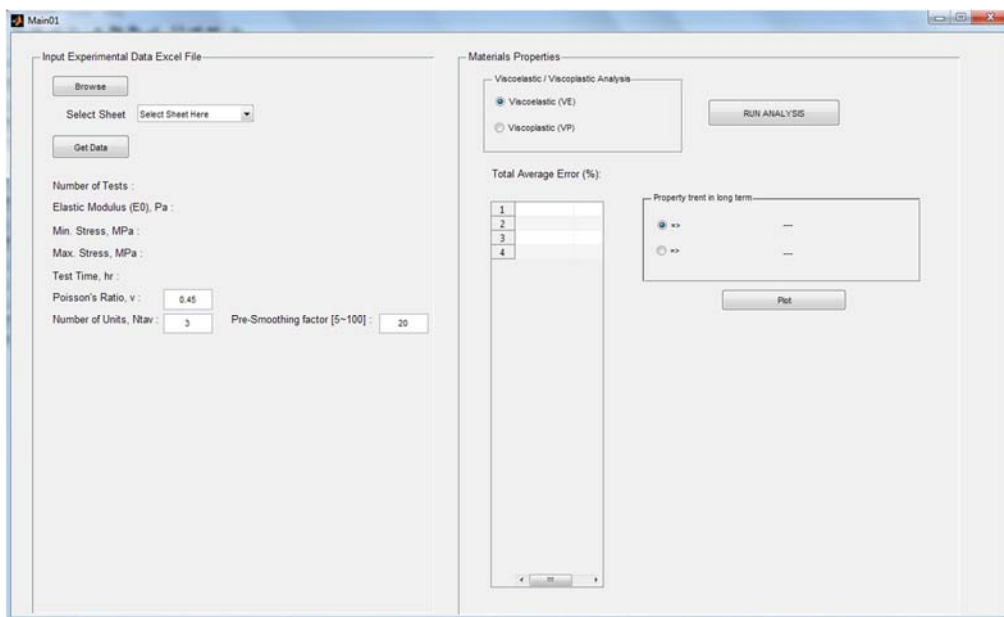
26	870.02	0.008015	0.01199	0.016005	0.016657	0.020175				
27	900.063	0.008049	0.012023	0.016132	0.016671	0.020241				
28	930.113	0.008049	0.012091	0.016166	0.016705	0.020342				
29	960.043	0.008049	0.012124	0.016199	0.016772	0.020375				

PIPE-24h | PIPE-07d | PIPE-02w | RES1-24h | RES1-24h-6 | RES2-24h | RES3-24h | RES4-24h

The sample file (above figure) shows different sheets for different material tests as: Pipe material for 24 hour test time, Pipe material for 7 day test time, Pipe material for two week test time, Material Res1, Material Res2, etc.

## Running FIITEST

To start, in MATLAB workspace type guide. This activates the GUI mode in which FITTEST file can be opened. Then press the Figure button ( ) to run the program. The program window appears as following



First step analysis starts with the Input Experimental Data Excel File. In this section press Browse button and locate/open the testdata.xlsx file. The name and file address will appear beside the Browse button. Use the drop/down option beside Select Sheet to choose one of the sheets within the uploaded data file which contains the experimental results of the material.

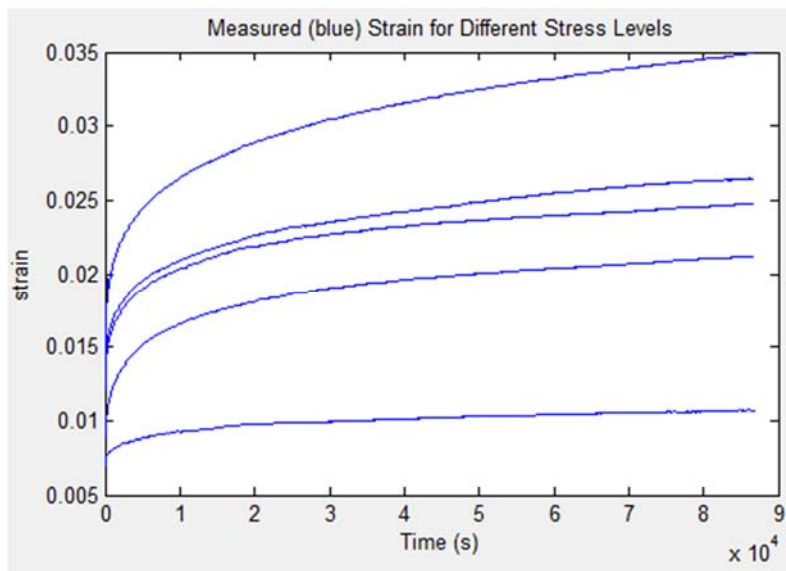
Press Get Data. The program uploads the test data and plots the strain vs time for all available stresses (following figure for sample test). Other information also are depicted which are: number of tests, instantaneous elastic modulus, minimum stress level, maximum stress level and test time (hr).

Three information regarding this material tests need to be given for analysis, as following.

Poisson's ratio: which a material property and is provided by material supplier. If not available, it is recommended to be set equal to 0.45

Number of Units, Ntav: which is the number of Kelvin units in Kelvin-Solid configuration model and is interpreted as the order of final expression

Pre-Smoothing factor [5~100]: which reduces the number of measured items and needs to be an integer number between 5 and 100. For example, entering 20 means that the program takes one data from each 20 available data. This has two benefits. First the run time reduces, second, the noises will be removed and the curve fitting will be more smooth.



Now the data are uploaded into the program FITTEST. The next step is performing the analysis. Two methods are introduced. Viscoelastic (VE) and Viscoplastic (VP). The first uses the exponential relations based on spring and dash-pot configuration and the second is based on the power law relations of plasticity theorem.

In Viscoelastic/Viscoplastic Analysis box choose one of either Viscoelastic (VE) or Viscoplastic (VP) analysis. Press RUN ANALYSIS button.

### **VE parameters**

By running VE analysis, the program calculates fitting parameters and a table of these parameters will be provided (following figure). Also mean fitting error which is the average of Mean Least Squares Deviations for all tests (curves) will be presented.

E00	5.1262e+08
v	0.4500
Ntav	3
m	0.5433
a	19.5922
b0	4.4311e+03
b1	210.5247
b2	2.7657
b3	1.0770
b4	-110.4567
c0	4.4200e-06
c1	-19.6318
c2	-0.5623
c3	-0.0039
c4	-8.1656e-04
d0	-2.4437
d1	-0.0244
d2	-0.0628
d3	4.8451
d4	14.3395
d5	0.7289

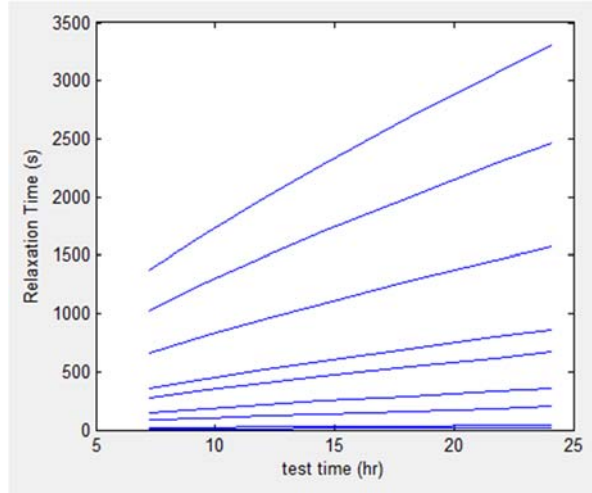
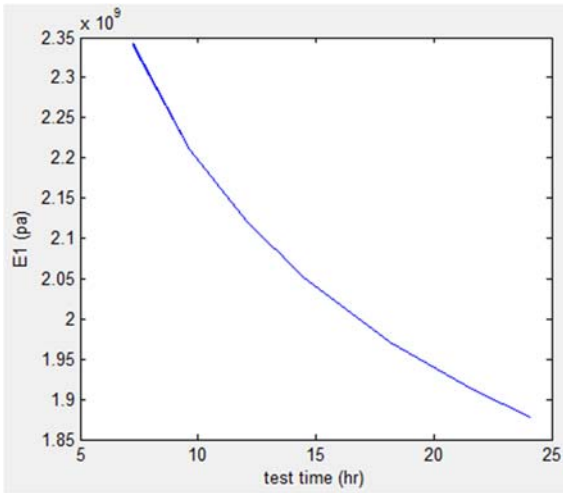
In right hand side the tool box Property trend in long term is provided which plots the behavior of two parameters  $E_1$  (first viscoelastic modulus) and  $\tau_1$  (first relaxation time). For this, one of either two following options needs to be chosen.

E1 vs Test-time (hr) for different stresses

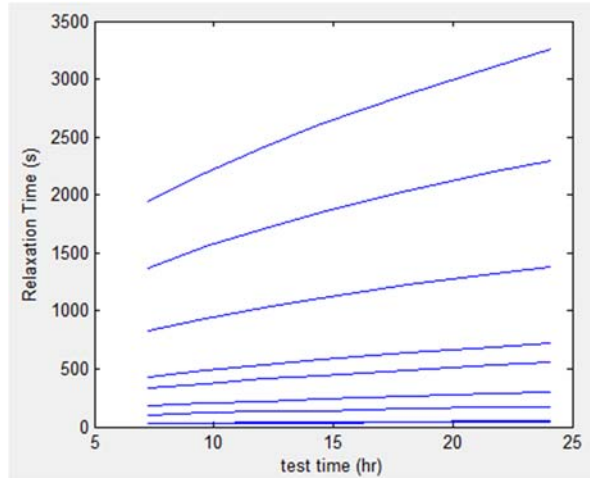
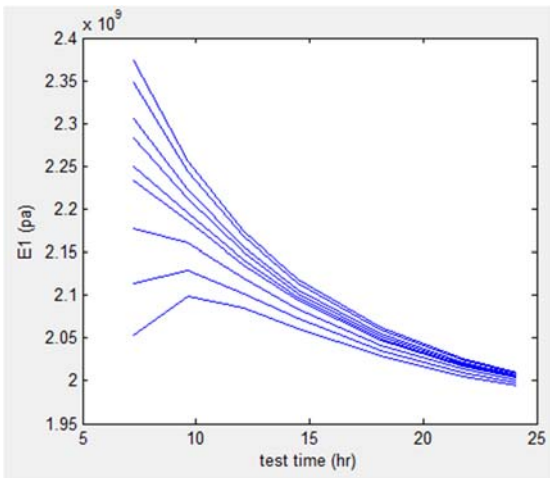
T1 vs Test-time (hr) for different stresses

By pressing the Plot button, the curves will be plotted. These curves serve as indicators of how the fitting suits for long term prediction. Since the analysis is a nonlinear optimization of finding the best fit, it would be a trial process and the analysis may need to be run for few times (refer to paper #1 for more details on the optimization process). This justifies the use of these plots as indicators of long term suitability of the fitting parameters. Following you see some example for different values of Ntav and Pre-smoothing factor.

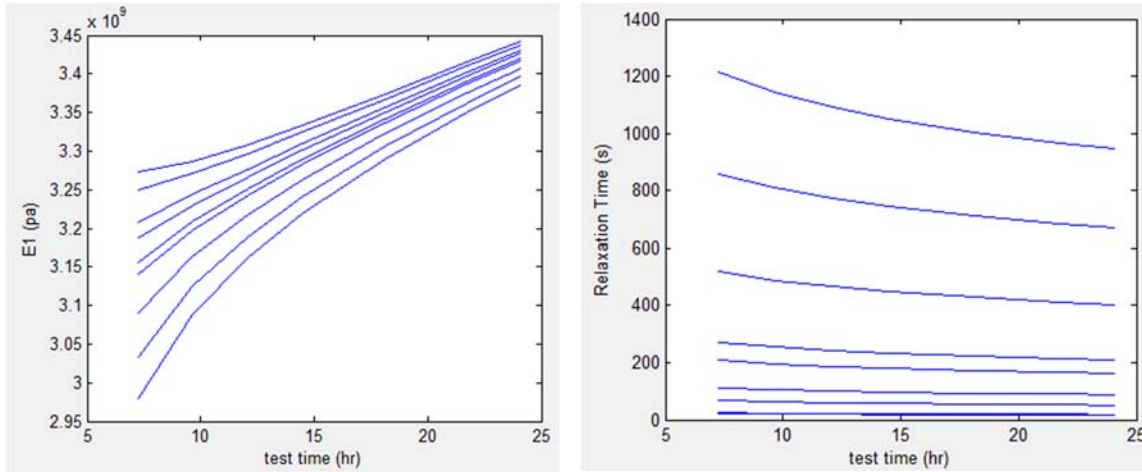




Case I: For  $N_{tav} = 3$  & *Pre-smoothing factor* = 20



Case II: For  $N_{tav} = 3$  & *Pre-smoothing factor* = 50



Case III: For  $N_{tav} = 5$  & *Pre-smoothing factor* = 50

Three cases are presented above which show how different values of  $N_{tav}$  and *Pre-smoothing factor* affect the materials behavior for long term prediction. Each curve represents results for stresses which are 2.68, 3.2, 4, 5.1, 5.58, 6.8, 8, 12 and 17. In Case I, curves for  $E_1$  for all stresses are identical and  $\tau_1$  increases versus test time. Same behavior can be observed in Case II, except  $E_1$  depends on stresses. In both cases,  $E_1$  decreases and  $\tau_1$  increases versus test time, which means that parameters of both cases are able to be used for long term prediction. In Cases III, we see different behavior of material parameters (increase of  $E_1$  and decrease of  $\tau_1$  versus test time) which means that the parameters are not acceptable.

### VP parameters

By running VP analysis, the program calculates fitting parameters and a table of these parameters will be provided (following figure). Also mean fitting error which is the average of Mean Least Squares Deviations for all tests (curves) will be presented.

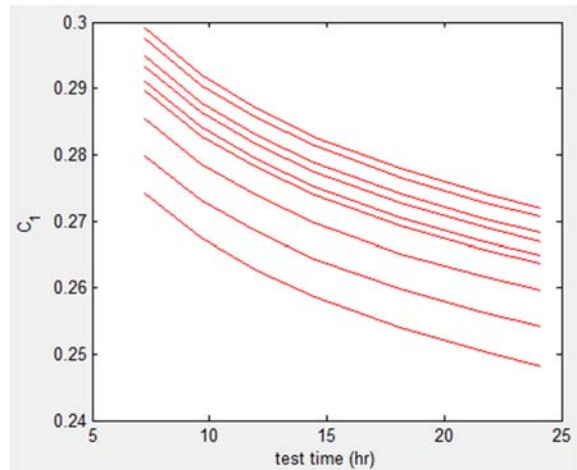
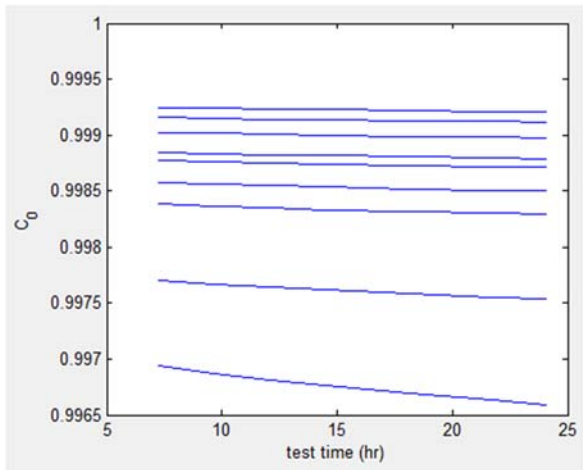
E00	5.1262e+08
v	0.4500
N	2
b1	7.8260e-05
b2	-3.8243e-05
b3	5.3416e-06
b4	-0.0049
b5	-0.0127
b6	-0.0111
m1	0.0687
m2	0.1124
sa	-0.0972
T1	-0.0013
d0	-0.0323
d1	5.1343e-05
d2	-0.0210
d3	0.0089
d4	0.0076
d5	-0.0047
d6	-0.0077
d7	-0.0038
d8	-0.0143
d9	-0.0110
T2	0.0381

In *Property trend in long term* tool box the behavior of two parameters  $C_0$  and  $C_1$  can be plotted. For this, one of either two following options needs to be chosen.

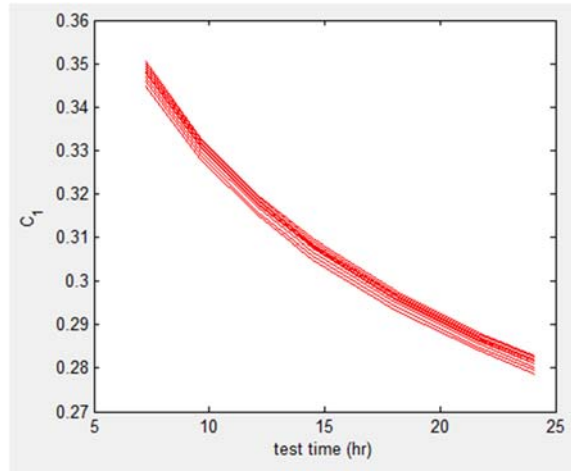
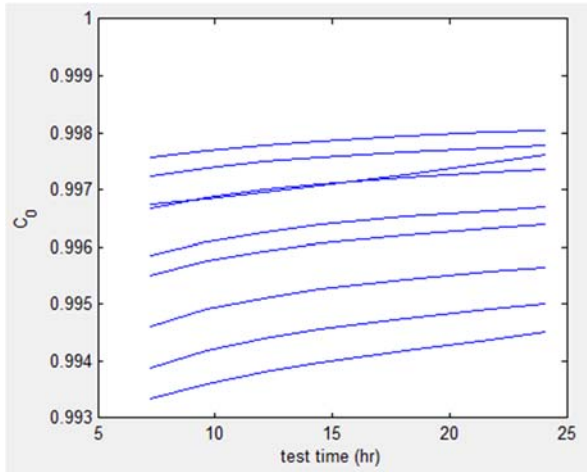
- $C_0$  vs Test-time (hr) for different stresses
- $C_1$  vs Test-time (hr) for different stresses

By pressing the **Plot** button, the curves will be plotted. Similar to VE analysis, these curves serve as indicators that show how the fitting suits for long term prediction. Following you see some examples for different values of *Pre-smoothing factor*. For VP analysis,  $N_{tav}$  represents the number of nonlinear term in constitutive equation and is set to be equal to one.

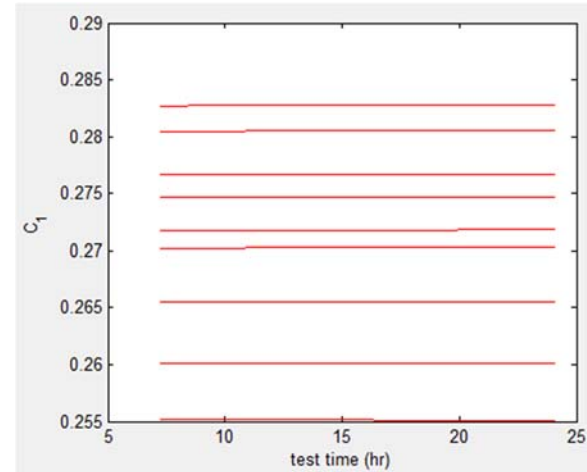
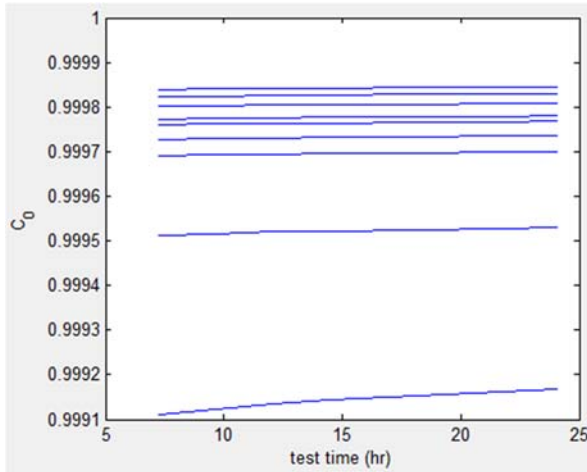
Here, decreasing both parameters of  $C_0$  and  $C_1$  versus test time is a good sign and indication of suitability of fitting parameters for long term behavior prediction (Case I).



Case I: For Pre-smoothing factor = **20**



Case II: For Pre-smoothing factor = 100



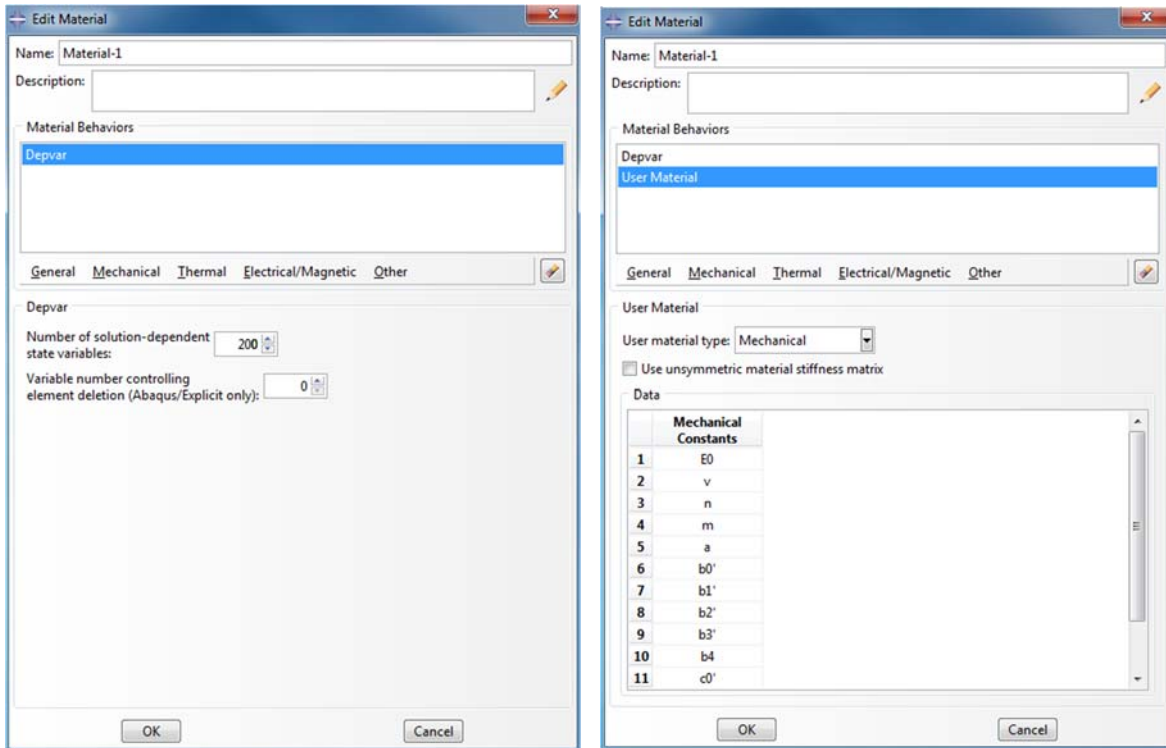
Case III: For Pre-smoothing factor = 10

### Finite Element Analysis using VISCOMAT

This step includes modeling the structure in ABAQUS software and invoking the VISCOMAT UMAT for analysis.

#### Material Definition

Material needs to be defined based on the actual material properties. In *Material Manager* a new material is created. For this a Name has to be defined. For the material behavior. Two parts, *Depvar* and *User Material*, need to be defined from *General* subsection. For *Depvar*, *number of solution-dependent state variables* is set to 200.



User material properties depend on the analysis types which are specified by the name of the material. Name of the material must follow specified rules. The starting four letters define the type of the analysis and must match the definitions in UMAT library. This letters are:

## NVE

These letters stand for Nonlinear ViscoElastic and is used for analyzing the nonlinear viscoelastic behavior. This material definition is used when Long term analysis is expected, using long term properties of material obtained from the FITTEST program. It needs 21 material constants as following:

- PROPS ( 1 ) =E0 , instantaneous module of elasticity
- PROPS ( 2 ) =v , Poisson's ratio
- PROPS ( 3 ) =n , number of Kelvin units
- PROPS ( 4 ) =m , scale factor for module of elasticity of each Kelvin unit
- PROPS ( 5 ) =a , scale factor for relaxation time of each Kelvin unit
- PROPS ( 6 ) =b0'
- PROPS ( 7 ) =b1'
- PROPS ( 8 ) =b2'
- PROPS ( 9 ) =b3'
- PROPS ( 10 ) =b4'
- PROPS ( 11 ) =c0'
- PROPS ( 12 ) =c1'

PROPS(13)=c2 '  
PROPS(14)=c3 '  
PROPS(15)=c4 '  
PROPS(16)=d0 '  
PROPS(17)=d1 '  
PROPS(18)=d2 '  
PROPS(19)=d3 '  
PROPS(20)=d4 '  
PROPS(21)=d5 '

Non-defined properties, above, are fitting constants.

## **NVP**

These letters stand for Nonlinear ViscoPlastic and is used for analyzing the nonlinear viscoplastic behavior. This material definition is used when Long term analysis is expected, using long term properties of material obtained from the FITTEST program. It needs 24 material constants as following:

PROPS(1)=E0 , instantaneous module of elasticity  
PROPS(2)=v , Poisson's ratio  
PROPS(3)=n , number of Kelvin units  
PROPS(4)=b1  
PROPS(5)=b2  
PROPS(6)=b3  
PROPS(7)=b4  
PROPS(8)=b5  
PROPS(9)=b6  
PROPS(10)=m1  
PROPS(11)=m2  
PROPS(12)=sa  
PROPS(13)=T1  
PROPS(14)=d0  
PROPS(15)=d1  
PROPS(16)=d2  
PROPS(17)=d3  
PROPS(18)=d4  
PROPS(19)=d5  
PROPS(20)=d6  
PROPS(21)=d7  
PROPS(22)=d8  
PROPS(23)=d9  
PROPS(24)=T2

Non-defined properties, above, are fitting constants.

## **LVEP**

These letters stand for Linear ViscoElastic Prony and is used for analyzing the linear viscoelastic behavior. This material definition is used when material properties of material are available in the form of Prony series. It needs at least 5 material constants as following:

PROPS(1)=E0 , instantaneous module of elasticity  
PROPS(2)= $\nu$  , Poisson's ratio  
PROPS(3)=n , number of Kelvin units  
PROPS(4)=E1 , module of elasticity for first Kelvin unit  
PROPS(5)=T1 , relaxation time for first Kelvin unit  
PROPS(6)=E2 , module of elasticity for second Kelvin unit  
PROPS(7)=T2 , relaxation time for second Kelvin unit  
PROPS(8)=E3 , module of elasticity for third Kelvin unit  
PROPS(9)=T3 , relaxation time for third Kelvin unit  
PROPS(10)=. . .

Constants for up to 20 Kelvin units can be used.